PHD

Metal mediated organic transformations

Butters, Christopher

Award date:
1995

Awarding institution:
University of Bath

METAL MEDIATED ORGANIC TRANSFORMATIONS

submitted by Christopher Butters

for the degree of PhD

of the University of Bath

1995

ProQuest LLC
789 East Eisenhower Parkway
P.O. Box 1346
Ann Arbor, MI 48106-1346

Summary

The work described in this thesis is concerned with the synthesis and reactivity of $CpMo(CO)_2$-derived π-allyl and π-diene complexes and related compounds, particularly with regard to selective transformations of the coordinated organic ligand. In order to put this topic into context, the Introduction contains a short review of some of the previous work carried out in this area, and illustrates how these complexes can be used as stoichiometric reagents in organic synthesis. In addition, the chemistry associated with the corresponding $Fe(CO)_3$-derived π-diene and π-dienyl complexes is included for comparative purposes.

The Results and Discussion is split into four separate sections. Section 2.1 reports the formation of the 4-oxo-η^3-cyclohexenyl complex $[Mo(\eta^3\text{-}C_6H_7O)(CO)_2(\eta^5\text{-}C_5Me_5)]$ (92). Selective elaboration of the coordinated cyclohexenyl ligand is demonstrated by the methods of *O*-protonation, hydride abstraction, enolate alkylation and nucleophilic addition.

Section 2.2 is concerned with the synthesis of the molybdenum-cyclopentadiene complex $[Mo(\eta^4\text{-}C_5H_6)(CO)_2(\eta^5\text{-}C_5Me_5)]$ (112). This complex undergoes an interesting hydrogen transfer reaction when formed under concentrated conditions. The elaborative methods of deprotonation/electrophilic addition and nucleophilic addition are briefly examined.

Section 2.3 describes the selective synthesis of certain 4-oxo-η^3-butenyl complexes analogous to (92), and details their reaction with $NaBH_4$ and simple organometallic reagents. The *syn* to *anti* isomerisation of these complexes is achieved using a protonation/deprotonation procedure. A preliminary study on their suitability for resolution *via* enzyme catalysed hydrolysis is also reported.

Section 2.4 discusses the synthesis of the novel η^3-γ-lactonyl complex $[Mo(\eta^3\text{-}C_4H_3O_2)(CO)_2(\eta^5\text{-}C_5Me_5)]$ (162) and its η^5-indenyl and η^5-cyclopentadienyl analogues. These complexes undergo an allyl-oxygen cleavage in their reaction with benzylamine or methoxide anion. Overall substituent addition takes place at the γ-carbon atom of

the lactone ring; evidence for initial nucleophilic attack at molybdenum is presented. A preliminary investigation into the protonation of an η^3-γ-lactonyl complex is also detailed.

Finally there follows an Experimental section and an Appendix containing crystallographic data.

Acknowledgements

First and foremost, I would like to express my gratitude to Professor Michael Green for making my three years of research at Bath both enjoyable and productive. I would also like to thank Dr. Martin Wills for his helpful advice and comments throughout the course of this work.

The results detailed in this thesis could not have been presented without the assistance of many others. I am particularly indebted to Dr. Mary Mahon for the six crystallographic studies, which have made an important contribution to this work. I would like to thank Dr. R. J. Deeth for an EHMO calculation, and Dr. R. Kinsman for teaching me advanced NMR techniques. I am grateful to Dr. M. E. Vamon Rao, Monika Kursawe and Dr. Nick Carr for conducting some preliminary experiments. Special thanks must go to all the technical staff within the department, especially to Robert Stevens, Ahmed Sheibani and Alan Carver, who provided an excellent support service. I would also like to thank my fellow laboratory companions for helping to create an enjoyable working atmosphere.

I thank the SERC and BP Research, Sunbury-on-Thames, for their financial assistance in the form of a CASE award.

Finally, I wish to thank my family and friends for their continued support and encouragement. In particular, I would like to thank Emma Lenz for her help with the typing of this thesis, and for her friendship throughout the last seven years of my university life.

Memorandum

The work described in this thesis was carried out by the author between October 1991 and September 1994 within the School of Chemistry at the University of Bath, under the supervision of Professor Michael Green. Unless otherwise indicated, the work is original and has not been submitted for any other degree.

Christopher Butters

Contents

Abbreviations

Cp	η^5-cyclopentadienyl
Cp*	η^5-pentamethylcyclopentadienyl
In	η^5-indenyl
R	alkyl or aryl group
Me	methyl
Et	ethyl
Pr	propyl
Bu	butyl
Ac	acetyl
Ph	phenyl
Ts	4-toluenesulphonyl
TBDMS	*t*-butyldimethylsilyl
DMTS	dimethylthexylsilyl
L	ligand
M	metal
X	halide or counter ion
n	normal
i	iso
s	secondary
t	tertiary
thf	tetrahydrofuran
Py	pyridine
DDQ	2,3-dichloro-5,6-dicyano-1,4-benzoquinone
LDA	lithium diisopropylamide
PLE	pig liver esterase
Nu	nucleophile
E	electrophile

B	base
Δ	heat
atm.	atmosphere
aq.	aqueous
hν	photolysis
h	hour
min	minute
d	day
mol	mole
mmol	millimole
mg	milligram
cm	centimetre
e.e.	enantiomeric excess
TLC	thin layer chromatography
IR	infrared
NMR	nuclear magnetic resonance
EHMO	extended Hückel molecular orbital
HOMO	highest occupied molecular orbital
LUMO	lowest unoccupied molecular orbital

Relating to Infrared Data

ν_{CO}	wavenumber of carbonyl band (cm^{-1})
v	very
s	strong
m	medium
w	weak
br	broad

Relating to NMR data

ppm	parts per million
Hz	hertz
MHz	megahertz
J	scalar coupling constant
δ	chemical shift
s	singlet
d	doublet
t	triplet
q	quartet
m	multiplet
br	broad

Relating to mass spectral data

FAB	fast atom bombardment
NBA	*n*-butylalcohol
X	unidentified fragment

1. INTRODUCTION

1.1 Stoichiometric Organotransition Metal Complexes In Organic Synthesis

The study of the preparation of organotransition metal complexes and their influence on the course of chemical reactions constitutes an area of chemistry that has been developing rapidly over the last three decades. Enormous advances in our understanding of the structure and reactivity of organotransition metal compounds have taken place. These insights have prepared the way for applications of these compounds to the ever burgeoning field of organic synthesis,[1-4] both as stoichiometric reagents and as catalysts.

The use of organotransition metals for organic synthesis involves three stages: (i) the interaction of an organic compound with a transition metal species to form an intermediate transition metal complex (complexation); (ii) a chemical reaction on the coordinated ligand (elaboration or functionalisation); (iii) recovery of the organic compound (decomplexation). It is the reactions of these intermediate transition metal complexes that are of interest to the synthetic chemist.

In general, coordination of an organic compound to a transition metal markedly alters the properties of the compound (*via* a change in electron density) such that it will undergo completely different types of reactions from the free molecule. According to the nature of the metal species, such coordination can activate or deactivate the organic ligand towards a particular reaction. This latter property allows organotransition metal species to be used as protecting or stabilising groups in organic synthesis.

When a metal species activates an organic ligand towards nucleophilic attack, it can direct both the stereo- and regio-chemistry of the reaction. These concepts have provided unique strategies for synthesising complex stereo- and regio-defined products. Recent research has started to focus on extending these methods to enantiospecific organic synthesis, allowing access to a number of important optically active molecules, many of which have significant biological properties.

From general considerations, the practical use of catalytic methods is considered preferable. However, the development of convenient pathways to stoichiometric

organotransition metal reagents, and their regeneration and recycling, can also make this approach profitable, especially when *multiple sequential* stereo- and regio-specific functionalisations are involved. It is precisely this field in which the application of organotransition metals of high selectivity appears very promising. Indeed, the elegant synthetic work of S. G. Davies[5,6] serves to underline the potential of this area.

In recent years, stoichiometric metal π-complexes of various unsaturated ligands have been used to significant advantage in the stereocontrolled construction of substituted cyclic, acylic and heterocyclic compounds. Established systems include the use of $[CpMo(CO)_2(\eta^3\text{-allyl})]$,[7-9] $[(\eta^4\text{-diene})Fe(CO)_3]$,[7-10] $[(\eta^6\text{-arene})Cr(CO)_3]$[11] and $[(CO)_5Cr{=}C(OR)R']$[12] complexes.

As an appropriate introduction to this thesis, the discussion will focus primarily on the systems of iron [$Fe(CO)_3$-derived π-diene and π-dienyl complexes] and molybdenum [$CpMo(CO)_2$-derived π-allyl and π-diene complexes], which share a number of similarities in their chemistry. The synthesis and use of the $Fe(CO)_3$-derived complexes has been more intensively investigated than that of the related molybdenum compounds. This stems largely from the fact that they are very easily prepared and the starting materials are readily available. As a consequence, the iron systems have enjoyed a fairly long history, whilst the molybdenum complexes that we shall discuss are more recent, and so their chemistry is less well known.

1.2 Methods of Complexation

The first stage in a synthetic route requiring the use of organotransition metals involves the complexation of an organic compound (often pre-functionalised) with a transition metal species to form a transition metal complex. Ideally such complexation processes will be economical and have widespread application. This section describes the general methods available for the preparation of stable $Fe(CO)_3$- and $CpMo(CO)_2$-derived η^4-1,3-diene complexes.

1.2.1 Preparation of (η^4-1,3-diene)$Fe(CO)_3$ Complexes

Butadiene-$Fe(CO)_3$ was prepared as long ago as 1930 by Reihlen *et al.*,[13] but practically no development in the area took place until more recently. During the 1960s a number of acyclic 1,3-diene complexes were studied by Pettit[14] and others, and Birch initiated a programme aimed at developing the chemistry of cyclohexadiene complexes.

The general procedure for the preparation of (η^4-1,3-diene)$Fe(CO)_3$ complexes involves direct reaction of a diene (acyclic, cyclic or heterocyclic) with $Fe(CO)_5$, $Fe_2(CO)_9$ or $Fe_3(CO)_{12}$. The exchange of CO for diene may be achieved photochemically, thermally[15] or chemically[16] (Fig. 1). A wide variety of substituents on the diene can be tolerated[8] and this makes the process particularly conducive towards organic synthesis.

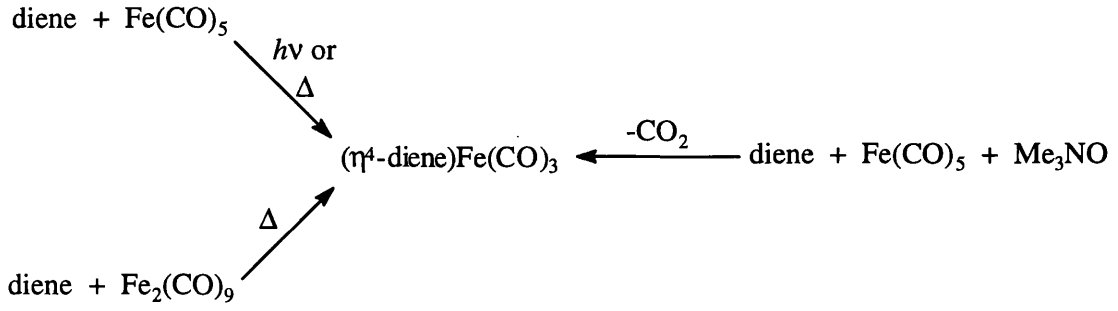

Figure 1

The use of $Fe(CO)_5$ is preferable for large scale work, owing to its lower cost (although this complex is volatile and toxic). Furthermore, $Fe(CO)_5$ will convert 1,4-dienes to their corresponding 1,3-diene complexes. In this case the use of substituted dienes invariably leads to mixtures of products. For example, dihydroanisole derivatives such as (1) give approximately equimolar mixtures of products (2) and (3).[17] Although these are readily separated by column chromatography, it is preferable to pre-conjugate the diene when complex (2) is required[18] (Fig. 2).

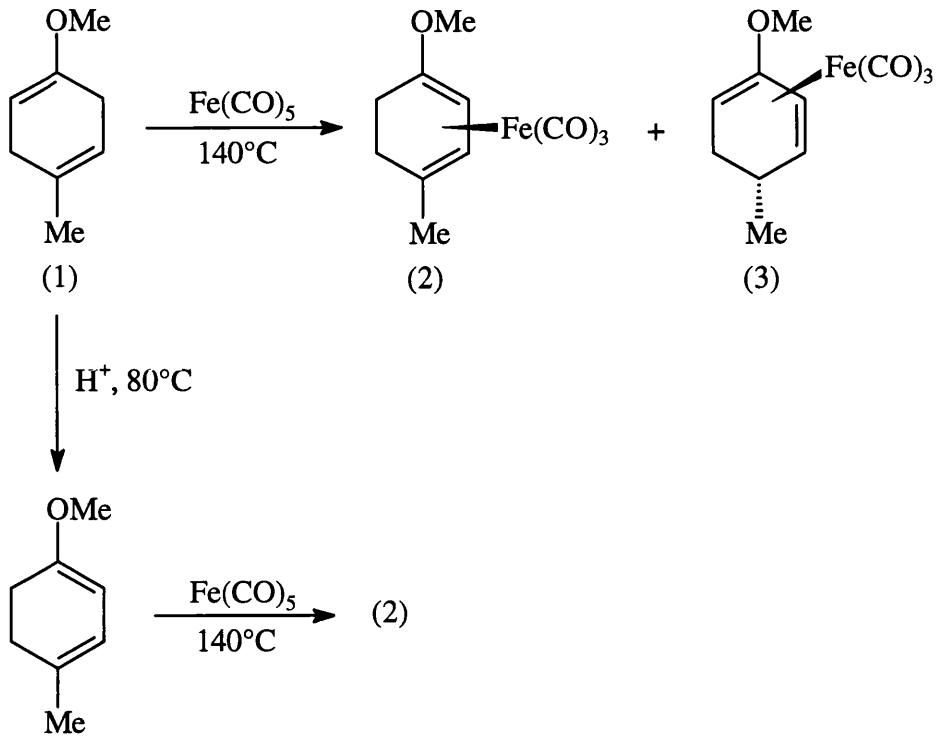

Figure 2

The unconjugated diene, 4-vinylcyclohexane (4), will also produce a 1,3-diene $Fe(CO)_3$ complex mixture. The product ratios vary depending on the conditions employed.[19]

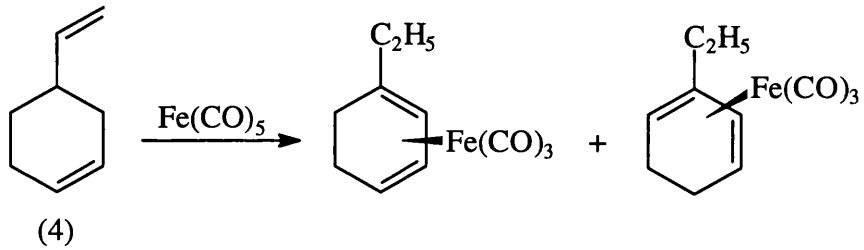

Δ	5	:	1
hν	1	:	5

Figure 3

Nonacarbonyldiiron [and the less commonly used trimer, $Fe_3(CO)_{12}$] can be used under milder conditions than $Fe(CO)_5$, but is generally more useful with conjugated dienes.[20] It has been shown to be particularly good for the formation of heterodiene complexes (Fig. 4).

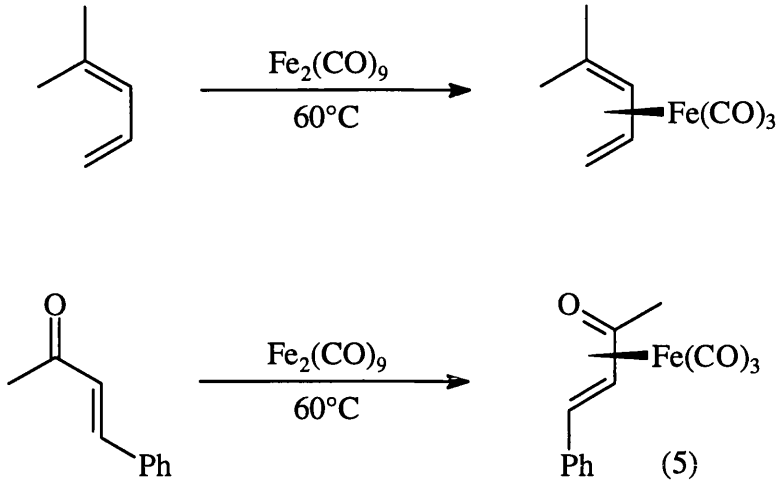

Figure 4

The benzylideneacetone complex (5) and related systems have proved to be very useful as $Fe(CO)_3$ transfer reagents for the synthesis of diene complexes that are difficult to obtain using standard procedures[21] (Fig. 5).

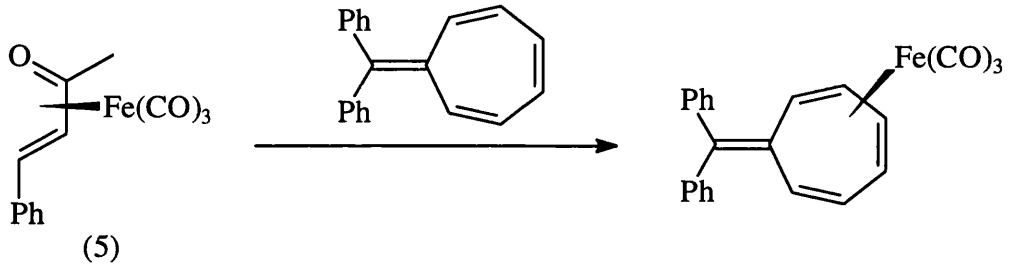

Figure 5

The mechanism of this exchange is believed to proceed through an intermediate with both the benzylideneacetone and the new ligand coordinated,[22,23] as shown in Figure 6.

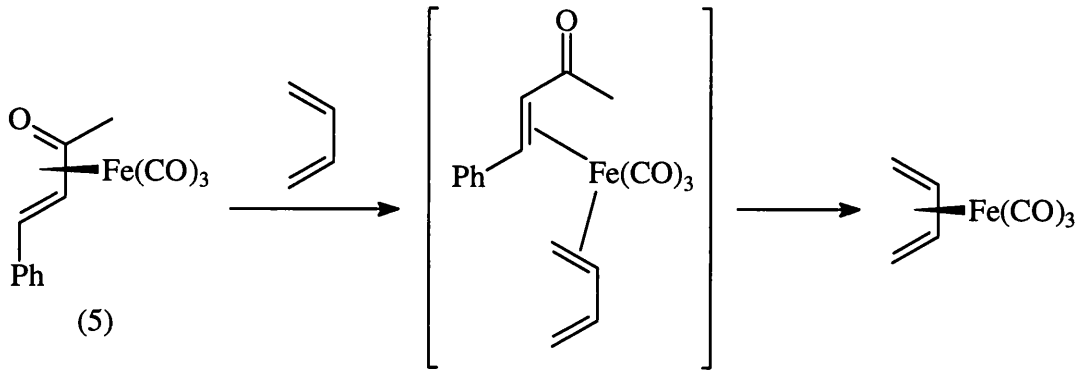

Figure 6

Several other methods for the preparation of (η^4-1,3-diene)$Fe(CO)_3$ complexes are known. Among these are some interesting ring-opening reactions of vinyl- and methylene-cyclopropanes[24,25] (Fig. 7).

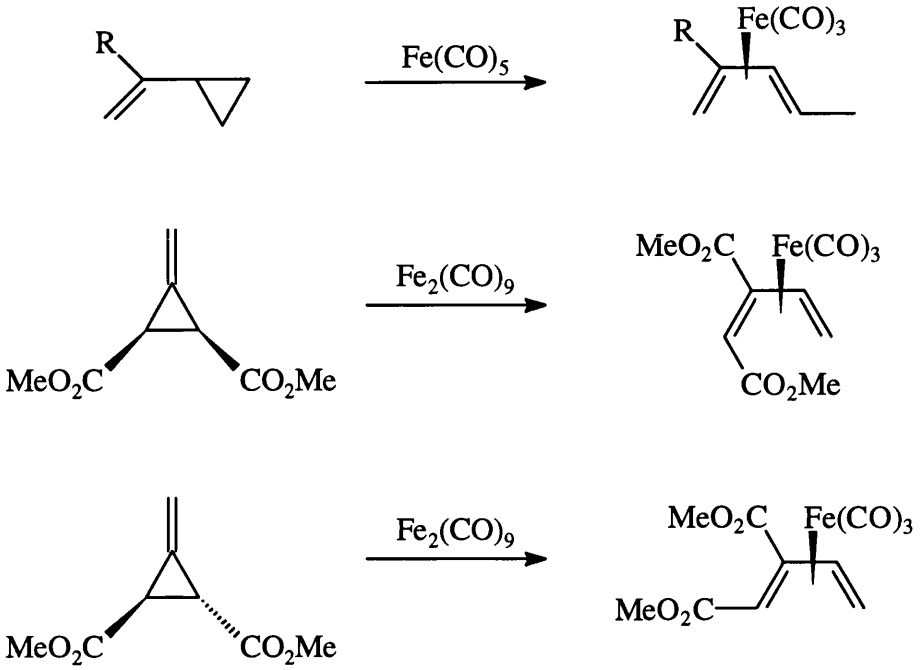

Figure 7

Vinyl epoxides also undergo rearrangement to diene complexes[26] (Fig. 8).

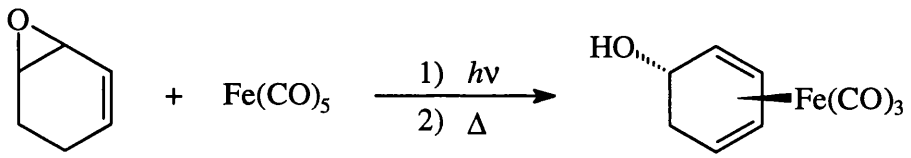

Figure 8

Finally, cyclohexenyl bromides react with iron carbonyls to give cyclohexadiene-$Fe(CO)_3$ complexes[27] (Fig. 9).

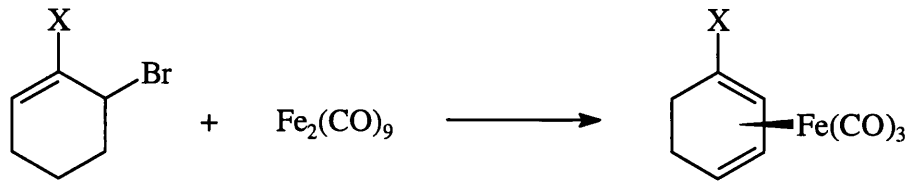

X = H, Cl

Figure 9

1.2.2 Preparation of (η^4-1,3-diene)$Mo(CO)_2Cp$ and Related Complexes

These complexes are cationic since they are coordinated to a $Mo(II)(CO)_2Cp$ group. The fundamental chemistry surrounding the synthesis of such species was developed by Faller and Green in the mid-1970s. One of the original methods used for their preparation involves prior construction of an η^3-allyl-$Mo(CO)_2Cp$ complex, *via* the requisite allylic halide.[28] This procedure is outlined in Figure 10, for the formation of the molybdenum η^3-cyclohexenyl complex (6). Subsequent hydride abstraction using trityl cation leads to the η^4-cyclohexadiene complex (7).[29]

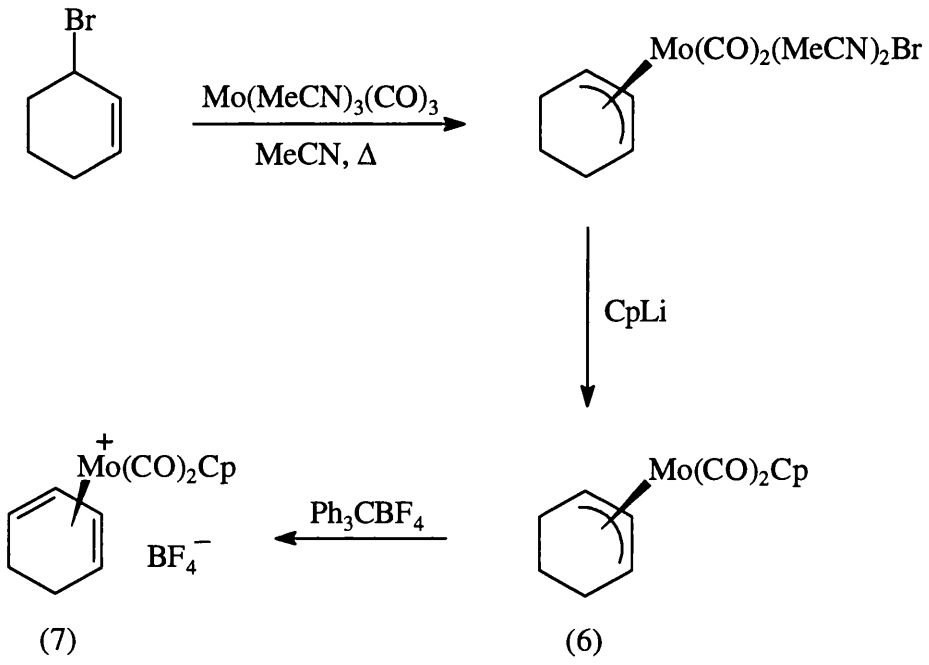

Figure 10

While this approach can be used to prepare the corresponding cycloheptadiene complex (8),[30] or simple acyclic complexes such as (9),[31,32] it is restricted by the availability of regiochemically pure allylic halides. Hence, very few functionalised η^4-diene complexes have been made using this process. The η^4-cyclopentadienone complex (10)[33] is one such example (Fig. 11).

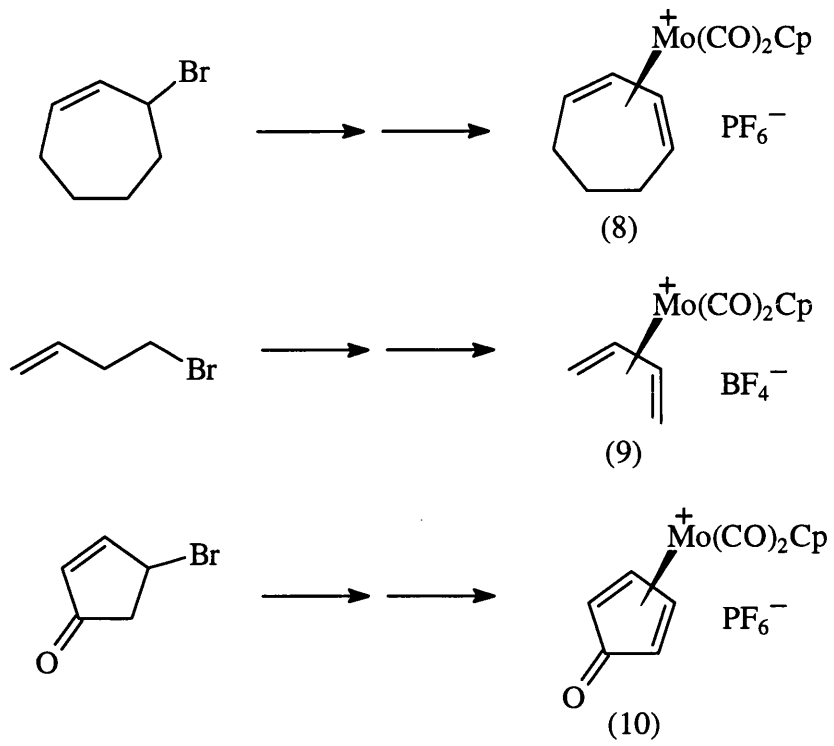

Figure 11

Attempts to extend this methodology using allylic acetates in place of allylic halides have met with limited success.[34-36] Liebeskind has recently established a more favourable approach employing the use of allylic diphenylphoshinates as starting materials.[37]

A potentially more general procedure for the preparation of η^4-1,3-diene molybdenum complexes, involving direct attachment of $[Mo(CO)_2L]$ (where L = η^5-C_9H_7 or η^5-C_5Me_5) to the diene, has been developed by Green and co-workers. This process can be achieved in two ways.

The first method involves treating a mixture of the required diene and the dimeric species $[Mo(CO)_3L]_2$ [L = η^5-C_9H_7 (11) or η^5-C_5Me_5 (12)] with silver tetrafluoroborate.[38,39] This results in a redox reaction, and the splitting of the dimeric species to generate the corresponding complex (Fig. 12).

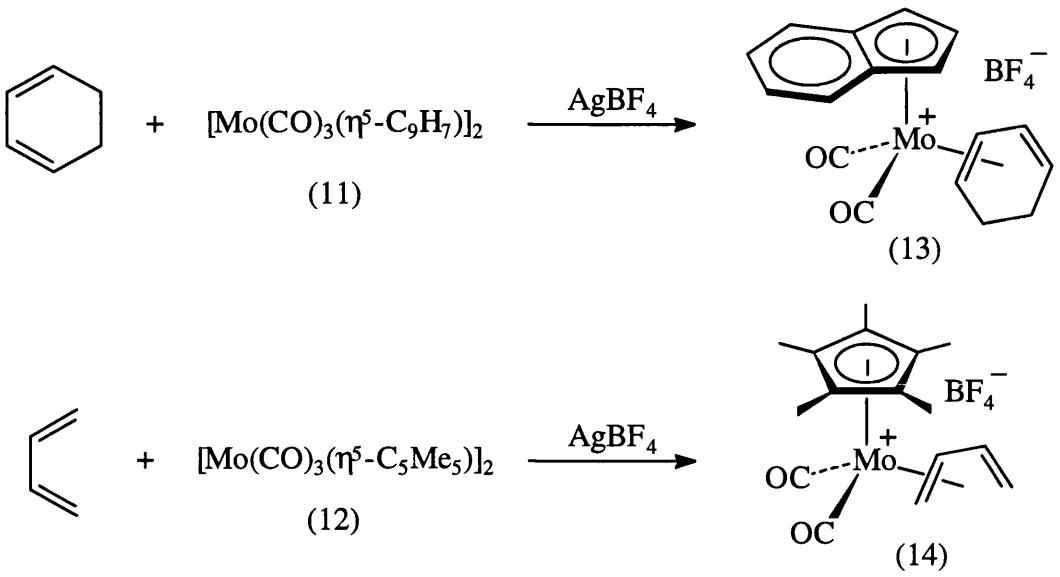

Figure 12

Molybdenum-(η^4-1,3-diene) complexes derived from simple readily available 1,3-dienes (e.g. buta-1,3-diene, isoprene, 2,3-dimethylbuta-1,3-diene, *trans*-penta-1,3-diene, cyclo-octatetraene and cyclohexa-1,3-diene) can be prepared in this manner. However, the presence of highly reactive $AgBF_4$ precludes the use of 1,3-dienes bearing sensitive functional groups.

The second method involves the use of the molybdenum *cis*-bis(acetonitrile) cation $[Mo(NCMe)_2(CO)_2L][BF_4]$ [L = η^5-C_9H_7 (15) or η^5-C_5Me_5 (16)]. This contains two labile acetonitrile ligands which are readily displaced on treatment with a diene species[38-45] (Fig. 13, overleaf). The relatively mild complexation conditions make this procedure an attractive and highly generalised synthetic route to the 1,3-diene complexes. Of particular note is the preparation of the methoxy-substituted cyclohexadiene complex (17). Complexes of this type have proved to be useful building blocks in the synthesis of natural products.[46]

The bis(acetonitrile) cations (15) and (16) are readily prepared, in a similar manner, *via* a series of simple steps from molybdenum hexacarbonyl. This is illustrated in Figure 14 for the η^5-indenyl species.

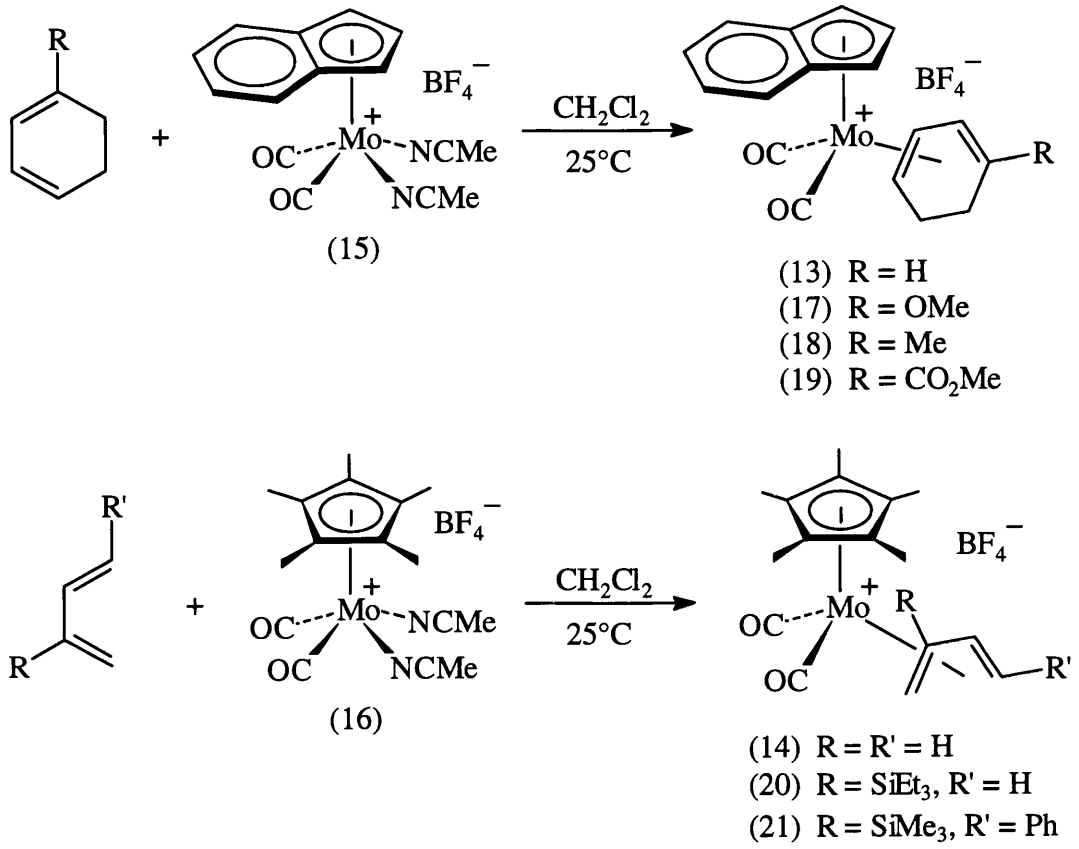

Figure 13

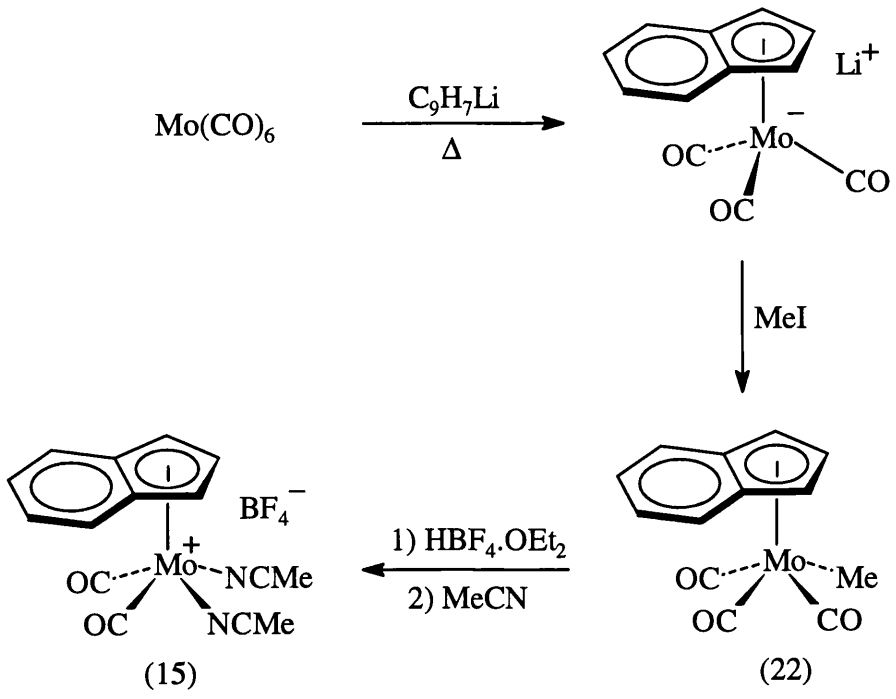

Figure 14

In a comparable study to the work done by Green, Krivykh has shown that molybdenum η^4-diene complexes can also be formed by the action of dienes and strong protic acid on dimeric species[47,48] (Fig. 15). However, the reported yields for this oxidative method are low, although they can be improved with the application of ultraviolet radiation. A further limitation is the use of strong acid which prohibits the use of dienes bearing acid-sensitive functional groups.

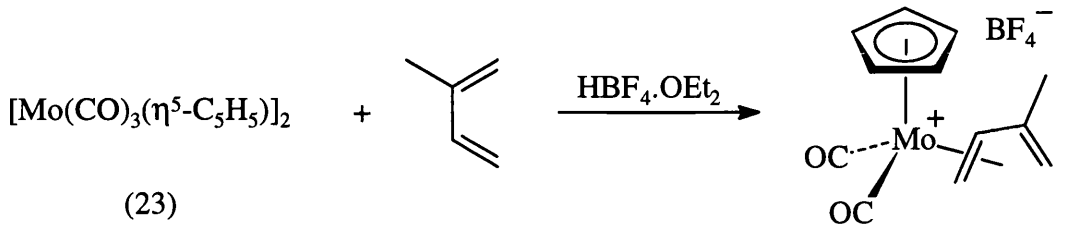

(23) (24)

Figure 15

Slightly better yields may be obtained by a ligand exchange reaction on a neutral η^3-allyl complex in the presence of strong acid.[48,49] For example, treatment of (25) with $HBF_4.OEt_2$ and excess cyclohexadiene leads to the formation of the corresponding η^4-cyclohexadiene complex (7) (Fig. 16). This process is thought to proceed *via* the η^2-propene intermediate (26),[50] which functions as a labile precursor to the formally 14-electron (or doubly unsaturated) Lewis acid $[Mo(\eta^5\text{-}C_5Me_5)(CO)_2]^+$. The Lewis acid species so formed reacts rapidly with any dienes present to generate a stable 18-electron complex.

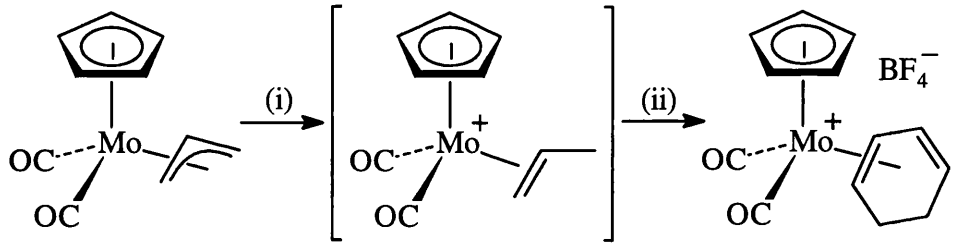

(25) (26) (7)

Figure 16. (i) $HBF_4.OEt_2$; (ii) cyclohexa-1,3-diene.

1.3 Bonding, Structure and Fluxionality in $Fe(CO)_3$- and $CpMo(CO)_2$-Derived Complexes

Before embarking on a discussion of the chemistry associated with $Fe(CO)_3$- and $CpMo(CO)_2$-derived complexes, it will be of value to summarise some of the important points regarding the bonding, structure and fluxionality in these systems.

1.3.1 Bonding of Hydrocarbon Ligands to Transition Metals

The stability and reactivity of hydrocarbon complexes of transition metals can be attributed to bonding effects. A simple model[51,52] proposed by Dewar, Chatt and Duncanson has been used to explain the bonding of ethylene to a transition metal. This is illustrated in Figure 17.

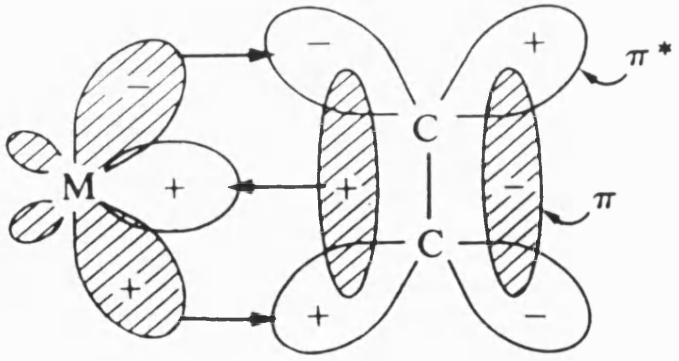

Figure 17. Dewar-Chatt-Duncanson bonding model.

According to this model the bonding consists of two components: (i) the unsaturated hydrocarbon donates electrons from its π-orbital to the metal (forward-donation); (ii) the metal donates its d-electrons into the anti-bonding π*-orbital of the olefin (back-donation). The overall effect is a reduction of electron density in the π-orbital and an increase in electron density in the π*-orbital. The theory explains very elegantly why the carbon-carbon bond weakens on coordination, and hence becomes more susceptible to addition reactions.

The same principles apply to polyenes bonded to transition metals, except that interactions between the double bonds must also be considered. Conjugated dienes have delocalised orbitals of differing energies and symmetries, and therefore offer a larger variety of combinations with the metal atomic orbitals, resulting in more stable metal-carbon bonds. The bonding of conjugated dienes to transition metals has been reviewed[53,54] and will not be elaborated upon here.

1.3.2 Structure and Fluxionality in $Fe(CO)_3$- and $CpMo(CO)_2$-Derived Complexes

Development of structural techniques has paralleled the development of organotransition metal chemistry and frequently contributed to it. One of the most studied groups of compounds in this regard have been the (1,3-diene)$Fe(CO)_3$ complexes, the simplest of which is the butadiene complex (27) (Fig. 18). Complexes of this type have 'piano stool' structures in which the plane of the carbonyl carbons lies parallel to the plane of the carbons bonded to the metal atom.

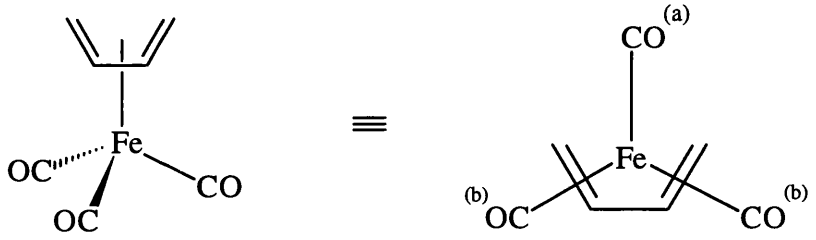

(27)

Figure 18. 'Piano stool' structure: (a) apical position, (b) basal position.

X-ray analysis of (27) shows a rigid structure in which two of the carbonyl ligands are in equivalent environments (basal positions), while the third carbonyl is unique (apical position). However, the room temperature ^{13}C-{^1H} NMR of (27) shows only one peak for these ligands indicating that this conformation is not adhered to in solution.[55,56] This experimental data is most reasonably explained by a rapid exchange process involving rotation of the $Fe(CO)_3$ moiety about its *pseudo*-C_3 axis, whereby the olefin retains its planarity.

Fluxional behaviour can also be observed in (1,3-diene)$Mo(CO)_2Cp$ complexes. For example, the molybdenum-1,3-diene cation (9) has been shown to exist as an equilibrium mixture of conformers, designated *exo* or *endo*, with the former predominating[31,32] (Fig. 19). (The terms *exo* and *endo* refer to the orientation of the diene moiety with respect to the cyclopentadienyl ligand.) Conversion between these conformers is possible by simple olefin rotation about the vector from the metal to the centre of the diene.

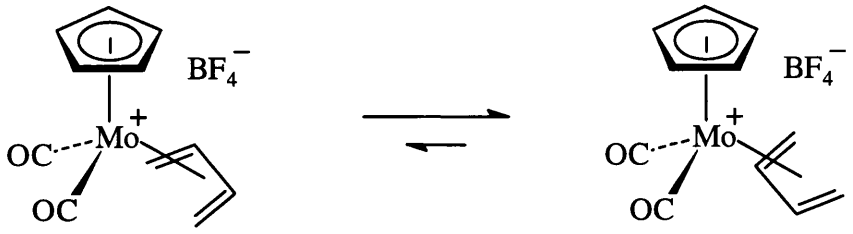

(9a) *exo*-conformer (9b) *endo*-conformer

Figure 19

Substituted cations such as (28) may also exhibit *cis-trans* isomerisation in addition to *exo-endo* conformational averaging.[31] This is thought to be occurring *via* the process illustrated in Figure 20, involving the formation of a solvated metallo-cyclopentene intermediate. Configurational interconversion of the *syn-* and *anti-* substituents (R^1 and R^2) may be achieved by a flip of the metallocycle envelope followed by collapse to the η^4-butadiene structure. Passage through a metallocyclopentene intermediate also serves to interconvert conformational isomers, although this is a path of higher energy than the corresponding rotational motion described above.

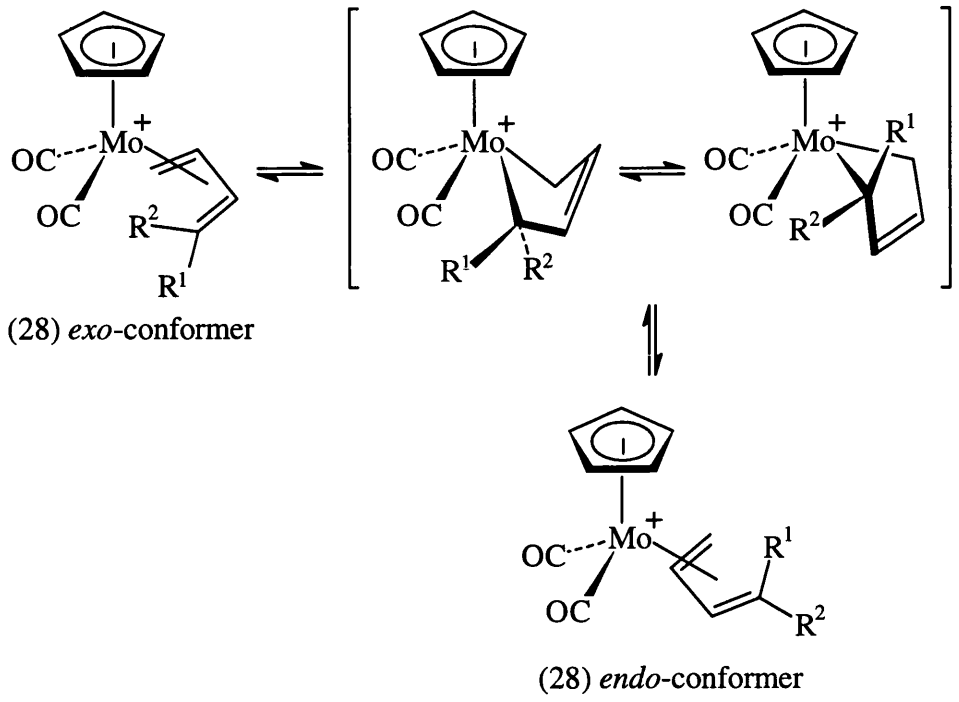

Figure 20. Metallocycle envelope flip mechanism.

It should be noted that in the vast majority of these 1,3-diene complexes the 1,3-diene ligand is coordinated to the transition metal in the planar η^4-*s-cis* configuration. Only recently has the η^4-*s-trans* geometry been identified[43,44,57-60] (Fig. 21).

η^4-*s-cis* configuration η^4-*s-trans* configuration

Figure 21

In addition to the η^4-diene complexes, η^3-allyl complexes have also been shown to exhibit *exo-endo* conformational isomerism.[61-64] As before, interconversion of these isomers is possible by a simple rotational mechanism (Fig. 22).

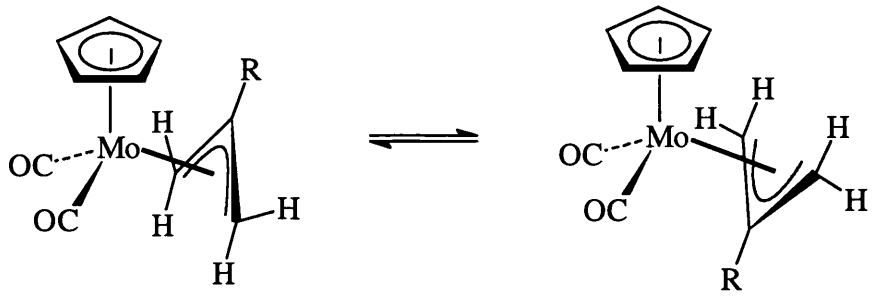

exo-conformer *endo*-conformer

Figure 22

In the ^{1}H NMR spectrum of these allyl complexes, the *syn*- and *anti*-protons of the terminal CH_2 groups are generally non-equivalent. Frequently, however, dynamic behaviour is observed in solution which renders the terminal protons equivalent on the NMR time scale. The most likely mechanism to explain this phenomenon is a rapid π-σ-π conversion, which at the σ-stage allows free rotation around the carbon-carbon and the metal-carbon bonds (Fig. 23). In this manner, *syn*- and *anti*-protons can exchange their position.

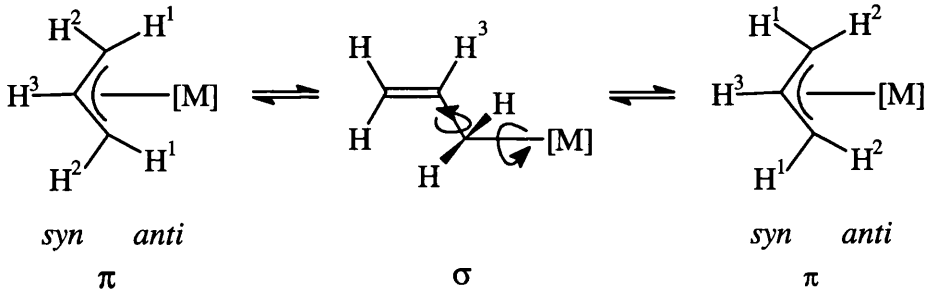

Figure 23

1.4 Elaboration of the Coordinated Organic Ligand by Stoichiometric Nucleophilic Addition

The selective introduction of functionality into a transition metal-coordinated organic compound can be achieved by a variety of methods. In recent years, much attention has been paid to the elaboration of coordinated unsaturated species by

nucleophilic attack. This section describes some of the progress made in this area, with particular regard to the $Fe(CO)_3$- and $CpMo(CO)_2$-derived cationic complexes.

1.4.1 General Factors Governing Nucleophilic Addition to Coordinated Unsaturated Species

Unsaturated hydrocarbons, such as ethylene, butadiene or benzene, do not normally undergo nucleophilic addition or substitution reactions. However, when these molecules are coordinated to electron-withdrawing transition metal centres they can be attacked by a wide range of nucleophiles. Cationic transition metal centres act as stronger electron-withdrawing groups than neutral metal centres, and as a result they are much more susceptible to nucleophilic attack. This enhanced reactivity is a consequence of metal-ligand bonding, which results in a transfer of electron density from the π-system of the hydrocarbon to the positively charged metal centre. Thus, coordination to a metal cation can be compared with nucleophilic attack on unsaturated organic species activated by an electron-withdrawing group (e.g. Michael addition or attack on species such as bromonium ions) (Fig. 24).

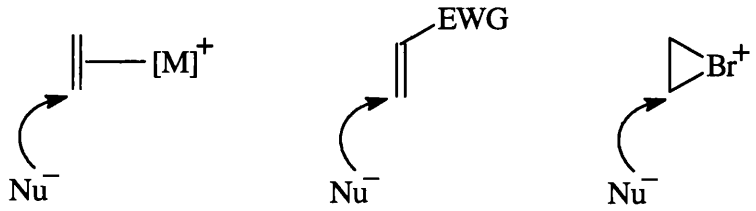

Figure 24

Both the regio- and stereo-selectivity of nucleophilic addition is influenced by coordination to a cationic metal species. The stereoselectivity is determined by whether addition occurs on the *exo*-face (i.e. on the side of the ligand away from the metal), or the *endo*-face of the unsaturated hydrocarbon, whereas the regioselectivity is determined by the preferred site of addition to the polyene. Both factors are strongly influenced by the nature of the transition metal species.

A number of X-ray crystallographic and spectroscopic studies[65,66] has shown that coordinately saturated, 18-electron, transition metal species generally undergo nucleophilic attack on the *exo*-face of the ligand. However, coordinately unsaturated (e.g. 16-electron) species can undergo *exo*- or *endo*-facial attack, depending on the conditions employed. These effects are neatly exemplified by the contrasting reactions of the two allyl species (29) and (30). Hydroxide addition to the coordinately unsaturated species (29) results in exclusive *exo*-facial attack,[34] whereas the 16-electron species (30) will undergo acetate attack on either the *exo*-or *endo*-face of the polyene, depending upon ligand concentration[67] (Fig. 25).

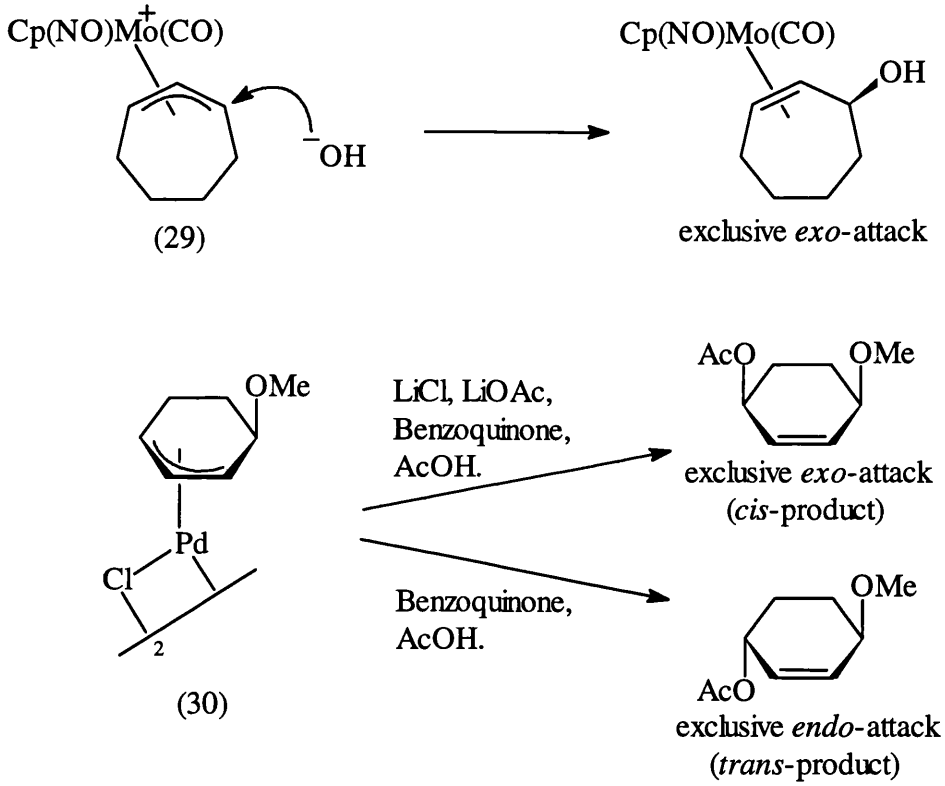

Figure 25

It should be noted, however, that it is not always possible to control the stereochemistry of addition to 16-electron complexes in this way and such reactions can often lead to mixtures of products.[67] Hence, in most processes the use of coordinately saturated species is preferred.

Based upon perturbation-theoretical considerations, Davies, Green and Mingos have proposed three general rules (D.G.M. Rules) which predict the regiochemistry of addition to 18-electron organotransition metal cations for reactions that are kinetically rather than thermodynamically controlled.[68] Applications of theses rules require the ligands to be classified as *even* (η^2, η^4, η^6) or *odd* (η^3, η^5). Furthermore, a distinction between *closed* (cyclic conjugated) and *open* ligands is necessary.

Rule 1: Nucleophilic attack occurs preferentially at *even* coordinated polyenes.

Rule 2: Nucleophilic addition to *open* coordinated polyenes is preferred to addition to *closed* polyene ligands.

Rule 3: For *even*, *open* polyenes, nucleophilic attack always occurs at the terminal carbon atom; for *odd*, *open* polyenyls, attack at the terminal carbon occurs only if the metal species is a strong electron-withdrawing group.

An accurate prediction of the site of nucleophilic attack can be obtained by the sequential application of these rules. This is illustrated in the example shown in Figure 26. Rule 1 eliminates the possibility of attack at the *odd* polyenyl ligand, the η^3-allyl. Rule 2 predicts preferred attack at the *open* η^4-butadiene and Rule 3 predicts attack at the terminal carbon of the ligand.

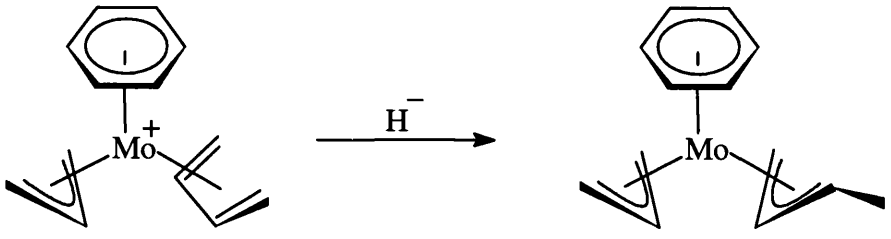

Figure 26

1.4.2 Nucleophilic Addition to $Fe(CO_3)$-Derived η^4-Diene and η^5-Dienyl Complexes

Neutral (η^4-1,3-diene)$Fe(CO)_3$ complexes carry no charge and therefore are generally unreactive towards most nucleophiles. Indeed, these complexes have been

shown to behave as nucleophiles themselves, undergoing a Friedel-Crafts type of acylation reaction[69,70] (Fig. 27).

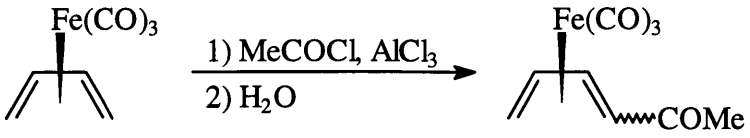

Figure 27

Relatively few cases of nucleophilic addition to (η^4-1,3-diene)$Fe(CO)_3$ complexes have been reported.[8-10] Most of these involve the formation of anionic intermediates that can subsequently be quenched with an electrophilic species. For example, Semmelhack and Herndon have shown that highly reactive carbanions will attack the coordinated diene (31) to give an intermediate anionic π-allyl complex (32)[71] (Fig. 28). This can be further manipulated *via* reaction with trifluoroacetic acid to give the substituted cyclohexenes (33), (34) and (35).

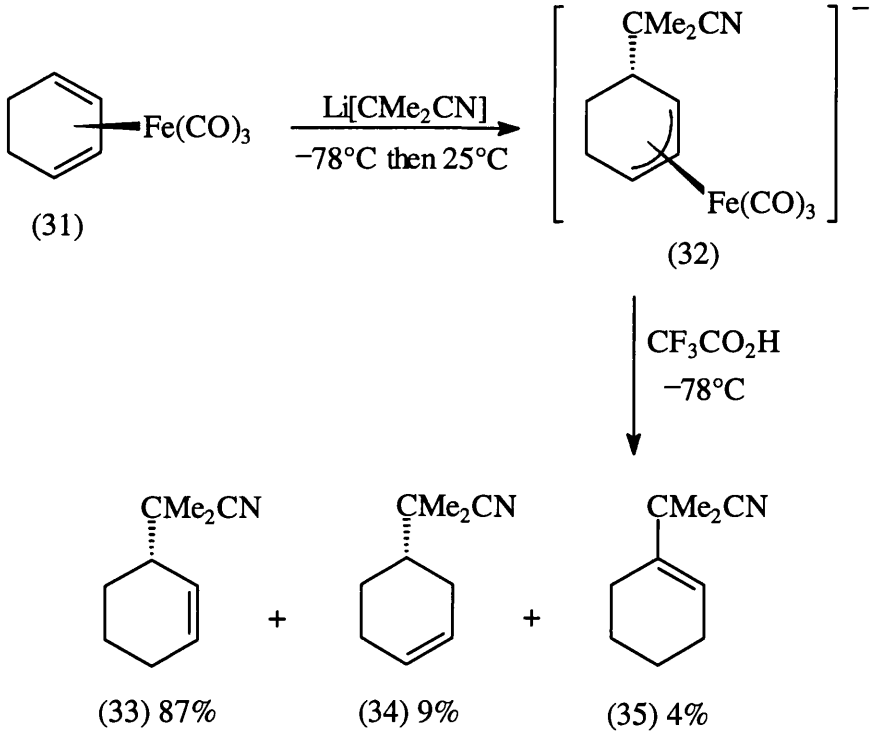

Figure 28

The synthetic applications of nucleophilic attack on (η^4-1,3-diene)$Fe(CO)_3$ complexes are limited. However, conversion of these species to cationic η^5-dienyliron

complexes, which are much more reactive towards nucleophiles, opens up many opportunities for synthesis.

In the acyclic series, the (η^5-dienyl)$Fe(CO)_3$ complexes[10] can be formed in two different forms, *cisoid* (36a) or *transoid* (36b) as shown in Figure 29. Furthermore, for each of these species, depending on the nature of substituents, *cis* and *trans* derivatives can exist.

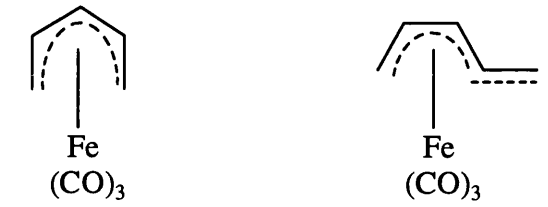

(36a) *cisoid* (36b) *transoid*

Figure 29

The cations are usually prepared by reaction of alcohols such as (37a) or (37b) with strong acids ($HClO_4$ or HBF_4) in acetic anhydride, followed by addition of anhydrous ether. These cations react with various nucleophiles giving adducts of the type (38) or (39) or mixtures of both (Fig. 30).

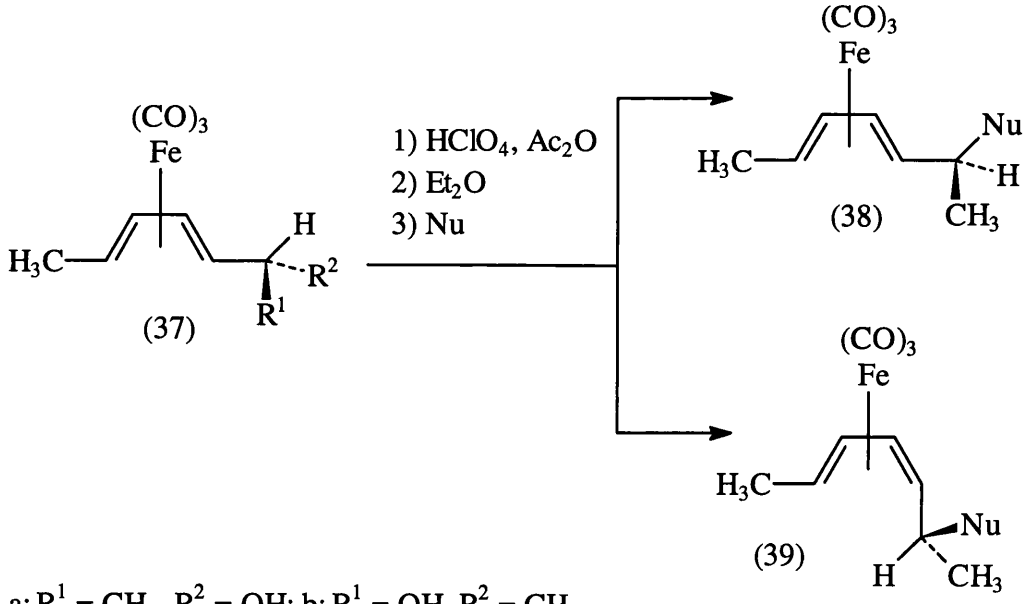

a: $R^1 = CH_3$, $R^2 = OH$; b: $R^1 = OH$, $R^2 = CH_3$.
Nu = ROH, RNH_2, PR_3, R_2Cd, electron-rich aromatics, hydride donors.

Figure 30

It is important to note that in each case the reaction shown in Figure 30 occurs stereoselectively and affords only one diastereoisomer in both type (38) and (39) derivatives. However, the mixtures of products obtained in such acyclic systems gives rise to limitations with this methodology. For this reason the majority of the work on nucleophilic additions to (η^5-dienyl)$Fe(CO)_3$ complexes has been confined to cyclic polyenyl systems, in particular the cyclohexadienyl complexes, owing to their ready availability. The chemistry of cyclohexadienyliron complexes is fairly extensive,[1-3,8] hence the discussion will be restricted to some of the more important features.

The general procedure for the preparation of (η^5-cyclohexadienyl)$Fe(CO)_3$ cations involves hydride abstraction from the corresponding (η^4-1,3-diene) complex[72] (Figure 31). Hydride removal usually occurs on the *exo*-face of the coordinated ligand. When substituted diene complexes are involved,[17,73] the reaction shows interesting and useful regioselectivity, explained in terms of steric and electronic effects of the substituent.

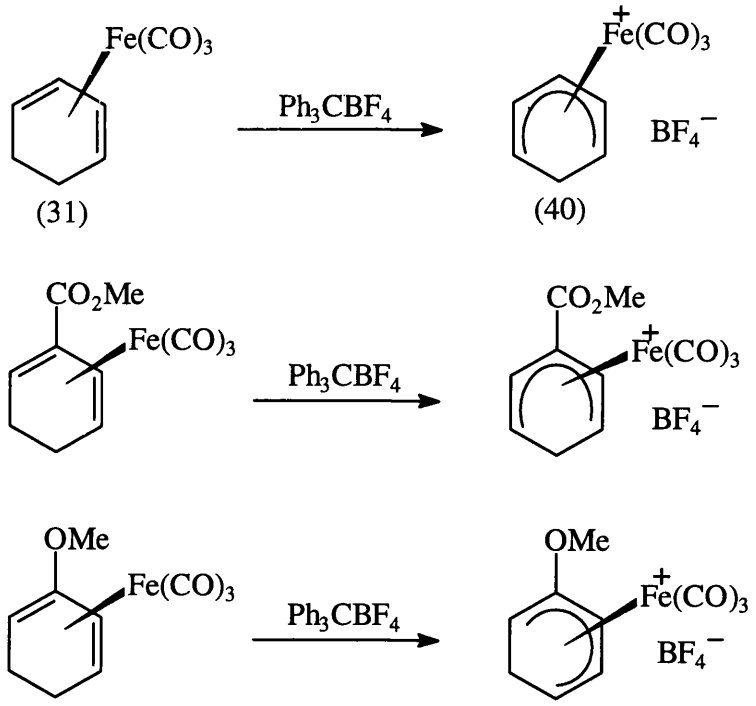

Figure 31

Once formed, these η^5-dienyl cations are highly reactive towards nucleophiles and this serves as an excellent method for the preparation of substituted cyclic diene

complexes. As before, the reaction is both regio- and stereo-selective, nucleophilic addition occurring at the dienyl terminus and *anti* to the $Fe(CO)_3$ group,[17,74-77] the general reaction being shown in Figure 32. The cyclohexadienyl cation (40) can be reacted with a number of different nucleophiles, regenerating the functionalised η^4-diene complex (41).

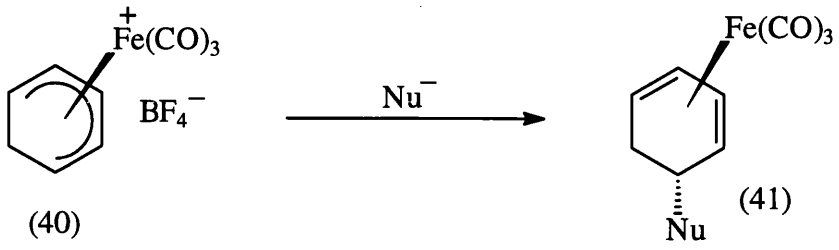

Nu^- = OH^-, CN^-, R_2CuLi, R_2Cd, R_2Zn, R_2NH, PR_3, ArH, enolates, enols, enamines, allylsilanes, enolsilanes.

Figure 32

During the early studies on these complexes, it was found that the use of alkyllithiums and Grignard reagents were problematic, giving poor yields of alkylation product - the major product being the dimeric species (42) (Fig. 33). This problem can be overcome by carrying out the reaction in methylene chloride (instead of ether or tetrahydrofuran, the solvents normally used for such reagents), at low temperature.[78]

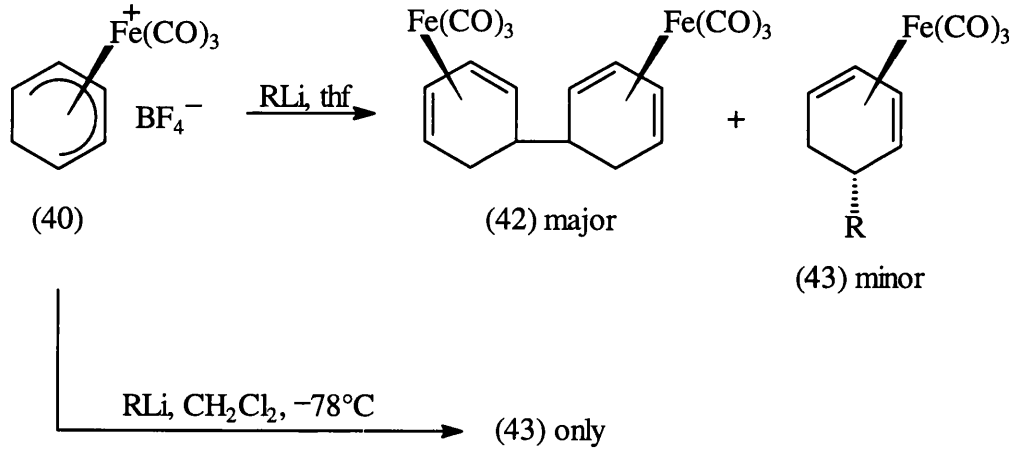

Figure 33

The hydride abstraction/nucleophilic addition process (described above) can be repeated, allowing the stereospecific *cis* introduction of two vicinal (1,2-relationship) substituents on a cyclohexane ring system[79,80] (Fig. 34). This multiple functionalisation strategy has been used extensively by Pearson,[7] with the aim of constructing stereodefined subunits of macrolide antibiotics.[81] The corresponding cycloheptadiene ring system has also been shown to undergo such sequential nucleophilic additions, providing access to *cis*-1,3-difunctionalised products.[80,82,83]

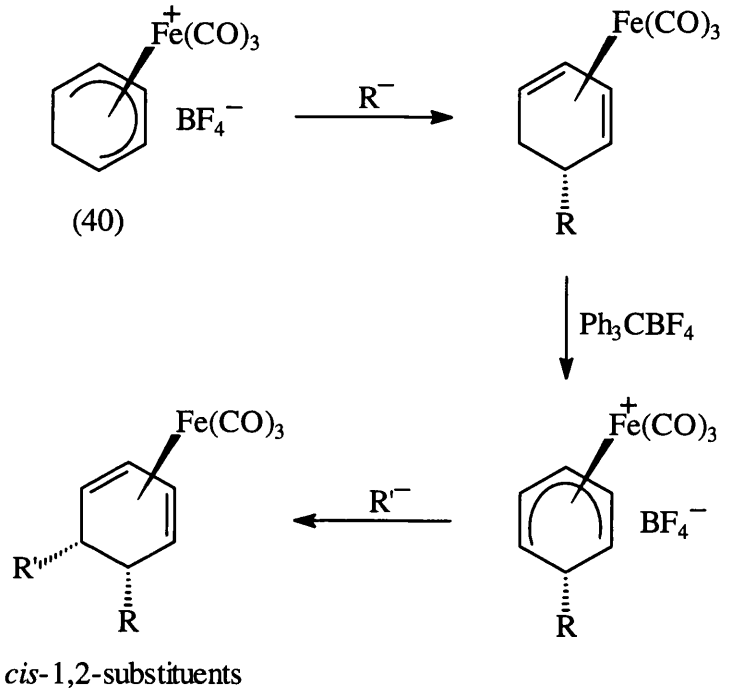

Figure 34

When nucleophilic addition is carried out on substituted cyclohexadienyl complexes, the site of nucleophilic attack is controlled primarily by electronic factors, although *severe* steric hindrance can have an effect. The regioselectivity of addition to some methoxy-substituted cyclohexadienyl complexes is shown in Figure 35.

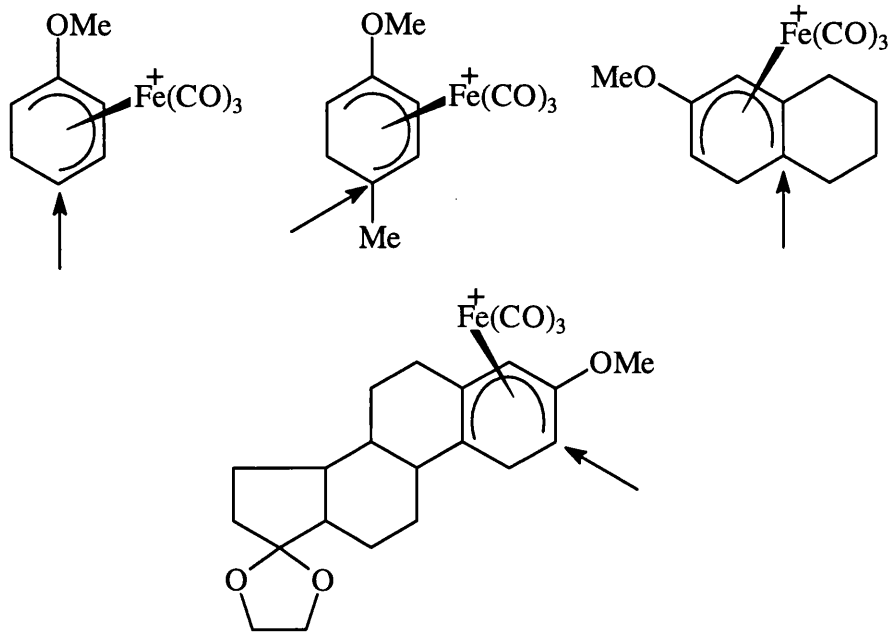

Figure 35

By proper choice of reaction conditions, the regioselectivity of nucleophilic addition to substituted cyclohexadienyl cations can be controlled. This, coupled with the stereocontrol obtained with such reactions, has provided access to multifunctional, stereodefined cyclohexadiene complexes, which have been used in the construction of a variety of important organic molecules. Figure 36 outlines the use of this methodology in the synthesis of the spiro[4,5] compound (44),[84] present in a number of naturally occurring sesquiterpenes.

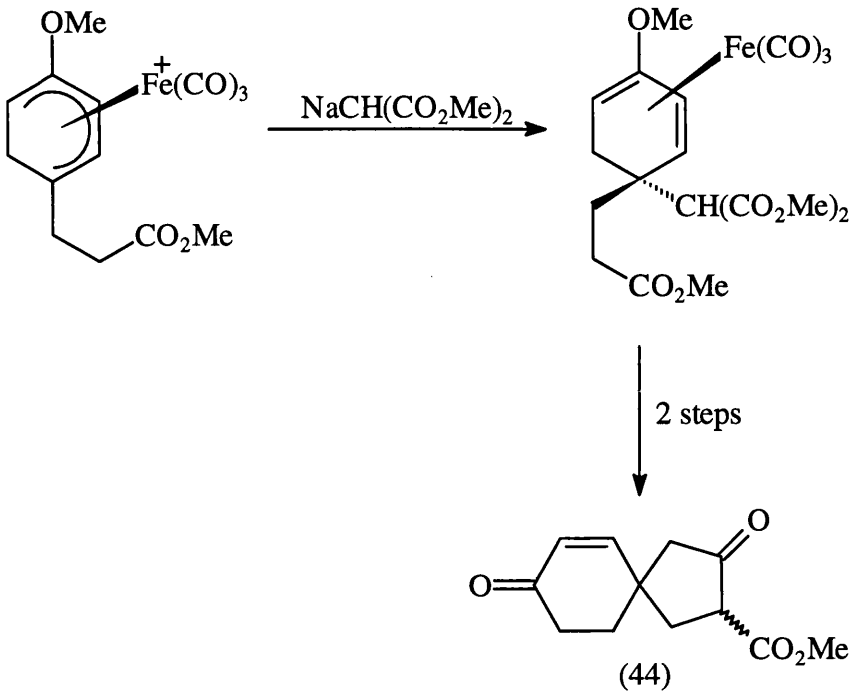

(44)

Figure 36

1.4.3 Nucleophilic Addition to Cationic $CpMo(CO)_2$-Derived η^3-Allyl and η^4-Diene Complexes and Related Species

Cationic η^4-diene complexes of molybdenum are readily prepared and, as expected, are highly reactive towards nucleophilic attack. They generally behave according to the D.G.M. Rules - nucleophilic addition to the diene occurring at a terminal carbon atom, with attack on the face of the ligand away from the metal.

Some of the initial work in this area was done independently by Faller[31,32] and Green[38] on acyclic 1,3-diene complexes. For example, nucleophilic addition of enamines to the η^4-1,3-diene cations (9) or (45) affords the corresponding *anti*-η^3-allyl complexes (46) and (47) respectively (Fig. 37).

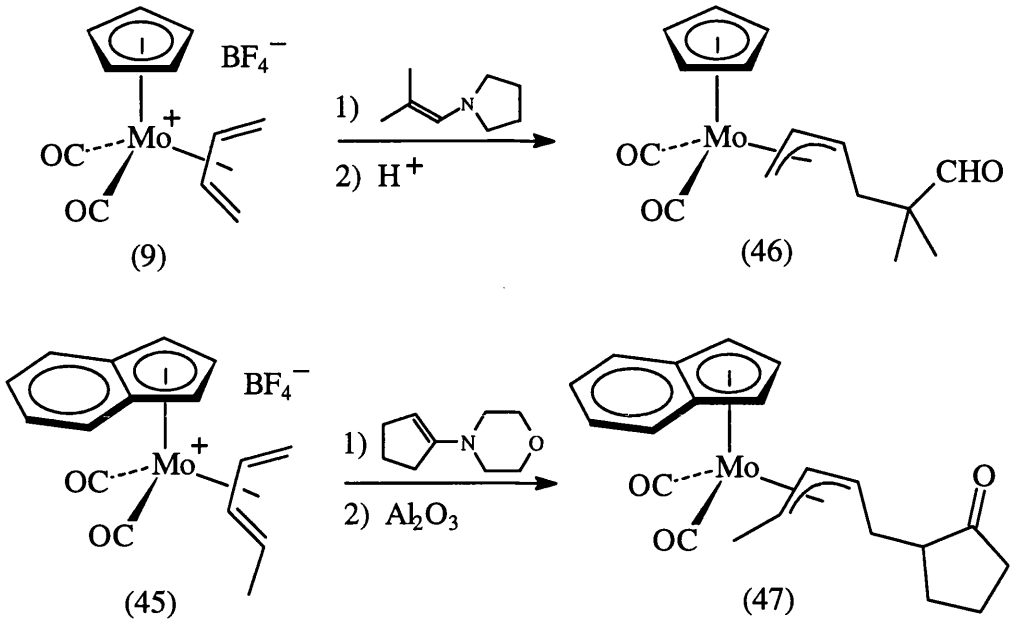

Figure 37

Reactions of this type were soon extended to cyclic systems, which offered increased opportunities for selective nucleophilic attack, owing to their rigid structure. As in the case of the corresponding iron systems, the chemistry of the η^4-cyclohexadiene molybdenum complexes has received much attention.

The reaction of η^4-cyclohexadiene cations with nucleophiles follows a fairly predictable course, giving η^3-allyl complexes. The range of nucleophiles is quite similar to those used with dienyliron systems. For example, the readily prepared η^4-diene cation (7) undergoes nucleophilic attack with Grignard reagents, enamines and enolates to generate the substituted η^3-allyl (48)[29,85] (Fig. 38). These additions take place at the terminus of the diene unit and on the face of the diene away from the metal (selective *exo*-attack).

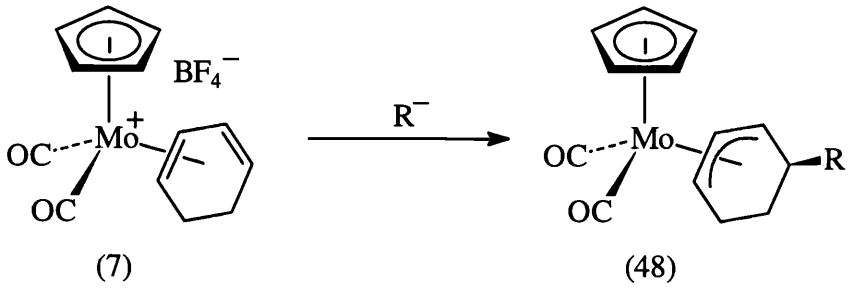

Figure 38

The neutral η^3-allyl species (48) thus formed can be activated towards a second nucleophilic attack by reconversion to an η^4-diene cation.[29,85] This can be achieved *via* hydride abstraction using the bulky trityl cation, which removes a hydride from the *exo*-face of the allyl ligand (Fig. 39). For most species, the steric bulk of the first nucleophile will direct the second attack, resulting in a *cis*-1,3-relationship of substituents.

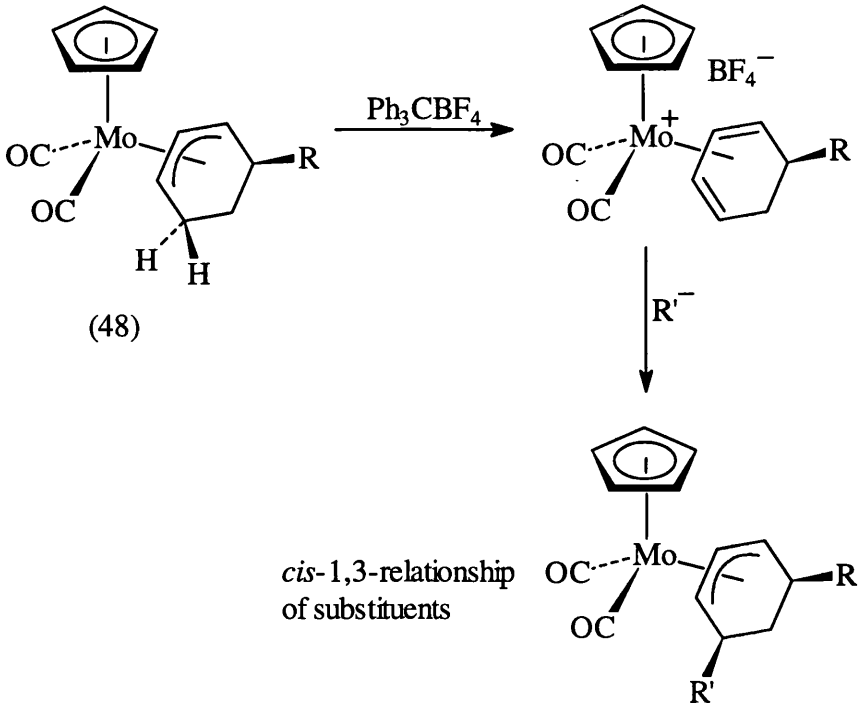

Figure 39

Similar double functionalisations have been carried out on the corresponding cycloheptadiene complexes, resulting in a *cis*-1,4-relationship of substituents.[30,86]

Another method for the reactivation of substituted η^3-allyl complexes toward nucleophilic addition involves nitrosyl exchange. This process was originally established by Faller using acyclic systems,[87,88] and was subsequently extended to the cyclic species.[29] For example, treatment of the neutral, substituted η^3-allyl complex (49) with nitrosonium ion results in the displacement of a carbonyl ligand for a nitrosyl ligand, a 3-electron donor, thus generating a cationic η^3-allyl species (50) (Fig. 40). This species

is susceptible to *exo*-facial nucleophilic attack, addition occurring at the terminus of the allyl species producing the highly stereodefined η^2-complex (51).

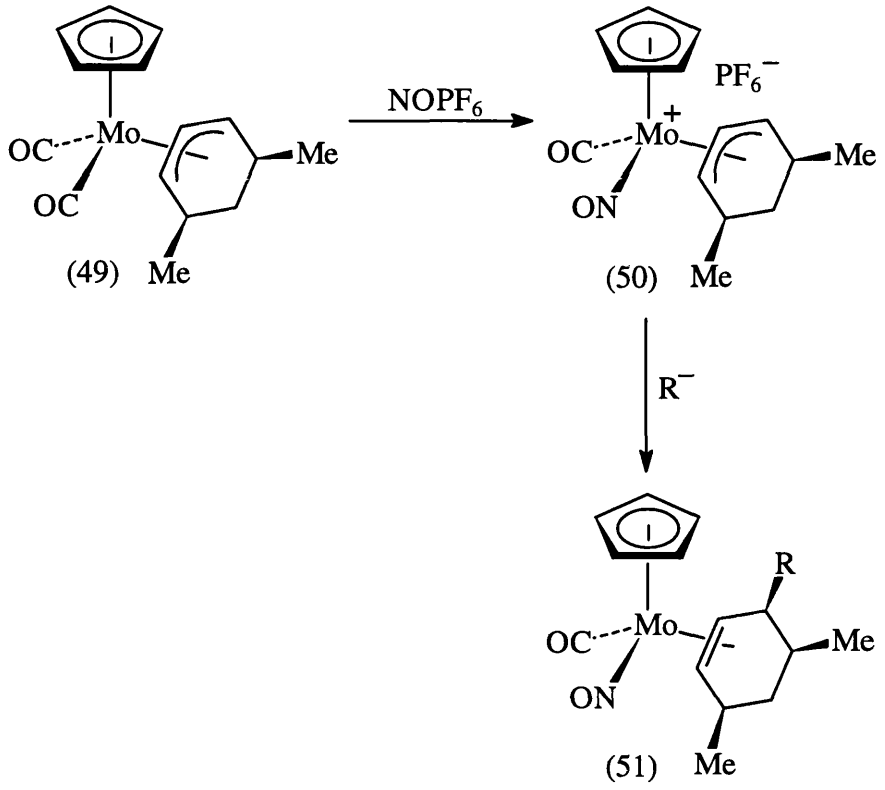

Figure 40

Some interesting regiocontrol has been noted with complexes of substituted cyclohexadienes. For example, complex (17) gives (52) on treatment with methylmagnesium iodide[39] (Fig. 41). This provides an alternative method for preparing substituted cyclohexadiene complexes, since (52) is readily converted to (18) on treatment with trityl cation.

Nucleophilic addition to the 1-substituted-1,3-diene (18) gives (53) as expected (Fig. 42), but hydride abstraction from (53) is unsuccessful using the trityl cation. However, treatment with DDQ in the presence of tetrafluoroboric acid does give the η^4-diene complex e.g. (54).[39]

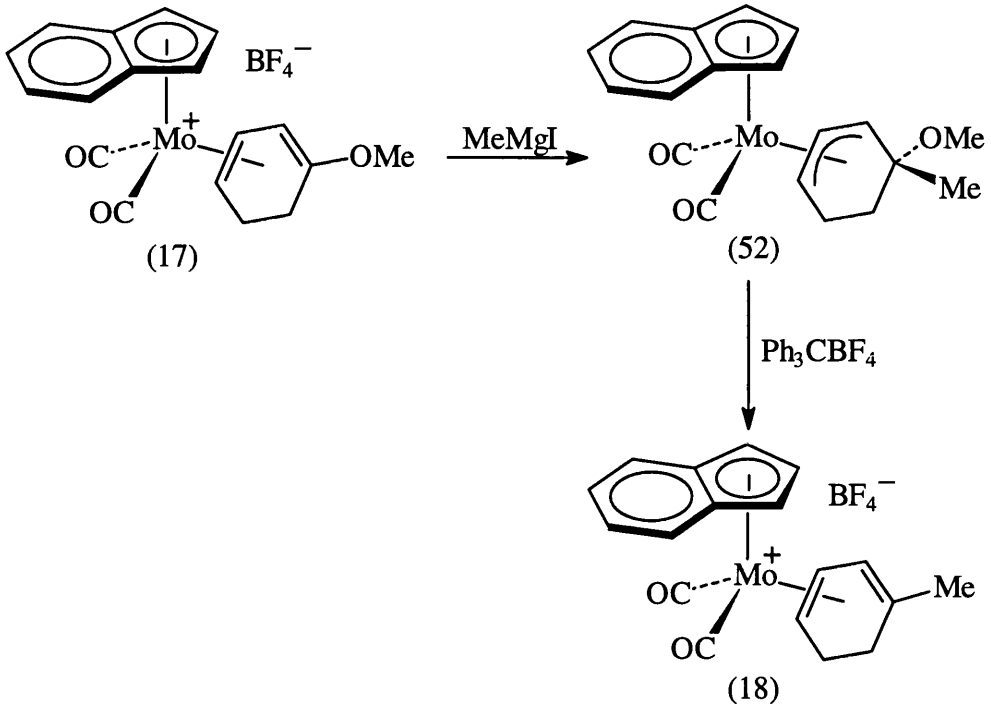

Figure 41

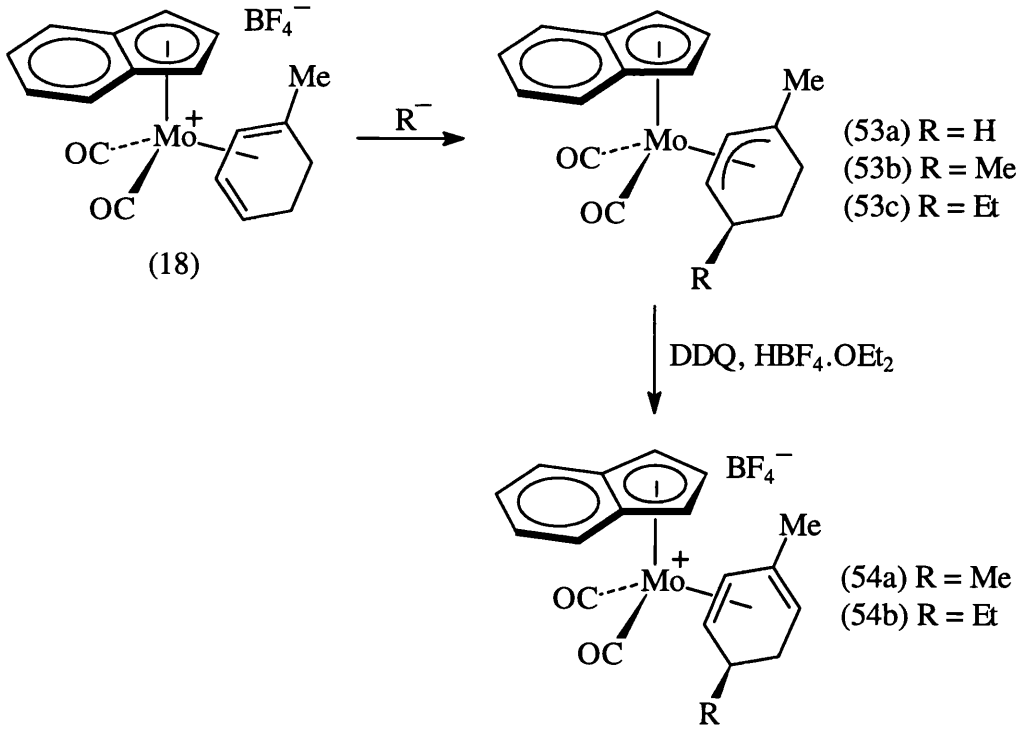

Figure 42

Interestingly, nucleophilic addition to the 2-substituted-1,3-diene (55) proceeds with complete regioselectivity to give (56)[39] (Fig. 43).

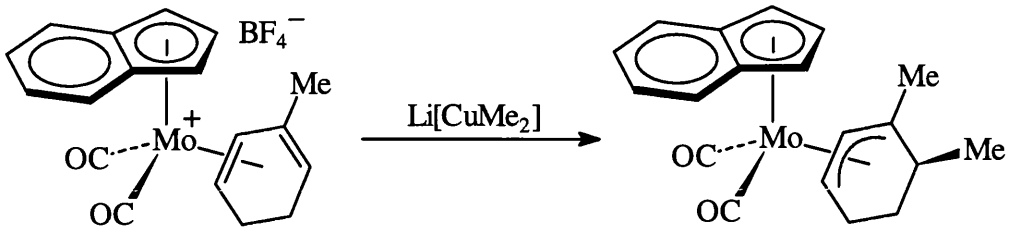

(55) (56)

Figure 43

1.5 Methods of Decomplexation

It has been shown that stoichiometric nucleophilic additions to transition metal coordinated organic ligands display a high degree of regio- and stereo-selectivity, consequently these reactions are potentially very useful in organic synthesis. Ultimately though, that potential can only be realised if there exists a method for the removal of the stereodefined product from the metal, without loss of stereochemical purity. This section reviews the main procedures available for the decomplexation of the organic compound from $Fe(CO)_3$- and $CpMo(CO)_2$-derived complexes.

1.5.1 Decomplexation from $Fe(CO)_3$-Derived Complexes

Synthetic routes requiring the use of $Fe(CO)_3$-derived η^4-1,3-diene and η^5-dienyl complexes invariably involve decomplexation from the diene species. This is simply because the η^4-1,3-diene ligand corresponds to the more stable organic entity and is readily removed without loss of stereochemistry.

A number of methods for the release of dienes from (η^4-1,3-diene)$Fe(CO)_3$ complexes have been reported (generally oxidative) and the particular method to be used depends upon the functionality present in the molecule. Oxidative decomplexation

has been reported using copper(II) chloride in ethanol,[89] ferric chloride in ethanol/hydrochloric acid,[90,91] and chromium(VI) oxidising agents (e.g. Collins' reagent)[92] (Fig. 44).

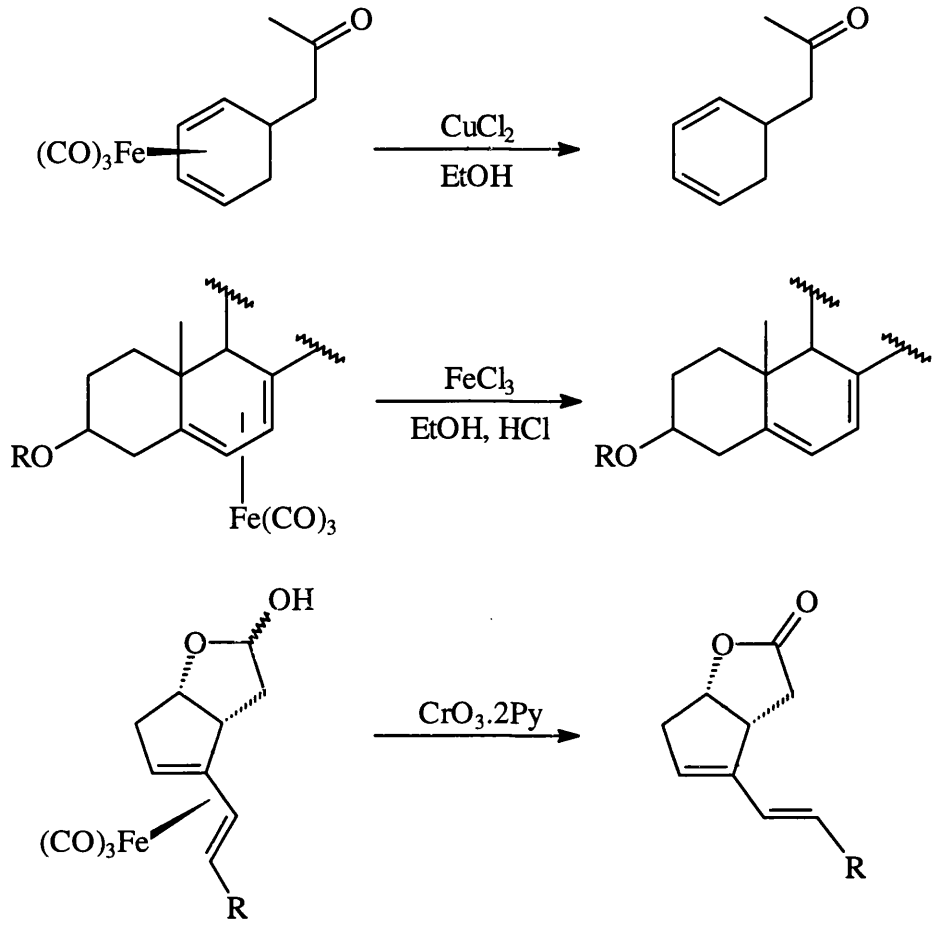

Figure 44

Ceric ammonium nitrate has been used extensively for the decomplexation of a variety of organometallics.[20,91] An example showing the removal of the hydroxy-cycloheptadiene compound (57) is illustrated in Figure 45.

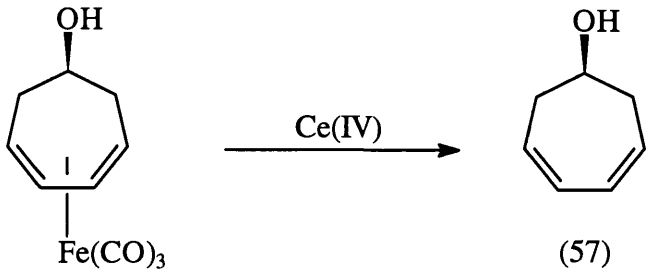

Figure 45

Trimethylamine-N-oxide has also found widespread application for the demetallation of (η^4-1,3-diene)Fe(CO)$_3$ complexes.[93-95] This reagent is often employed when traces of acid are to be avoided; it should be noted that most of the transition metal oxidising agents lead to acidic reaction conditions. For example, treatment of complex (58) with Me_3NO liberates the dienol ether (59) (Fig. 46). Species such as (59) are unstable towards acidic conditions and are readily hydrolysed to give enones. Hence, if this decomplexation had been carried out using $CuCl_2$/EtOH instead, the enone (60) would have been formed directly.

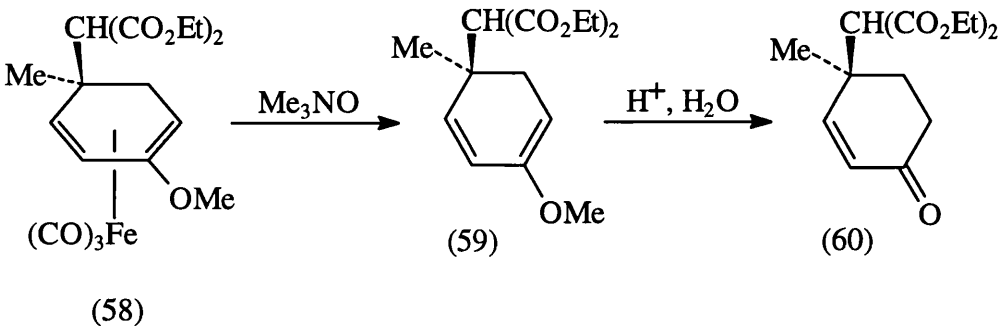

Figure 46

1.5.2 Decomplexation from CpMo(CO)$_2$-Derived Complexes and Related Species

In a similar manner to the iron systems, removal of the diene ligand from (η^4-1,3-diene)Mo(CO)$_2$L (L = Cp, Cp* or indenyl) complexes is a relatively straightforward procedure, and can be readily accomplished using oxidative methods. For example, treatment of the acyclic diene (61) with Me_3NO liberates (*E*,*E*)-undeca-1,3,5-triene (62),[39] a component of the Hawaiian seaweed *Dictyopteris plagiogramma* (Fig. 47).

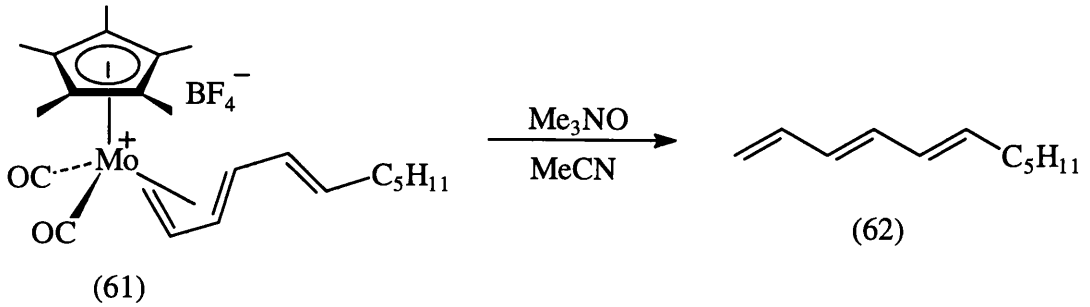

Figure 47

The corresponding η^5-indenyl cations have been shown to undergo decomplexation under milder conditions. Hence, (54b) reacts with CO to yield the free 1,3-diene (63)[39] (Fig. 48). The enhanced reactivity towards ligand substitution can be explained in terms of an η^5- to η^3-slippage[96] of the η^5-indenyl ligand.

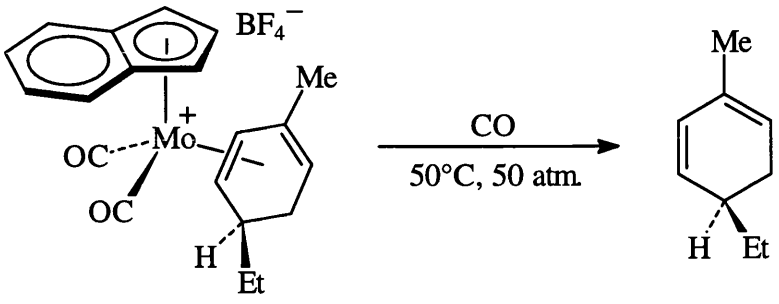

(54b) (63)

Figure 48

Displacement of the organic fragment from a molybdenum η^3-allyl species is slightly more complicated, since an η^3-allyl ligand does not correspond to a potentially stable organic entity. Therefore, any attempt to demetallate such a species will inevitably involve further functionalisation. The method of nitrosyl exchange followed by nucleophilic attack and oxidative decomplexation of the resultant η^2-olefin complex,[29] offers a solution to this problem. This is illustrated in Figure 49 (overleaf), where exposure of (64) to air effects demetallation, resulting in the formation of the stereochemically defined cyclohexene (65).

Recent research has focused on the development of new methods for regio- and stereo-controlled functionalisation/demetallation of η^3-allyl complexes. Pearson has devised an interesting intramolecular nucleophilic attack procedure that gives excellent regiocontrol.[85] Treatment of the carboxylic acid derivative (66) with an excess of iodine results in the formation of the cyclohexene lactone (69) (Fig. 50). This reaction is thought to proceed *via* the intermediates (67) and (68), with the presence of excess iodine causing an oxidative demetallation.

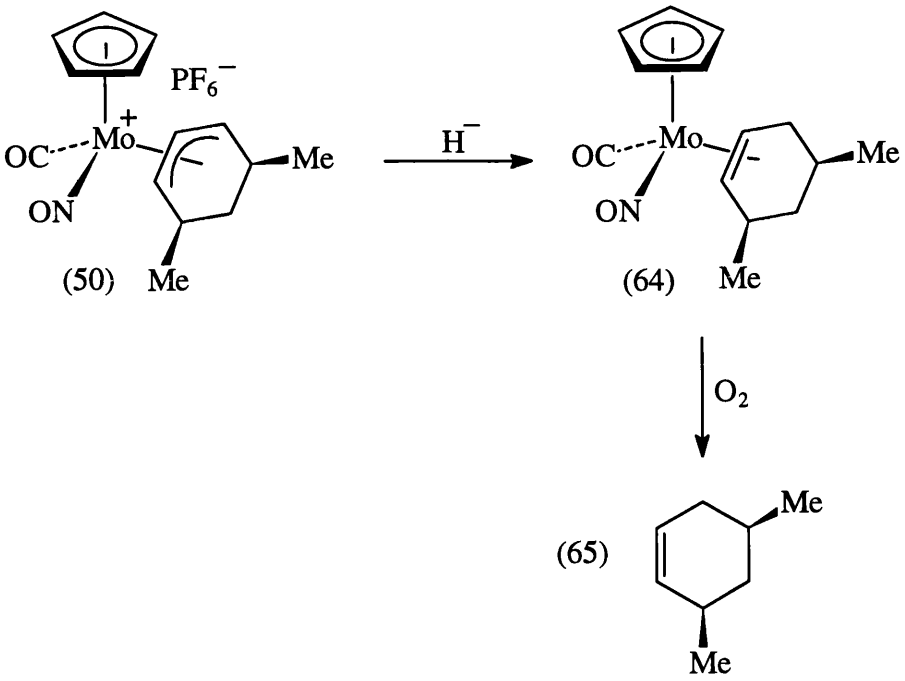

Figure 49

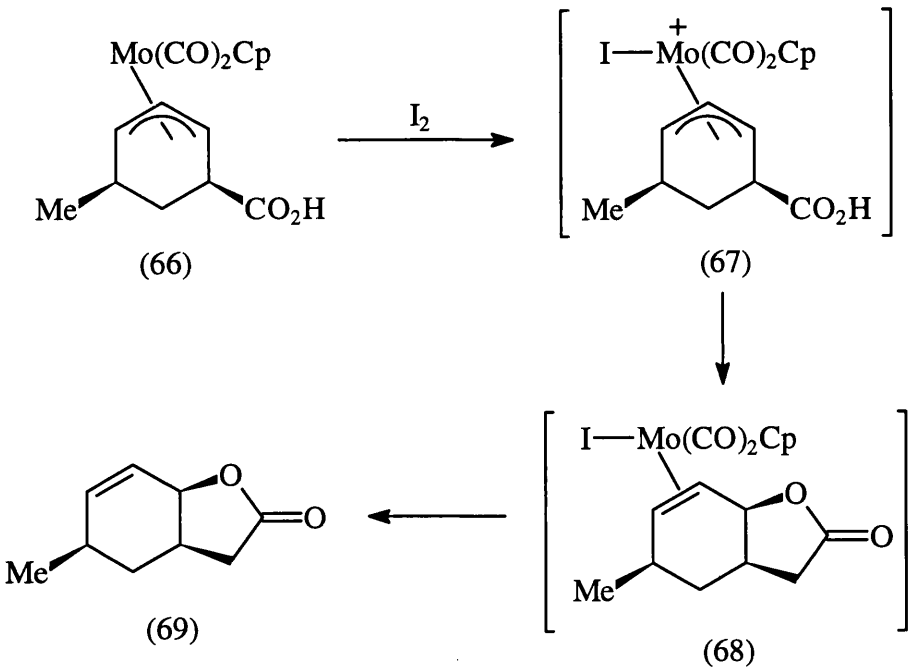

Figure 50

A similar process has been used by Liebeskind for the formation of *cis*-4,5-disubstituted-2-cyclopentenones.[33] For example, low temperature treatment of (70) with $IOCOCF_3$ results in attack of I^+ at molybdenum to give (71), which undergoes *anti* nucleophilic attack of CF_3COO^- to give the stereodefined product (72) (Fig. 51).

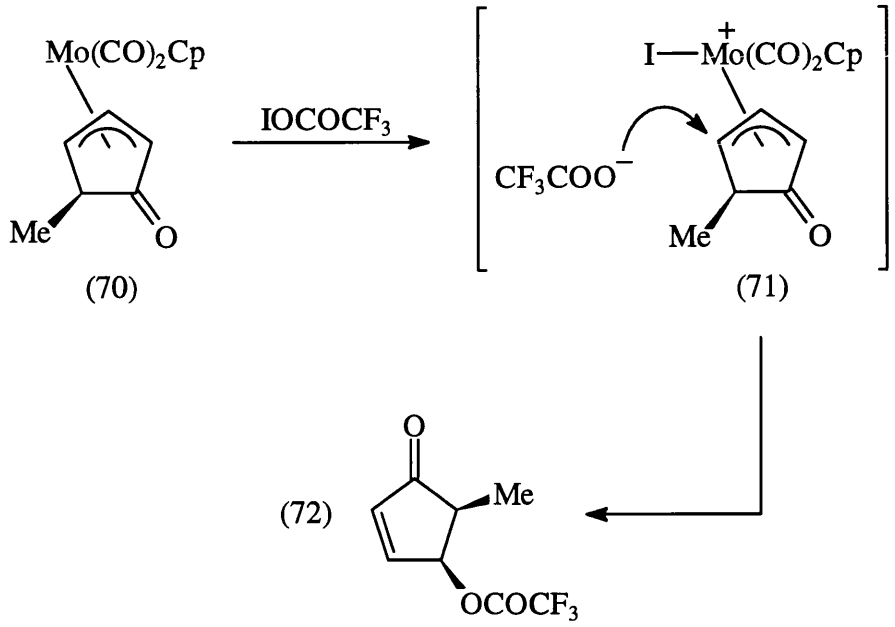

Figure 51

Finally, Faller has developed a new method of allyl elaboration/decomplexation involving electrophilic attack on modified η^3-allyl species. An example of this is illustrated in Figure 52. Treatment of the cationic η^3-allyl nitrosyl molybdenum species (73) with halide ions results in displacement of CO and the generation of a neutral halonitrosyl complex (74).[97] This species undergoes electrophilic attack by aldehydes, proceeding *via* coordination of the aldehyde oxygen to the metal centre, and concomitant η^3- to η^1-allyl conversion. Breakdown of the intermediate complex (75) results in the stereospecific formation of the homoallylic alcohol (76). In contrast to the nucleophilic additions described previously, addition occurs exclusively on the *endo*-face of the allyl moiety, as shown overleaf.

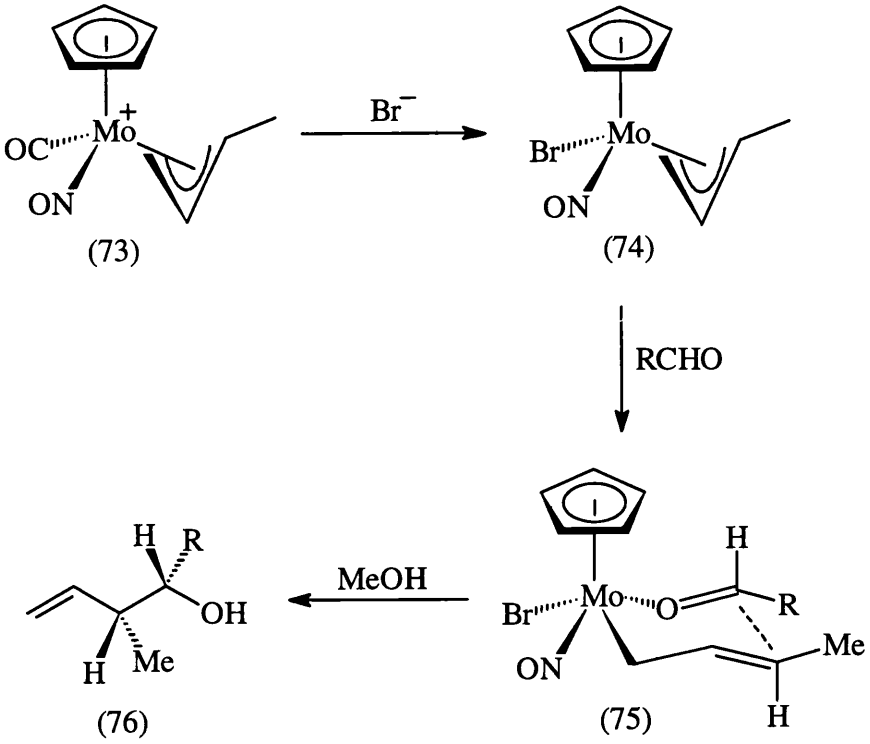

Figure 52

1.6 Extension to Chiral and Optically Active Systems

In the previous sections, the reactions of the iron and molybdenum complexes have been discussed only in terms of relative stereochemistry. It should be noted, however, that many of these complexes are chiral[98,99] (or have the potential to become chiral), existing as racemic mixtures. By extending the regio- and stereo-controlled chemistry associated with these species to enantiomerically pure systems, the synthesis of optically active compounds can be accomplished. This has important ramifications in organic chemistry, since many optically active molecules have significant biological properties, which makes them desirable target structures.

Several processes have been developed for the preparation of organotransition metal complexes in optically pure form. Early methods involved classical resolution of a racemic complex mixture. This is readily achieved by incorporating an asymmetric

functionality into a coordinated ligand and separating the resultant diastereoisomers. For example, Faller has made extensive use of the neomenthylcyclopentadienyl ligand for the resolution of allylmolybdenum complexes.[100,101] Access to optically pure (η^4-1,3-diene)$Fe(CO)_3$ is also possible using classical methods. Similarly, Green and co-workers have been able to resolve the keto-allyl complex (77) into both its enantiomers[103] *via* the sequence illustrated in Figure 53.

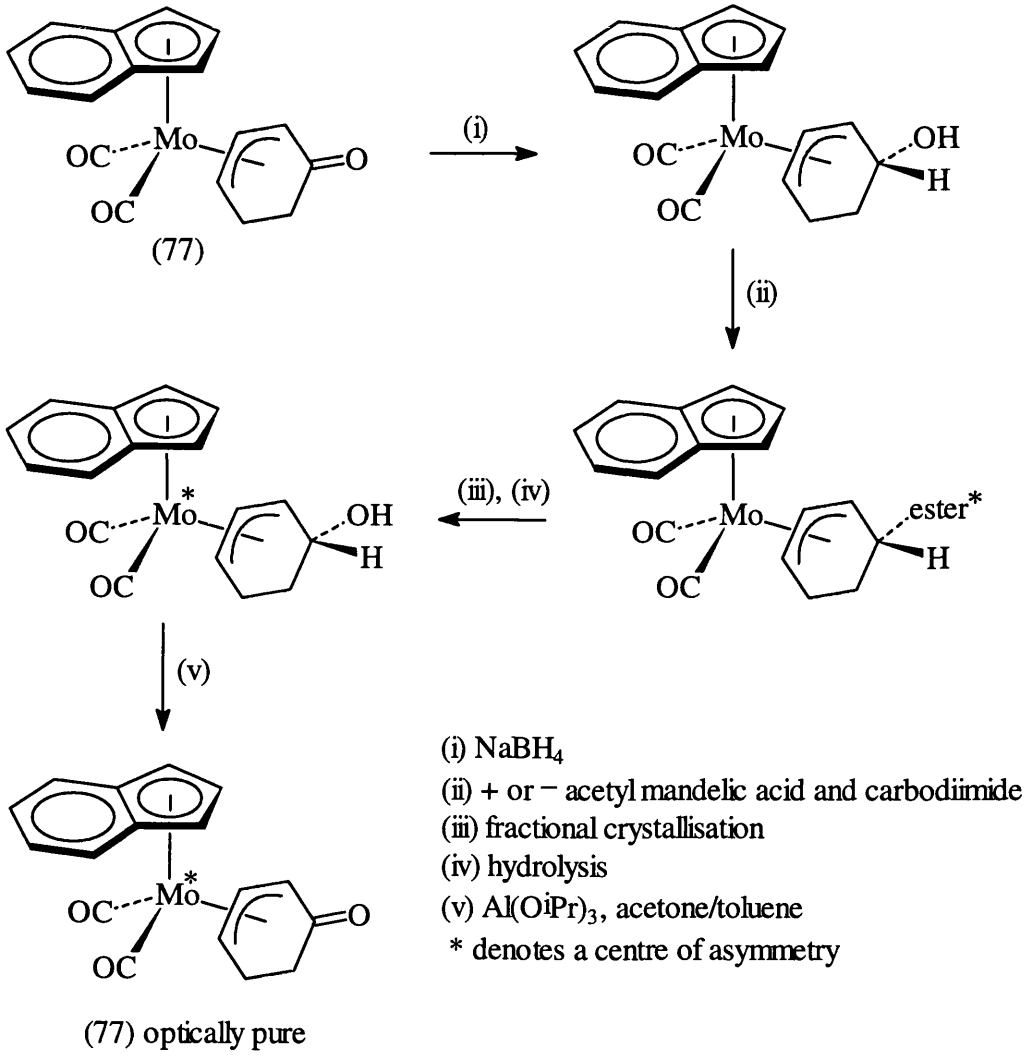

Figure 53

Since resolution is unattractive for applications in contemporary organic synthesis, other approaches towards enantioselectivity have been developed. Pearson has established a method of chiral recognition during the addition of optically active nucleophiles to diene-molybdenum and dienyliron complexes.[104-107] For example,

addition of an enantiomerically pure sulphoximinyl ester derived enolate to (7) gives, after desulphonylation, the functionalised product (78) in high enantiomeric excess (e.e.) (Fig. 54). Lower, but still significant asymmetric induction, was observed using the corresponding $Fe(CO)_3$ system.

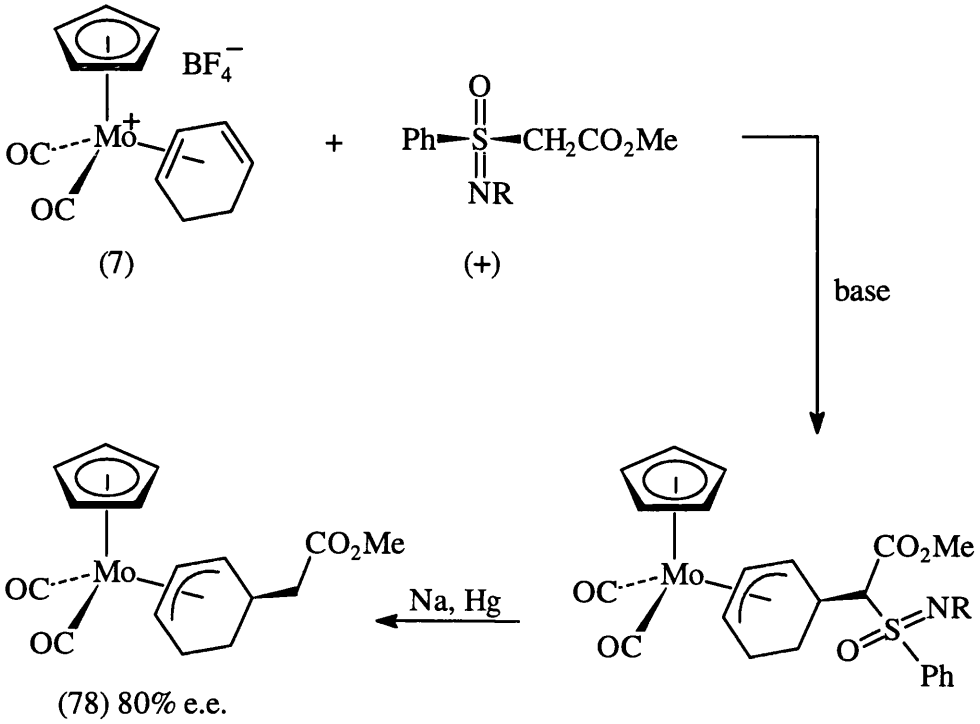

Figure 54. R = Ts, Me, TBDMS or DMTS.

A more direct method for obtaining homochiral products involves the introduction of enantioselectivity during the complexation of a substituted organic ligand. Stevenson's group have shown that an allylic ether group will direct the stereochemistry of complexation of a neighbouring diene.[108] This is especially useful for preparing optically pure cyclohexadiene complexes from readily available, optically pure cyclohexadiendiols (Fig. 55).

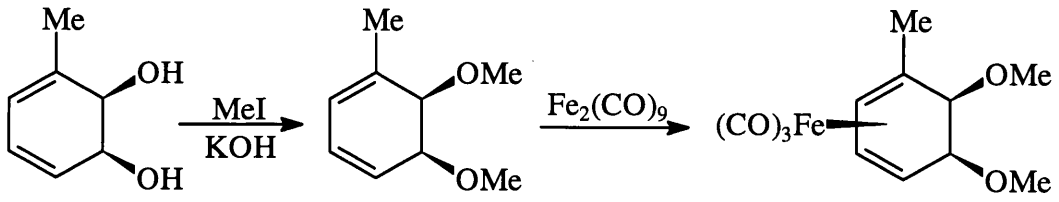

Figure 55

A similar procedure has been developed by Liebeskind during a study on homochiral synthesis using heterocyclic molybdenum complexes.[35,109] The allylic bromide (79) is readily available in optically active form from D- or L-arabinose, and can be converted enantiospecifically to the corresponding allyl complex (80).

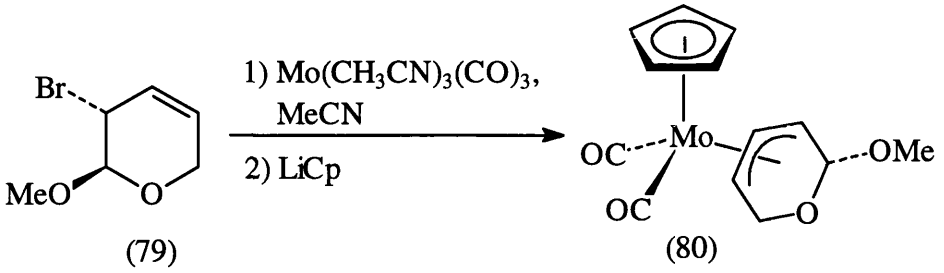

(79) (80)

Figure 56

In summary, the iron and molybdenum systems provide complimentary modes of regio- and stereo-control, offering a unique approach to the elaboration of complex organic compounds. The ability to introduce enantioselectivity into these systems utilises the full potential of this methodology, providing chemists with a useful route to the synthesis of optically active materials.

2. RESULTS AND DISCUSSION

2.1 Synthesis and Reactivity of 4-Oxo-η^3-cyclohexenyl Molybdenum Complexes

2.1.1 Introduction

During the course of an investigation into the chemistry of cationic molybdenum η^4-1,3-diene complexes, Green and co-workers found that reaction of 1-trimethylsilyloxycyclohexa-1,3-diene with the labile bis(acetonitrile) η^5-indenyl cation *cis*-$[Mo(NCMe)_2(CO)_2(\eta^5\text{-}C_9H_7)][BF_4]$ (15) led to the formation of the crystallographically identified 4-oxo-η^3-cyclohexenyl complex $[Mo(\eta^3\text{-}C_6H_7)(CO)_2(\eta^5\text{-}C_9H_7)]$ (77)[40] (Fig. 57). This transformation is believed to proceed *via* a fluoride-anion-induced desilylation of the initially formed diene cation (81).

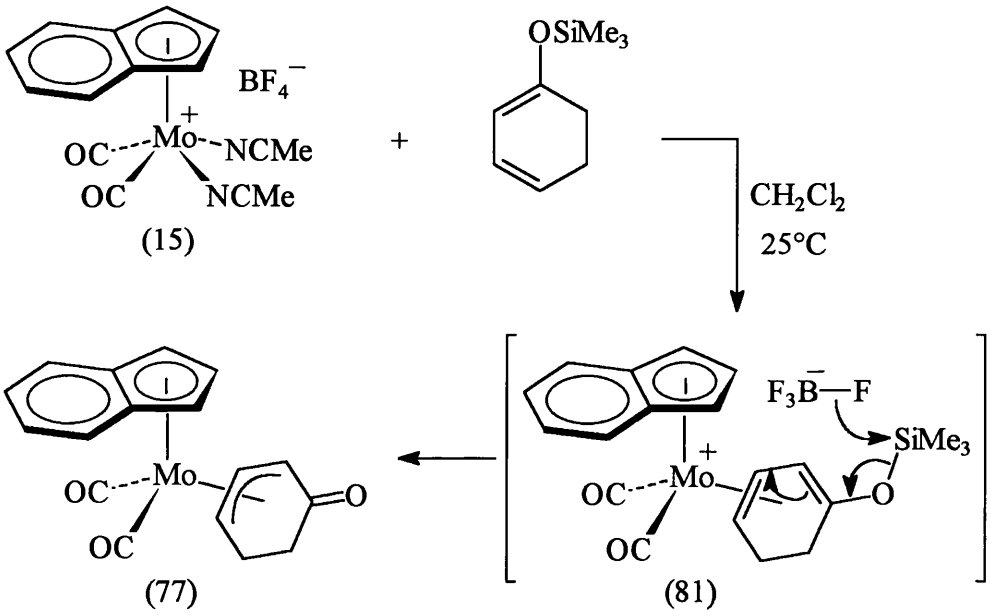

Figure 57

Access to (77) also proved possible by means of a demethylation reaction on the 1-methoxycyclohexa-1,3-diene cation (17) using strong bases such as sodium methoxide. This is illustrated in Figure 58, together with a summary of the chemistry associated with (77), which is dominated by organic transformations of the ketonic carbonyl group.

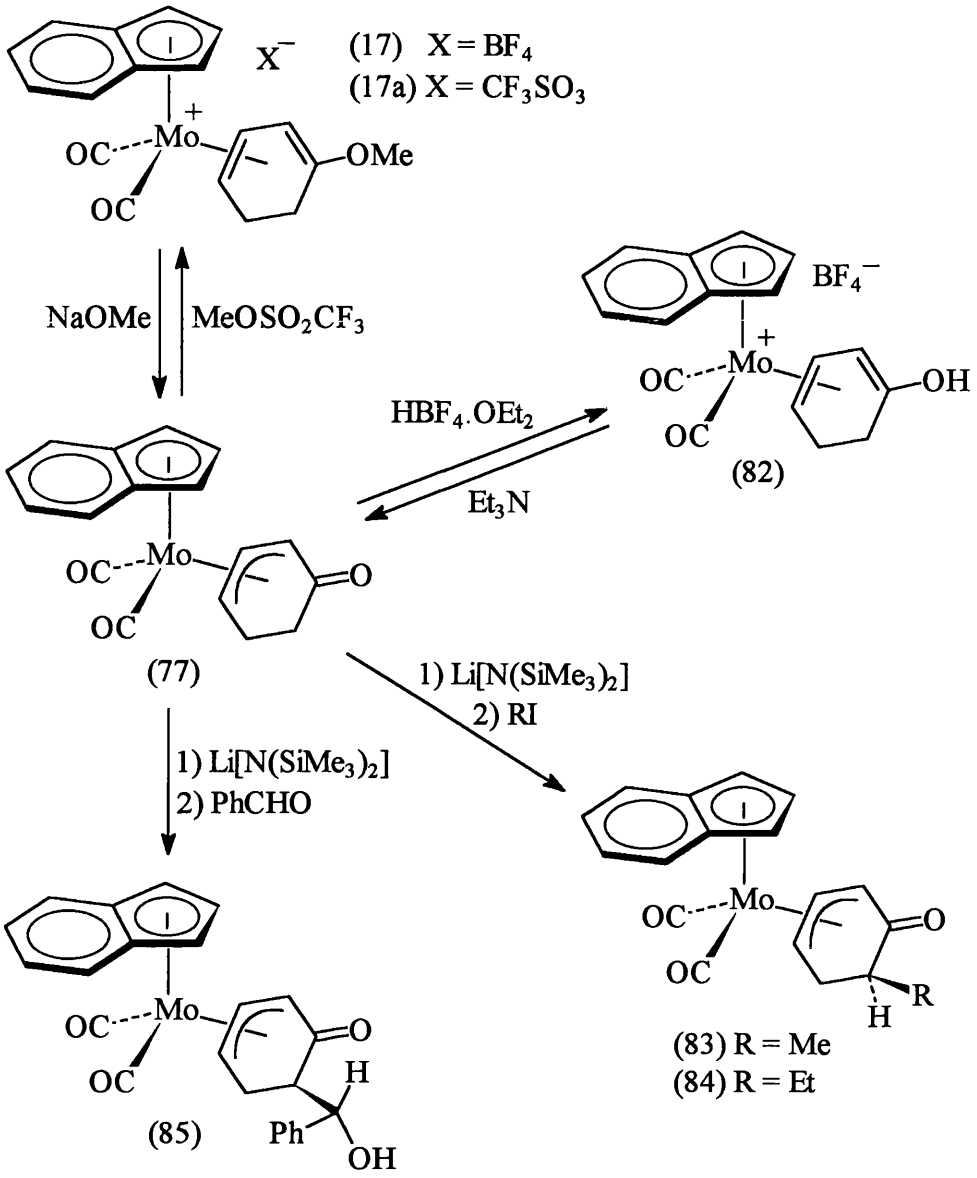

Figure 58

It is important to note that the products (83), (84) and (85) are obtained with complete diastereofacial selectivity due to the presence of the sterically large $Mo(CO)_2(\eta^5\text{-}C_9H_7)$ fragment, which effectively shields one face of the six-membered ring, resulting in selective *exo*-facial attack by electrophiles. The oxoallyl complex (77) has recently been prepared in optically active form using classical methods[103] (see Section 1.6). Thus, this methodology can be extended to give enantioselective reactions, allowing the products

to be formed with defined stereochemistry, thereby facilitating the construction of a variety of asymmetric organic molecules based on a six-membered ring.

The analogous 4-oxo-η^3-cyclohexenyl complexes of iron (86)[110] and ruthenium (87)[57] have also been synthesised within our group using 1-trimethylsilyloxycyclohexa-1,3-diene. However, from general synthetic considerations and in terms of potential applications, the molybdenum system appears to be the most promising. Further evidence of this is provided by reports from other researchers on the preparation and reactivity of related molybdenum complexes. In particular, Pearson has established the use of 5-oxoallyls contained within six-[7,111,112] seven-[7] and eight-membered[113] rings [(88), (89) and (90) respectively], whilst Liebeskind has recently developed the chemistry of the five-membered ring species (91)[33,114] (Fig. 59).

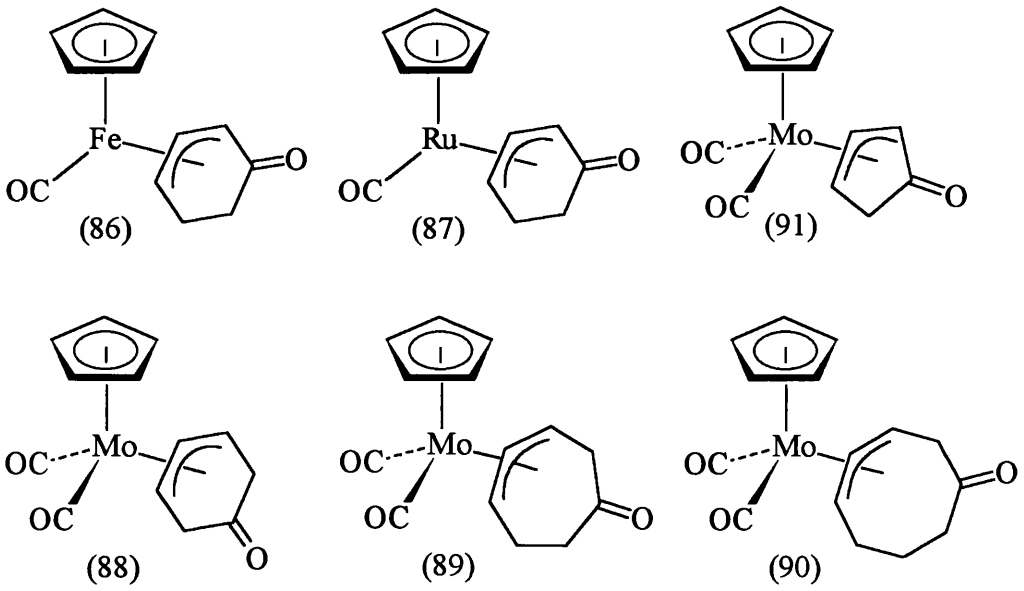

Figure 59

Given the importance of such systems for use in the stereocontrolled synthesis of complex organic molecules, we wanted to expand our working knowledge of the 4-oxo-η^3-cyclohexenyl molybdenum species. As a direct comparison to the indenyl complexes, it was decided to investigate the chemistry of the corresponding pentamethylcyclopentadienyl system.

2.1.2 Synthesis of $[Mo(\eta^3\text{-}C_6H_7O)(CO)_2(\eta^5\text{-}C_5Me_5)]$ (92)

The bis(acetonitrile) η^5-pentamethylcyclopentadiene cation *cis*-$[Mo(NCMe)_2(CO)_2(\eta^5\text{-}C_9H_7)][BF_4]$ (16) was readily prepared, starting from molybdenum hexacarbonyl, using an established procedure.[44] When a dichloromethane solution of (16) was heated to reflux in the presence of 1-trimethylsilyloxycyclohexa-1,3-diene, a smooth reaction ensued and a good yield (82%) of yellow *crystals* was isolated following chromatography on alumina. This product analysed for $[Mo(C_6H_7O)(CO)_2(C_5Me_5)]$ in accordance with the FAB mass spectrum and analytical data. Examination and comparison of the IR and NMR spectroscopic data with that of (77)[40] confirmed the structure as the 4-oxo-η^3-allyl complex (92) (Fig. 60).

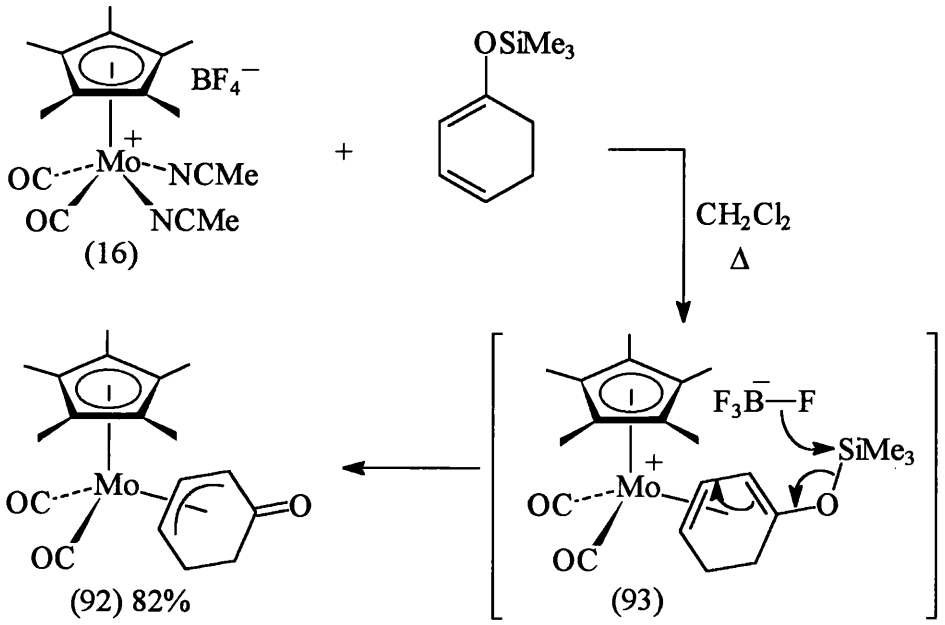

Figure 60

The IR spectrum displayed two distinct bands at 1952 and 1875 cm^{-1}, assignable to the metal coordinated carbonyls, along with a third band at 1630 cm^{-1} due to the ketonic carbonyl functionality. In addition to resonances attributed to the CO and η^5-C_5Me_5 ligands, the ^{13}C-{^1H} NMR spectrum showed resonances assignable to three metal coordinated allyl carbon atoms (74.8, 59.7 and 59.6 ppm), two methylene carbons (30.6 and 22.1 ppm) and a ketonic carbonyl at 197.7 ppm. The corresponding resonances

were also present in the ^{1}H NMR spectrum. Presumably (92) is formed by initial coordination of the diene to the metal to generate an η^4-diene cation (93), which is then desilylated by the BF_4^- counterion to afford the isolated complex.

The expected similarities in the spectroscopic data for (92) and the η^5-indenyl complex (77) imply that they exhibit the same structural characteristics. Complex (77) was the subject of a single crystal X-ray diffraction study[40,115] and its molecular structure is included here for comparative purposes (Fig. 62, overleaf). It was found that the η^3-cyclohexenyl ring is coordinated to molybdenum exclusively in the *exo*-configuration (the reciprocal *endo*-configuration is not observed as this would result in unfavourable steric interactions between the indenyl ligand and the C_6-ring). As with the majority of Mo(II) *exo*-η^3-allyls, the inner carbon atom of the allyl moiety is closer to the metal than that of the outer carbons.[29] The C_6-ring adopts a very flattened chair conformation where the methylene hydrogens bonded to C(3) and C(4) are nearly eclipsed. [N.B. This is in contrast to the previously mentioned iron and ruthenium complexes, (86) and (87), in which the C_6-ring adopts a flattened boat conformation]. The ring flattening is thought to occur as a result of conjugation between the η^3-allyl and the ketonic carbonyl group, which is reflected in the following bond distances: C(1)-C(2) 1.456(11) Å and C(2)-O(1) 1.211(12) Å. The observed C(1)-C(2) bond distance is shorter than a normal carbon-carbon single bond [*ca.* 1.53(1) Å],[116] whilst the C(2)-O(1) bond distance is slightly longer than that expected for a normal ketonic bond, but shorter that that considered as a zwitterion [*ca.* 1.26(1) Å].[116] This suggests some contribution from the resonance form shown in Figure 61.

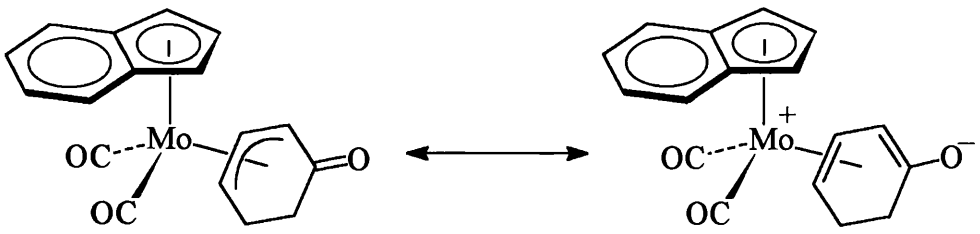

(77)

Figure 61

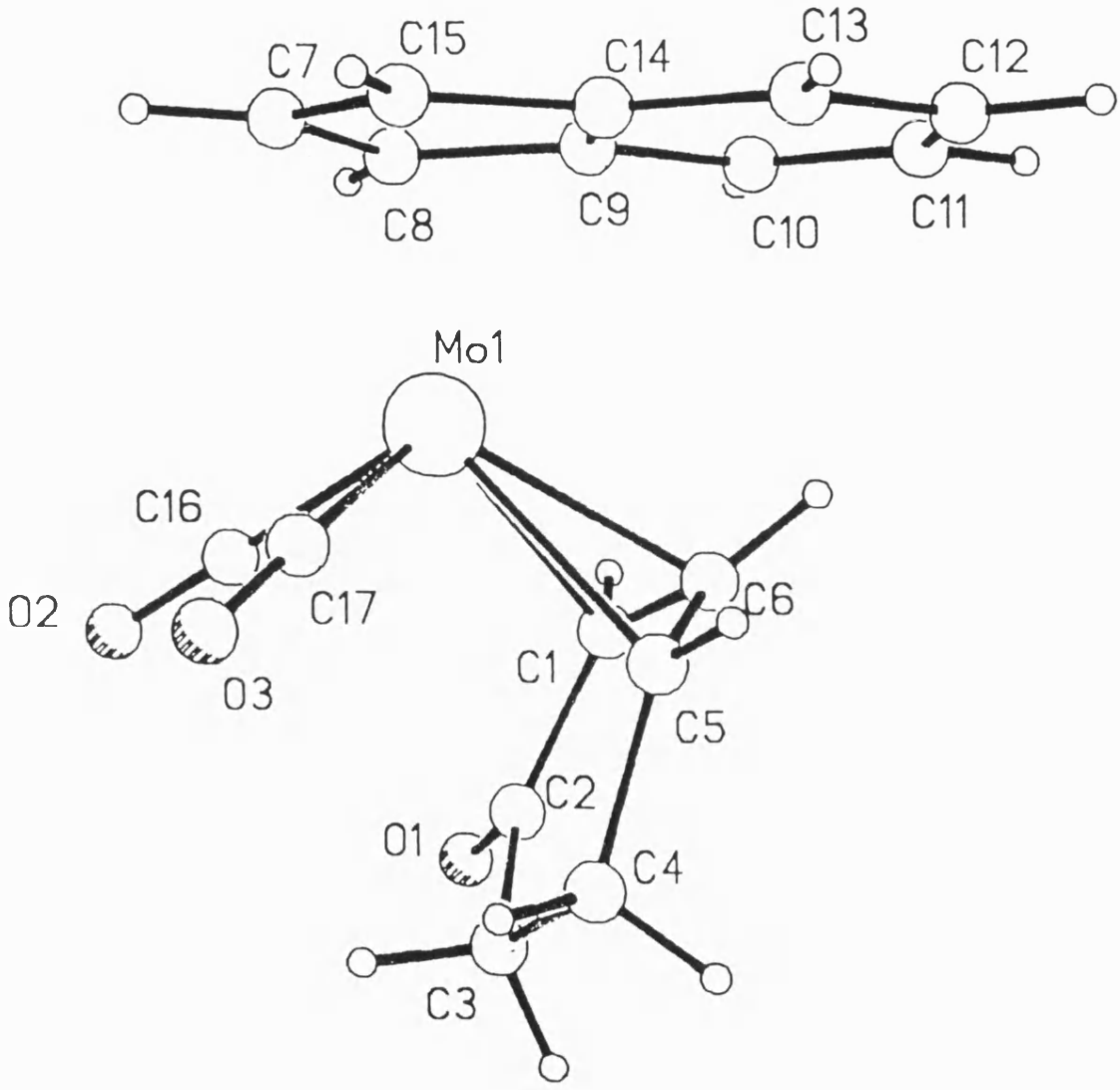

Figure 62. Molecular structure of $[Mo(\eta^3\text{-}C_6H_7O)(CO)_2(\eta^5\text{-}C_9H_7)]$ (77).

Given the above information, it is not unreasonable to assume that the η^5-C_5Me_5 complex (92) displays similar properties. In particular, the low frequency carbonyl band present in the IR spectrum of (92) (1630 cm^{-1}) is indicative of a π-interaction between the η^3-allyl and the ketone functionality. We can therefore assign the location of charge density within (92) as illustrated in Figure 63. Such a distribution is confirmed by the reactivity of complex (92), as will become evident in the following pages.

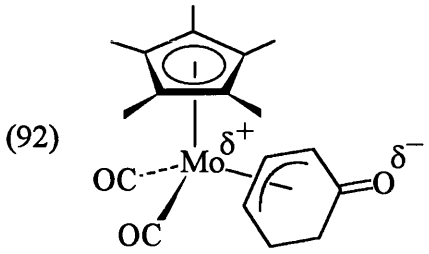

Figure 63

2.1.3 Elaboration *via* Protonation

A build up of negative charge on the oxygen atom of the ketonic carbonyl group present in (92) suggests that it should react readily with electrophiles. Indeed, this was found to be the case. A dichloromethane solution of (92) was treated at low temperature with $HBF_4.OEt_2$, which resulted in a darkening of the mixture and ultimately the isolation of an orange powder. The product was identified from analytical and spectroscopic data as the 1-hydroxy-η^4-1,3-diene cation (94), formed in high yield (70%) *via* selective *O*-protonation (Fig. 64).

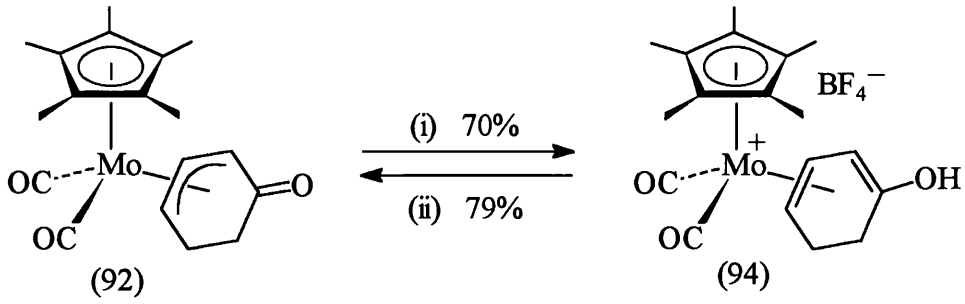

Figure 64. (i) $HBF_4.OEt_2$, CH_2Cl_2, -78°C; (ii) Et_3N.

Complex (94) can be viewed as a species containing the enol form of cyclohex-3-ene-1-one, stabilised by coordination to a cationic metal fragment. The reaction is readily reversible, (94) being reconverted to (92) in 79% yield on addition of triethylamine.

Interestingly, the η^4-1,3-diene ligand present in (94) would be expected to behave as an active substrate for the stereoselective introduction of nucleophiles. However, this avenue was only briefly explored. Reaction of (94) with $Na[BH_3CN]$ (thf, 0°C) gave a neutral complex which was readily purified by chromatography. The spectroscopic and analytical data suggested the presence of an hydroxy-substituted η^3-allyl complex. A closer examination of the ^1H NMR spectrum (with the aid of COSY spectra), revealed that the reaction had occurred *via* selective *exo*-attack of H^- on the hydroxy-substituted carbon. Hence, the product was identified as the allylalcohol complex (95) (Fig. 65). This complex can also be formed from a stereoselective reduction of (92) (see Section 2.1.6).

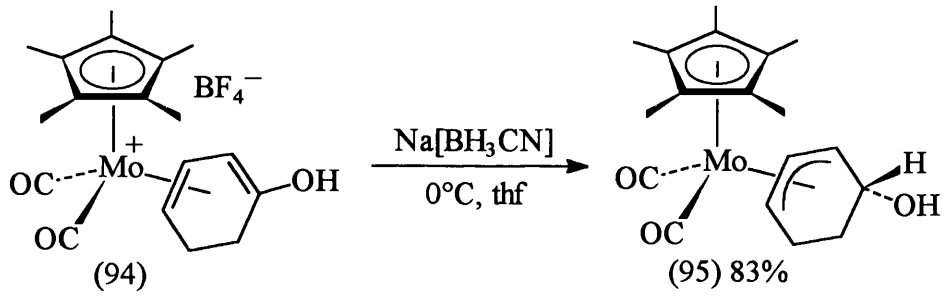

Figure 65

The presence of the electron-withdrawing oxygen substituent directs the site of nucleophilic attack to the more electron-deficient carbon at the terminus of the 1,3-diene. This is in good agreement with the regioselectivity previously observed for attack on the corresponding 1-methoxy-substituted η^5-indenyl complex (17)[40] (Fig. 66).

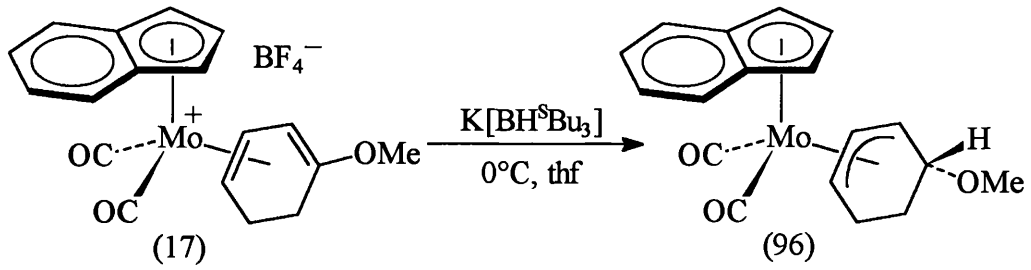

Figure 66

2.1.4 Elaboration *via* Hydride Abstraction

An established procedure for the elaboration of coordinated η^3-allyl ligands involves conversion to the corresponding η^4-1,3-diene cation *via* hydride abstraction[29,85] (see Section 1.4). This is readily accomplished with the use of the bulky trityl cation Ph_3C^+. While the reaction generally proceeds smoothly in most cases, it has been reported that certain η^3-allyl complexes are resistant to hydride removal using this reagent.[39,112] In particular, previous attempts to apply this methodology to the indenyl ketoallyl complex (77) have been unsuccessful.[115] Recently however, Liebeskind has reported that the C_5-oxoallyl complex (91) undergoes facile hydride abstraction using Ph_3CPF_6 to form the cationic cyclopentadienone complex (10) in high yield[35] (Fig. 67).

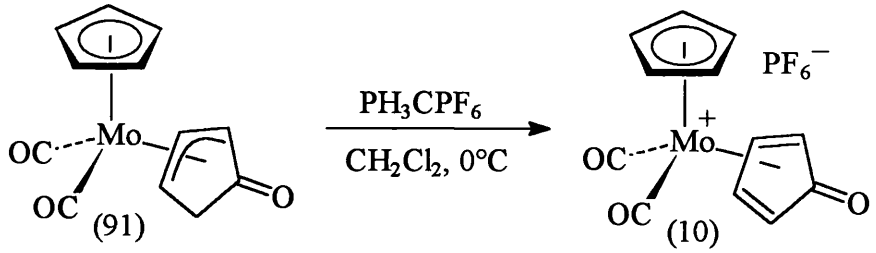

Figure 67

Encouraged by this result, it was decided to examine the reactivity of complex (92) with the trityl reagent. Special precautions were taken to ensure anhydrous conditions since Ph_3C^+ produces traces of acid in the presence of water:

$$Ph_3C^+ + H_2O \longrightarrow Ph_3COH + H^+$$

This prevents any competition from *O*-protonation as described above. Thus, the reaction was carried out under an argon atmosphere using 'flame-dried' equipment. Treatment of (92) with Ph_3CBF_4 in dichloromethane (introduced *via* vacuum distillation from P_2O_5) at 0°C, resulted in the formation of a particularly air-sensitive mustard-cream powder in high yield. The insolubility of the product in Et_2O suggested it to be a cationic complex. This was supported by the move to a higher frequency of the strong metal-carbonyl bands in the IR spectrum (2056 and 2012 cm^{-1}). In addition, two further less intense bands were observed at 1703 and 1686 cm^{-1}, characteristic of a conjugated

enone.[117] The ^{13}C-{^{1}H} NMR spectrum showed peaks at 95.8, 75.8, 73.9 and 67.8 ppm due to a 1,3-diene moiety, as well as a quaternary carbonyl carbon (194.3 ppm) and a methylene carbon (35.3 ppm). These assignments were reinforced by the ^{1}H NMR spectrum, with coordinated diene proton resonances at 5.75, 5.49, 4.23 and 3.51 ppm, and two strongly coupled, higher field resonances at 3.08 and 2.79 ppm due to the methylene protons. Hence, the product was identified as the oxo-η^4-1,3-diene cation (97), in good agreement with the microanalysis and mass spectral data (Fig. 68).

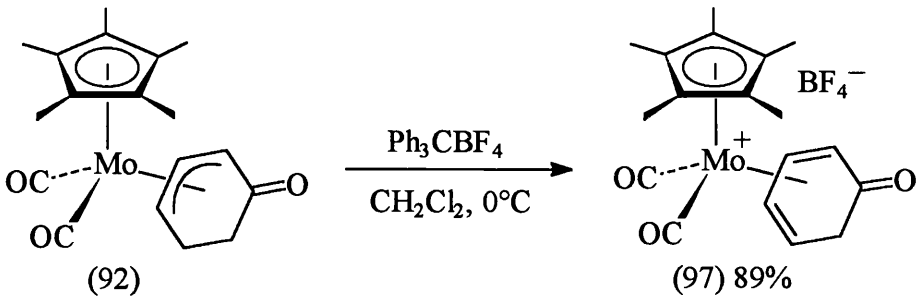

Figure 68

As a result of steric interactions between the metal and the bulky reagent, hydride abstraction takes place on the *exo*-face of the allyl ligand. The cyclohexadienone ligand present in the product (97) can be regarded as the keto tautomer of phenol, stabilised by coordination to a metal centre. To the best of our knowledge, this is the first example of such a compound where the metal centre is cationic, although similar neutral complexes containing $Fe(CO)_3$-derived ligands have previously been prepared.[118,119] Access to this compound creates the opportunity to regio- and stereo-selectively add nucleophiles to the terminus of the 1,3-diene chromophore present in (97). (The 1,3-diene, being coordinated to a cationic metal centre, would be the most likely site of nucleophilic attack, as opposed to the ketonic group).

It was decided to investigate the electrophilicity of complex (97) by reaction with a variety of nucleophiles, starting with simple systems involving sources of hydride anion. Treatment of (97) with K-Selectride (thf, 0°C) resulted in decomposition of the

reaction mixture as indicated by IR spectroscopy. However, the cyclohexadienone cation (97) was found to react with one molar equivalent of sodium borohydride (thf, 0°C) to regenerate the oxo-η^3-allyl complex (92) (Fig. 69) in 80% yield. This was confirmed from an examination of the IR and NMR spectral data and comparison with that from an authentic sample of (92).

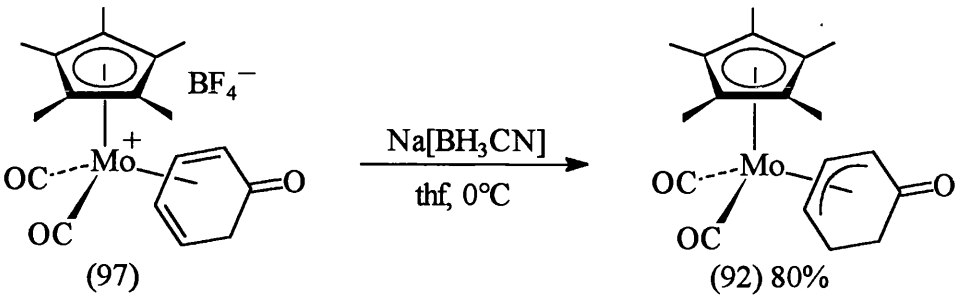

Figure 69

The above result indicated that the primary site of nucleophilic addition to (97) was at the terminus of the 1,3-diene chromophore, β to the keto-group (i.e. regiocontrol had been established). Encouraged by this information, an attempt was made to introduce more complex functionality into this system.

Complex (97) was treated with 1-pyrrolidino-1-cyclohexene as a means of accessing the η^3-allyl complex (98) (Fig. 70). However, the desired reaction did not occur and (98) was not formed.

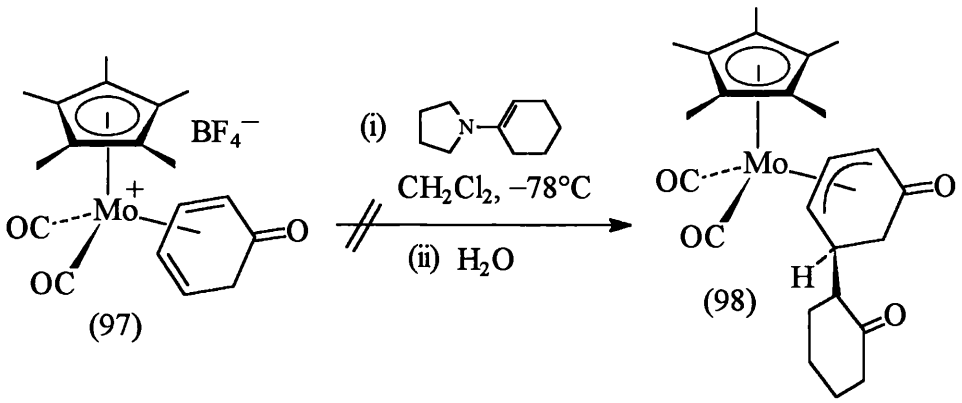

Figure 70

Instead, after work-up of the reaction, a red-purple solid was isolated as the main product. The IR spectrum of this species showed two metal-carbonyl bands at 1863

and 1833 cm^{-1} with no signal occurring for an organic carbonyl functionality. FAB mass spectrometry showed a molybdenum isotope pattern at 576 and the ^1H NMR spectrum gave a sharp singlet at 1.93 ppm, indicating the presence of one or more equivalent pentamethylcyclopentadienyl groups. This data suggested the presence of a high molecular weight species containing the $[Mo(\eta^5\text{-}C_5Me_5)(CO)_2]$ fragment. One known compound exhibiting similar properties is the dinuclear complex $[Mo(\eta^5\text{-}C_5Me_5)(CO)_2]_2$ (99)[120] (Fig. 71), also red-purple in colour. An authentic sample of (99) was obtained and its spectral data was compared with that of the unknown solid. The data was found to be in good agreement and thus the product was identified as the dimeric species (99).

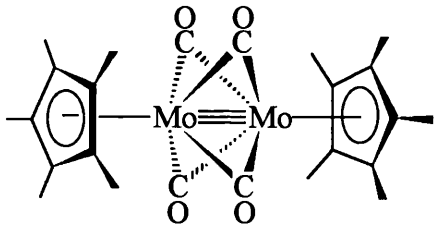

(99)

Figure 71

A reaction between our oxo-η^4-dienyl cation (97) and MeMgBr was also carried out, with the η^3-allyl complex (100) as the expected product (Fig. 72). Again, the desired reaction did not occur and (100) was not isolated.

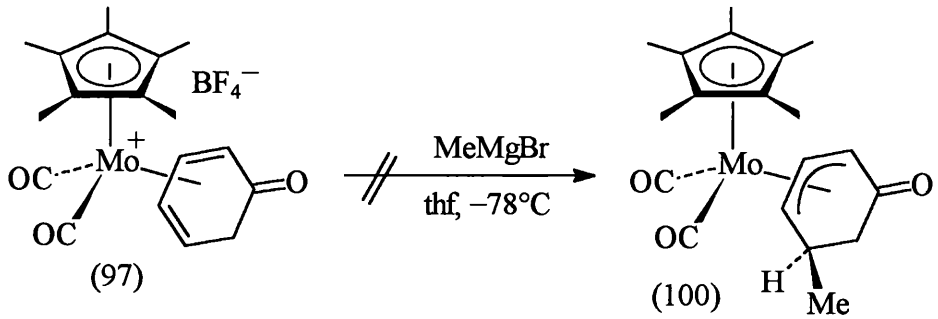

(97) (100)

Figure 72

As before, the major product of this reaction was identified as the molybdenum dinuclear complex (99). In both the enamine and the Grignard reactions, such a species

could only have been formed by removal of the η^4-organic fragment from (97) followed by coupling of two [Mo(η^5-C_5Me_5)$(CO)_2$] fragments. It was thought that the basicity of both the enamine and Grignard reagents was allowing this to occur [*via* removal of an acidic proton α to the keto-group in (97)]. In order to test this theory, we decided to investigate the reaction between (97) and a strong base.

Hence, complex (97) was treated with 1,8-bis(dimethylamino)naphthalene (proton sponge) (CH_2Cl_2, -78°C). It was found that the main product of the reaction was indeed the dimeric complex (99) (Fig. 73).

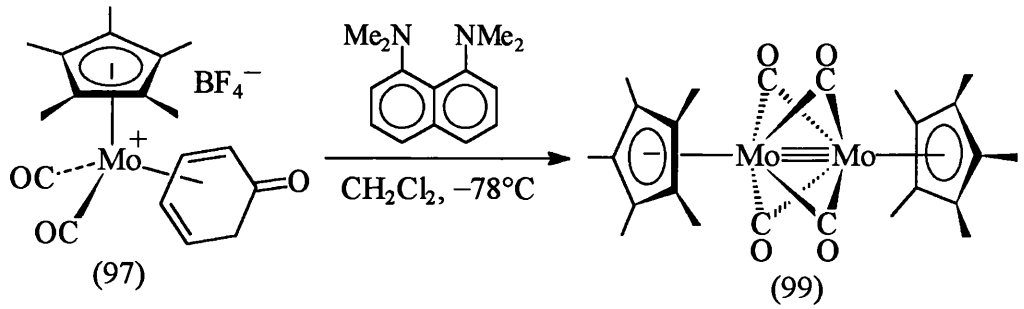

Figure 73

This led us to propose a mechanism [proceeding *via* an unstable Zwitterion (101)] to account for the observations of these base-induced reactions (Fig. 74, overleaf). Although in each case the decomplexed organic product was not isolated, it is probable that this species would have some sort of biaryl structure, as in (102). Presumably the reaction is driven by the thermodynamic stability of the molybdenum dimer (99).

It would appear that the addition of nucleophiles to complex (97) is dependent upon the nature of the nucleophile. This seems a reasonable suggestion as Grignard reagents are hard, basic nucleophiles whereas Na[BH_3CN] is a somewhat milder source of anion. Quite possibly, (97) will successfully add other mild sources of nucleophile reagent (e.g. cuprates) although such reactions were not attempted.

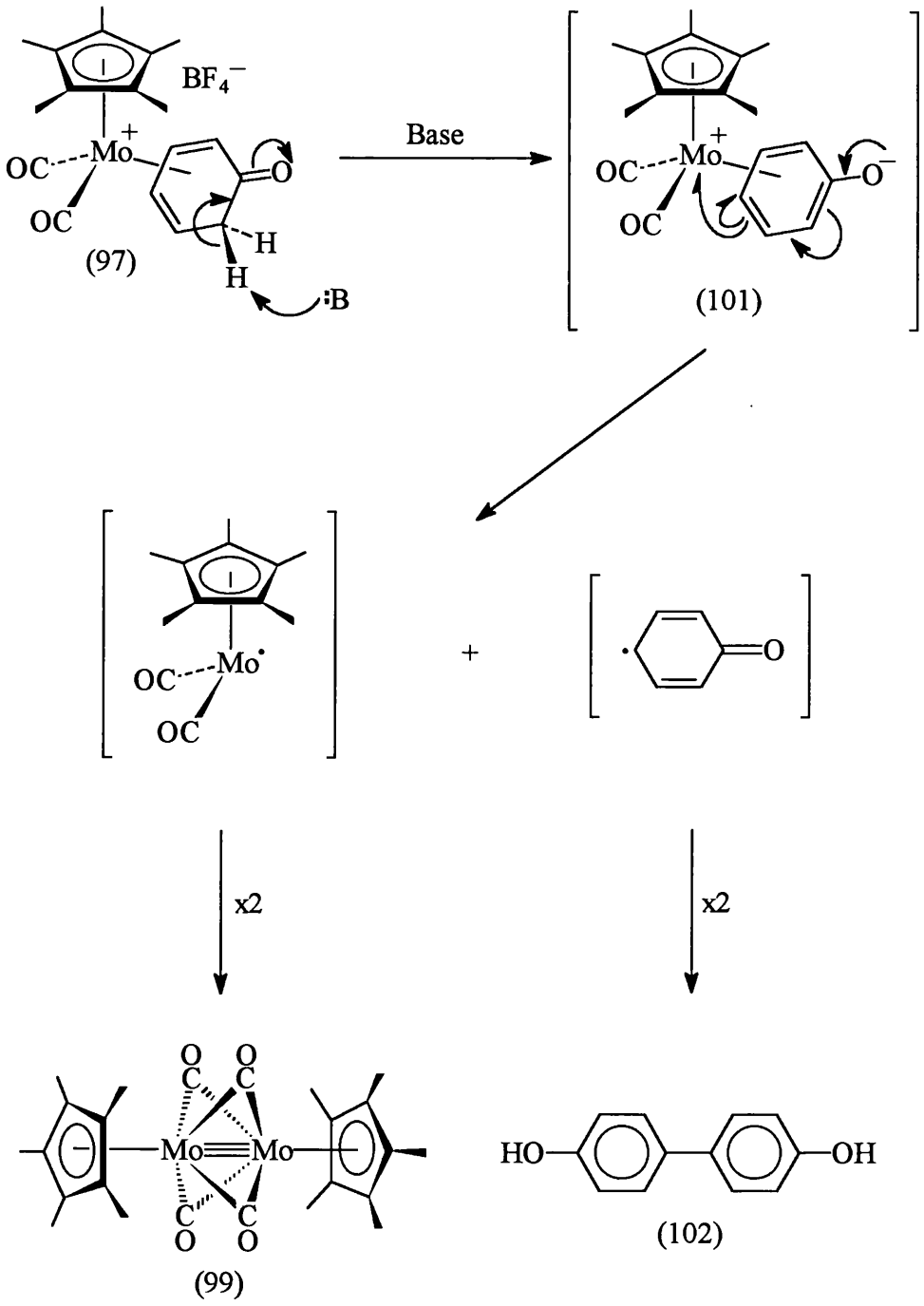

Figure 74

2.1.5 Elaboration *via* Alkylation of the Derived Lithium Enolate

Although nucleophilic attack at the terminus of a coordinated 1,3-diene chromophore remains a significant elaborative method, the presence of an uncoordinated functionality offers an alternative strategy for the stereoselective

introduction of substituents. In the case of the oxoallyl complex (92), simple organic transformations associated with the ketonic functionality are a possibility. More specifically, the opportunity of carrying out stereocontrolled carbon-carbon bond forming reactions *via* the formation of a metal enolate is particularly attractive.

By far the most important method for preparing metal enolates involves a metal-hydrogen exchange, although other methods commonly used in the preparation of simple organolithiums and Grignard reagents, such as oxidative metallation,[121] metal-hydrogen exchange,[122] or transmetallation,[123] have been used. The development of non-nucleophilic, highly basic reagents such as $Li[N(^{i}Pr)_2]$ (LDA), $Li[N(SiMe_3)_2]$ and $K[N(SiMe_3)_2]$ have made it possible to generate 'kinetic' enolates regioselectively at low temperatures in aprotic solvents. Under these conditions, the least hindered hydrogen atom is abstracted (Fig. 75) and subsequent alkylation can be achieved with full regiocontrol.

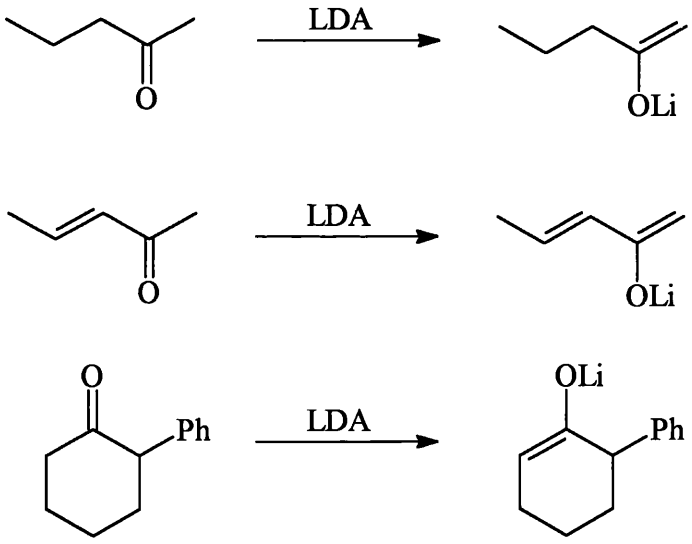

Figure 75. Formation of 'kinetic' enolates.

Reaction of the oxo-η^3-allyl complex (92) with $Li[N(SiMe_3)_2]$ (thf, -78°C) gave a dark red solution thought to be due to the intermediacy of an *E*-enolate anion (103). Treatment of the solution (at -78°C) with MeI afforded an 87% yield of the yellow *exo*-methyl-4-oxo-η^3-allyl complex (104) (Fig. 76).

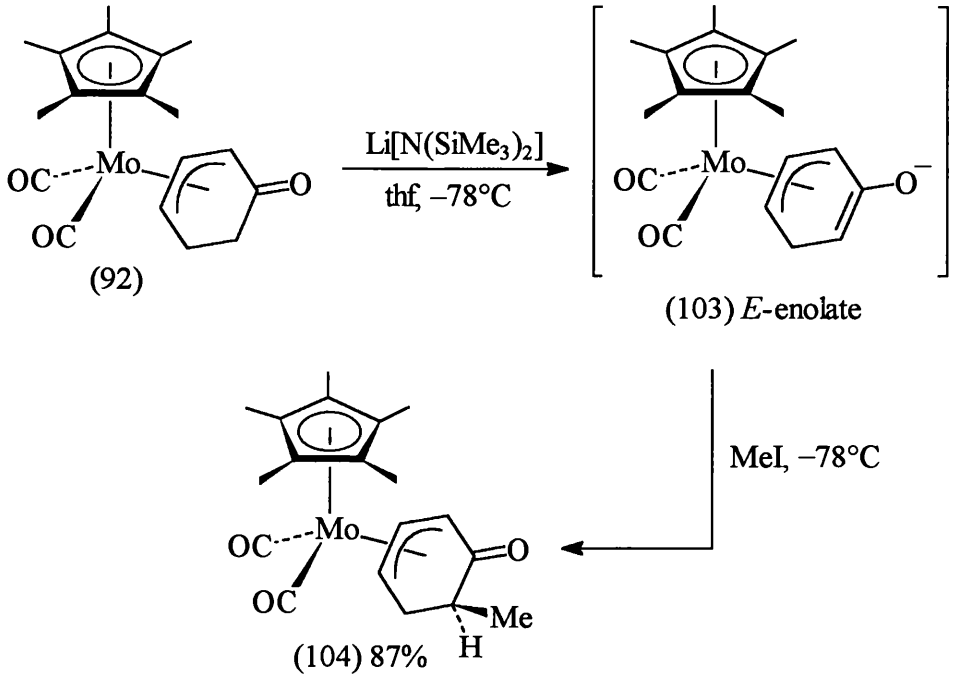

Figure 76

Analytical and spectroscopic data were consistent with the structure of the product (104). An examination of the proton-proton coupling constants in the ^{1}H NMR spectrum [and comparison with those in complex (92)] revealed that the methyl group had been added exclusively to the face of the cyclohexenyl ligand opposite to the metal (i.e. the *exo*-face). This stereocontrol is consistent with that previously reported for similar enolate systems.[7,40,57] The observed diastereofacial selectivity can be attributed to the presence of the bulky $Mo(CO)_2(\eta^5\text{-}C_5Me_5)$ fragment which effectively shields the *endo*-face of the six-membered ring resulting in selective attack by electrophiles on the *exo*-face of the *E*-enolate. It is important to note that a new chiral centre has been formed in this reaction.

An attempt was made to convert (104) to the corresponding η^4-1,3-diene cation (105) *via* hydride abstraction. However, treatment of (104) with Ph_3CBF_4 (anhydrous conditions, CH_2Cl_2, 0°C) did not give the desired product (Fig. 77). Monitoring by IR spectroscopy showed only the presence of the starting material (102), indicating that no reaction had taken place.

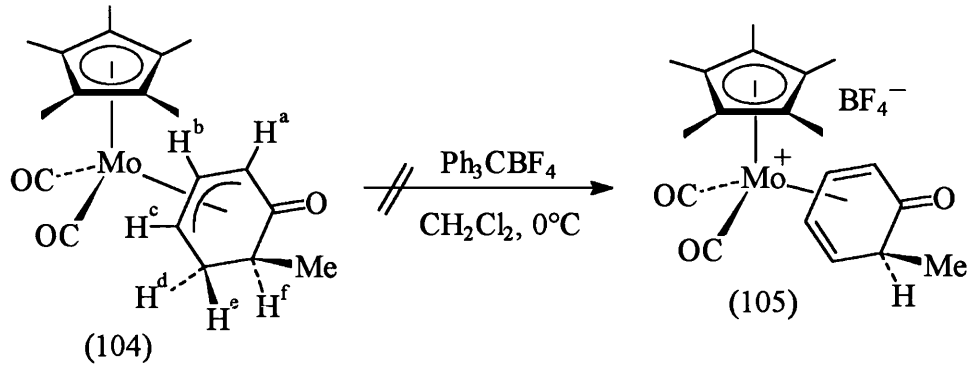

Figure 77

The unreactivity of (104) towards Ph_3CBF_4 compared with the unsubstituted oxoallyl complex (92) is presumably caused by the presence of an *exo*-substituent. The methyl group may hinder the approach of the bulky trityl cation such that abstraction of the *exo*-hydrogen (H^e) is prevented.

2.1.6 Elaboration *via* Nucleophilic Addition to the Ketonic Group

Nucleophilic addition to the ketonic group present in complex (92) offers further opportunities for the stereoselective introduction of substituents. Stereospecific reduction of (92) was achieved by reaction with sodium borohydride in methanol to afford the yellow crystalline hydroxyallyl complex (95) in 77% yield (Fig. 78).

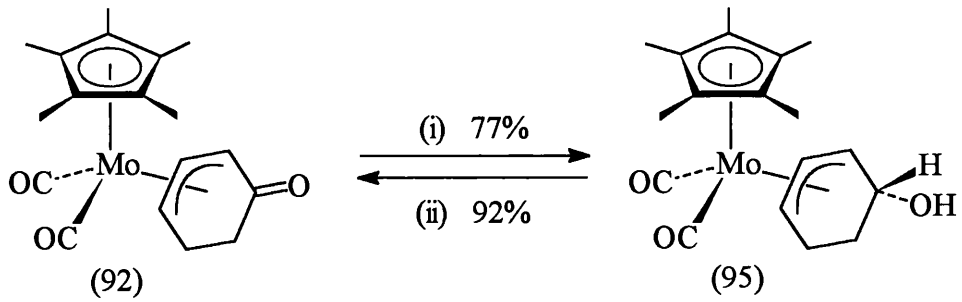

Figure 78. (i) $NaBH_4$, MeOH; (ii) $Al(^iPrO)_3$, acetone, toluene, Δ.

This reaction was found to be readily reversible, the oxoallyl complex (92) being regenerated in 92% yield *via* an Oppenauer oxidation.[124]

These results prompted us to consider some carbon-carbon bond forming reactions at the ketonic functionality involving the use of organometallic reagents.

Organolithium compounds, Grignard reagents and to a lesser extent organozinc compounds, are the most frequent choice of reagent for such reactions. However, although they generally react cleanly with aldehydes and ketones, there are several types of side reaction that can occur (enolization, reduction, condensation, Wurtz-type coupling etc.), particularly when hindered carbonyl substrates or bulky organometallic reagents are being employed. The ease with which the molybdenum complex (92) undergoes enolization alerted us to the possibility of side reactions when using such reagents. As a result, a slightly modified procedure was adopted, requiring the use of organocerium reagents.

Organocerium reagents are generated *in situ* by transmetallation reactions between organolithiums or Grignard reagents and anhydrous cerium (III) chloride[125-127] (Fig. 79).

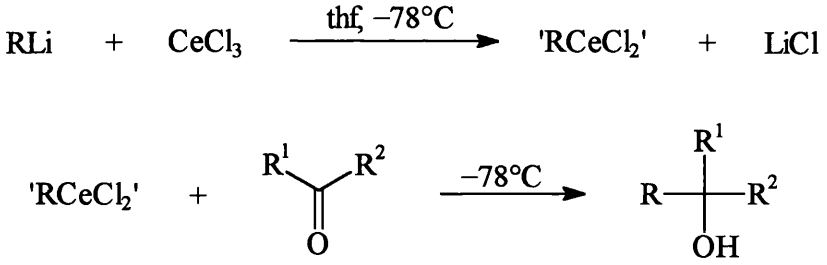

Figure 79

Alkyl (primary, secondary and tertiary), alkenyl, alkynyl, allyl and aryl organocerium compounds can all be prepared by this simple procedure. Little is known of the structure of these organoceriums, or the exact nature of the reactive species. Although they have been denoted as a σ-alkyl species ('$RCeCl_2$'), other compositions (e.g. $RM{\cdot}CeCl_3$, 'ate' complexes or species resulting from Schlenk-type equilibria)[128] cannot be ruled out.

Regardless of the true nature of the reactive nucleophiles, these reagents react efficiently with aldehydes and ketones, providing alcohols in yields that are often superior to those reported utilising Grignard or organolithium reagents. Particularly impressive is the ability of organocerium reagents to effect carbonyl addition whilst

completely suppressing the competing side reactions that would otherwise occur when using simple organometallics. This has been amply demonstrated by Imamoto,[125-127] who has reported many examples of addition to highly enolizable substrates and systems involving sterically hindered species (Fig. 80).

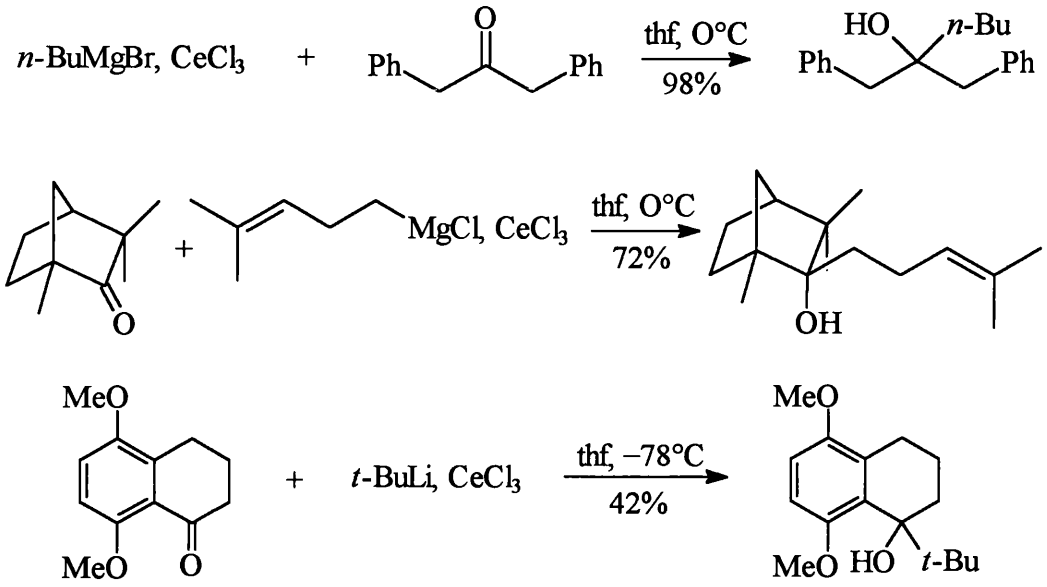

Figure 80

Thus, the oxoallyl complex (92) was treated with the organocerium reagent derived from phenyllithium and anhydrous cerium (III) chloride (thf, -78°C). A smooth reaction ensued and monitoring by IR spectroscopy showed the gradual consumption of (92) with the formation of two new metal-carbonyl bands, at slightly lower frequency (1925 and 1838 cm^{-1}), characteristic of the expected allylalcohol. Following aqueous work-up and column chromatography, a yellow product was obtained in high yield that analysed for $[Mo(C_{12}H_{13}O)(CO)_2(C_5Me_5)]$ in accordance with the microanalysis and FAB mass spectral data. Along with peaks due to the η^5-C_5Me_5 and cyclohexenyl ligands, the ^1H NMR spectrum displayed resonances at 7.69, 7.36 and 7.22 ppm attributed to the presence of a phenyl group and a singlet at 2.50 ppm assigned to the proton of an hydroxy group. Evidently, nucleophilic addition of phenyl had taken place at the ketonic functionality in (92) to afford the allylalcohol (106) (Fig. 81). This was supported by the ^{13}C-{^1H} NMR spectrum which clearly showed a new resonance at

75.1 ppm due to the quaternary carbon centre. As before, the stereochemistry of addition was controlled, leading to selective *exo*-facial attack and the formation of a chiral carbon centre.

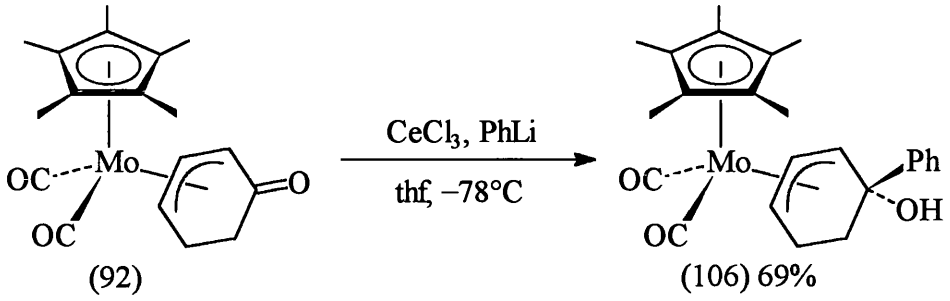

Figure 81

The same procedure was attempted using the methyl-substituted oxoallyl complex (105). The reaction proceeded smoothly and afforded the expected disubstituted allylalcohol product (107) (Fig. 82) in 72% yield, as confirmed by analysis and spectroscopy. The *exo*-facial attack of phenyl led to a *cis*-1,2-relationship of substituents on the cyclohexenyl ring and the formation of a second chiral carbon centre.

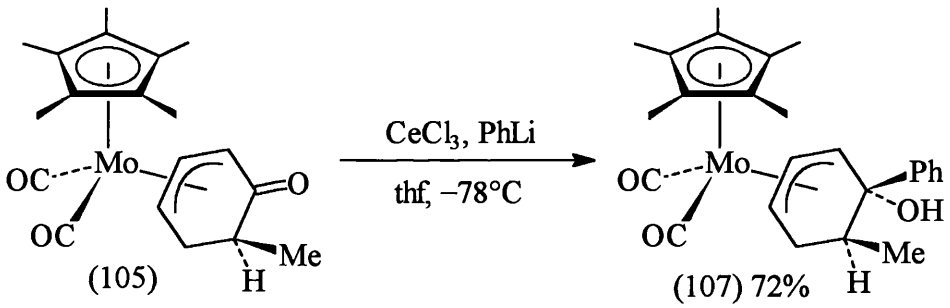

Figure 82

In order to provide a more detailed picture of the geometry and bonding within complex (107), a single crystal X-ray diffraction experiment was undertaken. The molecular structure is shown in Figure 83 together with the atomic numbering scheme used. An alternative representation from a 'side-on' viewpoint is illustrated in Figure 84. Selected bond lengths, angles and torsion angles are given in Table 1.

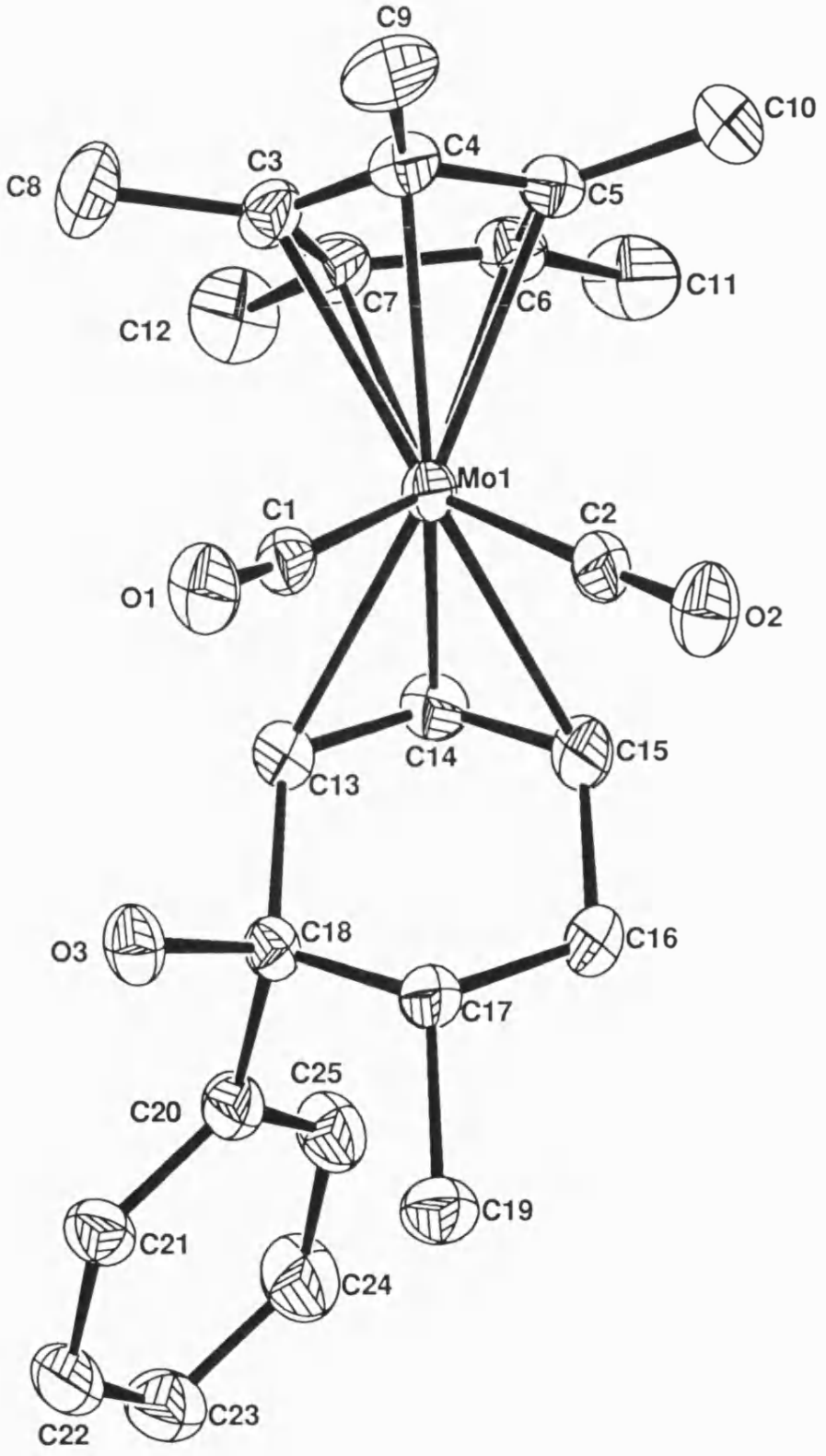

Figure 83. Molecular structure of $[Mo(\eta^3\text{-}C_{13}H_{15}O)(CO)_2(\eta^5\text{-}C_5Me_5)]$ (107).

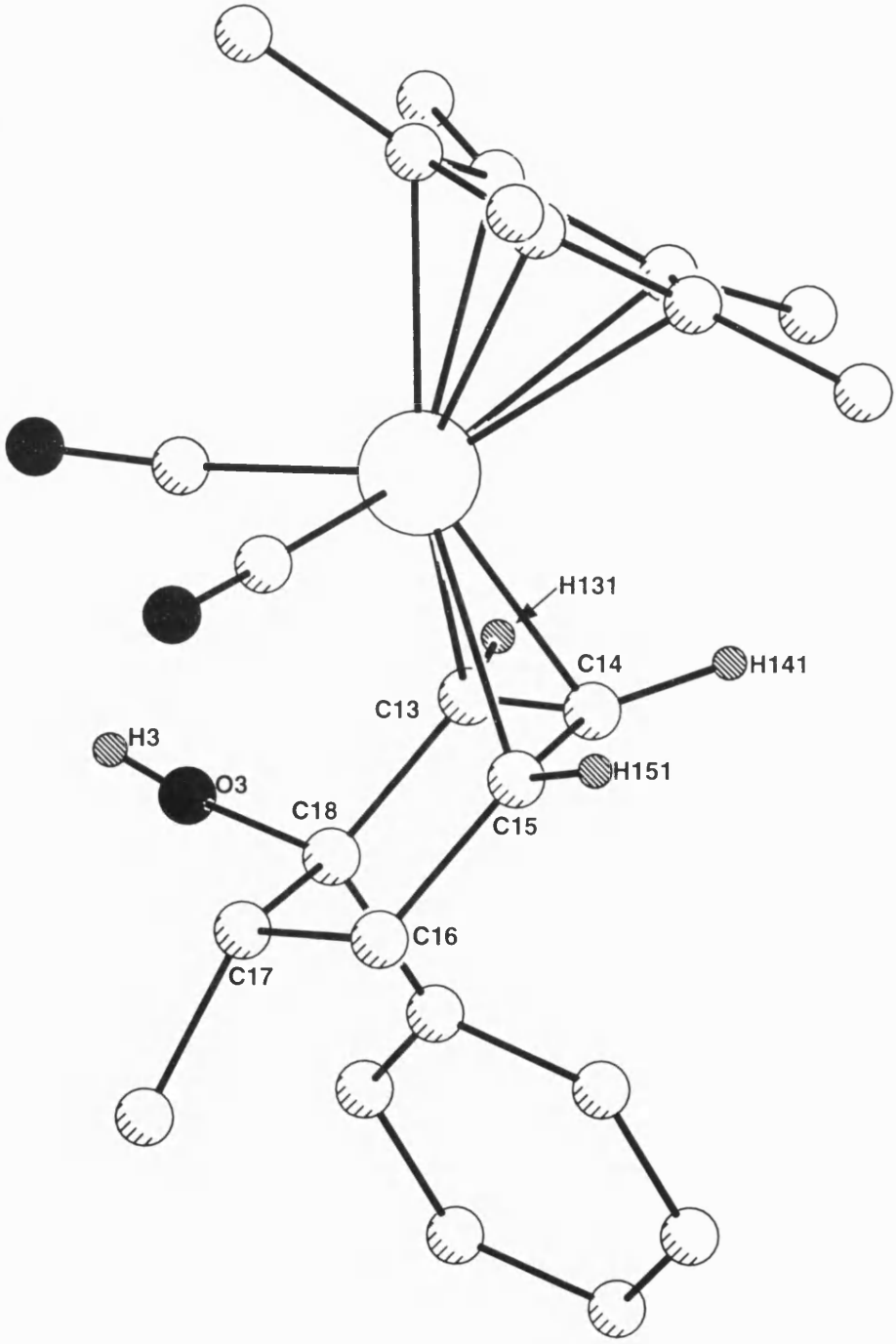

Figure 84. Alternative representation of $[Mo(\eta^3\text{-}C_{13}H_{15}O)(CO)_2(\eta^5\text{-}C_5Me_5)]$ (107).

Table 1 Selected bond lengths (Å), angles (°) and torsion angles (°) for complex (107) with estimated standard deviations in parenthesis.

Mo-C(1)	1.943(5)	Mo-C(2)	1.946(5)
Mo-C(3)	2.336(5)	Mo-C(4)	2.304(5)
Mo-C(5)	2.352(5)	Mo-C(6)	2.386(5)
Mo-C(7)	2.389(5)	Mo-C(13)	2.350(5)
Mo-C(14)	2.187(5)	Mo-C(15)	2.368(5)
C(1)-O(1)	1.161(5)	C(2)-O(2)	1.149(5)
C(13)-C(14)	1.417(5)	C(14)-C(15)	1.404(5)
C(15)-C(16)	1.510(6)	C(13)-C(18)	1.524(6)
C(18)-O(3)	1.433(4)	C(18)-C(20)	1.539(6)
C(1)-Mo-C(2)	82.0(2)	Mo-C(1)-O(1)	174.2(4)
Mo-C(2)-O(2)	178.7(4)	C(13)-C(14)-C(15)	115.9(4)
C(14)-C(13)-C(18)	119.0(4)	C(14)-C(15)-C(16)	118.9(4)
C(13)-C(14)-C(15)-C(16)	40.5(4)	C(14)-C(15)-C(16)-C(17)	-38.7(4)
C(15)-C(16)-C(17)-C(18)	38.1(4)	C(16)-C(17)-C(18)-C(13)	-39.6(3)
C(14)-C(13)-C(18)-C(17)	43.2(4)	C(18)-C(13)-C(14)-C(15)	-43.5(4)

Complex (107) displays a typical 'piano-stool' type arrangement in its solid-state structure. The central molybdenum atom can be formally described as seven-coordinate, being bonded to two terminal carbonyl ligands, an η^3-cyclohexenyl fragment and an η^5-pentamethylcyclopentadienyl ligand, which is considered to occupy three coordination sites. Both metal-carbonyl groups are essentially linear, within experimental error, with Mo-C-O angles of 174.2 and 178.7°, the Mo-C and C-O bond lengths being typical.[129] The two carbonyl ligands lie at an angle of 82.0° to one another. The η^5-C_5Me_5 ligand is essentially planar and is bound at a mean distance of 2.353 Å from the metal atom.

The cyclohexenyl ligand is bound to the metal *via* three carbon atoms as an η^3-allyl. This C(13)-C(14)-C(15) moiety is bonded *exo* with respect to the η^5-C_5Me_5 ring with Mo-C distances of 2.350(5), 2.187(5) and 2.368 (5) Å and a bond angle of 115.9°, typical for η^3-cyclohexenyl molybdenum complexes.[29,40] The cyclohexenyl ring can be seen to adopt a chair conformation, with a near-planar phenyl substituent in an axial position at C(18), along with methyl and hydroxyl substituents, both in equatorial positions, at C(17) and C(18) respectively. The phenyl and methyl groups are oriented away from the metal on the *exo*-face of the ring. Conversely, the hydroxyl moiety is positioned on the *endo*-face of this ligand (i.e. on the same side as molybdenum). This confirms that complex (107) has been formed with complete facial control.

Phenyl-substituted complexes such as (107) could have important applications in the synthesis of biaryl compounds. The biaryl axis is the central feature of a large number of pharmacologically active natural products of differing structure,[130] and also of an increasing number of chiral reagents.[131] With access to the oxoallyl complex (92) in optically pure form (*via* resolution) and the use of substituted phenyllithium reagents, it should be possible to prepare a range of homochiral biaryls by the route illustrated in Figure 85. Such reactions were beyond the scope of this preliminary investigation, however, it is envisaged that this methodology will be established in the near future.

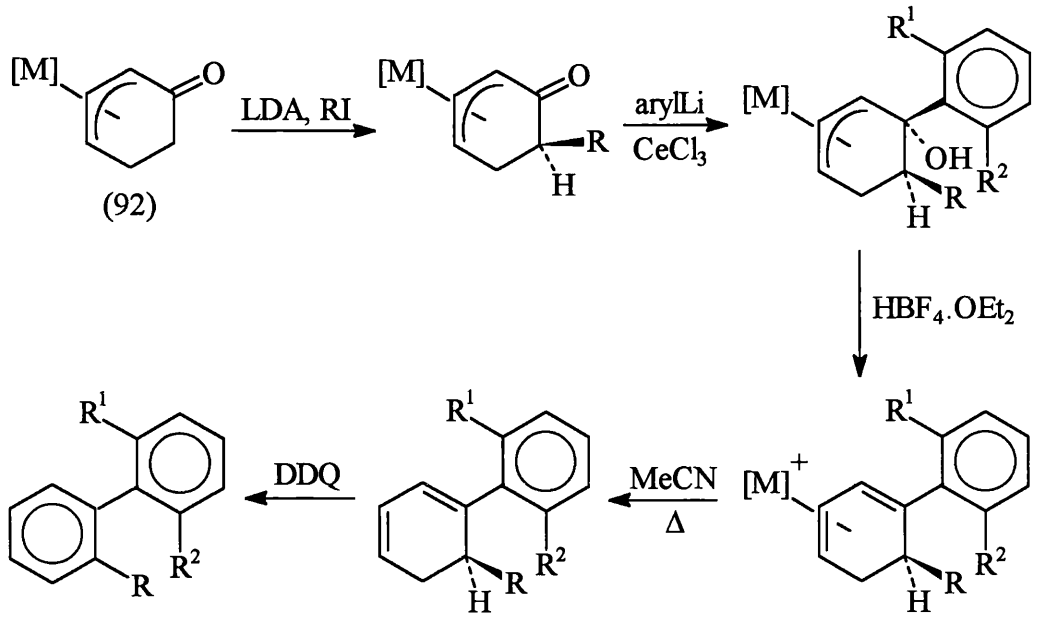

Figure 85. [M] = $[Mo(CO)_2(\eta^5\text{-}C_5Me_5)]$.

2.1.7 Summary and Conclusions

The oxoallyl complex $[Mo(\eta^3\text{-}C_6H_7O)(CO)_2(\eta^5\text{-}C_5Me_5)]$ (92) has been synthesised and shown to undergo a range of functionalisation reactions at different sites around the C_6 ring. Conversion to the corresponding cationic 1,3-diene complex (and thus activation towards nucleophiles) can be readily achieved by either *O*-protonation or hydride abstraction. Alternatively, enolate alkylation or nucleophilic addition reactions associated with the ketonic group can be successfully carried out. The presence of the metal fragment in (92) and its derivatives causes such functionalisation reactions to occur with complete stereoselectivity. Hence, by proper choice of reaction sequence, these complexes could be used to obtain highly regio- and stereo-defined products based on a C_6-ring. The possibility of extending this methodology to give enantioselective reactions offers considerable scope for the further development of this area.

2.2 Synthesis and Reactivity of $CpMo(CO)_2$-Derived C_5-Ring Complexes

2.2.1 Introduction

The development of methods for the stereocontrolled construction of substituted C_5-based ring systems (e.g. as in natural products such as the prostaglandins[132,133] and jasmonoids[134]) remains an important goal in synthetic organic methodology. The use of cyclopentenyl-based metal π-complex intermediates to control both the regio- and stereo-chemistry of substituent introduction has been explored in recent years.[135-137] Within the context of $CpMo(CO)_2$-derived compounds, the previously mentioned 4-oxoallyl complex (91) has been successfully employed as a scaffold for the stereospecific formation of 2-cyclopentenones.[33,114] Complex (91) is prepared from the requisite allylic bromide, 4-bromo-2-cyclopentenone, as outlined in Figure 86.

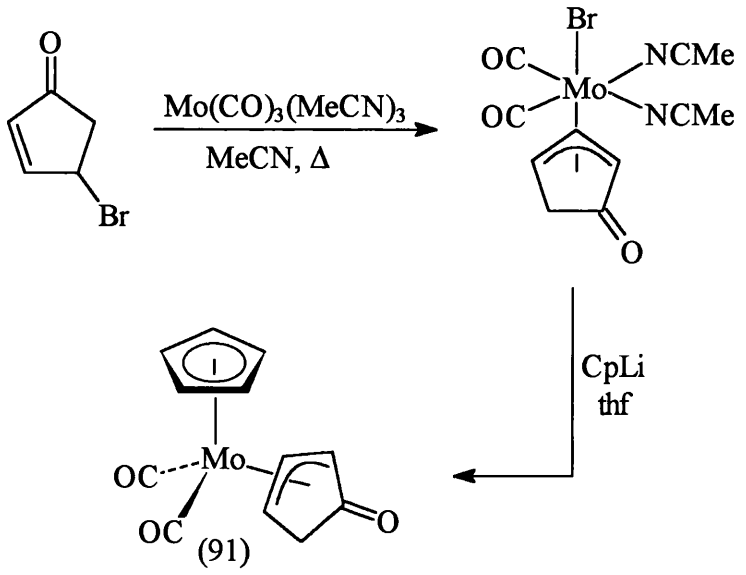

Figure 86

A potentially more attractive means of accessing such molybdenum C_5-ring complexes can be envisaged with the use of bis(acetonitrile) technology (see Sections 1.2.2 and 2.1). Although the *cis*-bis(acetonitrile) cations (15) and (16) have been used effectively for the direct complexation of cyclohexa-1,3-dienes, the corresponding complexation of cyclopentadienes has not been attempted. It was therefore decided to

investigate the synthesis and reactivity of a simple molybdenum-cyclopentadiene system using this methodology.

2.2.2 Synthesis of *cis*-[Mo(NCMe)$_2$(CO)$_2$(η^5-C$_5$H$_5$)][BF$_4$] (108)

Previous work carried out within our group on the complexation of 1,3-dienes to molybdenum centres has made use of the *cis*-bis(acetonitrile) cation [Mo(NCMe)$_2$-(CO)$_2$L][BF$_4$] [where L = η^5-C$_9$H$_7$ (15) or η^5-C$_5$Me$_5$ (16)]. Although the analogous η^5-cyclopentadienyl cation (108) was obtained[138] a number of years ago (by a rather unattractive procedure involving AlCl$_3$), it was reported to be unstable, with a tendency to decompose on isolation. Consequently, the reactivity of this species with 1,3-dienes had not been explored. It was found, however, that (108) could be readily prepared in a similar manner to (15) and (16) using the procedure shown in Figure 87. Molybdenum hexacarbonyl was treated with cyclopentadienylsodium to generate the molybdenum tricarbonyl anion (109). This species was not isolated but treated directly with MeI to afford [Mo(η^5-C$_5$H$_5$)(CO)$_3$Me] (110) (64% overall yield) as a yellow crystalline solid. Addition of HBF$_4$.OEt$_2$ to a solution of (110) in dichloromethane effected protonation of the methyl group. Subsequent treatment with acetonitrile led to the isolation of the mono-acetonitrile complex (111) in 90% yield, obtained as an orange-red solid. The *cis*-bis(acetonitrile) cation (108) was prepared by refluxing a solution of (111) in acetonitrile for 8 hours and isolated in 79% yield as a blood-red solid. In contrast to the previously reported observations,[138] (108) was found to be perfectly stable when kept under an inert atmosphere of nitrogen, and was fully characterised by microanalysis, IR, NMR and FAB mass spectrometry. As a result, (108) was chosen as a suitable substrate for the introduction of a cyclopentadiene ligand.

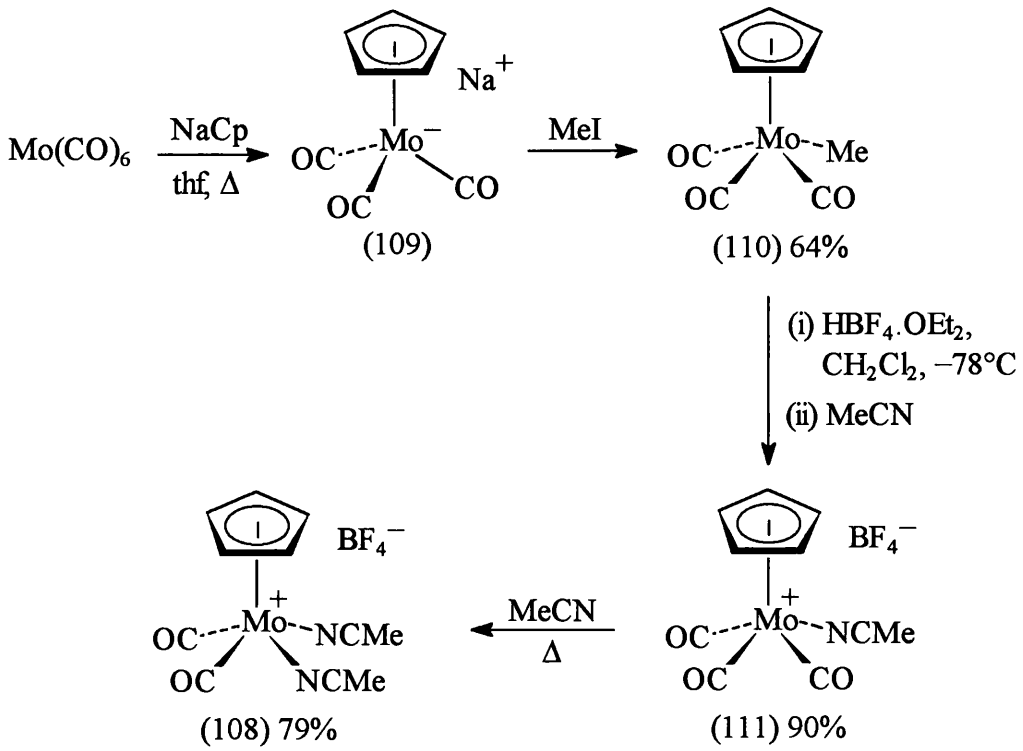

Figure 87

2.2.3 Synthesis of $[Mo(\eta^4\text{-}C_5H_6)(CO)_2(\eta^5\text{-}C_5H_5)][BF_4]$ (112)

Having established the ready availability of the η^5-cyclopentadienyl *cis*-bis(acetonitrile) cation (108), its reactivity with cyclopentadiene was examined. It was found that room temperature addition of excess, freshly distilled, cyclopentadiene to a relatively dilute solution of (108) in CH_2Cl_2 (*ca.* 0.01 mol dm^{-3}) led to facile ligand substitution and the formation of the desired cationic diene complex (112), obtained as a yellow powder in 90% yield (Fig. 88).

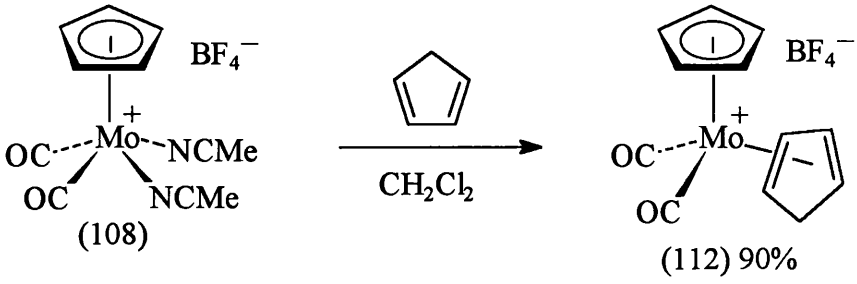

Figure 88

Complex (112) was found to be only soluble in polar solvents such as acetone, MeCN or $MeNO_2$, and sparingly soluble in CH_2Cl_2. The solution IR spectrum clearly showed two pairs of metal-carbonyl bands (2052 and 1998 cm^{-1}, 2025 and 1972 cm^{-1}), indicating the presence of both *exo* and *endo* conformers. The ^1H NMR spectrum displayed one set of time-averaged resonances with peaks at 6.35 and 4.65 ppm, assignable to the four symmetrically orientated diene protons, along with peaks at 3.90 and 3.50 ppm due to the methylene protons, in addition to the η^5-C_5H_5 peak at 5.85 ppm. The η^4-cyclopentadiene ligand in the ^{13}C-{^1H} NMR spectrum showed only three resonances at 85.5, 72.1 and 44.0 ppm (again reflecting the high symmetry of the diene).

The initial preparation (and subsequent solution handling) of the η^4-cyclopentadiene cation (112) was carried out using dilute conditions as described above. This was merely coincidental and did not form part of a pre-planned strategy. However, repeated attempts to form (112) under more concentrated conditions led to the serendipitous discovery of an interesting side-reaction. Infrared monitoring of the reaction between cyclopentadiene and a concentrated dichloromethane solution (108) (*ca.* 0.05 mol dm^{-3}) initially showed the presence of (108) and (112) along with the formation of a new species (ν_{CO} 2027 cm^{-1}). As the reaction progressed, the IR spectra revealed the gradual consumption of (108) and (112), and after three hours, only the strong band at 2027 cm^{-1} could be detected. Such a high frequency band suggested the formation of a monocarbonyl cationic species. Following standard work-up procedure, *via* the slow addition of Et_2O, a yellow solid was isolated. From an examination of the analytical and spectroscopic data, the product was readily identified as the known bis(η^5-cyclopentadienyl) cation[139] (113) (Fig. 89). In particular, the ^1H NMR spectrum clearly showed a high field resonance at -8.15 ppm, characteristic of the metal-hydrogen functionality present in this complex.

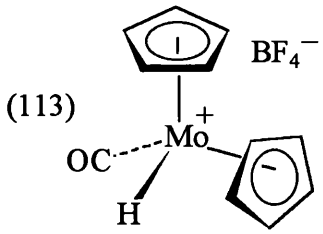

Figure 89

From the IR evidence it appears that the cationic complex (113) was generated from the initial formation of the η^4-cyclopentadiene complex (112) (Fig. 90), presumably *via* the loss of CO and a hydrogen transfer (the driving force of the reaction being the thermodynamic stability gained from forming a second η^5-cyclopentadienyl ligand). This was supported by the subsequent observation that (113) could be produced in near quantitative yield (89%) simply by stirring a concentrated solution of pure (112) in a suitable solvent (i.e. MeCN, $MeNO_2$ or acetone). When a saturated solution of (112) in $MeNO_2$ was left to stand at room temperature, the evolution of CO was clearly visible.

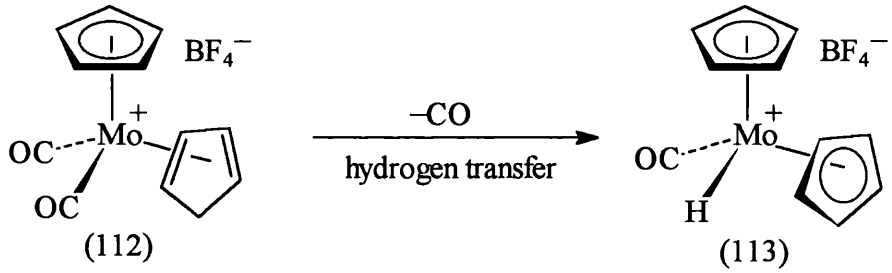

Figure 90

A detailed investigation into the kinetics of this reaction were beyond the scope of this work. However, (112) seemed to be reasonably stable in solution when kept at dilute concentrations (*ca.* 0.01 mol dm^{-3} or less).

The concentration dependent conversion of (112) to (113) implied that some sort of intermolecular hydrogen transfer reaction was taking place. On the basis of this information, a mechanism for this process can be suggested, which is shown in Figure 91. Loss of CO would lead to the creation of a 16-electron species (114), with a vacant coordination site at the metal. The binuclear combination of such species could then

form a cyclic intermediate (115) containing two metal-hydrogen agostic interactions. Subsequent break-up of this intermediate, *via* hydrogen transfer, would give rise to the thermodynamically more stable bis(η^5-cyclopentadienyl) cation (113).

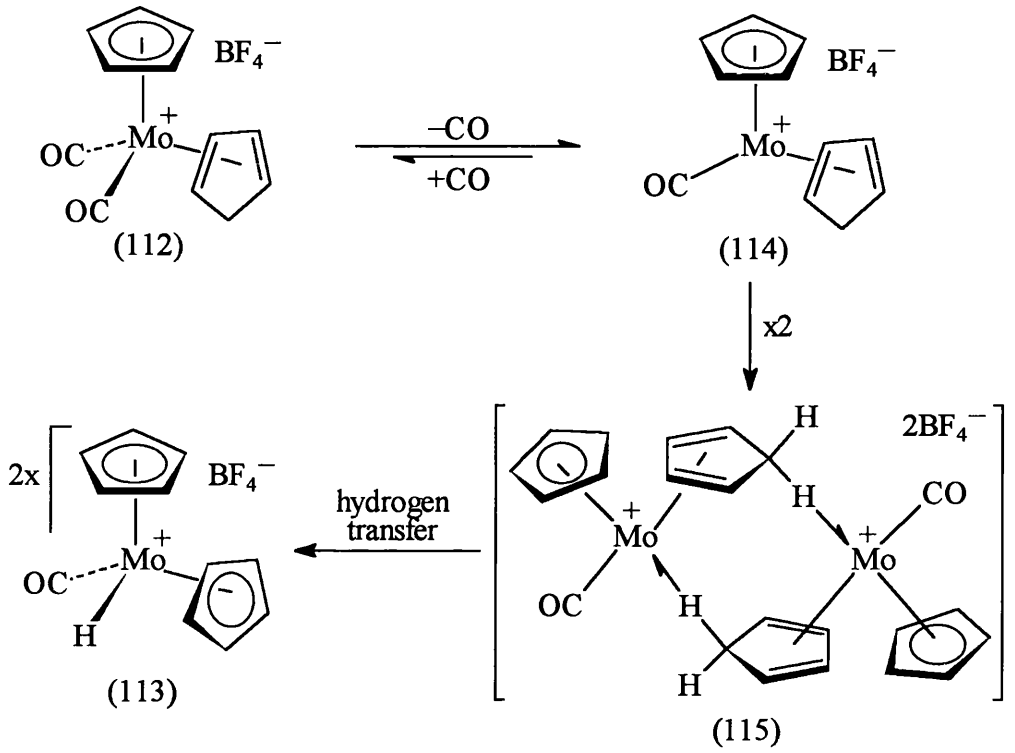

Figure 91

Interestingly, a search through the literature revealed that the η^4-cyclopentadiene cation (112) has previously been used by Beck for the synthesis of some binuclear molybdenum-rhenium carbonyl complexes.[140] However, no mention of the characterisation or stability of this complex was reported.

Although (112) could be readily synthesised under dilute conditions from the *cis*-bis(acetonitrile) cation (108), it was also thought worthwhile investigating whether this complex could be formed using related methodology established by Krivykh (see Section 1.2.2). The yellow π-allyl complex (25) was prepared in two steps from $Mo(CO)_6$ using the published procedure.[28] On adding one equivalent of $HBF_4.OEt_2$ to a cooled (-78°C) solution of (25) in dichloromethane, a deep red colouration was produced and the appearance of two high frequency metal-carbonyl bands in the IR

spectrum (2026 and 1975 cm^{-1}) was noted. This was attributed to the presence of the labile η^2-propene intermediate (26) (Fig. 92). Following the addition of excess, freshly distilled, cyclopentadiene, the solution was allowed to warm to room temperature resulting in the formation of a red-brown solidified mixture. It appeared that the product form this reaction was some sort of insoluble polymeric material, the identity of which was not ascertained. Clearly the desired η^4-cyclopentadiene cation is not available by this method.

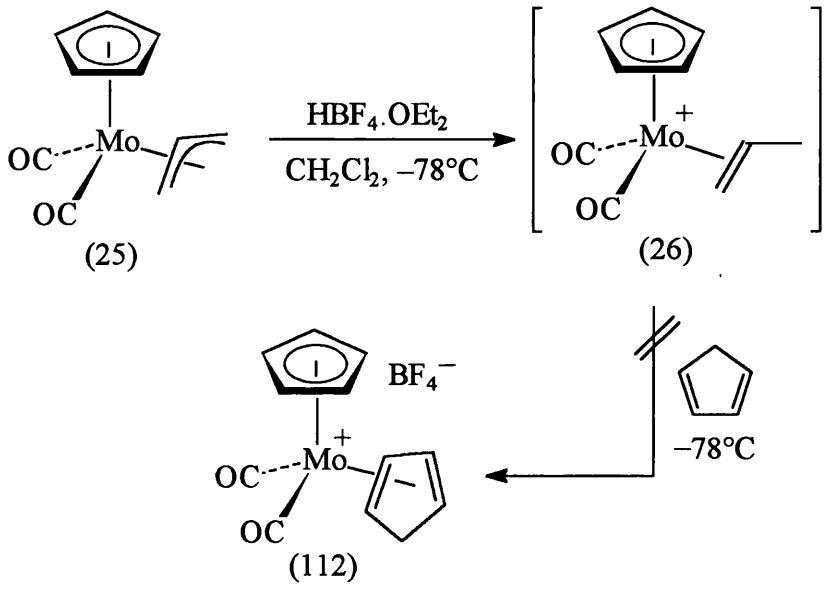

Figure 92

2.2.4 Deprotonation of $[Mo(\eta^4\text{-}C_5H_6)(CO)_2(\eta^5\text{-}C_5H_5)][BF_4]$ (112)

With access to the η^4-cyclopentadiene cation (112) the possibility of introducing functionality into the C_5-diene ligand was considered. It is known that treatment of the related cyclohexadiene-molybdenum complexes with base, results in the formation of η^3-dienyl complexes. For example, the η^5-indenyl complexes (13) and (18) both undergo smooth deprotonation reactions affording (116) and (117) respectively[39,112] (Fig, 93).

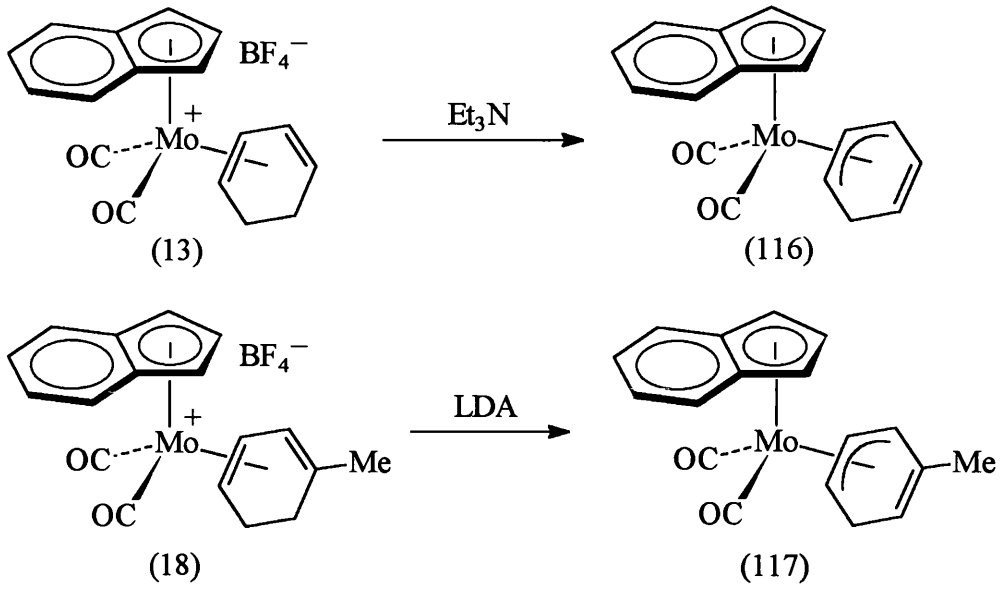

Figure 93

By applying similar procedures to the cyclopentadiene cation (112), it was envisaged that deprotonation would allow the formation of the corresponding dicyclopentadienyl complex (118) (Fig. 94). Such a species would be expected to contain a 'ring-slipped' system having η^3- and η^5-bonded cyclopentadienyl ligands.

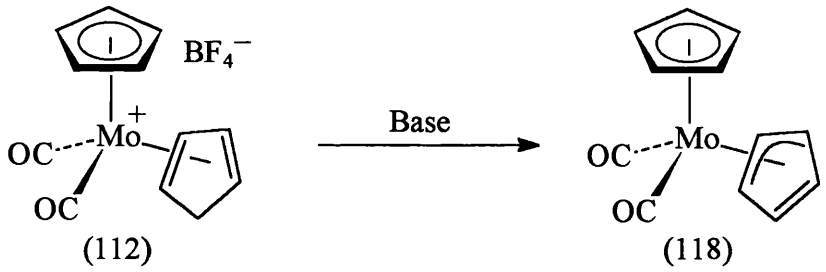

Figure 94

The analogous bis(cyclopentadienyl)tungsten dicarbonyl complex (119) has been prepared by Brintzinger.[141-144] He showed that when solutions of the monocarbonyl compound (120) were exposed to CO pressures of about 100 atm., complex (119) was formed as a blue material, in essentially quantitative yield, over a period of 12-15 hours (Fig. 95). However, no such transformations were observed at atmospheric pressures of CO. Interestingly, it was reported that the molybdenum complex (118) could not be prepared using this methodology.[141]

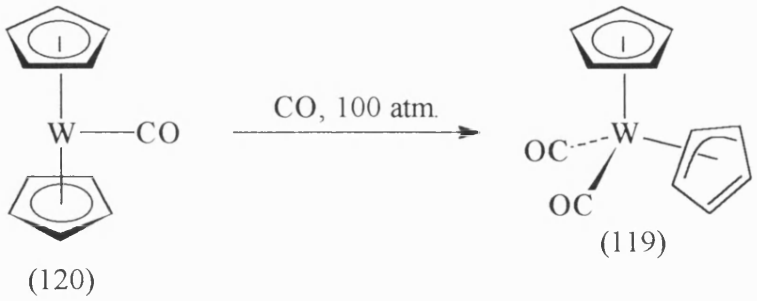

(120) (119)

Figure 95

The molecular structure of (119) has been determined by X-ray diffraction.[142] In this study it was confirmed that (119) contains a 'ring-slipped' system in which one of the cyclopentadienyl ligands is composed of a metal-coordinated η^3-allylic fragment (Fig. 96). As a result, this ligand adopts a bent arrangement in which the uncoordinated olefinic moiety is distorted from the plane passing through the three carbons of the η^3-allylic fragment (in contrast to the planar η^5-cyclopentadienyl ligand). Such a structure is necessary in order for (119) to satisfy the 18-electron rule.

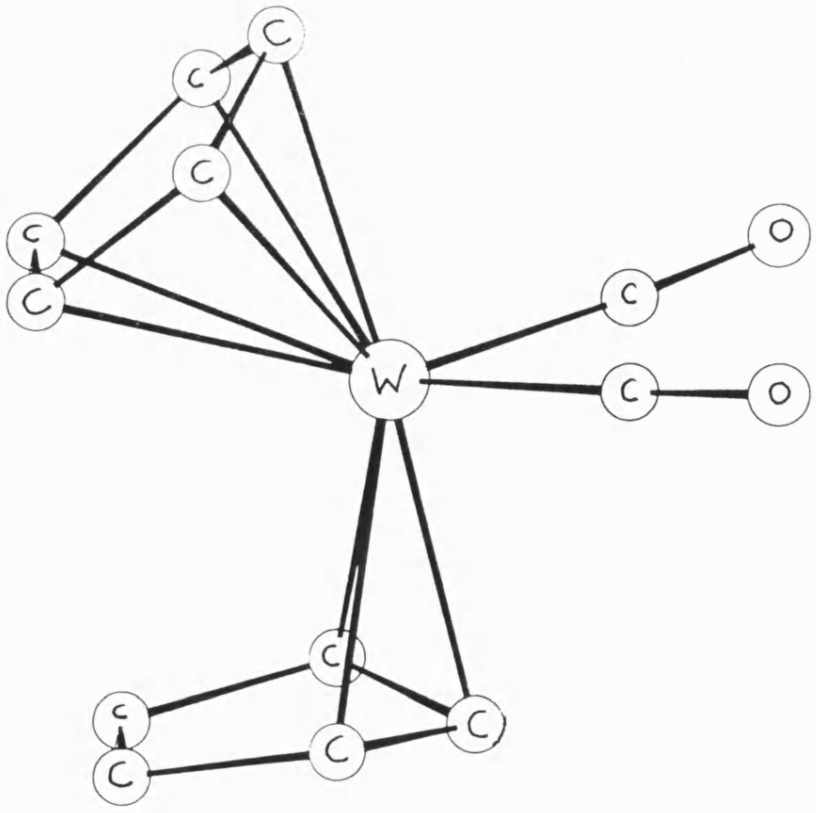

Figure 96. Molecular structure of $[W(\eta^3\text{-}C_5H_5)(CO)_2(\eta^5\text{-}C_5H_5)]$ (119).

It is not unreasonable to assume that the uncoordinated olefinic moiety present in (119) can undergo reactions that are normally associated with free alkenes, such as cyclisations or addition reactions.[145] The presence of the bulky metal fragment would be expected to control such reactions so that they occur stereospecifically. With regard to the tungsten complex (119), this type of chemistry has not previously been explored. It was therefore considered important to try to isolate the analogous molybdenum complex (118) [from the η^4-cyclopentadiene cation (112)] so that its potential as a precursor for the stereospecific elaboration of C_5-rings could be examined.

Thus, a cooled suspension of the yellow cation (112) (thf, -78°C) was treated with one equivalent of $Li[N(SiMe_3)]_2$ resulting in the immediate formation of a green solution. An IR spectrum of this solution showed the complete consumption of (112) and the formation of two new metal-carbonyl bands at 1952 and 1861 cm^{-1}, consistent with the presence of the desired η^3-cyclopentadienyl complex (118) [cf. IR data for the related tungsten complex (119) shows metal-carbonyl bands at 1955 and 1872 cm^{-1}]. However, after warming to room temperature and following usual work-up procedures, only the known bis(cyclopentadienyl) monocarbonyl complex $[Mo(\eta^5\text{-}C_5H_5)_2(CO)]$ (121)[146] was isolated. In a repeat of this reaction it was observed that (118) was only stable in solution at room temperature for about an hour. Monitoring by IR spectroscopy revealed the gradual consumption of (118) with the simultaneous growth of a single metal-carbonyl band at 1916 cm^{-1}, due to the formation of (121). It was therefore concluded that the η^3-cyclopentadienyl complex (118) could be readily formed at low temperature but was too unstable to be isolated (in accordance with the observations of Brintzinger),[143,144] preferring instead to rearrange to the monocarbonyl complex (121), *via* loss of CO and concomitant η^3- to η^5- conversion of a cyclopentadienyl ligand (Fig. 97).

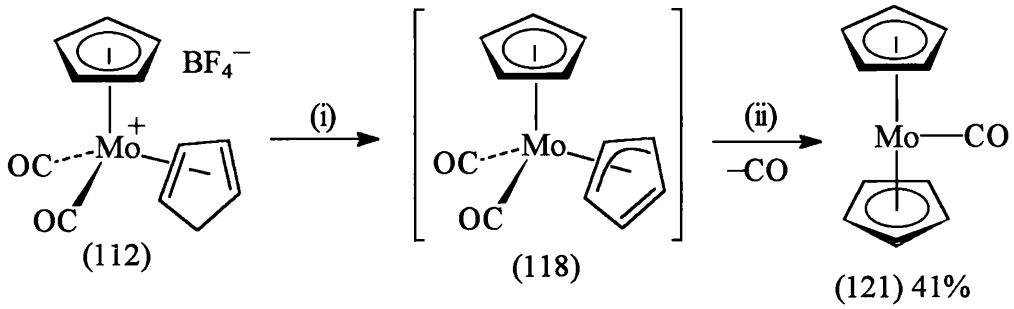

Figure 97. (i) $Li[N(SiMe_3)_2]$, thf, -78°C; (ii) warm to 25°C.

Although (118) could not be isolated, it is possible that the stereospecific elaboration of its uncoordinated olefinic fragment can be accomplished by examining its reactivity at low temperature. This avenue was not thoroughly explored, although its feasibility was demonstrated in a related reaction. A dilute dichloromethane solution of the π-allyl complex (25) was treated at low temperature (-78°C) with two equivalents of $HBF_4.OEt_2$ followed by addition of 2,4-cyclopentadien-1-yltrimethylsilane. After warming to room temperature and work-up of the reaction mixture, the η^4-cyclopentadiene cation (112) was isolated as the only product in 70% yield [N.B. when this reaction was repeated using concentrated conditions, the expected formation of (113) was observed]. A mechanism for this reaction can be suggested and is shown in Figure 98. The first step involves the precedented ligand substitution reaction to give the 1,3-diene cation (122). Presumably this undergoes a facile fluoride-anion-induced desilylation to generate the η^3-cyclopentadienyl intermediate (118). The presence of excess acid would be expected to cause an *exo*-facial electrophilic addition of H^+ at the uncoordinated olefinic fragment in (118), leading to the formation of the product (112).

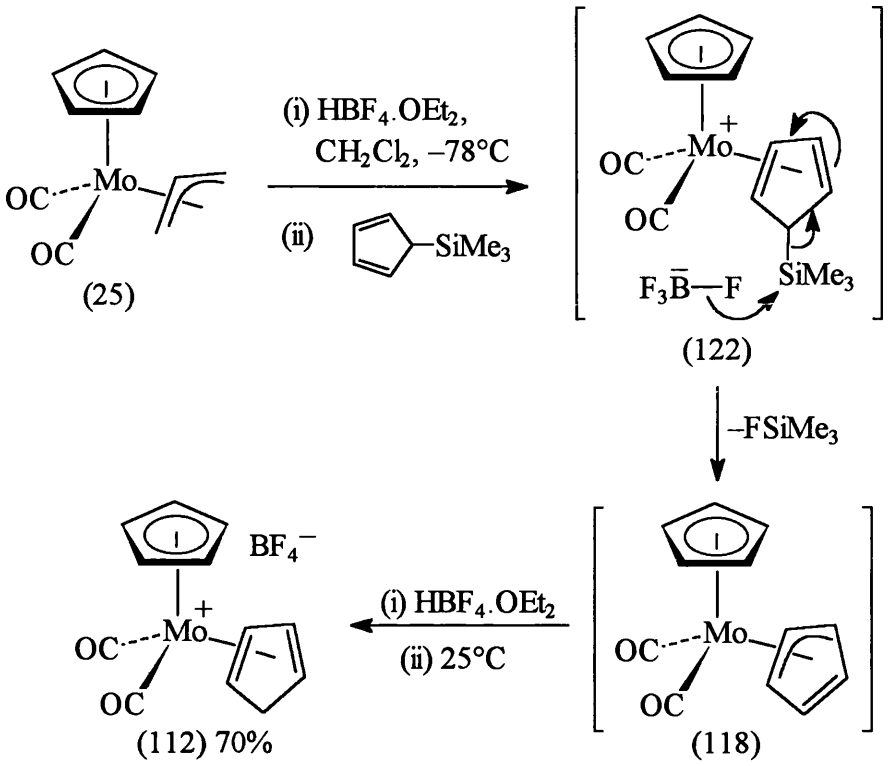

Figure 98

The success of the above reaction implies that the low temperature generation and subsequent reaction of (118) with electrophilic species, offers a potential strategy for the formation of stereochemically defined, substituted cyclopentadienes.

2.2.5 Nucleophilic Addition to $[Mo(\eta^4\text{-}C_5H_6)(CO)_2(\eta^5\text{-}C_5H_5)][BF_4]$ (112)

Following established concepts, it was expected that nucleophilic addition reactions to the terminus of the 1,3-diene chromophore present in complex (112) would provide a method of accessing stereospecifically substituted η^3-cyclopentenyl complexes. However, this area was only briefly investigated.

Treatment of (112) with sodium cyanoborohydride (thf, -78°C) resulted in smooth conversion to the η^3-cyclopentenyl complex (123),[147] obtained as a yellow powder in 70% yield (Fig. 99).

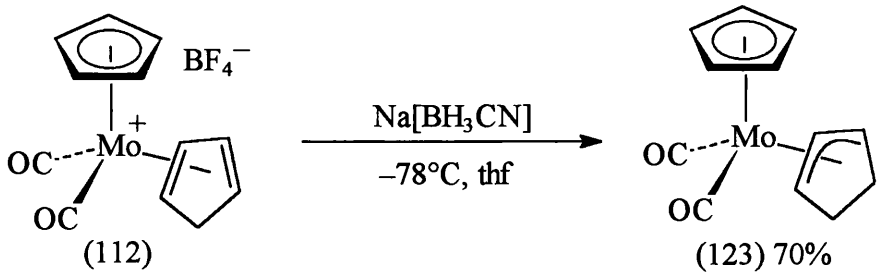

Figure 99

The IR spectrum of (123) showed two metal-carbonyl bands at 1935 and 1854 cm^{-1}, characteristic of a neutral η^3-allyl complex. The ^{13}C-{^1H} NMR spectrum displayed only three peaks for the η^3-cyclopentadienyl ligand at 60.5 (central allyl carbon), 57.9 (terminal allyl carbons) and 30.1 ppm (methylene carbons), attributed to the symmetrical orientation of the complex. A similar equivalence was observed in the ^1H NMR spectrum. Presumably (123) is formed *via exo*-facial attack of H^- at the terminus of the 1,3-diene moiety in (112).

Encouraged by this result, the reaction between (112) and a Grignard reagent was attempted. Low temperature treatment of (112) with one equivalent of MeMgI (thf, -78°C) resulted in the formation of a red/mauve solution. Monitoring by IR spectroscopy showed the complete consumption of (112) and the formation of two new metal-carbonyl bands at 1937 and 1862 cm^{-1}, implying the formation of a neutral η^3-allylic product. However, all attempts to isolate this species using standard work-up procedures were thwarted by its extremely sensitive nature. Hence, on the evidence of the IR data, the product can only be tentatively identified as the expected methyl-substituted η^3-cyclopentenyl complex (124) (Fig. 100).

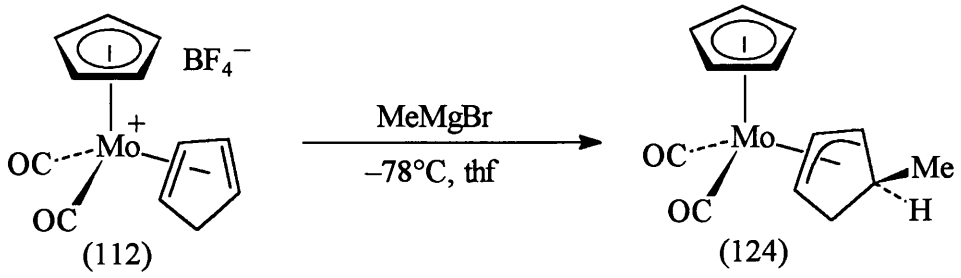

Figure 100

Unfortunately, a more detailed investigation of this reaction and the use of other nucleophilic reagents was not attempted, due to a lack of time. Further work is needed in this area in order to establish the methodology.

2.2.6 Summary and Conclusions

The synthesis of the η^4-cyclopentadiene cation $[Mo(\eta^4\text{-}C_5H_6)(CO)_2(\eta^5\text{-}C_5H_5)][BF_4]$ (112) has been achieved and it has been shown that this complex undergoes an interesting hydrogen transfer reaction when formed under concentrated conditions. From an initial investigation into the reactivity of (112), it is evident that the methods of deprotonation/electrophilic addition, and nucleophilic addition, could have potential as useful strategies for the elaboration of the coordinated C_5-ligand. However, further work needs to be done in this area in order to establish these principles.

In view of the formation of complex (112), it is reasonable to expect that substituted cyclopentadienes could be directly coordinated to a molybdenum centre using bis(acetonitrile) technology. This methodology should therefore provide a general route to a range of molybdenum-cyclopentadiene complexes. It is worth noting that the use of 1-trimethylsilyloxycyclopenta-1,3-diene (readily accessible from cyclopent-3-enone, which itself is formed[148] by palladium(0)-catalysed rearrangement of 3,4-epoxycyclopentene) would allow a more convenient preparation of Liebeskind's 4-oxo-η^3-cyclopentenyl complex (91), *via* a fluoride-anion-induced desilylation (Fig. 101).

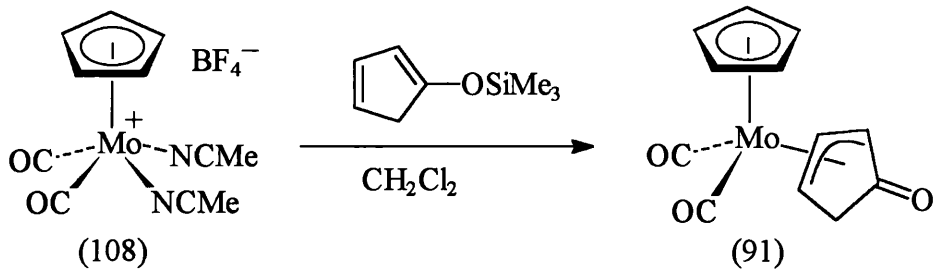

(108) (91)

Figure 101

2.3 Synthesis and Reactivity of 4-Oxo-η^3-butenyl Molybdenum Complexes and Related Compounds

2.3.1 Introduction

As a result of experience gained from the synthesis and reactivity of the 4-oxo-η^3-cyclohexenyl complex $[Mo(\eta^3\text{-}C_6H_7O)(CO)_2(\eta^5\text{-}C_9H_7)]$ (77) (see Section 2.1.1), Green and co-workers initiated a programme to examine the chemistry of the corresponding acyclic systems. Previous work in this area[43,44] has established the ready availability of the 4-oxo-η^3-butenyl complexes (125) and (126) from the reaction between the bis(acetonitrile) cation *cis*-$[Mo(NCMe)_2(CO)_2L][BF_4]$ [where L = η^5-C_9H_7 (15) or η^5-C_5Me_5 (16)] and 1-trimethylsilyloxybuta-1,3-diene (Fig. 102, overleaf). These complexes being formed from a non-rigid diene, can adopt four possible structural configurations, designated *exo-syn* (a), *endo-syn* (b), *exo-anti* (c) and *endo-anti* (d). [The overall orientation of the allyl ligand gives rise to *exo-endo* isomerism (see Section 1.3.2), while the terms *syn* and *anti* refer to the position of the aldehydic substituent relative to the C_3 backbone of the allyl ligand]. It was found that (125) and (126) are formed as isomeric mixtures of these species, being predominantly composed of the *syn* isomers (none of the *endo-anti* isomer was detected in either case, presumably as a result of steric interactions).

A rational explanation for these observations has been proposed,[44] based on the nature of the initially formed silyloxydiene intermediate (Fig. 103). Formation of the *syn*-oxoallyls takes place *via* the intermediacy of an *s-trans*-diene cation, whilst the *anti*-oxoallyls are derived from the corresponding *s-cis*-diene intermediate. The initial coordination of the silyloxydiene gives rise to the *s-trans*-diene intermediate (the kinetic product). It is the competition between the rate of fluoride-anion-induced desilylation of this species and the rate of formation of the *s-cis*-diene cation that is responsible for the ratio of isomers observed. The presence of a highly nucleophilic fluoride anion results in the short-lived presence of the *s-trans*-diene cation, thereby affording a greater proportion of the *syn* isomer.

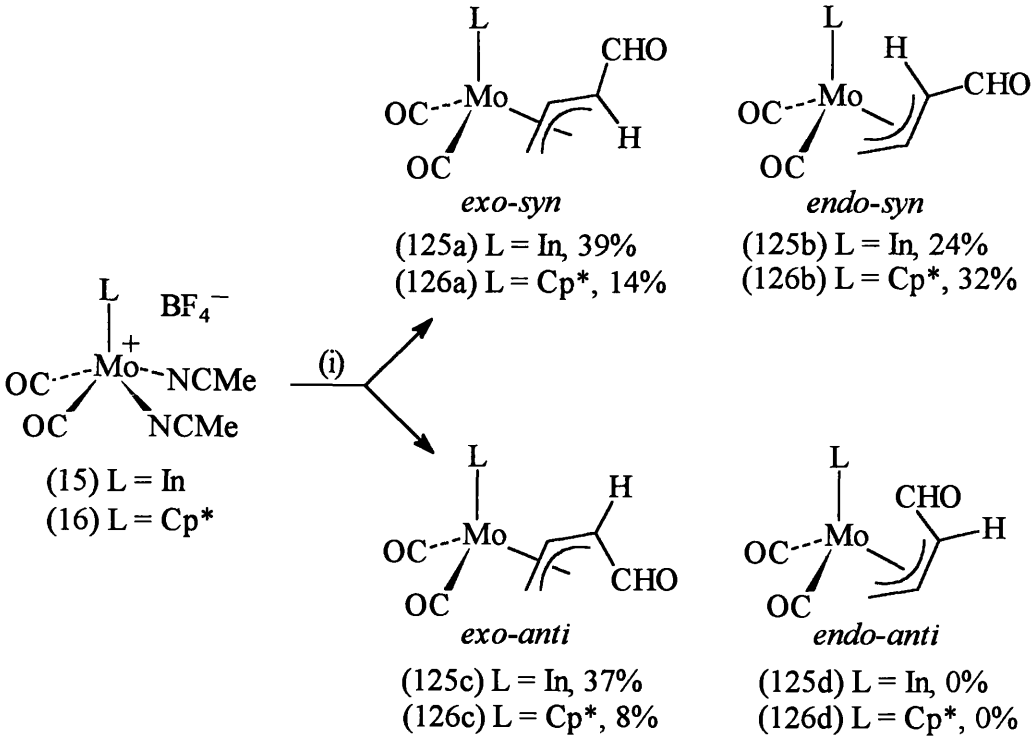

Figure 102. (i) 1-Trimethylsilyloxybuta-1,3-diene.

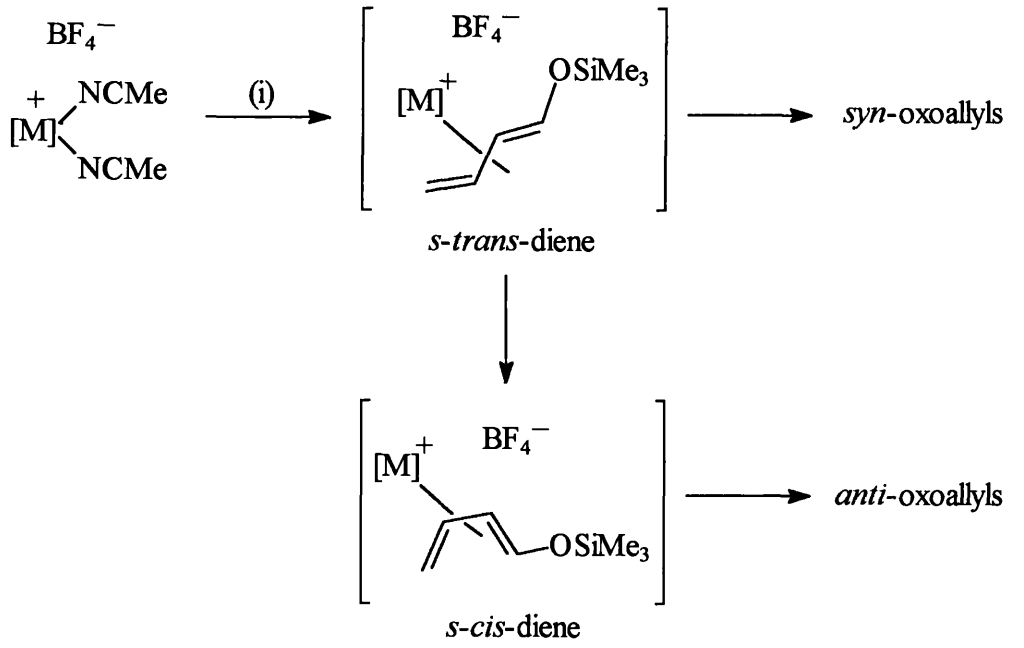

Figure 103. [M] = $Mo(CO)_2L$, L = η^5-C_9H_7 or η^5-C_5Me_5;
(i) 1-Trimethylsilyloxybuta-1,3-diene.

The *syn* and *anti* isomers of (126) can be readily separated by column chromatography, however this is not possible for the η^5-indenyl species (125). Alternatively, exclusive isolation of the *anti* isomers of both (125) and (126) can be achieved *via* a *syn* to *anti* conversion using a simple protonation/deprotonation procedure (see Section 2.3.2).

Complexes (125) and (126) have also been shown to successfully undergo Wittig reactions.[44] [This is in contrast to the behaviour of the cyclic ketoallyl complexes (77) and (92), for which the presence of acidic α-protons precludes the use of Wittig reagents.[40]]

In a recent study, Liu and co-workers have investigated the functionalisation of some related *syn*-η^3-butenyl complexes, and demonstrated their potential for use as precursors to a variety of stereodefined organic compounds.[149-151]

We wished to further develop the chemistry of the 4-oxo-η^3-butenyl complexes by examining alternative approaches to their selective synthesis and expanding our knowledge of the reactivity associated with such systems. The following sub-sections describe the additional work that has been carried out in this area. (N.B. For comparative purposes, selected NMR data is given at the end of certain sub-sections.)

2.3.2 A Protonation/Deprotonation Procedure for the *Syn* to *Anti* Conversion of 4-Oxo-η^3-butenyl Complexes

During the course of their initial investigation Green and co-workers discovered an interesting isomerisation process for the *syn* to *anti* conversion of the 4-oxo-η^3-butenyl molybdenum complexes (125) and (126).[43,44] This process, which proceeds *via* a protonation/deprotonation sequence, has been rationalised as a result of a mechanistic study on complex (126) and is illustrated in Figure 104. It was found that low temperature (-78°C) addition of $HBF_4.OEt_2$ to a dichloromethane solution of the *syn*-oxoallyl complex (126a), (126b) (3:7 mixture) leads to the initial formation of the thermally unstable *exo-s-trans* (30%) and *endo-s-trans* (70%) hydroxybutadiene cations

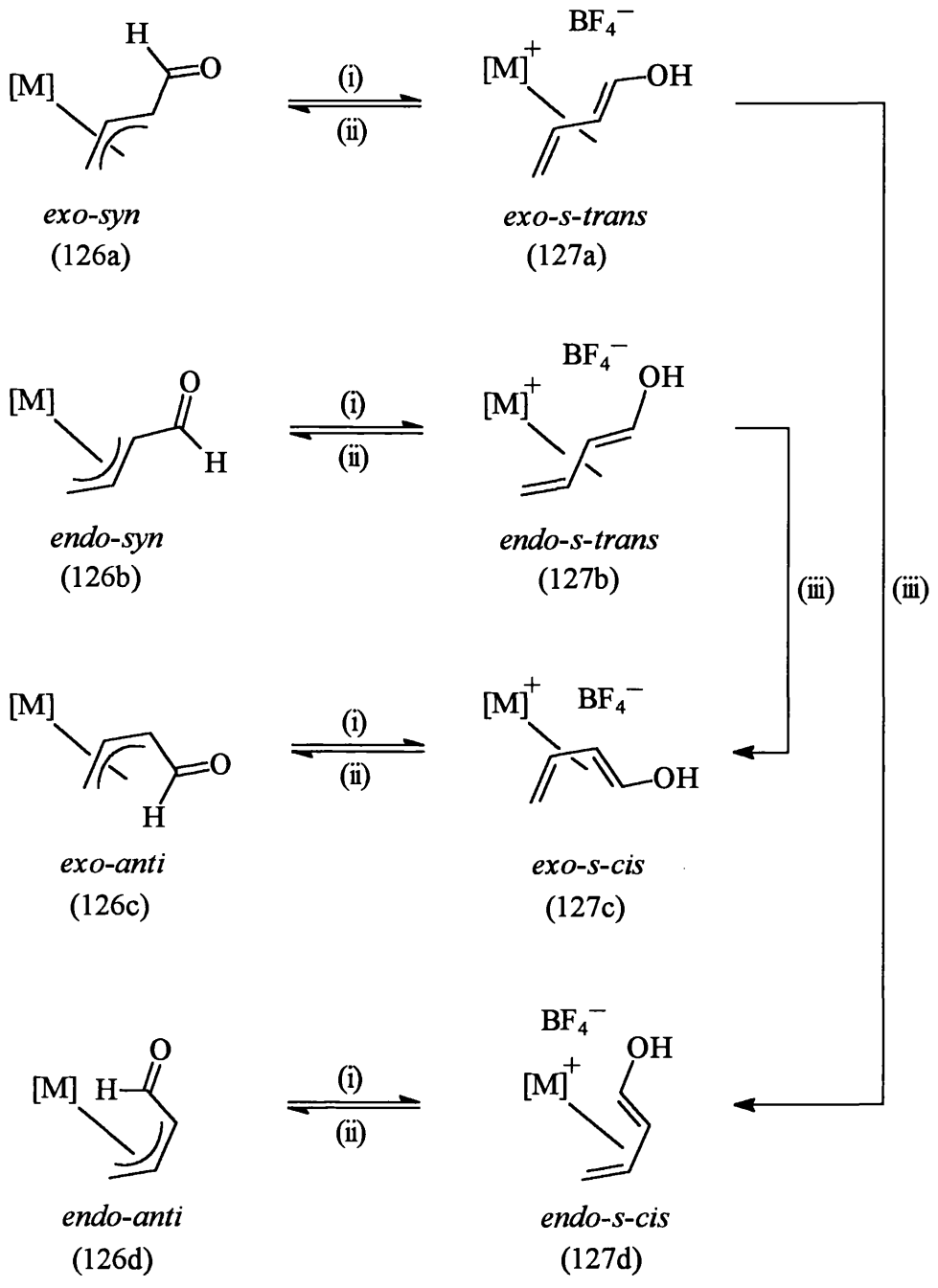

Figure 104. [M] = $Mo(CO)_2(\eta^5\text{-}C_5Me_5)$. (i) $HBF_4.OEt_2$, CH_2Cl_2, -78°C; (ii) Et_3N, CH_2Cl_2, -78°C; (iii) warming to room temperature.

(127a) and (127b). Addition of triethylamine to (127a), (127b) at -78°C regenerates the *syn*-oxoallyl starting mixture (126a), (126b). Alternatively, on warming to room temperature, these species undergo an irreversible rearrangement to the corresponding *exo-s-cis* and *endo-s-cis* diene cations (127c) and (127d), which are non-interconverting and can be isolated as an isomeric mixture. This represents an overall rotation about the central C^2-C^3 axis, which is assumed to take place *via* a coordinatively unsaturated η^2-diene species. Deprotonation of (127c), (127d) with triethylamine generates the *anti*-oxoallyls (126c), (126d) from which only the *exo-anti* isomer (126c) can be isolated. Protonation of (126c) gives, in turn, the *exo-s-cis* cation (127c). Thus, overall a *syn*-allyl $\rightleftharpoons$ *s-trans*-diene $\rightarrow$ *s-cis*-diene $\rightleftharpoons$ *anti*-allyl structural relationship has been established for the molybdenum oxoallyl complexes (125) and (126).

In view of these results, it was decided to examine whether such a *syn* to *anti* isomerisation process could be effected using oxoallyl complexes containing metal centres other than molybdenum. The analogous ruthenium system was the initial choice of study for this investigation. Thus, the yellow ruthenium *exo-syn*-oxoallyl complex (128a) was readily prepared according to an established procedure[57,58] (Fig. 105). Although this complex is obtained as an isomeric mixture, exclusive isolation of the *exo-syn* isomer can be obtained by fractional crystallisation.

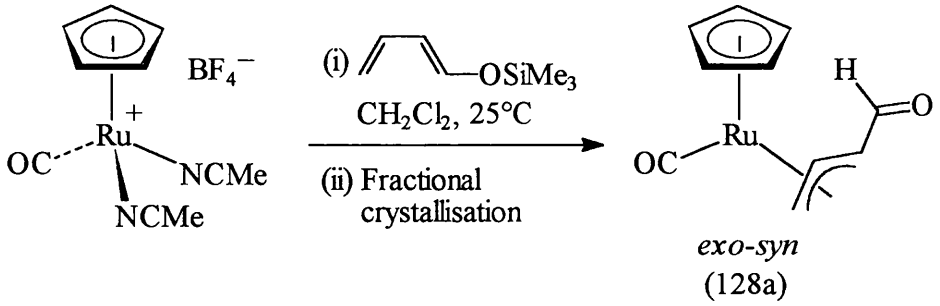

Figure 105

Complex (128a) was subjected to the protonation/deprotonation sequence. Treatment of a cooled (-78°C) dichloromethane solution of (128a) with $HBF_4.OE_2$ was followed by warming to room temperature. Monitoring by IR spectroscopy revealed the complete consumption of (128a) and the formation of a new product (ν_{CO} /cm^{-1} at

2010), tentatively identified as an *endo-s-cis*-diene cation (129d) (in accordance with the proposed mechanism). This species was not isolated but treated directly with triethylamine to afford exclusively the *endo-anti*-oxoallyl complex (128d) as a pale yellow solid in 87% yield. Clearly, a *syn* to *anti* isomerisation had taken place, presumably *via* a similar system mechanism to that proposed for the molybdenum system (Fig. 106).

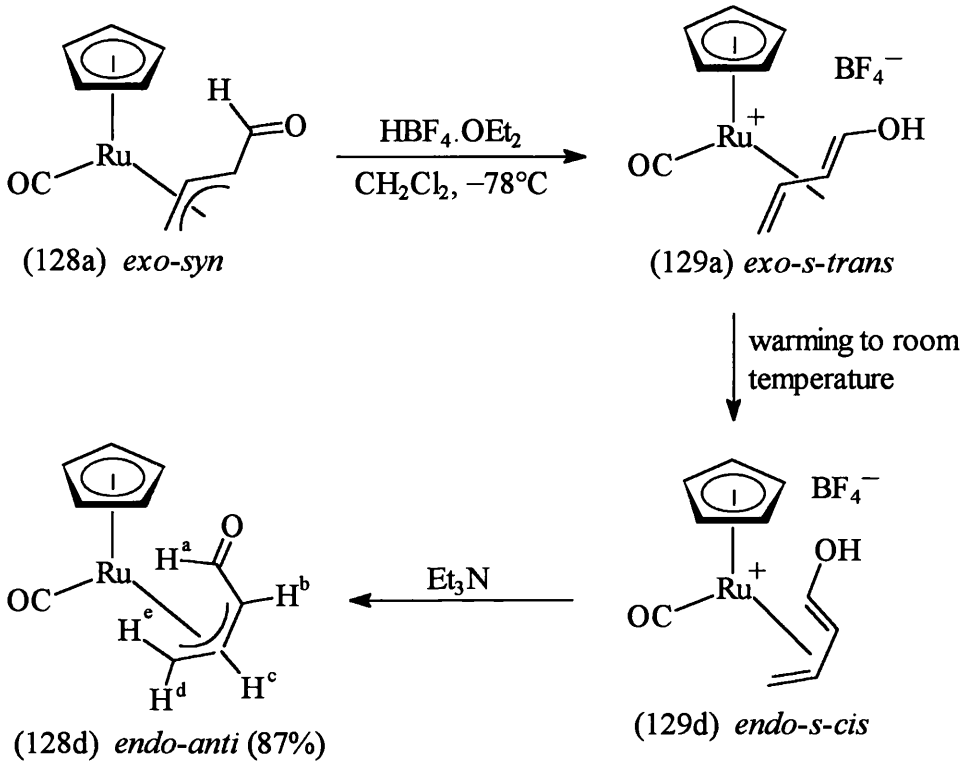

Figure 106

The assignment of an *endo-anti* configuration for the product (128d) was based on certain NMR parameters. Differentiation between *syn* and *anti* isomers can be derived from the vicinal ^{3}J(H-H) couplings of the allylic protons, in particular $^{3}J(H^{b}H^{c})$ which is transoid in nature for the *syn* isomers and cisoid for the *anti*, decreasing as might be expected in the case of the latter. Marked differences in chemical shift like wise allow *exo* and *endo* isomers to be distinguished[44,64] (see Table 2, page 89).

A similar protonation/deprotonation sequence was also carried out on the corresponding iron system. The orange iron *exo-syn*-oxoallyl complex (130a) was

readily prepared using an established route[110] (Fig. 107). Notably the product is isolated as a single isomer in this reaction.

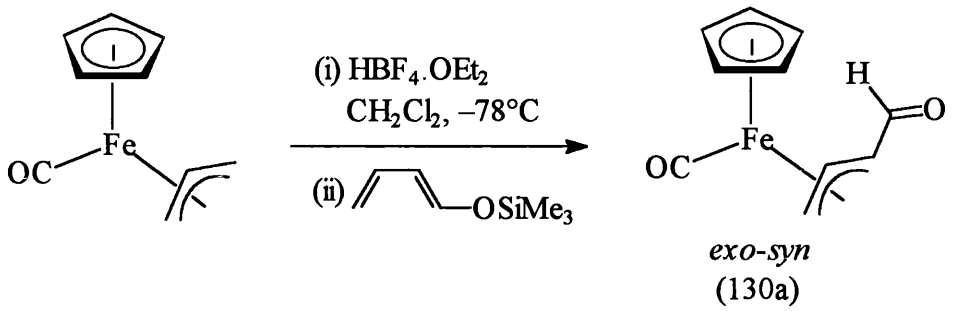

Figure 107

Low temperature addition of $HBF_4.OEt_2$ (-78°C) to a dichloromethane solution of (130a) caused the mixture to immediately turn red in colour, presumably due to the formation of an *exo-s-trans*-diene cation (131a). Subsequent warming to room temperature followed by treatment with triethylamine afforded the *endo-anti* oxoallyl complex (130d) as a yellow powder in 92% yield. An examination and comparison of the NMR data confirmed the structural orientation of the product. Again, this *syn* to *anti* isomerisation can be explained in terms of the proposed mechanism (Fig. 108).

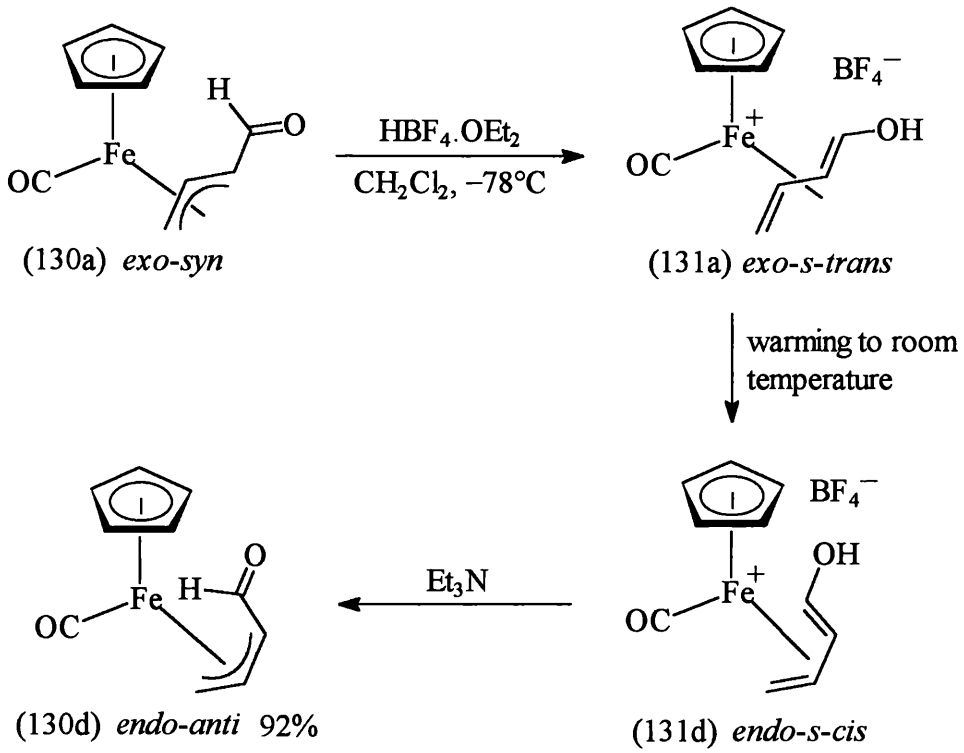

Figure 108

Table 2

^{1}H NMR data for the oxoallyl complexes [M(η^3-$CH_2CHCHCHO$)(CO)(η^5-C_5H_5)]

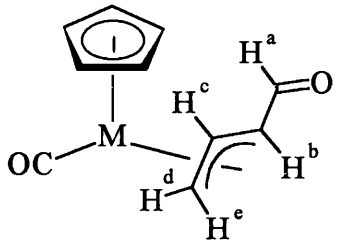

Complex	(128a)*	(128d)*	(130a)*	(130d)†
M	Ru	Ru	Fe	Fe
Isomer	*exo-syn*	*endo-anti*	*exo-syn*	*endo-anti*
$\delta(H^a)$	9.00	7.78	9.37	7.35
$\delta(H^b)$	2.46	4.40	1.44	4.30
$\delta(H^c)$	4.20	4.66	5.33	5.25
$\delta(H^d)$	2.67	3.19	3.08	3.05
$\delta(H^e)$	1.53	2.16	1.19	1.31
$J(H^aH^b)$	5.5	7.7	6.1	7.3
$J(H^bH^c)$	9.2	6.8	9.8	7.3
$J(H^cH^d)$	7.0	7.9	7.2	7.9
$J(H^cH^e)$	11.1	11.4	11.5	11.9

Shifts in ppm downfield form TMS. Coupling constants in Hz.

* In a CD_2Cl_2 solution, 20°C.

† In a $CDCl_3$ solution, 20°C.

The success of the above reactions suggests that the *syn*-allyl ⇌ *s-trans*-diene → *s-cis*-diene ⇌ *anti*-allyl structural relationship established for the molybdenum oxoallyls, is also inherent in the analogous ruthenium and iron systems. Thus, the protonation/deprotonation sequence can be used as a general method for the *syn* to *anti* isomerisation of oxoallyl complexes.

2.3.3 Selective Synthesis of *Anti*-4-oxo-η^3-butenyl Complexes using Acetoxy-1,3-butadiene.

The asymmetry associated with the 4-oxo-η^3-butenyl complexes (due to the presence of the oxoallyl ligand) causes them to be chiral. It should therefore be possible to resolve these compounds into their respective enantiomers. The classical method, previously used for the resolution of the analogous cyclic ketoallyl complex (77) (see Section 1.6), could be used for this purpose. However, the uneconomical nature of this process prompted us to examine an alternative route by which we might obtain optically pure oxoallyl complexes.

The use of biotransformations for enantioselective organic synthesis is an area that has been developing rapidly over the last decade.[152] In a recent publication,[153] Crout and co-workers reported the use of an enzyme, pig liver esterase (PLE), for the catalytic enantioselective hydrolysis of the ester-substituted $Fe(CO)_3$ complex (132) (Fig. 109). This process, which proceeds by way of a kinetic resolution, offers a simple and efficient means of accessing compounds in optically active form.

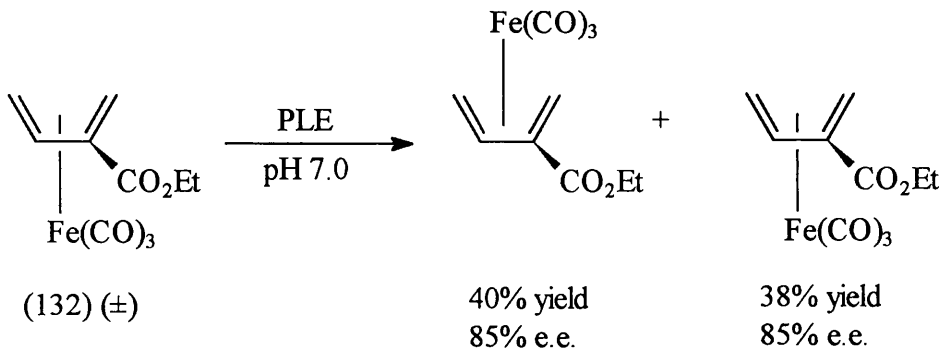

Figure 109

It was thus envisaged that a similar approach could be used for the enantioselective resolution of our molybdenum oxoallyl complexes. This requires a modification to our existing methodology in which an ester functionality is introduced at the complexation stage. The proposed route by which we hoped to efficiently obtain enantiomerically pure oxoallyls is illustrated in Figure 110 for the η^5-pentamethyl-cyclopentadienyl system.

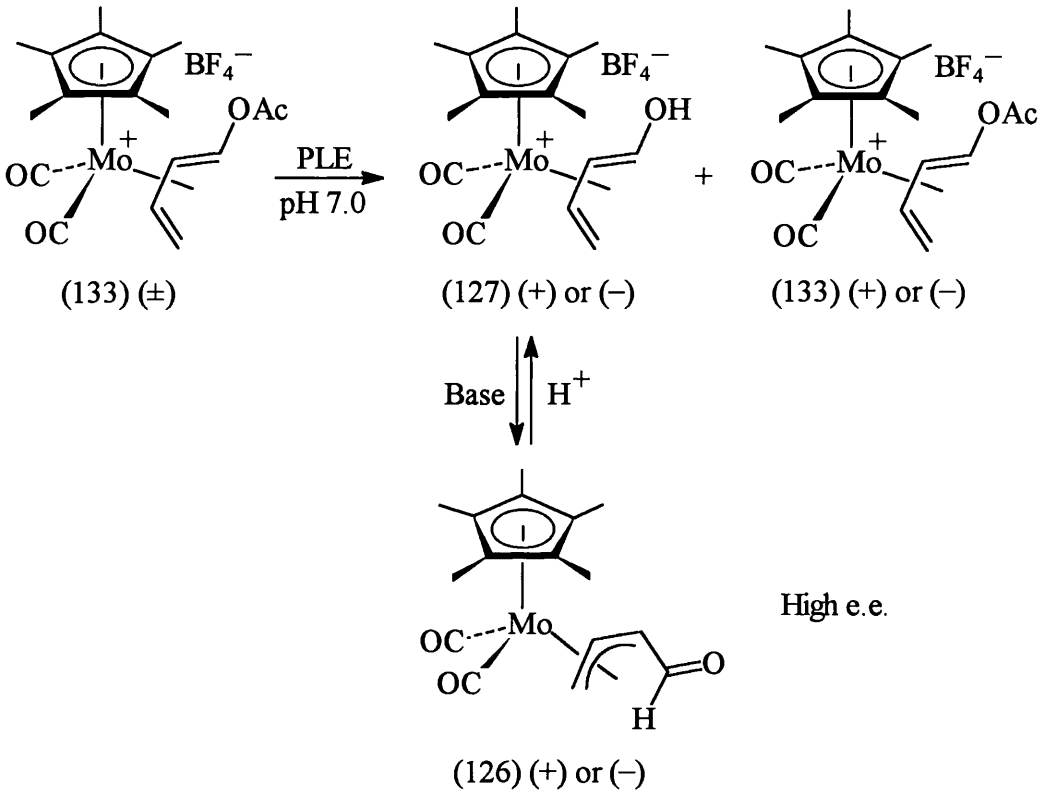

(133) (±) (127) (+) or (–) (133) (+) or (–)

(126) (+) or (–) High e.e.

Figure 110

In order to study the viability of this process it was necessary to isolate the acetoxy-diene complex (133). Treatment of the η^5-C_5Me_5 *cis*-bis(acetonitrile) cation (16) with 1-acetoxy-1,3-butadiene (CH_2Cl_2, 4 d) resulted in smooth conversion to (133), isolated as a green solid in 71% yield (Fig. 111). The IR spectrum of this species showed two clear high frequency metal-carbonyl bands at 2053 and 2006 cm^{-1}, characteristic of a cationic η^4-1,3-diene complex, along with a band at 1759 cm^{-1} due to the presence of the organic carbonyl functionality. The ^1H NMR spectrum displayed a set of broadened resonances at 6.08 (H^c), 5.97 (H^b), 4.58 (H^a), 2.57 (H^d) and 1.05 ppm

(H^e), which could be unequivocally assigned to an *s-cis* configuration of the diene moiety (an *s-trans*-diene would be expected to show much lower-field chemical shifts for H^a and H^e due to their more exposed orientation in space in this configuration).[44]

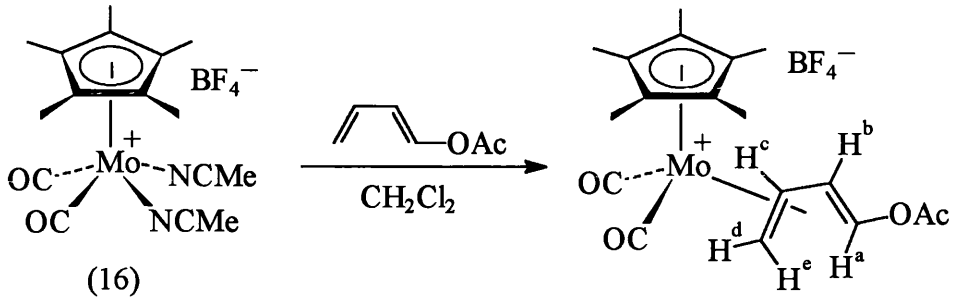

Figure 111

Having established the ready availability of the η^5-pentamethylcyclopentadienyl acetoxy-diene cation (133), its suitability for resolution *via* enzymatic hydrolysis was exmined. Invariably such biotransformations are carried out in an aqueous buffer solution at controlled pH (ideally pH 7-8 for PLE).[152] It was essential that (133) was stable under such conditions (i.e. not susceptible to water-induced hydrolysis or decomposition). Hence, the stability of this cation in water was studied. IR monitoring of a stirred aqueous solution (pH 7) of (133) revealed approximately 35% conversion (after 1 h) to a hydrolysis product, exhibiting bands at 1960, 1883 and 1644 cm^{-1} (characteristic of a neutral oxoallyl complex). As a result of this experiment, we concluded that (133) was far too sensitive towards hydrolysis, and thus would not be suitable for PLE enzymatic resolution.

The exact identity of the hydrolysis product derived from (133) was subsequently found to be the *exo-anti*-oxoallyl complex (126c). The use of more basic conditions in a two-phase reaction [CH_2Cl_2/$NaHCO_3$ (aq.) *ca.* pH 8.5] afforded (126c) as a yellow crystalline solid in 81% yield (Fig. 112). Examination and comparison of the spectroscopic data for this species readily confirmed the exclusive formation of the *exo-anti* isomer.[44] In particular, the chemical shifts for the allyl ligand in the ^1H NMR are consistent with an *exo* conformation (see Table 4, p.102). Similarly, the magnitude

of the $J(H^bH^c)$ coupling constant (7.1 Hz) implies a cisoid relationship between H^b and H^c, indicative of an *anti*-configuration [these protons are transoid in nature when in the *syn* configuration, giving a higher value for this coupling constant (*ca.* 9.4 Hz)].[44]

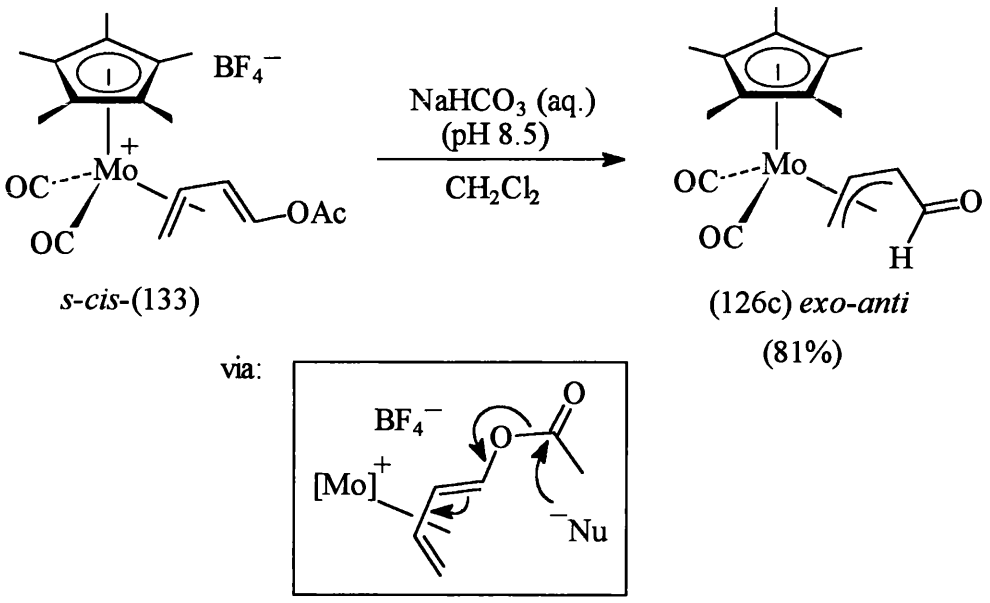

Figure 112

The selective formation of the *exo-anti*-oxoallyl complex (126c) by the above process provides conclusive evidence that *anti*-oxoallyls are formed directly from the corresponding *s-cis*-diene precursor (cf. Section 2.3.1). It is also interesting to note that the presence of an *endo-anti* isomer was not detected. Presumably this is because the energy barrier for *exo-endo* interconversion of *anti*-(126) is too high for this process to occur at room temperature.

In order to throw further light on the nature of the bonding and orientation within an *exo-anti*-oxoallyl configuration, complex (126c) was the subject of a single crystal X-ray diffraction study. The molecular structure of (126c) is illustrated in Figure 113, with selected bond lengths and interbond angles being listed in Table 3.

The central molybdenum atom can be described as seven-coordinate, being bonded to two terminal carbonyl ligands, an η^3-*anti*-oxoallyl fragment and an η^5-pentamethylcyclopentadienyl ligand, which is considered to occupy three coordination sites. Both metal-carbonyl groups are essentially linear, within experimental error, with

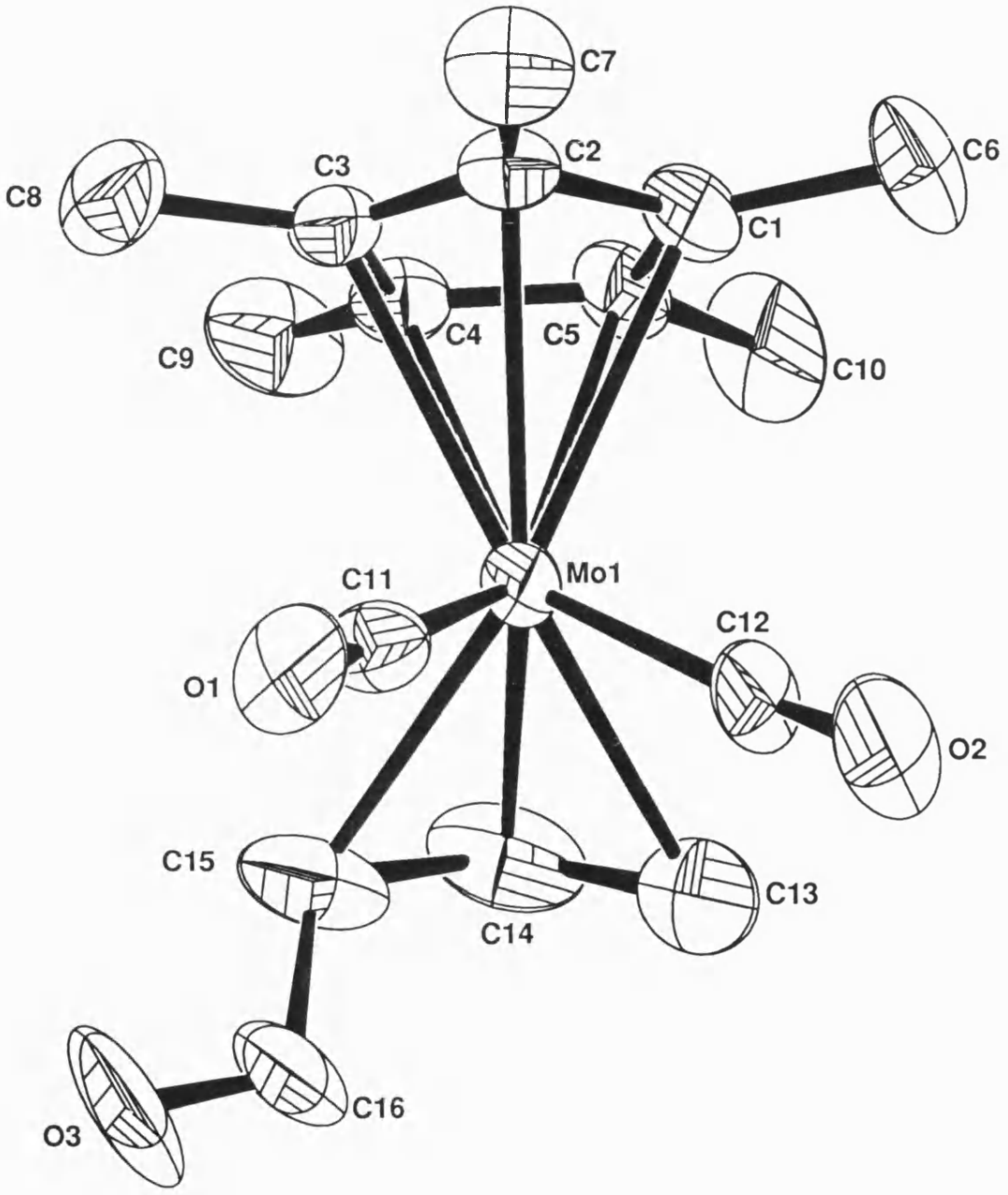

Figure 113.

Molecular structure of *exo-anti*-[Mo(η^3-$CH_2CHCHCHO$)$(CO)_2$(η^5-C_5Me_5)] (126c).

Table 3

Selected bond lengths (Å) and angles (°) for complex (126c) with estimated standard deviations in parenthesis.

Mo-C(1)	2.339(10)	Mo-C(2)	2.319(11)
Mo-C(3)	2.322(10)	Mo-C(4)	2.366(10)
Mo-C(5)	2.373(10)	Mo-C(11)	1.915(17)
Mo-C(12)	1.971(16)	Mo-C(13)	2.303(14)
Mo-C(14)	2.176(13)	Mo-C(15)	2.297(13)
C(11)-O(1)	1.153(17)	C(12)-O(2)	1.126(15)
C(13)-C(14)	1.401(18)	C(14)-C(15)	1.439(20)
C(15)-C(16)	1.555(21)	C(16)-O(3)	1.246(23)
Mo-C(11)-O(1)	174.7(13)	Mo-C(12)-O(2)	174.7(16)
C(11)-Mo-C(12)	80.4(7)	C(13)-C(14)-C(15)	123.5(12)
C(14)-C(15)-C(16)	121.7(14)	C(15)-C(16)-O(3)	125.4(16)

Mo-C-O bond angles of 174.7°, the Mo-C and C-O bond lengths being typical.[129] These two carbonyl ligands lie at an angle of 80.4° to one another. The C_5Me_5 ligand is essentially planar, being bonded to molybdenum at a mean bond distance of 2.344 Å.

The *anti*-oxoallyl ligand is bound *via* C(13), C(14) and C(15) to the metal, with O(3) of the aldehydic carbonyl group bent away from the molybdenum atom at a non-bonding distance of 3.979 Å. The η^3-allyl backbone can be seen to adopt an *exo* orientation with respect to the η^5-C_5Me_5 ligand, the C(13)-C(14)-C(15) bond angle of 123.5° being typical[154] of acyclic η^3-allyl complexes. As with the majority of Mo(II) *exo*-η^3-allyls, the inner carbon atom of the allyl moiety is closer to the metal [Mo-C(14) 2.176(13) Å] than both the outer carbons [Mo-C(13) 2.303(14) and Mo-C(15) 2.297(13) Å].[29,154] Finally, it is interesting that the carbon-carbon interatomic distances

of 1.401(18) and 1.439(20) Å within the metal bound part of the ligand are somewhat unsymmetrical. This, together with the bond distances C(16)-O(3) 1.246(23) and C(15)-C(16) 1.555(21) Å, implies some degree of π-conjugation between the η^3-allyl and the aldehydic carbonyl group.[116] Hence, the overall structure can be viewed as the sum of the two resonance forms shown in Figure 114. The partial diene character can be expected to exert a greater degree of rigidity within the oxoallyl ligand.

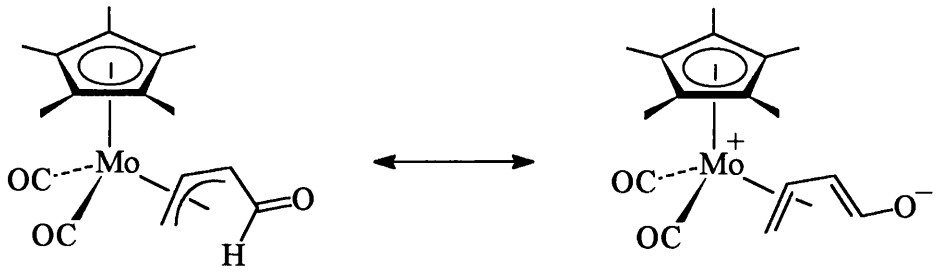

(126c) *exo-anti*

Figure 114

This latter observation is typical for 4-oxo-η^3-allyl complexes [cf. the cyclic ketoallyl complex (77)][40] and readily accounts for the low frequency aldehydic carbonyl band present in the IR spectrum of these species [ν_{CO}/cm^{-1} (126c) 1644].

Along with the above mentioned η^5-C_5Me_5 acetoxy-diene complex (133), the analogous η^5-C_5H_5 species was simultaneously prepared and examined for its potential as a candidate for enzymatic resolution. Treatment of the η^5-C_5H_5 *cis*-bis(acetonitrile) cation (108) with 1-acetoxy-1,3-butadiene (CH_2Cl_2) resulted in comparatively faster conversion (2 d) to the corresponding cationic acetoxy-substituted η^4-diene (134), isolated as a rather insoluble yellow solid in 85% yield (Fig. 115). As in the case of (133), the IR spectrum for this cation (134) showed two high frequency metal-carbonyl bands at 2068 and 2020 cm^{-1}, along with a band at 1759 cm^{-1} due to the carbonyl in the ester moiety. Similarly, the ^1H NMR spectrum displayed a set of broadened resonances for the diene protons at 6.48 (H^b), 6.29 (H^c), 6.07 (H^a), 3.01 (H^d) and 2.38 (H^e) ppm, characteristic of an *s-cis* configuration. The broadening of the signals presumably arises as a result of fluxional behaviour within the diene ligand (see Section 1.3.2).

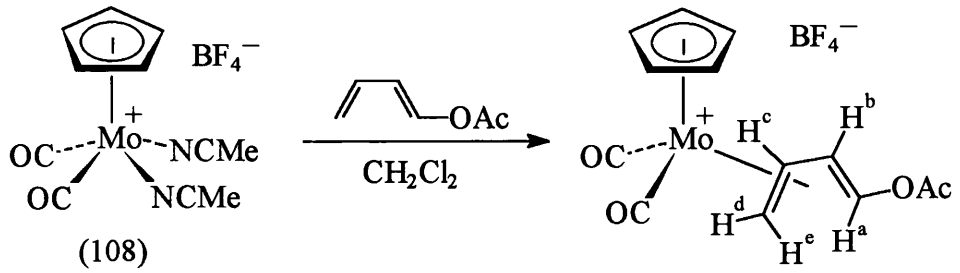

s-cis-(134) 85%

Figure 115

Complex (134) was also subjected to water stability tests in order to determine its suitability for resolution *via* enzymatic hydrolysis. IR monitoring of a stirred aqueous solution (pH 7) of (134) revealed approximately 60% conversion (after 1 h) to the hydrolysis product (an oxoallyl complex), exhibiting bands at 1973, 1896 and 1649 cm^{-1}. This implied that (134) was even more sensitive to hydrolysis than the corresponding η^5-C_5Me_5 cation (133), and therefore would also be unsuitable for PLE-catalysed resolution. [The difference in reactivity between (133) and (134) can be attributed to the respective stabilising properties provided by the η^5-C_5Me_5 and η^5-C_5H_5 ligands. The η^5-C_5Me_5 ligand has the stronger electron-donating effect, helping to stabilise the positive charge at molybdenum in (133), making this cation less susceptible to nucleophilic attack (hydrolysis)].

The exact nature of the oxoallyl hydrolysis product was subsequently determined. Comlpete conversion to this species was effected with the use of more basic conditions. Thus, reaction of (134) in a two-phase system (CH_2Cl_2/$NaHCO_3$(aq.) *ca.* pH 8.5) afforded the oxoallyl complex (135) as a yellow solid in 87% yield (Fig. 116). The IR spectrum of (135) shows a low frequency band for the aldehydic-carbonyl group (1649 cm^{-1}) suggesting a degree of conjugation with the η^3-allyl. An examination of the room temperature ^1H NMR spectrum of complex (135) revealed two sets of broadened resonances in the ratio 10:1. This was attributed to the presence, in solution, of two interconverting isomeric forms, *exo-anti* (135c) (major isomer) and *endo-anti* (135d) (minor isomer). Differences in chemical shift were used to distinguish between

exo and *endo* forms.[44] A low temperature NMR experiment was necessary in order to determine the coupling constants (see Table 4). On lowering the temperature of the NMR probe to -40°C, exchange between the two isomeric forms was slowed and the spectrum showed well-resolved resonances for (135c) and (135d) in the ratio 15:1. The magnitudes of the vicinal coupling constants between H^b and H^c [(135c), $J(H^bH^c)$= 7.0 Hz; (135d) $J(H^bH^c)$ = 6.2 Hz] confirmed the *cis* relationship of these protons in (135c) and (135d), and hence the assignment of the *anti* configuration. A low temperature ^{13}C-{^1H} NMR spectrum was also needed in order to obtain well-resolved resonances.

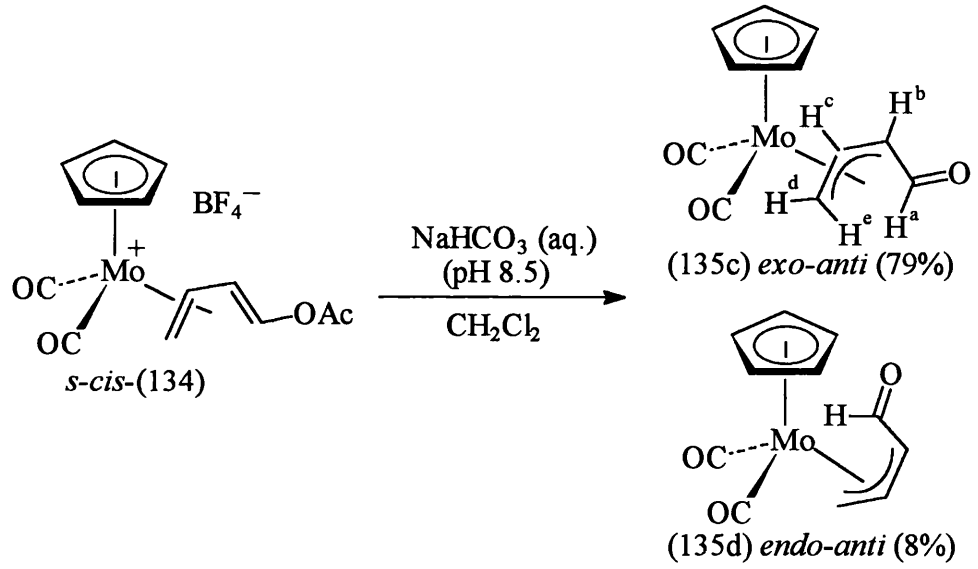

Figure 116

The above process again illustrates the selective formation of an *anti*-oxoallyl complex from the corresponding *s-cis*-diene cation. Interestingly in the case of (135), a small amount of the *endo-anti* isomer (135d) was observed, implying that the energy barrier for *exo-endo* interconversion in *anti*-(135) is lower than in the corresponding η^5-C_5Me_5 complex *anti*-(126).

As regards enzymatic resolution, it is evident that both the η^5-C_5Me_5 and η^5-C_5H_5 acetoxy-diene cations (133) and (134) are too readily hydrolysed in the presence of water, and hence are unsuitable for this methodology. It is conceivable that the use of other ester-substituted diene cations such as (136) and (137) (Fig. 117) (in which steric or electronic factors might slow down the rate of water-induced

hydrolysis), might allow convenient access to optically pure oxoallyl complexes. These possibilities are currently under investigation within our group.

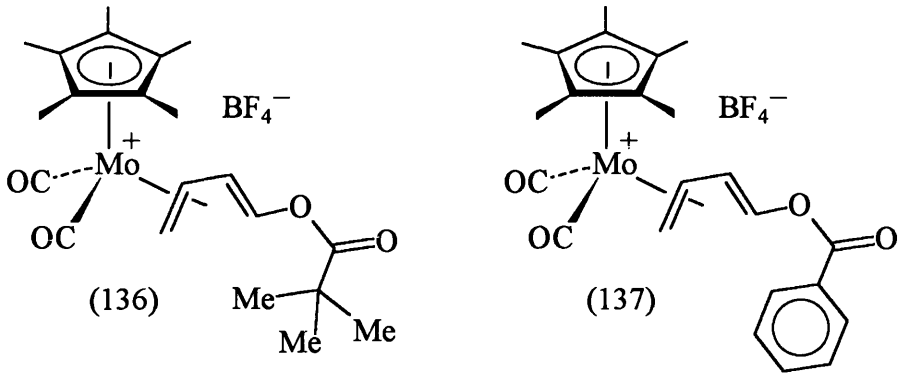

Figure 117

The use of acetoxy-1,3-butadiene for the selective preparation of *anti*-oxoallyls *via* the Krivykh[48,49] procedure [as opposed to the use of bis(acetonitrile) ligand substitution] was also attempted. In these reactions, the use of strong acid prevented the isolation of the acetoxy-diene intermediate. Low temperature treatment of [Mo(η^3-C_3H_5)(CO)$_2$(η^5-C_5H_5)] (25) (CH_2Cl_2, -78°C) with $HBF_4.OEt_2$ and 1-acetoxy-1,3-butadiene, followed by warming to room temperature and basic work-up, afforded the η^5-C_5H_5 oxoallyl complex (135) in 54% yield (Fig. 118). As before, (135) was found to be a 10:1 mixture of the *exo-anti* and *endo-anti* isomers (135c) and (135d).

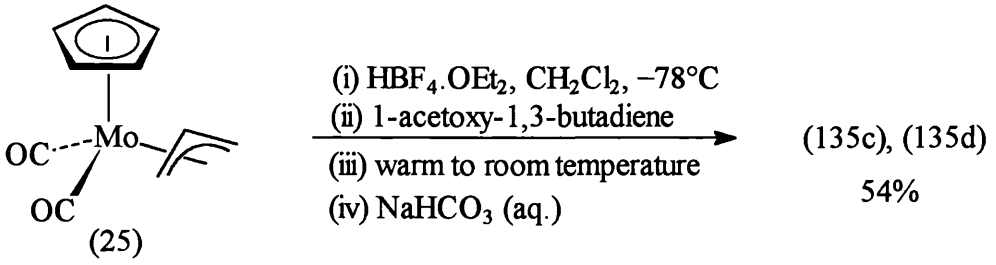

Figure 118

An analogous procedure was used to access the corresponding tungsten system. Allyl ligand substitution from [W(η^3-C_3H_5)(CO)$_2$(η^5-C_5H_5)] (138)[64] with 1-acetoxy-1,3-butadiene led to the isolation of the tungsten oxoallyl complex (139) as a crystalline yellow solid, in 43% yield (Fig. 119). The IR spectrum of (139) showed two metal-

carbonyl bands at 1966 and 1885 cm^{-1}, along with a low frequency aldehydic-carbonyl band at 1651 cm^{-1} (again suggesting a degree of conjugation with the η^3-allyl). As with the η^5-C_5H_5 complex (135), the room temperature NMR spectrum of (139) displayed two sets of broadened resonances, this time in the ratio 14:1. These were assigned to the presence, in solution, of the two interconverting isomers, *exo-anti* (139c) (major isomer) and *endo-anti* (139d) (minor isomer). A low temperature NMR experiment was necessary in order to determine the coupling constants (see Table 4). On lowering the temperature of the NMR probe to -30°C, exchange between the two isomeric forms was slowed and the spectrum showed well-resolved resonances for (139c) and (139d) in the ratio 20:1. The magnitude of the $J(H^bH^c)$ coupling constants [(139c), 6.9 Hz; (139d) 6.6 Hz] confirmed the *anti* orientation of the oxoallyl ligand. Sharp resonances in the ^{13}C-{^1H} NMR spectrum could also only be obtained at low temperature (-30°C).

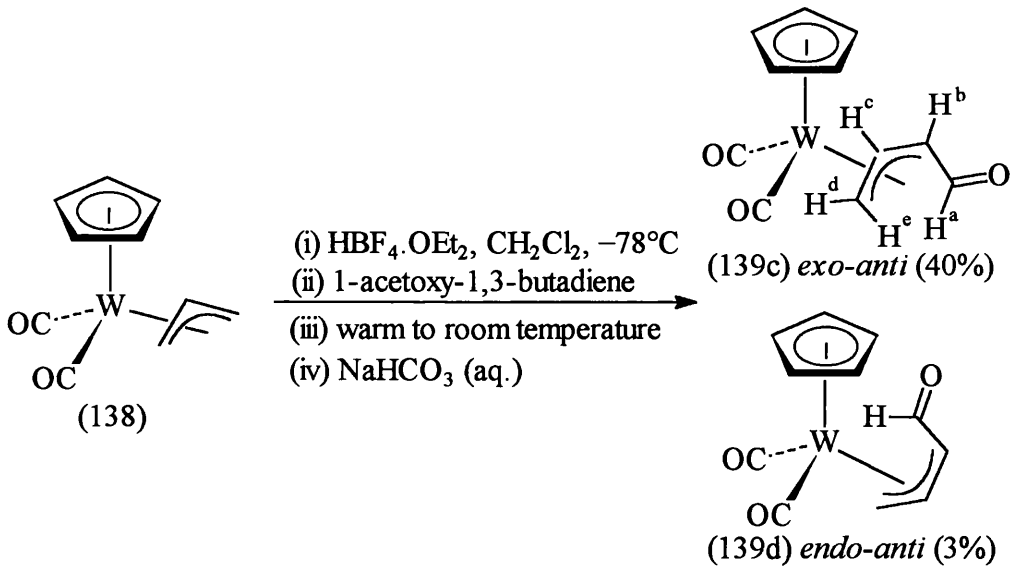

Figure 119

Finally, exclusive access to the η^5-C_9H_7 molybdenum *exo-anti*-oxoallyl complex (125c) was also achieved using this methodology, *via* the corresponding η^3-allyl complex (140)[64] (Fig. 120). Complex (125c) was isolated as a yellow crystalline solid in 49% yield.

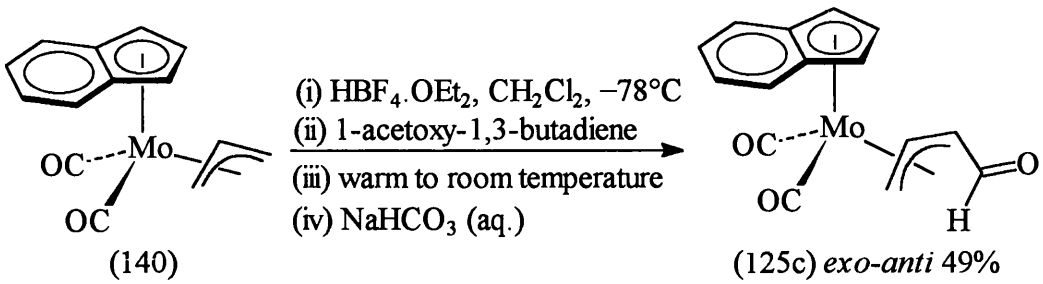

(140) (125c) *exo-anti* 49%

Figure 120

An examination and comparison[44] of the analytical and spectroscopic data readily confirmed the singular presence of the *exo-anti* isomer (125c). It is particularly interesting to note the relatively high upfield chemical shift observed for the *exo* oriented H^c, caused by the anisotropic shielding effect of the indenyl ring (see Table 4, overleaf).

Table 4

^{1}H NMR data for the oxoallyl complexes [M(η^3-$CH_2CHCHCHO$)$(CO)_2(\eta^5$-L)]

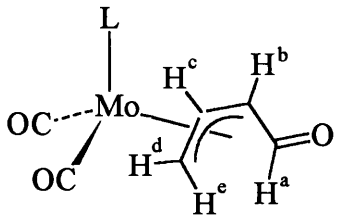

Complex	(125c)*	(126c)*	(135c)†	(135d)†	(139c)‡	(139d)‡
M	Mo	Mo	Mo	Mo	W	W
L	C_9H_7	C_5Me_5	C_5H_5	C_5H_5	C_5H_5	C_5H_5
Isomer	*exo-anti*	*exo-anti*	*exo-anti*	*endo-anti*	*exo-anti*	*endo-anti*
$\delta(H^a)$	6.86	7.00	6.98	7.71	6.89	7.63
$\delta(H^b)$	3.35	3.42	4.00	4.28	4.02	4.24
$\delta(H^c)$	0.40	3.51	4.78	4.46	4.39	4.47
$\delta(H^d)$	2.52	2.28	3.02	2.77	2.90	2.64
$\delta(H^e)$	1.83	1.75	1.68	2.65	1.78	2.55
$J(H^aH^b)$	8.2	7.8	7.9	7.9	8.2	8.3
$J(H^bH^c)$	7.4	7.1	7.0	6.2	6.9	6.6
$J(H^cH^d)$	8.7	8.4	8.2	7.3	8.2	6.8
$J(H^cH^e)$	12.2	11.6	11.9	11.2	11.2	9.9

Shifts in ppm downfield from TMS. Coupling constants in Hz.

* In a CD_2Cl_2 solution, 20°C.

† In a CD_2Cl_2 solution, -40°C.

‡ In a CD_2Cl_2 solution, -30°C.

2.3.4 Reactivity of *Anti*-4-oxo-η^3-butenyl Complexes Towards $NaBH_4$ Reduction

Having established an efficient procedure for preparing 4-oxo-η^3-butenyl complexes exclusively in the *anti* configuration, we turned our attention to examining the reactivity of these compounds, with particular regard to standard organic transformations of the aldehydic functionality. The synthesis of the derived alcohols, *via* $NaBH_4$ reduction, was the initial area of investigation.

Addition of $NaBH_4$ to a methanolic solution of the η^5-C_5H_5 *anti*-oxoallyl complex (135) [present as a 10:1 mixture of (135c) and (135d)] resulted in a fast reaction (0.5 h), and, following chromatographic work-up, a yellow crystalline solid was isolated in 65% yield. Spectroscopic and analytical data supported the formulation of the expected hydroxyallyl complex [$Mo(\eta^3$-$CH_2CHCHCH_2OH)(CO)_2(\eta^5$-$C_5H_5)$] (141). An examination of the ^1H NMR data showed the presence of a single set of well-resolved resonances for the hydroxyallyl ligand at 4.12 (H^c), 3.93 (H^b), 3.78 (H^a), 2.94 (H^d), 2.14 (H^f), 1.50 (OH) and 141 ppm (H^e), readily assignable to the *exo-anti* isomer (141c) (Fig. 121) (see Table 6). Following a deuteration experiment (see below), it was evident that the resonance at H^f was that arising from the incoming nucleophile, H^-. Comparison of the NMR data with that of similar complexes (see Table 6, page 112), suggested that the newly-formed hydroxyl group was orientated away from the metal (i.e. *trans*). Presumably, this *trans* metal-hydroxy relationship arises from initial attack of H^- on the *exo*-face of the oxoallyl (135), followed by a rapid rotation about the C^1-C^2 bond to give the less sterically demanding product (141c). The magnitude of the $J(H^bH^f)$ coupling constant (11.0 Hz), suggesting a transoid relationship between H^b and H^f, provides further evidence for this structure.

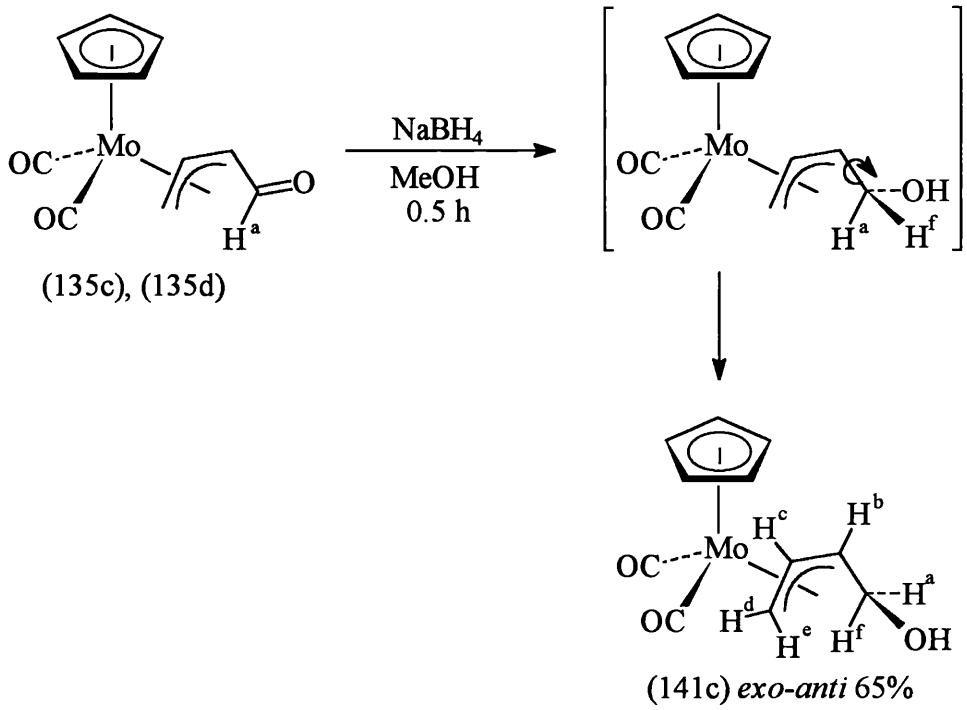

Figure 121

A reaction between *anti*-(135) and $NaBD_4$ (MeOH, 0.5 h) allowed the incorporation of deuterium into the structure to give the analogous *exo-anti*-hydroxyallyl complex (142c) (Fig. 122) as a yellow crystalline solid in 67% yield, fully characterised by analysis and spectroscopy. The ^1H NMR spectrum showed proton resonances at chemical shifts similar to those in (141c), with the distinct absence of a peak corresponding to H^f [hence, H^f in (141c) is equivalent to D in (142c)].

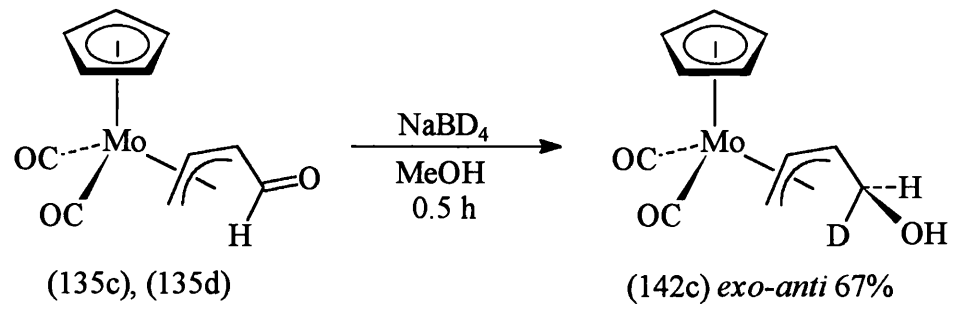

Figure 122

Both the above-mentioned reductions, leading to the formation of the hydroxyallyls (141c) and (142c), were rapid, being complete in under 0.5 h. However, prolonged stirring of the respective reaction mixtures gave rise to the serendipitous

discovery of an interesting side-reaction. An excess of $NaBH_4$ was added to a methanolic solution of *anti*-(135). After stirring for 0.5 h at ambient temperature, monitoring by TLC indicated total conversion to the expected hydroxyallyl complex (141c). On stirring for a further 2 h, TLC monitoring showed the gradual formation of an additional product. The reaction was continued for a total of 30 h, and TLC analysis of the resulting mixture revealed the complete consumption of (141c), with the new product being the only detectable species. Following aqueous work-up and column chromatography, this product was isolated as a hexane-soluble, yellow crystalline solid in 69% yield.

From an examination of the NMR spectra, it was evident that an η^3-butenyl complex, adopting an *exo-anti* configuration, had been formed. The ^1H NMR spectrum of this compound displayed almost identical resonances to those in the hydroxyallyl complex (141c) (minus the broad signal of a hydroxyl group), along with a strong singlet at 3.21 ppm, characteristic of a methoxy-substituent. The corresponding resonance at 57.2 ppm in the ^{13}C-{^1H} NMR spectrum similarly implied the presence of a methoxy functionality. On the basis of this evidence, the structure of the product was tentatively identified as the methoxyallyl complex *exo-anti*-[Mo(η^3-CH_2CHCH-CH_2OMe)$(CO)_2$(η^5-C_5H_5)] (143c) (Fig. 123). This formulation was supported by the microanalysis and FAB mass spectral data.

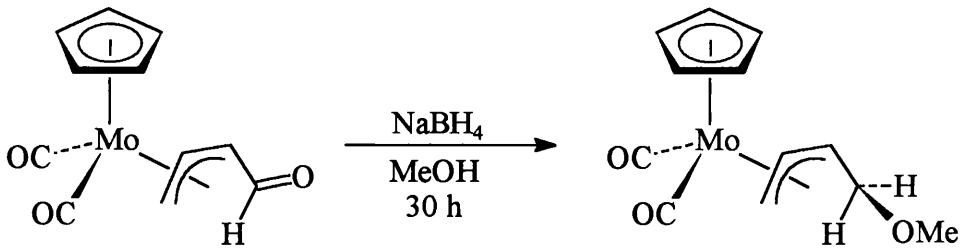

(135c), (135d) (143c) *exo-anti* 69%

Figure 123

The molecular structure of (143c) was confirmed from a single crystal X-ray diffraction study and is illustrated in Figure 124. Selected bond lengths and interbond angles are listed in Table 5. The molybdenum atom can be described as formally seven-

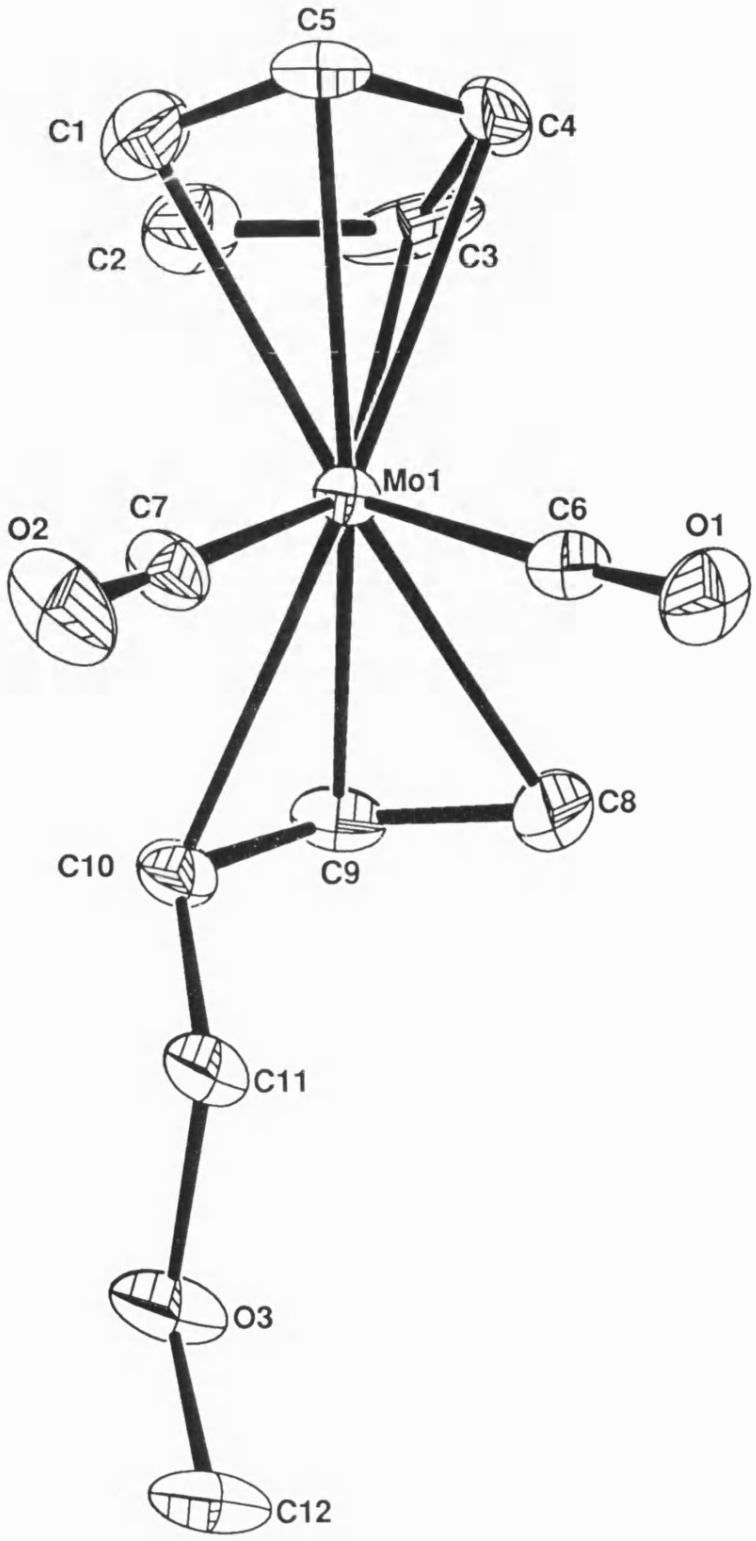

Figure 124

Molecular structure of *exo-anti*-[Mo($CH_2CHCHCH_2OMe$)$(CO)_2(\eta^5$-$C_5H_5)$] (143c).

Table 5

Selected bond lengths (Å) and angles (°) for complex (143c) with estimated standard deviations in parenthesis.

Mo-C(1)	2.345(8)	Mo-C(2)	2.365(7)
Mo-C(3)	2.340(7)	Mo-C(4)	2.308(7)
Mo-C(5)	2.298(6)	Mo-C(6)	1.942(7)
Mo-C(7)	1.967(7)	Mo-C(8)	2.325(7)
Mo-(C9)	2.216(6)	Mo-C(10)	2.342(6)
C(6)-O(1)	1.168(7)	C(7)-O(2)	1.152(7)
C(8)-C(9)	1.416(9)	C(9)-C(10)	1.409(8)
C(10)-C(11)	1.486(7)	C(11)-O(3)	1.421(6)
O(3)-C(12)	1.408(8)		
Mo-C(6)-O(1)	177.2(4)	Mo-C(7)-O(2)	178.0(4)
C(6)-Mo-C(7)	80.9(3)	C(8)-C(9)-C(10)	119.7(5)
C(9)-C(10)-C(11)	121.0(5)	C(10)-C(11)-O(3)	109.0(4)
C(11)-O(3)-C(12)	111.2(5)		

coordinate, bound to two terminal carbonyl ligands, a cyclopentadienyl ring and a methoxy-substituted η^3-allylic organic fragment. The metal-carbonyls are essentially linear, having unexceptional Mo-C and C-O bond distances, and lie at an angle of 80.9° to one another. The η^5-C_5H_5 ring is almost planar and is bound at a mean distance of 2.331 Å from the metal atom.

The η^3-allylic organic fragment adopts an *anti* configuration being bonded to molybdenum *via* three carbon atoms, which lie symmetrically underneath the two carbonyl ligands. This C(8)-C(9)-C(10) moiety is bonded *exo* with respect to the η^5-C_5H_5 ring, with Mo-C distances of 2.325(7), 2.216(6) and 2.342(6) Å, and a bond angle of 119.7°, typical of η^3-allylic molybdenum complexes.[29,154] The methoxy-

substituent is oriented away form the metal (i.e. *trans* to molybdenum), the C-O and O-C bond lengths being unexceptional.[116]

Based on our previous knowledge of oxoallyl chemistry, a mechanism for the formation of (143c) can be suggested (Fig. 125). Evidently, the initial step in the process involves reduction of the aldehyde (135c), (135d) to give the hydroxyallyl complex (141c). This presumably undergoes electrophilic attack from a trivalent boron species (i.e. 'BH_3', which is generated *in situ* and can act as a Lewis acid) at the oxygen atom of the hydroxyl moiety, thereby producing an excellent leaving group. Subsequent back-side attack from the metal atom results in the rapid elimination of $HOBH_3^-$ and the formation of an η^4-diene cation (9). Nucleophilic addition of MeO^- (from the methanolic solvent) to the terminus of the 1,3-diene (on the *exo*-face of this ligand) leads to the observed methoxyallyl product (143c).

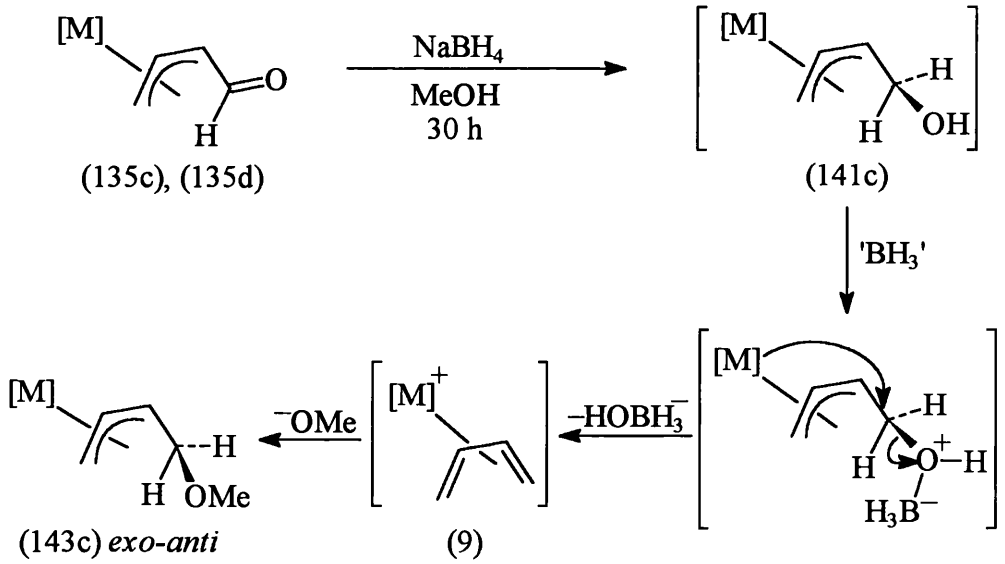

Figure 125. [M] = $Mo(CO)_2(\eta^5\text{-}C_5H_5)$.

Clearly, the key step in this mechanistic sequence involves conversion of (141c) to (9) *via* an electrophilic addition/elimination reaction. In order to substantiate this process, the reaction between (141c) and an electrophilic reagent was examined. Low temperature treatment of (141c) with $HBF_4.OEt_2$ (CH_2Cl_2, -78°C) resulted in the formation of a yellow precipitate. This was isolated and, following purification, was

readily identified as the known *s-cis*-η^4-butadiene cation (9),[31] obtained as a yellow powder in 85% yield (Fig. 126).

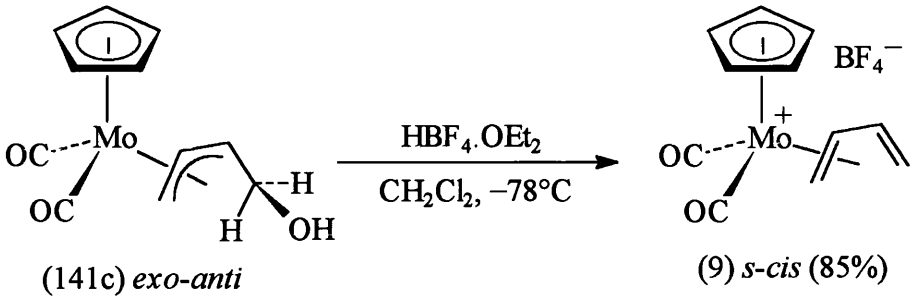

(141c) *exo-anti* (9) *s-cis* (85%)

Figure 126

The success of this reaction confirmed that (141c) readily undergoes electrophilic attack at oxygen (in this case *via* protonation), followed by elimination to afford (9).

Further evidence for the intermediacy of (9) in the formation of (143c) came from the results of a deuteration experiment. An excess of $NaBD_4$ was added to a methanolic solution of the *anti*-oxoallyl complex (135) and the resultant yellow mixture was stirred at ambient temperature for 30 h. Standard chromatographic work-up led to the isolation of a hexane-soluble yellow solid in 60% yield. An examination of the analytical and spectroscopic data revealed that the product was a 1:1 mixture of deuterio-isomers (144c) and (145c), both with an *exo-anti* configuration of methoxy substituents (Fig. 127, overleaf). Interestingly, the ^1H NMR spectrum showed that the deuterium atom in (145c) was in an *anti* position relative to the η^3-allyl moiety (as illustrated).

These observations can be readily interpreted in terms of our suggested mechanism (Fig. 128, overleaf). The initial product in the above reaction is the hydroxyallyl complex (142c). Electrophilic attack from an *in situ*-generated trivalent boron species, 'BD_3', takes place at the oxygen atom, *trans* to molybdenum, followed by a rapid elimination to generate the η^4-diene intermediate (146) (with deuterium in an *anti* position relative to the diene). Nucleophilic addition of MeO^- can then equally occur at both ends of the η^4-diene ligand (on its *exo*-face) and thus (144c) and (145c) are formed in the ratio 1:1.

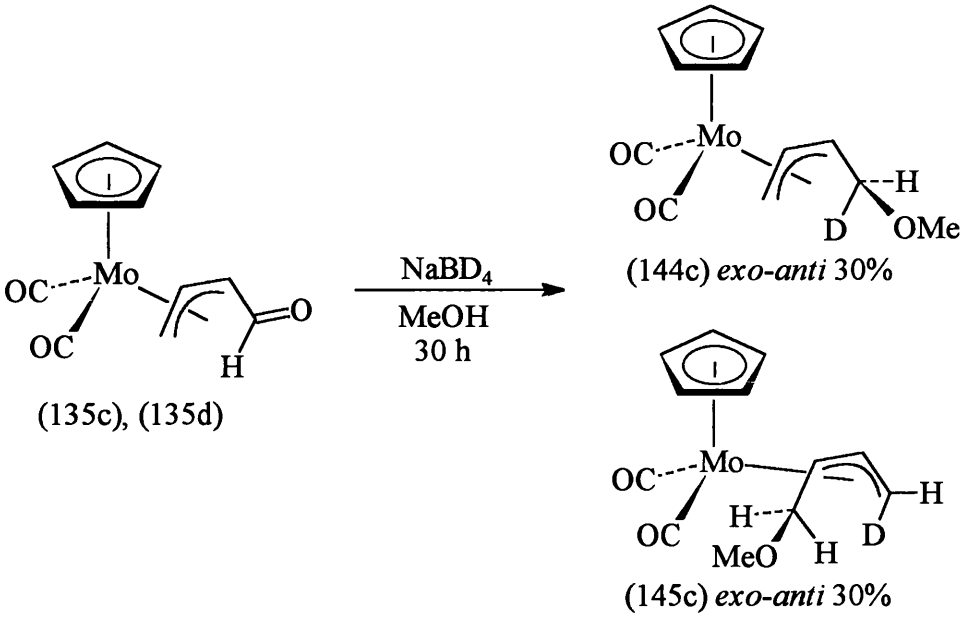

Figure 127

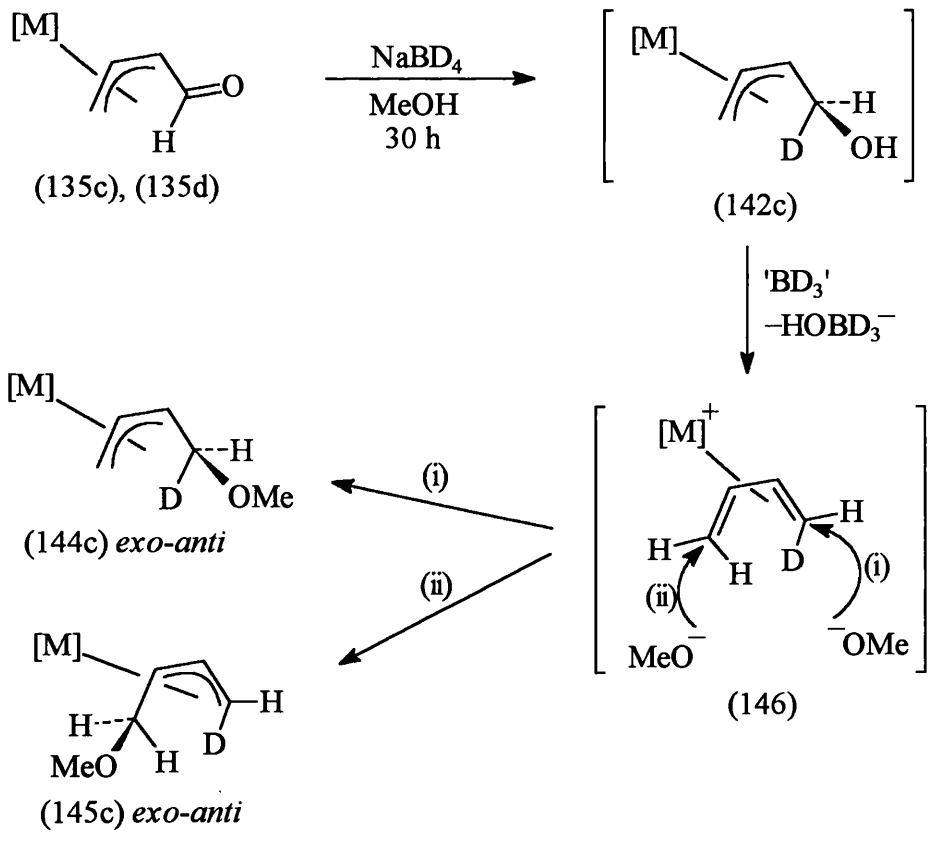

Figure 128. [M] = $Mo(CO)_2(\eta^5\text{-}C_5H_5)$.

The reactivity of the η^5-C_5Me_5 *exo-anti*-oxoallyl complex (126c) towards $NaBH_4$ was also examined. Treatment of a methanolic solution of (126c) with $NaBH_4$ followed by stirring at ambient temperature for 1 h, resulted in the formation of the corresponding *exo-anti*-hydroxyallyl complex (147c), isolated as a yellow solid in 62% yield (Fig. 129). An examination of the spectroscopic data revealed comparable similarities to the analogous η^5-C_5H_5 complex (141c), implying the same structural orientation of the η^3-hydroxyallyl ligand (see Table 6, overleaf).

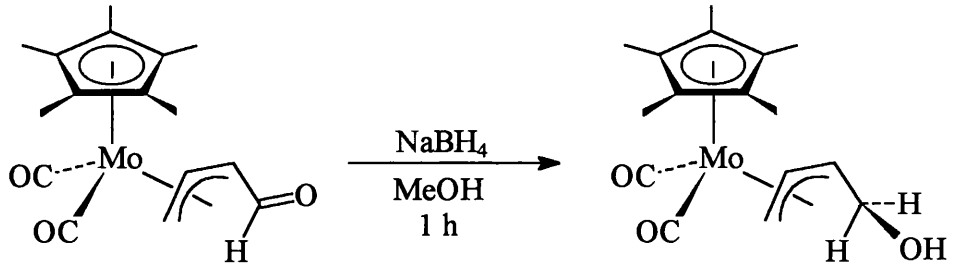

(126c) *exo-anti* (147c) *exo-anti* 62%

Figure 129

As before, an extended reaction time led to the formation of a methoxy-substituted compound. Treatment of a methanolic solution of (126c) with $NaBH_4$ followed by stirring at ambient temperature for 2 d gave the *exo-anti*-methoxyallyl complex (148c), obtained as a yellow solid in 65% yield (Fig. 130). Spectroscopic data was similarly in close accordance with the analogous η^5-C_5H_5 complex (143c), again suggesting the same structural orientation of the η^3-methoxyallyl ligand (see Table 6).

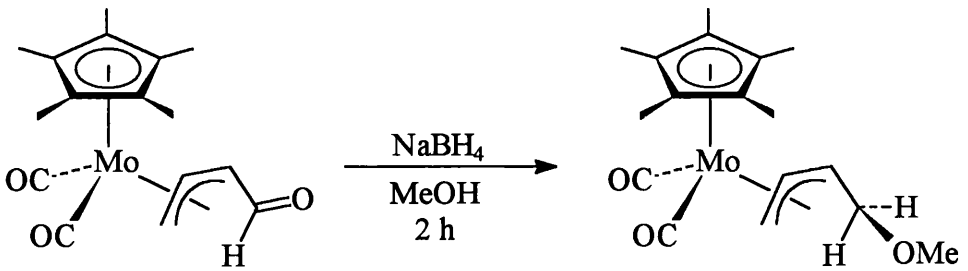

(126c) *exo-anti* (148c) *exo-anti* 65%

Figure 130

Table 6

^{1}H NMR data for the oxyallyl complexes [Mo(η^3-$CH_2CHCHCH_2OR$)$(CO)_2$(η^5-L)]

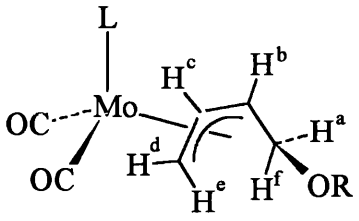

Complex	(141c)*	(143c)†	(147c)†	(148c)†
L	C_5H_5	C_5H_5	C_5Me_5	C_5Me_5
R	H	Me	H	Me
Isomer	*exo-anti*	*exo-anti*	*exo-anti*	*exo-anti*
$\delta(H^a)$	3.78	3.62	3.64	3.56
$\delta(H^b)$	3.93	3.77	3.22	3.05
$\delta(H^c)$	4.12	4.21	2.85	2.92
$\delta(H^d)$	2.94	2.96	2.25	2.25
$\delta(H^e)$	1.41	1.35	1.46	1.43
$\delta(H^f)$	2.14	1.82	2.07	1.80
$J(H^aH^b)$	-	3.7	3.6	3.6
$J(H^aH^f)$	11.0	11.0	11.4	10.9
$J(H^bH^c)$	7.7	7.7	7.6	7.8
$J(H^bH^f)$	11.0	11.2	11.2	11.1
$J(H^cH^d)$	7.5	7.6	7.6	7.5
$J(H^cH^e)$	11.4	11.4	11.9	11.2

Shifts in ppm downfield from TMS. Coupling constants in Hz.

* In a $CDCl_3$ solution, 20°C.

† In a CD_2Cl_2 solution, 20°C.

2.3.5 Reactivity of *Anti*-4-oxo-η^3-butenyl Complexes towards Organometallic Reagents

The *anti*-oxoallyl complexes were also used as substrates for the stereocontrolled addition of carbon nucleophiles. These reactions were carried out using readily available organometallic reagents.

Addition of methylmagnesium iodide to a solution (thf, -20°C) of the yellow complex *anti*-(135) [present as a 10:1 mixture of (135c) and (135d)] resulted in a smooth reaction, the progress of which was readily monitored by IR spectroscopy. This showed the rapid consumption of the starting material with the subsequent formation of a new product (ν_{CO}/cm^{-1} at 1943 and 1850). Upon completion of the reaction, chromatographic work-up afforded a hexane-soluble yellow powder in 70% yield. The spectroscopic and analytical data supported the formulation of the expected secondary alcohol complex [Mo(η^3-$CH_2CHCHCH(OH)Me$)$(CO)_2$(η^5-C_5H_5)]. In particular, the ^1H NMR showed resonances at 4.01 (H^c), 3.82 (H^b), 3.04 (H^d), 2.89 (H^a), 2.35 (OH), 1.44 (H^e) and 1.18 ppm (Me), indicating the presence of an hydroxy-substituted η^3-butenyl ligand in an *exo-anti* configuration (see Table 7, page 116). Hence, the product was readily identified as the *exo-anti*-hydroxyallyl complex (149c) (Fig. 131).

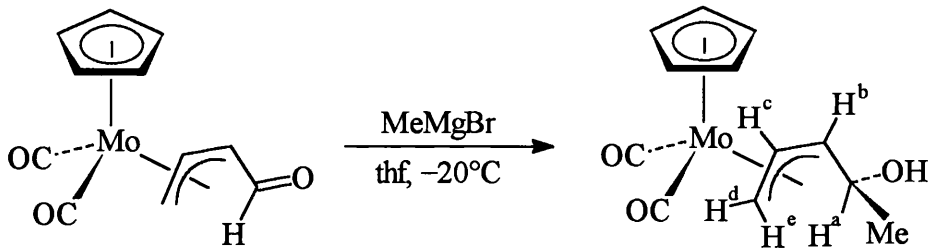

(135c), (135d) (149c) *exo-anti* 70%

Figure 131

The metal fragment directs the attack of Me^- to the *exo*-face of the oxoallyl ligand, resulting in a stereocontrolled addition and the formation of chiral carbon centre. The methyl group in (149c) is presumably orientated away from the metal. This was confirmed from an examination of the vicinal coupling constant between H^a and H^b [$J(H^aH^b)$ = 8.3 Hz] suggesting that these protons adopt a transoid relationship.

Reaction of *anti*-(135) with ethylmagnesium bromide (thf, 0°C) resulted in smooth conversion to the corresponding ethyl-substituted *exo-anti*-hydroxyallyl complex (150c), isolated as a hexane-soluble yellow crystalline solid in 53% (Fig 132). The identity and structural orientation of this complex was confirmed by the close accordance of the relevant spectroscopic data with that derived from (149c) (see Table 7, page 116). Again the reaction proceeds *via exo*-facial attack of Et^- at the aldehyde to give a stereodefined chiral carbon centre.

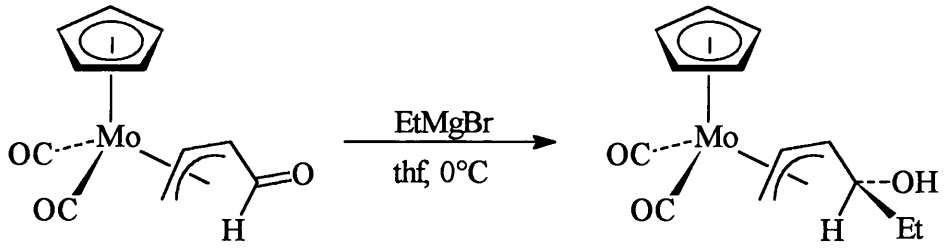

(135c), (135d) (150c) *exo-anti* 53%

Figure 132

Similarly, treatment of *anti*-(135) with phenylmagnesium chloride (thf, 0°C) resulted in a facile reaction and the formation of a hexane-soluble yellow solid in 57% yield. An examination and comparison of the spectroscopic and analytical data readily identified the product as the phenyl-substituted *exo-anti*-hydroxyallyl complex (151c) (Fig. 133).

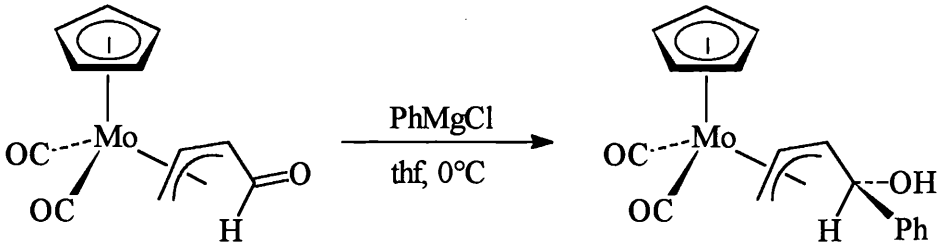

(135c), (135d) (151c) *exo-anti* 57%

Figure 133

A reaction between the η^5-C_5Me_5 *exo-anti*-oxoallyl complex (126c) and an organolithium reagent was also examined. Low temperature addition of methylithium to a solution of (126c) (thf, -78°C) gave rise to the formation of the methyl-substituted

exo-anti-hydroxyallyl complex (152c), again isolated as a hexane-soluble yellow solid in 75% yield (Fig. 134). An examination of the spectroscopic data revealed comparable similarities to the analogous η^5-C_5H_5 complex (149c), implying the same structural orientation of the η^3-hydroxyallyl ligand (see Table 7, overleaf).

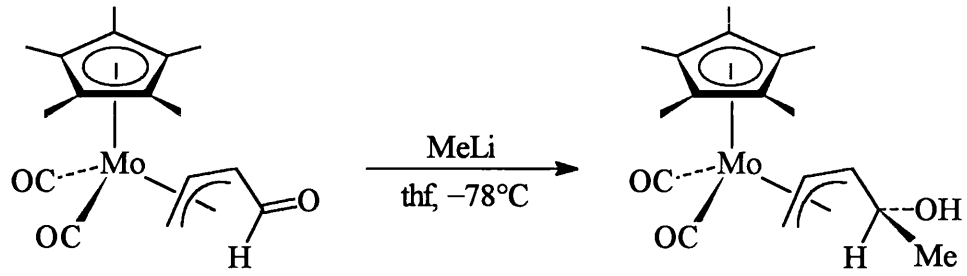

(126c) *exo-anti* (152c) *exo-anti* 75%

Figure 134

Table 7

^{1}H NMR data for the hydroxyallyl complexes

[Mo(η^3-$CH_2CHCHCH(OH)R$)$(CO)_2$(η^5-L)]

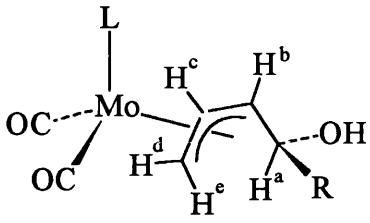

Complex	(149c)*	(150c)†	(151c)†	(152c)*
L	C_5H_5	C_5H_5	C_5H_5	C_5Me_5
R	Me	Et	Ph	Me
Isomer	*exo-anti*	*exo-anti*	*exo-anti*	*exo-anti*
$\delta(H^a)$	2.89	2.63	3.67	2.87
$\delta(H^b)$	3.82	3.79	4.01	3.12
$\delta(H^c)$	4.01	4.00	3.85	2.71
$\delta(H^d)$	3.04	3.05	3.04	2.32
$\delta(H^e)$	1.44	1.41	1.58	1.53
$J(H^aH^b)$	8.3	8.5	8.9	8.2
$J(H^bH^c)$	7.9	8.1	8.4	7.8
$J(H^cH^d)$	7.9	7.9	7.9	8.4
$J(H^cH^e)$	11.7	11.6	11.7	11.7

Shifts in ppm downfield from TMS. Coupling constants in Hz.

* In a CD_2Cl_2 solution, 20°C.

† In a $CDCl_3$ solution, 20°C.

2.3.6 Attempted Oxidation of [Mo(η^3-$CH_2CHCHCH(OH)Me$)$(CO)_2$(η^5-C_5H_5)] (149c)

It has previously been mentioned that the cyclic hydroxyallyl complex (96) readily undergoes smooth conversion to the corresponding ketoallyl complex (92) under the conditions of an Oppenauer oxidation[124] (see Section 2.1.6). By extending this methodology to the analogous acyclic hydroxyallyl species, it was envisaged that ketoallyl complexes such as (153) could be prepared (Fig. 135).

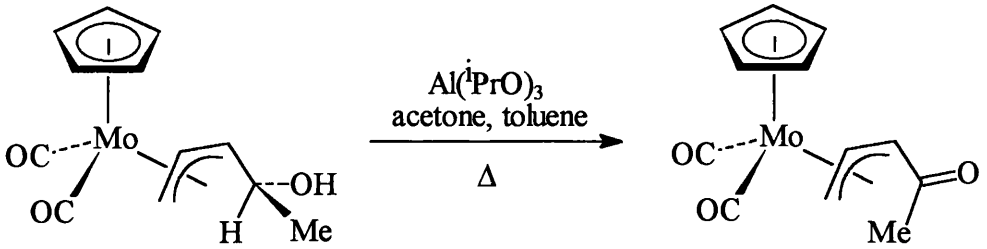

(149c) *exo-anti* (153)

Figure 135

In order to examine the feasibility of this process, an attempt was made to prepare (135) from the methoxy-substituted *exo-anti*-hydroxyallyl complex (149c) under standard Oppenauer oxidation conditions. Thus, aluminium isopropoxide was added to a solution of (149c) (acetone, toluene) and the mixture was heated to reflux. Monitoring by TLC indicated the gradual consumption of (149c) with the subsequent formation of a new product, the reaction being complete in 5.5 h. Following standard chromatographic work-up, a hexane-soluble yellow solid was isolated in 47% yield. From an initial examination of the spectroscopic and analytical data, it was evident that the expected ketoallyl complex (153) had not been formed. It was subsequently found that the product from this reaction was an *exo-anti*-η^3-pentadienyl complex (154c) (Fig. 136, overleaf), which presumably arises as a result of an elimination reaction. The IR spectrum displayed two distinct metal-carbonyl bands at 1950 and 1867 cm^{-1}, along with a less intense band at 1617 cm^{-1}, assignable to the olefinic fragment. The ^1H NMR spectrum showed *exo*-η^3-allyl proton resonances at 4.50 (H^b), 4.19 (H^c), 2.84 (H^d) and 1.47 ppm (H^e), along with three proton resonances due to the *anti*-olefinic fragment at

4.99 (H^g), 4.72 (H^f) and 4.33 ppm (H^a). The corresponding resonances were also observed in the ^{13}C-{^1H} NMR spectrum.

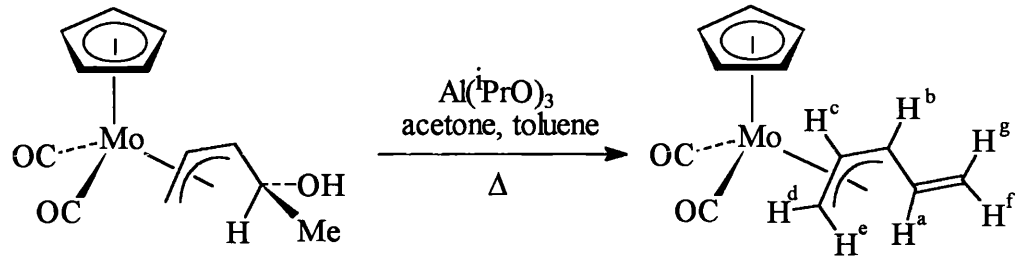

(149c) *exo-anti* (154c) *exo-anti* 47%

Figure 136

In order to confirm the exact structural nature of this product (154c), a single crystal X-ray diffraction experiment was carried out. Figure 137 shows the geometry of the molecule and the atomic numbering scheme used. Selected bond lengths and angles are given in Table 8.

The molybdenum atom can be described as formally seven-coordinate, bound to two carbonyl ligands, a cyclopentadienyl ring, and an *exo-anti*-η^3-pentadienyl fragment. The metal-carbonyl groups are essentially linear and lie at an angle of 78.9° to one another, having unexceptional Mo-C and C-O interatomic distances.[129] The η^5-C_5H_5 ring is almost planar and is bound at a mean distance of 2.351 Å from the metal atom.

The η^3-pentadienyl ligand is bound *via* C(8), C(9) and C(10) to the metal and can be seen to adopt an *anti* configuration, with C(11) being bent away from the molybdenum atom at a non-bonding distance of 3.281 Å. The η^3-allyl backbone is orientated *exo* with respect to the η^5-C_5H_5 ligand and lies symmetrically underneath the two carbonyl ligands. The C(8)-C(9)-C(10) moiety has a bond angle of 120.3°, with Mo-C bond distances of 2.338(6), 2.234(6) and 2.400(6) Å, which is typical for Mo(II) *exo*-η^3-allyl complexes.[29,154] The C(10)-C(11) bond distance of 1.446(8) Å is shorter than a standard carbon-carbon single bond [*ca.* 1.530 Å],[116] whilst the non-coordinated double bond [C(11)-C(12)] distance of 1.334(8) Å is longer than that expected for a standard terminal carbon-carbon double bond [*ca.* 1.299 Å]. This latter observation

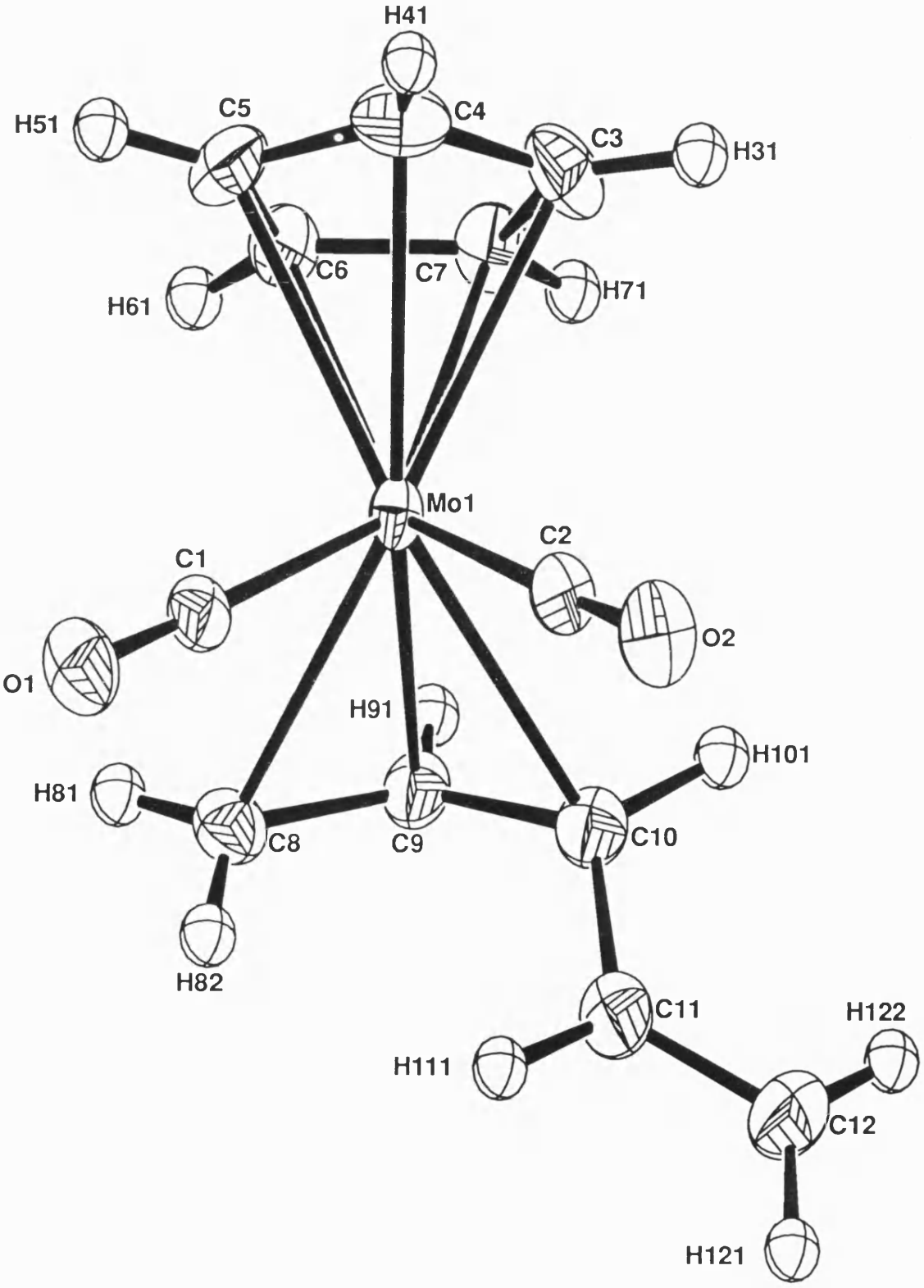

Figure 137

Molecular stucture of *exo-anti*-[Mo(η^3-$CH_2CHCHCHCH_2$)(CO_2)(η^5-C_5H_5)] (154c).

Table 8

Selected bond lengths (Å) and angles (°) for complex (154c) with estimated standard deviations in parenthesis.

Mo-C(1)	1.939(6)	Mo-C(2)	1.957(6)
Mo-C(3)	2.332(7)	Mo-C(4)	2.310(7)
Mo-C(5)	2.344(7)	Mo-C(6)	2.380(6)
Mo-C(7)	2.389(6)	Mo-C(8)	2.338(6)
Mo-C(9)	2.234(6)	Mo-C(10)	2.400(6)
C(1)-O(1)	1.160(7)	C(2)-O(2)	1.149(6)
C(8)-C(9)	1.412(7)	C(9)-C(10)	1.426(7)
C(10)-C(11)	1.446(8)	C(11)-C(12)	1.334(8)
C(1)-Mo-C(2)	78.9(3)	C(8)-C(9)-C(10)	120.3(5)
C(9)-C(10)-C(11)	123.5(5)	C(10)-C(11)-C(12)	124.5(6)

implies that there is a degree of π-conjugation between the η^3-allyl and olefinic fragments.

The physical and spectroscopic properties of complex (154c) bear considerable similarity to those of its oxo counterpart (135c) (see Section 2.3.2). A significant shift to lower wavenumber is, however, observed on comparison of their respective IR spectra [ν_{CO}/cm^{-1} (135c) 1973, 1896; (154c) 1950, 1867], indicating that the level of π-conjugation in (154c) is less than that in (135c). Presumably, complex (154c) could be obtained more directly from *anti*-(135) by means of a Wittig reaction.

The above result would seem to indicate that the ketoallyl complex (153) is not available from Oppenauer oxidation of (149c). Clearly, a competing elimination reaction predominates under these conditions. The use of an alternative oxidative

procedure (e.g. Swern oxidation) should allow access to complexes of type (153). However, due to a lack of time, such reactions were not investigated.

2.3.7 Summary and Conclusions

The majority of the work discussed in the above sections has been concerned with the chemistry of 4-oxo-η^3-butenyl complexes and a few useful conclusions can be drawn from these studies. Perhaps the most obvious point to note is the demonstration of the *syn*-allyl $\rightleftharpoons$ *s-trans*-diene $\rightarrow$ *s-cis*-diene $\rightleftharpoons$ *anti*-allyl structural relationship inherent in the formation and protonation of the oxoallyls. Thus, the *syn*-oxoallyls can be readily converted to the corresponding *anti* isomers *via* a simple protonation/ deprotonation sequence. Alternatively, *anti*-oxoallyl complexes can be prepared directly *via* the initial formation of an *s-cis*-acetoxy-diene cation.

A preliminary study on an efficient method of resolving the 4-oxo-η^3-butenyl complexes has been carried out. In this regard, the *s-cis*-acetoxy-diene cations have been examined as potential substrates for PLE hydrolytic resolution. However, these species were found to be unsuitable for such a process. Variation of the ester functionality should allow this methodology to be successfully established in the near future.

The 4-oxo-η^3-butenyl complexes have also been shown to undergo nucleophilic additions at the aldehydic group. The presence of the metal fragment plays an important role in the outcome of such reactions, both in terms of steric and electronic factors. As a result, these reactions occur stereoselectively and could therefore find potential usage in the area of stereocontrolled organic synthesis. With access to the oxoallyl complexes in optically pure form, it should be possible to carry out enantioselective syntheses, thereby realising the full potential of this area.

2.4 Synthesis and Reactivity of Molybdenum Heterocyclic Complexes

2.4.1 Introduction

During the course of an investigation into metal-acetylene chemistry, Green and co-workers established the formation of several interesting η^3-bonded (allyl-substituted) lactonyl complexes.[155,156] For example, $[Mo(COCF_3)(CO)_3(\eta^5\text{-}C_5H_5)]$ (155) was found to react thermally with an excess of but-2-yne (hexane, 60°C) to afford the red crystalline σ-bonded vinylketone complex (156) (Fig. 138). This species readily undergoes a reaction with a donor ligand, such as CO, to form the η^3-γ-lactonyl complex (157).

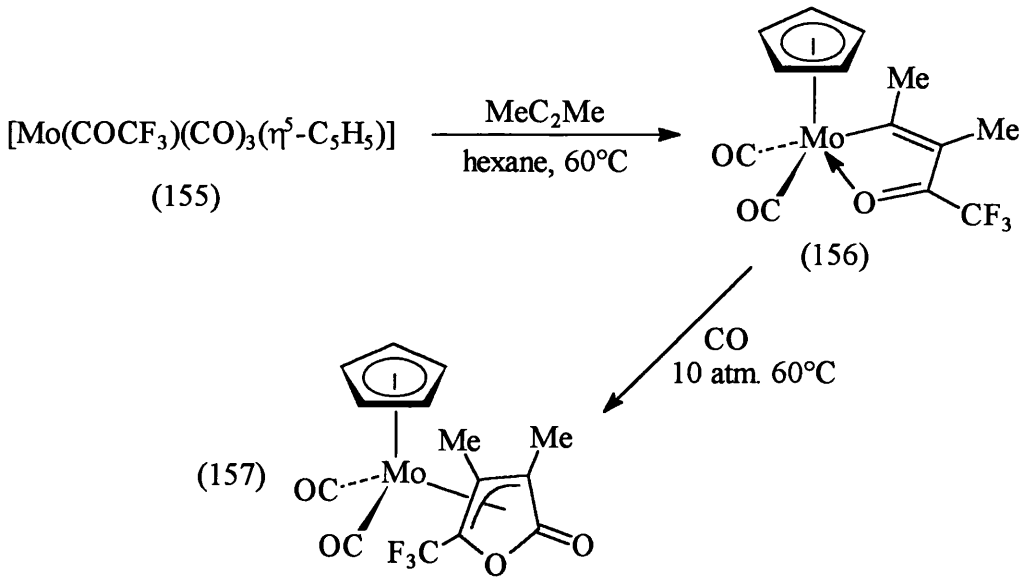

Figure 138

The subsequent reactivity of complex (157) has not been investigated. Indeed, there have been surprisingly few studies of the synthetic potential of isolated transition metal π-complexes of unsaturated heterocycles.[157-161] Recently however, Liebeskind and co-workers have reported the preparation of several pyranyl-derived π-complexes of molybdenum and demonstrated their application to organic synthesis.[35,109] One such complex is the η^3-δ-lactonyl species (159), which is prepared *via* the allylic bromide (158) (Fig. 139).

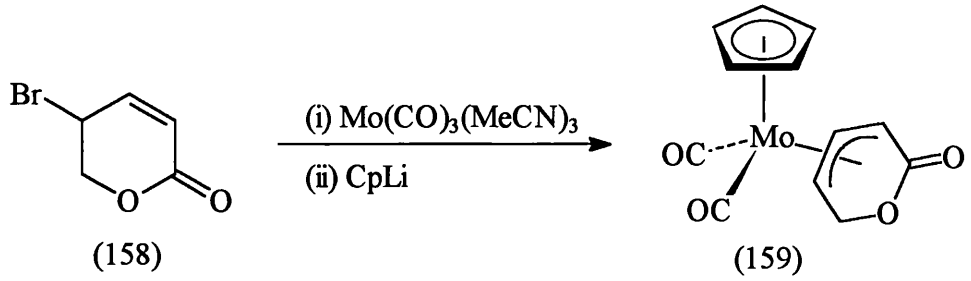

Figure 139

A simple strategy for the stereocontrolled introduction of substituents to the lactonyl fragment in these complexes has been developed (Fig. 140). The procedure is based on the precedented *exo*-facial addition of nucleophiles to cationic $CpMo(CO)_2(\eta^4\text{-diene})$ complexes and results in the overall replacement of the lactonyl carbonyl group. This methodology has also been extended to an optically active system allowing the enantiospecific synthesis of several substituted dihydro- and tetrahydro-pyrans.[35,109]

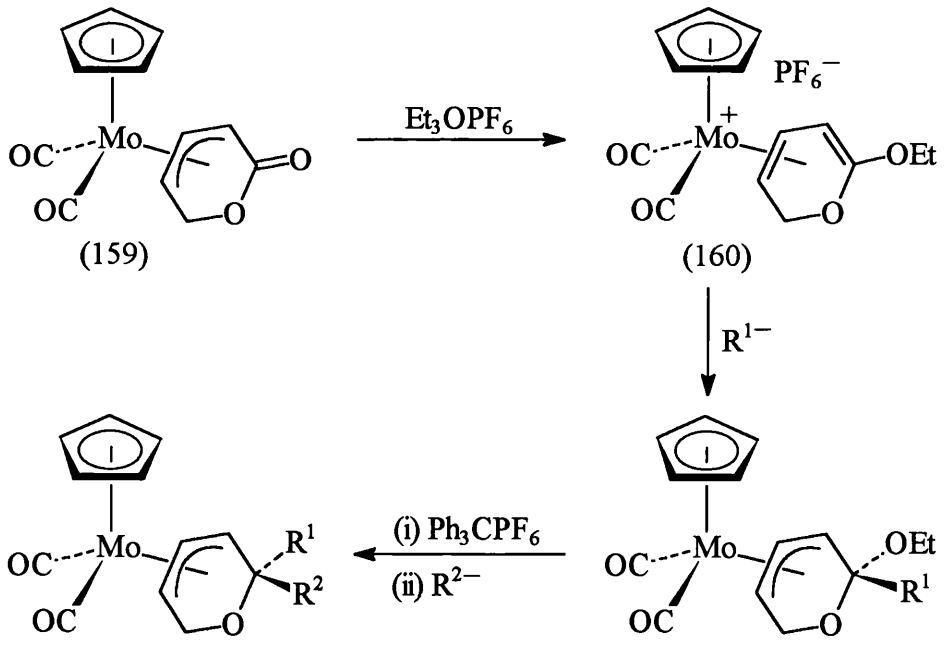

Figure 140

A potentially more attractive means of accessing such molybdenum-heterocyclic complexes can be envisaged with the use of our established bis(acetonitrile) technology. It was therefore decided to adopt this procedure in order to examine the synthesis and reactivity of some furanyl-derived π-complexes of molybdenum.

2.4.2 Synthesis of Furanyl-Derived π-Complexes of Molybdenum

Our initial efforts in this area were concerned with the direct complexation of furan to a $[CpMo(CO)_2]^+$ fragment by means of a ligand substitution reaction. However, all attempts to carry out such a procedure proved to be unsuccessful. An excess of furan was added to a dichloromethane solution of the η^5-C_5H_5 *cis*-bis-(acetonitrile) cation (108) and the resultant mixture was left to stir under standard conditions for 7 d. Monitoring by IR spectroscopy showed that no reaction had taken place. Heating the reaction mixture to reflux similarly did not lead to the formation of the desired η^4-furan complex (161) (Fig. 141). Attempts to prepare (161) using the related Krivykh procedure [i.e. *via* the η^3-allyl complex (25) (see Section 1.2.2)] were also unsuccessful.

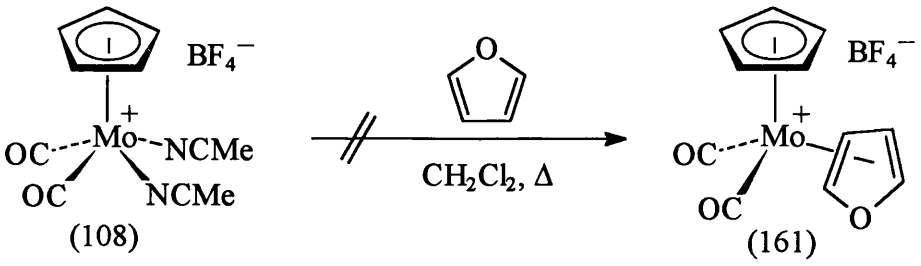

Figure 141

Undeterred by the failure of the above reaction, the direct complexation of a substituted furan to a molybdenum centre was examined. It was found that room temperature addition of excess 2-(trimethylsilyloxy)furan to a dichloromethane solution of the η^5-C_5Me_5 *cis*-bis(acetonitrile) cation (16) led to facile ligand substitution and the formation of a novel η^3-γ-lactonyl complex (162) (Fig. 142), obtained as a bright yellow powder in 62% yield. Presumably this reaction proceeds *via* a fluoride-anion-induced desilylation mechanism.

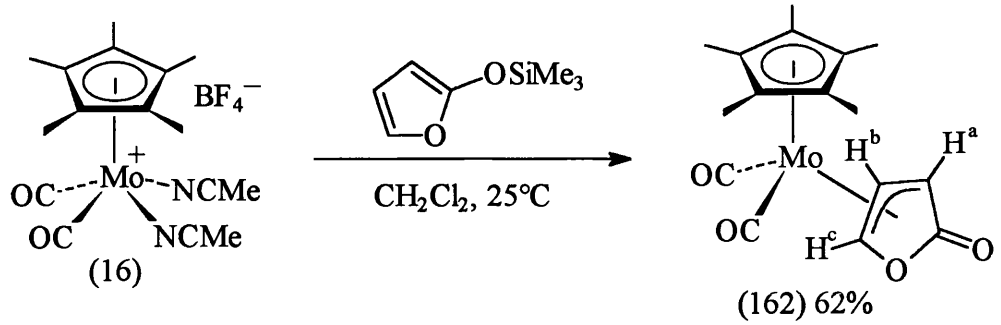

Figure 142

The solution IR spectrum of (162) displayed a major set of carbonyl bands at 1968, 1892 (metal-carbonyls) and 1748 cm^{-1} (γ-lactone carbonyl), along with a corresponding minor set of carbonyl bands at 1985, 1917 and 1721 cm^{-1}. The two sets of bands were in the ration 3:1 (in CH_2Cl_2) suggesting the presence of *exo* and *endo* conformers of (162). This was confirmed from an examination of the NMR spectral data. The room temperature ^1H NMR spectrum showed a single set of broadened resonances (due to *exo-endo* fluxional interconversion) at 6.38 (H^c), 4.99 (H^b), 3.02 (H^a) and 1.92 ppm (C_5Me_5). Low temperature NMR spectra were needed in order to distinguish between the two conformers and to determine the coupling constants. On lowering the temperature of the NMR probe to -80°C, exchange between the conformations was slowed, and the spectrum displayed two sets of well-resolved resonances in the ratio 7:1. An examination of the respective chemical shift values indicated that the *exo*-conformation was the predominant conformer in solution, at least at low temperature.

In order to establish the nature of the bonding and orientation within complex (162), a single crystal X-ray diffraction experiment was carried out. The molecular structure is shown in Figure 143, together with the atomic numbering scheme used. An alternative representation from a 'side-on' viewpoint is illustrated in Figure 144. Selected bond lengths, angles and torsion angles are given in Table 9.

Complex (162) crystallises in the *exo* conformation, thus confirming the predominance of the *exo* conformer as this compound approaches the solid state.

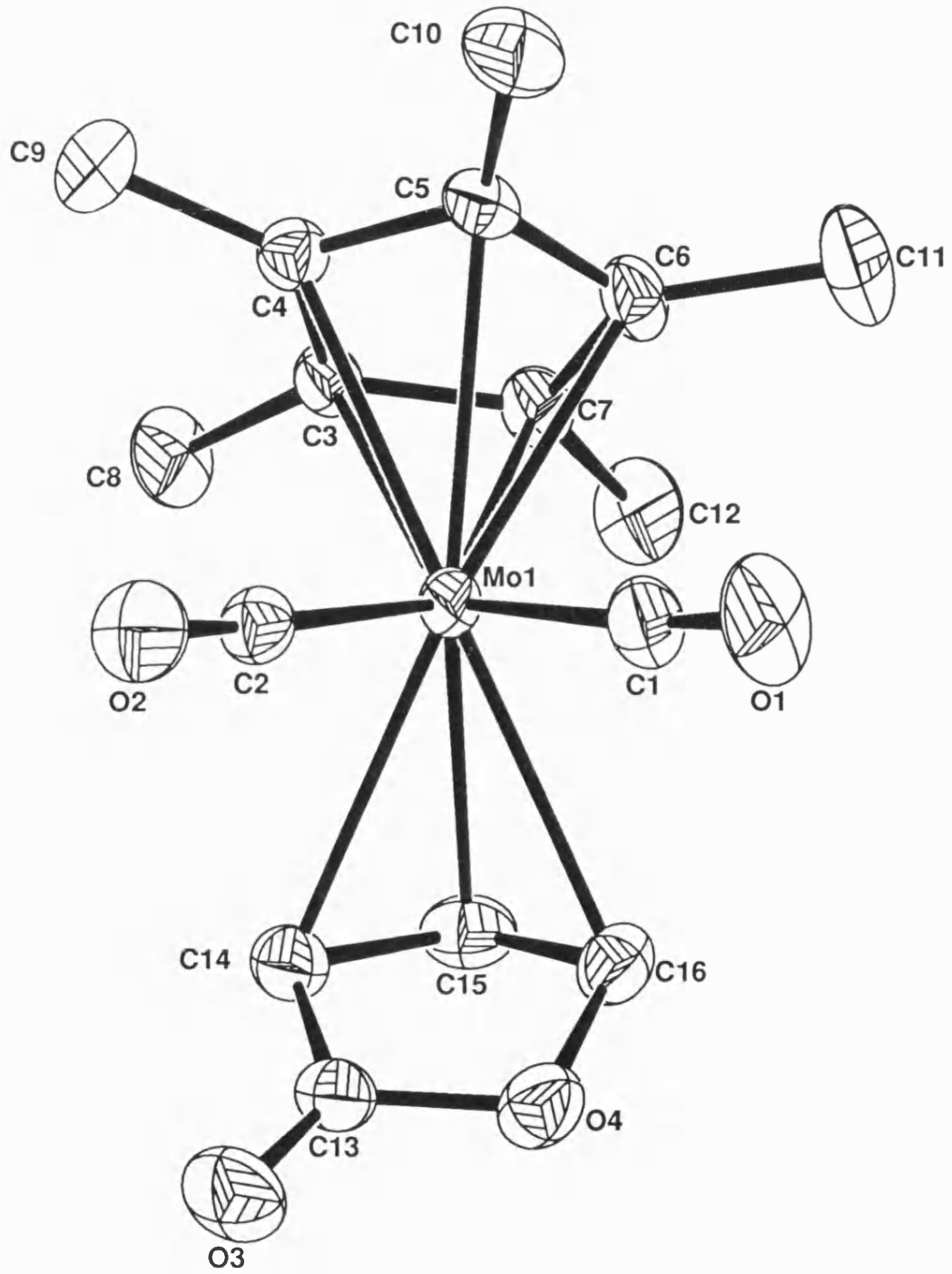

Figure 143. Molecular structure of $[Mo(\eta^3\text{-}C_4H_3O_2)(CO)_2(\eta^5\text{-}C_5Me_5)]$ (162).

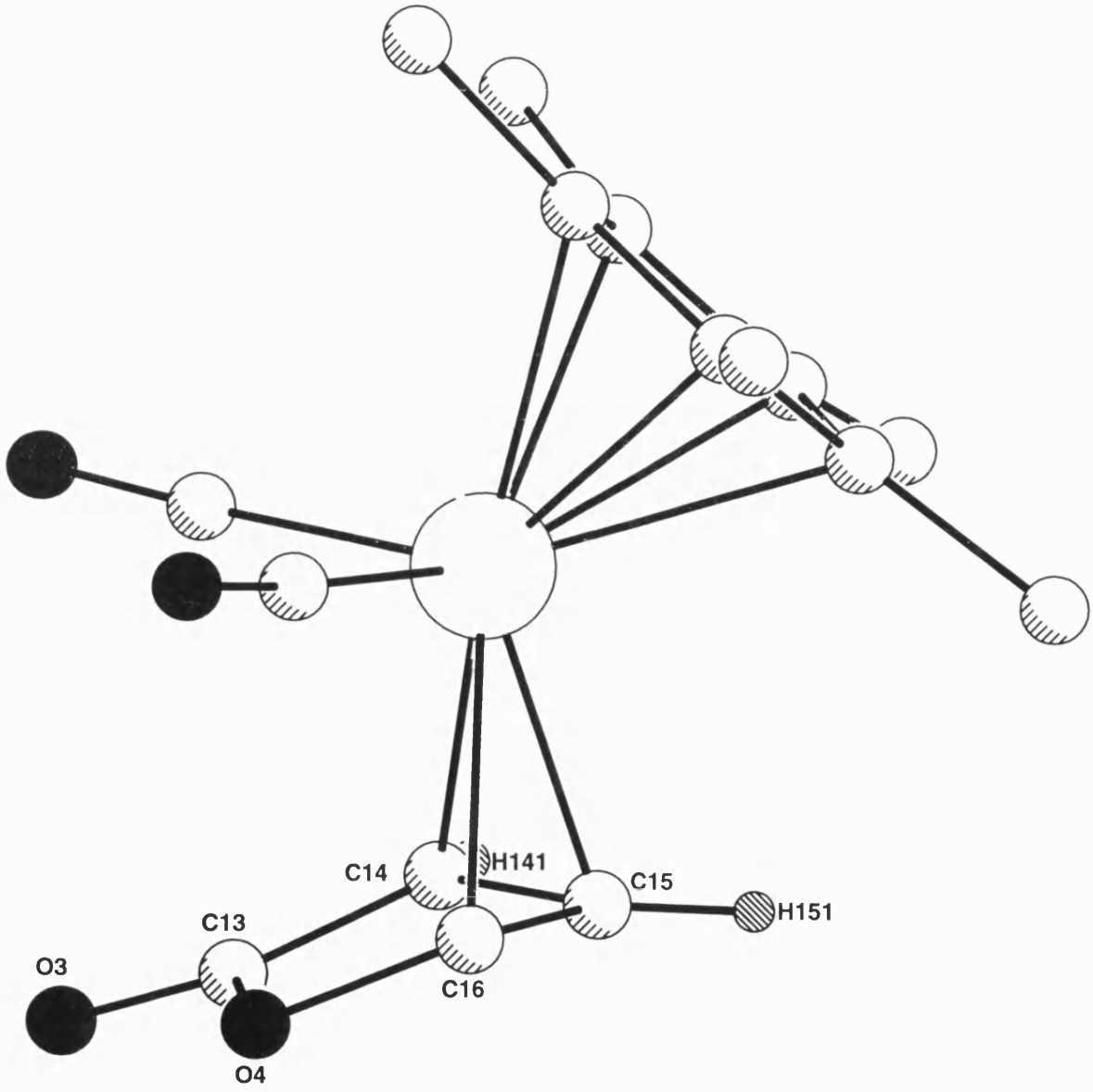

Figure 144. Alternative representation of $[Mo(\eta^3\text{-}C_4H_3O_2)(CO)_2(\eta^5\text{-}C_5Me_5)]$ (162).

Table 9

Selected bond lengths (Å), angles (°) and torsion angles (°) for complex (162) with estimated standard deviations in parentheses.

Mo-C(1)	1.942(6)	Mo-C(2)	1.969(6)
Mo-C(3)	2.391(5)	Mo-C(4)	2.352(5)
Mo-C(5)	2.296(5)	Mo-C(6)	2.318(5)
Mo-C(7)	2.374(5)	Mo-C(14)	2.369(6)
Mo-C(15)	2.189(5)	Mo-C(16)	2.358(6)
C(1)-O(1)	1.151(5)	C(2)-O(2)	1.139(6)
C(13)-O(3)	1.205(5)	C(13)-O(4)	1.388(5)
C(16)-O(4)	1.431(5)	C(13)-O(14)	1.439(6)
C(14)-C(15)	1.415(7)	C(15)-C(16)	1.390(7)
C(1)-Mo-C(2)	83.7(3)	Mo-C(1)-O(1)	175.6(3)
Mo-C(2)-O(2)	177.1(3)	C(13)-C(14)-C(15)	107.5(4)
C(14)-C(15)-C(16)	103.6(4)	C(15)-C(16)-O(4)	110.3(4)
C(13)-C(14)-C(15)-C(16)	-21.1(4)	C(14)-C(15)-C(16)-O(4)	24.5(4)
C(13)-O(4)-C(16)-C(15)	-18.2(4)	C(16)-O(4)-C(13)-C(14)	4.1(4)
O(4)-C(13)-C(14)-C(15)	10.7(4)		

The central molybdenum atom can be formally described as seven-coordinate, being bonded to two terminal carbonyl ligands, an η^3-γ-lactonyl fragment and a pentamethyl-cyclopentadienyl ligand. Both metal-carbonyl groups are essentially linear, within experimental error, with Mo-C-O angles of 175.6 and 177.1°, the Mo-C and C-O bond lengths being typical.[129] These two carbonyl ligands lie at an angle of 83.7° to one

another. The C_5Me_5 ligand is essentially planar and is bound at a mean distance of 2.346 Å from the metal atom.

The γ-lactonyl fragment is bound to the metal *via* three carbon atoms as an η^3-allyl. This C(14)-C(15)-C(16) moiety adopts an *exo* orientation with respect to the η^5-C_5Me_5 ring, with a bond angle of 103.6° due to the constrained nature of the five-membered heterocyclic ring. As with the majority of Mo(II) exo-η^3-allyls, the inner carbon atom of the allyl moiety is closer to the metal [Mo-C(15) 2.189(5) Å] than both the outer carbons [Mo-C(14) 2.369(6) Å and Mo-C(16) 2.358(6) Å].[29,154] The lactonyl fragment can be seen to exist in an envelope-type conformation with the lactone moiety bent away from the metal out of the plane of the allyl carbon atoms. Finally, it should be noted that the carbon-carbon interatomic distances within the metal-bound part of this ligand are somewhat unsymmetrical [C(14)-C(15) 1.415(7) and C(15)-C(16) 1.390(7) Å]. This, together with the bond distances C(13)-C(14) 1.439(6) and C(13)-O(3) 1.205(5) Å, implies some degree of π-conjugation between the η^3-allyl and the lactone carbonyl group.[116]

The analogous η^5-cyclopentadienyl system was also examined. Addition of excess 2-(trimethylsilyloxy)furan to a dichloromethane solution of (108) led to the formation of the desired η^3-γ-lactonyl complex (163) in 55% yield, obtained as a bright yellow powder (Fig. 145). It was found that complex (163) could be similarly prepared using the Krivykh procedure [i.e. *via* the η^3-allyl complex (25) (see Section 1.2.2)], albeit in much lower yield (37%).

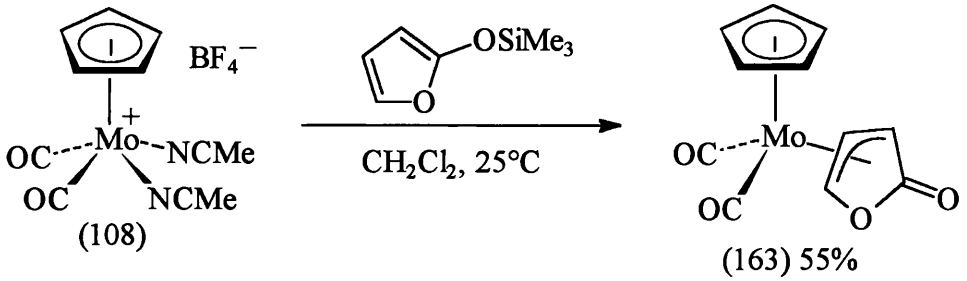

(108)

(163) 55%

Figure 145

As in the case of complex (162), the IR and NMR spectral data for (163) indicated the presence of *exo* and *endo* conformers in solution. The IR spectrum displayed two distinct sets of carbonyl bands in the ratio 2:1. The room temperature NMR spectrum showed a set of time-averaged broadened resonances and thus, low temperature experiments were necessary in order to distinguish between the conformers and determine the coupling constants. On lowering the temperature of the NMR probe to -60°C, exchange between the conformations was slowed, and the spectrum displayed two sets of well-resolved resonances in the ratio 7:1. As before, an examination of the chemical shift values for the η^3-lactonyl protons indicated that the *exo* conformer was the major isomer present in solution.

The corresponding reaction between 2-(trimethylsilyloxy)furan and the η^5-indenyl *cis*-bis(acetonitrile) cation (15) proceeded in a similar fashion, to afford the anticipated η^3-γ-lactonyl complex (164) in 57% yield, as a bright yellow solid (Fig. 146).

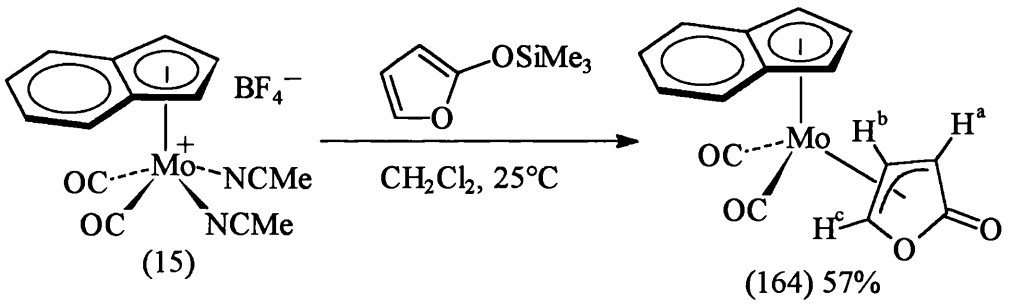

Figure 146

Complex (164) was found to exhibit only one set of carbonyl bands in its solution IR spectrum (at 1979, 1904 and 1752 cm^{-1}). The room temperature ^1H NMR spectrum displayed one set of slightly broadened resonances indicating the possibility of a conformational equilibrium. However, on lowering the temperature of the NMR probe to -45°C, the spectrum showed only one set of well-resolved resonances, with peaks for the η^3-lactonyl protons at 6.62 (H^c), 3.14 (H^a) and 1.26 ppm (H^b). Such chemical shift values were unequivocally assigned to the singular presence of an *exo* conformer. In particular, the relatively high upfield shift observed for the central allyl

proton (H^b) is typical[64] of (η^5-indenyl)$Mo(CO)_2$(*exo*-η^3-allyl) complexes, being caused by the anisotropic shielding effect of the indenyl ring. The absence of an *endo* conformer [cf. complexes (162) and (163)] can be attributed to the unfavourable steric interactions that would occur between the η^5-indenyl ligand and the lactone moiety in an *endo* configuration.

2.4.3 Reactivity of Molybdenum η^3-γ-Lactonyl Complexes Towards Nucleophilic Addition

Having established the ready availability of the novel η^3-γ-lactonyl molybdenum complexes, their reactivity towards nucleophilic addition was examined. The addition of nucleophiles to the corresponding η^3-δ-lactonyl complexes[35] used by Liebeskind has not been reported (the stereocontrolled elaboration of such species proceeding *via* initial electrophilic attack - see Section 2.4.1, Figure 140). However, it was anticipated that such additions would occur at the lactone carbonyl functionality present in these complexes (in accordance with standard organic reactions), possibly resulting in cleavage of the lactonyl ring.

The reaction between the η^5-indenyl-η^3-γ-lactonyl complex (164) and benzylamine was our initial area of study. When two molar equivalents of benzylamine were added to a dichloromethane solution of (164), a smooth reaction ensued and work-up afforded a good yield (85%) of a bright yellow powder. Significantly, when this reaction was repeated using only one molar equivalent of benzylamine, a much lower yield (*ca.* 8%) of this product was obtained. The pure material was found to be only soluble in polar solvents (acetone, MeCN), being slightly soluble in dichloromethane. An initial examination of the analytical and spectroscopic data supported the formulation [$Mo(C_{11}H_{12}NO_2)(CO)_2(\eta^5\text{-}C_9H_7)$], indicating that a molecular equivalent of benzylamine had been incorporated into the structure. Following the results of a single crystal X-ray diffraction experiment, the product was

identified as the novel zwitterionic η^2-olefinic complex (165) (Fig. 147), containing formalised positive and negative charges at nitrogen and molybdenum respectively.

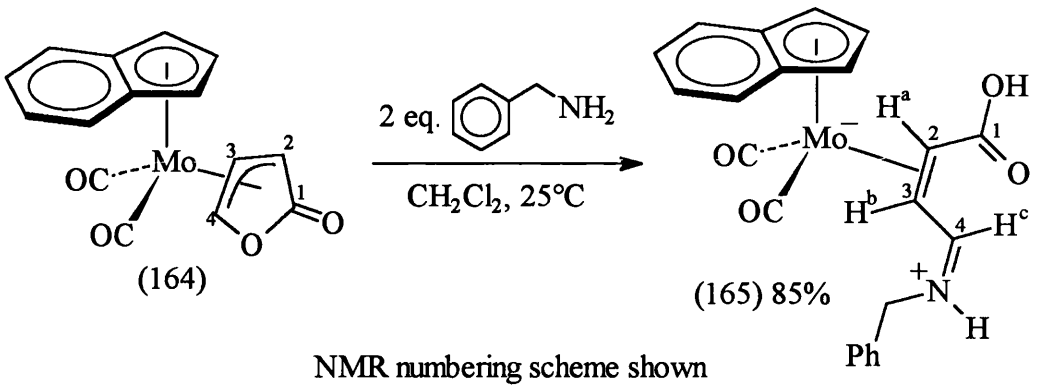

NMR numbering scheme shown

Figure 147

The molecular structure and atomic numbering scheme used are shown in Figure 148. Selected bond lengths, angles and torsion angles are given in Table 10. Complex (165) displays a typical 'piano-stool' type arrangement, in which the central molybdenum atom is bonded to two terminal carbonyl ligands, an η^2-olefinic fragment and an η^5-indenyl ring. The metal-carbonyl groups lie at an angle of 79° to one another and are both essentially linear, within experimental error, with Mo-C-O angles of 178.6° and 175.7°. The Mo-C and C-O bond lengths show some deviation from typical values,[129] suggesting increased back-bonding from the metal (as expected for a metal anion). Notably, a ring slippage pattern was observed in the metal-indenyl bonding. The carbon atoms C(4), C(5) and C(6) lie closer to the molybdenum centre at distances of 2.320(9), 2.302(10) and 2.328(9) Å, compared with the distances Mo-C(3) 2.445(9) and Mo-C(7) 2.431(8) Å. This allyl-ene, metal-ligand pattern is a common feature in metal-indenyl bonding.[162]

The remaining organic ligand is bonded to molybdenum in an η^2-fashion, *via* a *cis*-disubstituted olefin (the substituents being an iminium moiety and a carboxylic acid group), and orientated such that the hydrogen atoms H(141) and H(131) lie underneath the indenyl ligand. The iminium moiety (i.e. the $PhCH_2N^+HCH$ fragment) is positioned away from the metal such that the N(1)-C(15) and C(13)-C(14) double bonds are

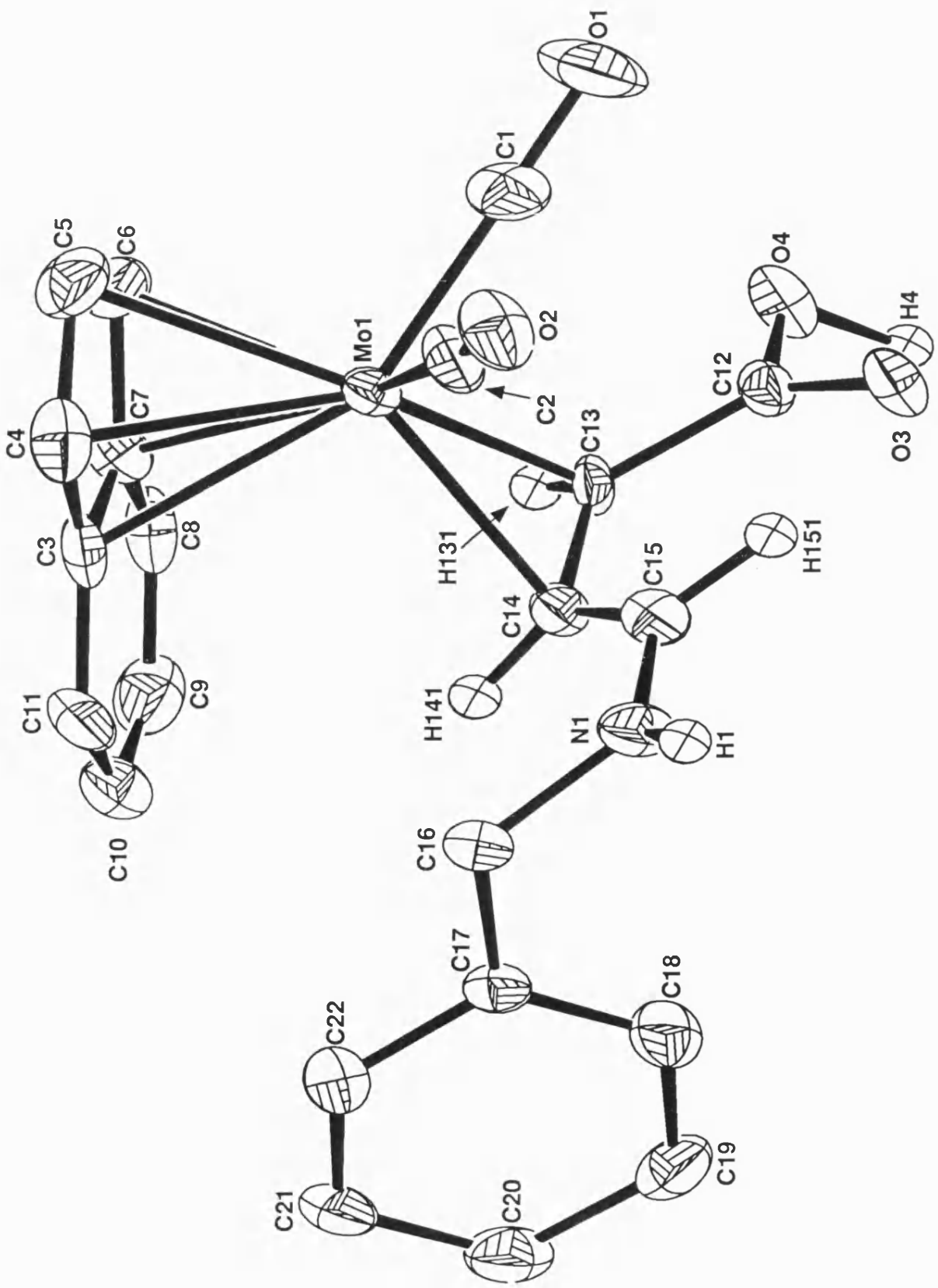

Figure 148. Molecular structure of $[Mo(\eta^2\text{-}C_{11}H_{12}NO_2)(CO)_2(\eta^5\text{-}C_9H_7)]$ (165)

Table 10

Selected bond lengths (Å), angles (°) and torsion angles (°) for complex (165) with estimated standard deviations in parentheses.

Mo-C(1)	1.929(9)	Mo-C(2)	1.938(10)
Mo-C(3)	2.445(9)	Mo-C(4)	2.230(9)
Mo-C(5)	2.302(10)	Mo-C(6)	2.328(9)
Mo-C(7)	2.431(8)	Mo-C(13)	2.237(8)
Mo-C(14)	2.272(9)	C(1)-O(1)	1.177(9)
C(2)-O(2)	1.158(9)	C(12)-O(3)	1.259(9)
C(12)-O(4)	1.319(8)	C(12)-C(13)	1.449(10)
C(13)-C(14)	1.450(10)	C(14)-C(15)	1.382(10)
N(1)-C(15)	1.333(9)	N(1)-C(16)	1.467(9)
C(1)-Mo-C(2)	79.9(4)	Mo-C(1)-O(1)	178.6(6)
Mo-C(2)-O(2)	175.7(7)	C(12)-C(13)-C(14)	124.3(7)
C(13)-C(14)-C(15)	123.6(7)	C(14)-C(15)-N(1)	127.1(7)
C(12)-C(13)-H(131)	113.1(40)	C(14)-C(13)-H(131)	117.7(41)
C(13)-C(14)-H(141)	119.7(40)	C(15)-C(14)-H(141)	116.3(40)
C(12)-C(13)-C(14)-C(15)	21.3(1)	C(13)-C(14)-C(15)-N(1)	-177.3(6)
C(16)-N(1)-C(15)-C(14)	-14.7(1)		

effectively *trans* to each other. The carboxylic acid moiety lies underneath the two metal-carbonyl ligands.

The η^2-olefin is bound to the metal asymmetrically with Mo-C bond distances of 2.237(8) and 2.272(9) Å, which are both considerably shorter than the typical[129] molybdenum-olefin bond distance (2.369 Å). Such values are consistent with a significantly increased degree of back-bonding from the metal. This is also reflected in

the C(13)-C(14) bond distance [1.450(10) Å] which is closer to the length of a standard carbon-carbon single bond (1.530 Å)[116] than that of a standard *cis*-disubstituted carbon-carbon double bond (1.317 Å)[116]. Thus, the C(13) and C(14) carbon atoms can be considered to have a degree of sp^3-character. The bond angles about these atoms provide further evidence of this. For example, the C(12)-C(13)-H(131) bond angle of 113.1° is lower than the 120° expected for an sp^2-hybridised moiety (sp^3-hybridisation corresponds to a bond angle of 109.5°). Finally, it is interesting to note the shortened carbon-carbon bond lengths C(12)-C(13) 1.449(10) Å, and particularly C(14)-C(15) 1.382(10) Å. This, coupled with the observed bond distances C(12)-O(3) 1.259(9) and N(1)-C(15) 1.333(9) Å, implies a certain amount of π-delocalisation around the six atom moiety from N(1) to O(3).

The solution IR and NMR spectroscopic data for (165) is in good agreement with the solid state X-ray structural observations. The IR spectrum displayed strong metal-carbonyl bands at 1933 and 1842 cm^{-1} along with a weaker band at 1653 cm^{-1} (carboxylic acid carbonyl group). Such relatively low frequency bands can be explained in terms of the back-bonding and π-delocalisation effects described above. In addition to resonances assigned to the indenyl and benzyl groups, the ^1H NMR spectrum showed two broadened peaks at 9.72 and 6.61 ppm (CO_2H and NH) along with three further resonances at 6.79 (H^c), 1.70 (H^a) and 1.13 ppm (H^b). It is interesting to note the relatively high-field chemical shift values observed for H^a and H^b, which can be attributed to the increased amount of sp^3-character associated with the olefinic carbons to which these protons are attached. The magnitude of the vicinal ^3J(H-H) coupling constants between H^a, H^b and H^c confirmed the geometry of the η^2-olefinic ligand. Thus, $J(H^aH^b)$ = 7.4 Hz, implying that H^a is *cis* to H^b, whereas $J(H^bH^c)$ = 11.2 Hz, indicative of a transoid relationship between H^b and H^c. The corresponding resonances were also exhibited in the ^{13}C-{^1H} NMR spectrum which, in particular, displayed peaks at 177.7 (C^1), 133.9 (C^4), 55.2 (C^3) and 41.9 ppm (C^2).

The formation of the zwitterionic complex (165) as the sole reaction product clearly showed that the anticipated attack of benzylamine at C^1 (NMR numbering) of the

η^3-γ-lactonyl complex (164) (i.e. the carbonyl carbon) had not taken place. Instead, overall addition of a $PhCH_2NH$ fragment had occurred at C^4 in (164) (i.e. at the γ-allyl carbon adjacent to the heterocyclic oxygen). In order to rationalise this process, it was therefore necessary to obtain more detailed information regarding the relative charge distribution in a molybdenum η^3-γ-lactonyl complex. This was achieved by means of an Extended Hückel Molecular Orbital (EHMO) calculation[163] which was carried out for the η^5-C_5H_5 γ-lactonyl complex (162). The X-ray crystallographic coordinates and bond parameters for (162) were used as the data set for the calculation, all hydrogens being idealised to a distance of 1.10 Å from their respective carbon atoms. The calculated electronic charges for the molybdenum atom and the η^3-γ-lactonyl ligand are shown in Figure 149. Representations of the theoretical HOMO (highest occupied molecular orbital) and LUMO (lowest unoccupied molecular orbital) were also obtained, and these are illustrated in Figures 150 and 151 respectively (overleaf).

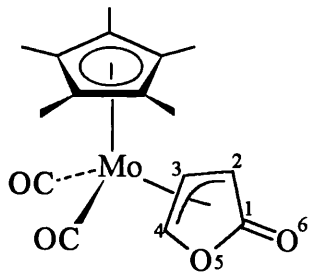

$C^1 = +1.180$ $O^5 = -0.753$
$C^2 = -0.107$ $O^6 = -1.131$
$C^3 = -0.078$ $Mo = +1.106$
$C^4 = +0.404$

Relative charge distribution for $[Mo(\eta^3\text{-}C_4H_3O_2)(CO)_2(\eta^5\text{-}C_5Me_5)]$ (162)

Figure 149

The calculations clearly show a high degree of localised positive charge (+1.180) at C^1 (the carbonyl carbon), as expected. The γ-carbon atom, C^4 [corresponding to the overall site of addition to (164)], also displays a small amount of positive charge (+0.404). However, the molybdenum centre is significantly more electropositive, having a localised charge of +1.106. These observations suggest that the formation of the zwitterionic η^2-olefin complex (165) takes place *via* initial attack of benzylamine at the metal atom, followed by a rearrangement reaction in which a $PhCH_2NH$ moiety is effectively transferred to C^4.

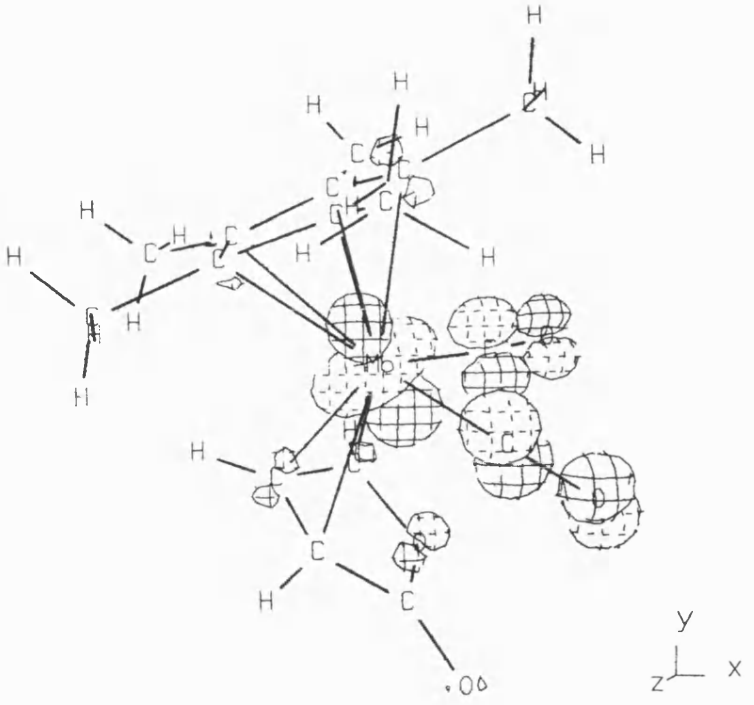

Figure 150. Theoretical HOMO plot for $[Mo(\eta^3\text{-}C_4H_3O_2)(CO)_2(\eta^5\text{-}C_5Me_5)]$ (162).

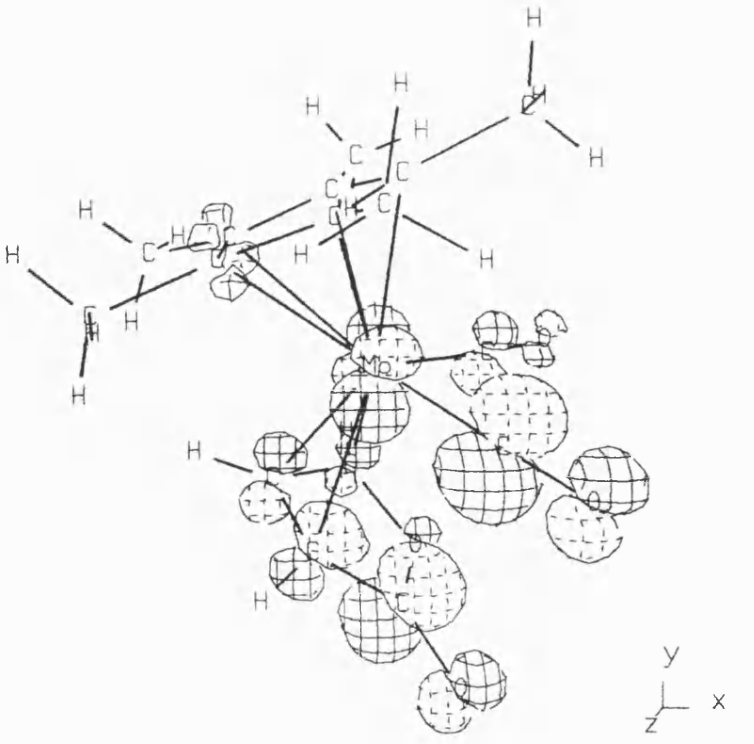

Figure 151. Theoretical LUMO plot for $[Mo(\eta^3\text{-}C_4H_3O_2)(CO)_2(\eta^5\text{-}C_5Me_5)]$ (162).

In the light of the above information, a mechanism for the formation of (165) can be proposed (Figure 153, overleaf). Direct *N*-coordination of benzylamine to the molybdenum centre in (164) would be expected to occur with concomitant η^3- to η^1-slippage of the lactone ligand to form (166). A second molecule of benzylamine can then effect deprotonation to generate a molybdenum anion (167) containing a molybdenum-amido group (i.e. a Mo-NHR σ-bond). This species undergoes a reductive elimination reaction in which the amido moiety is transferred to C^4, thus giving rise to an anionic η^2-olefin intermediate (168). Subsequent electron redistribution *via* the nitrogen lone-pair, results in cleavage of the lactone ring and protonation of the organic carbonyl moiety to form the zwitterionic η^2-olefin complex (165). It is interesting to note that (165) is isolated as a zwitterion and is perfectly stable in this form. Presumably direct rearrangement to the corresponding neutral η^3-allyl species (169) [which can be considered as a resonance form of (165)] is an energetically unfavourable process.

The corresponding reaction between the η^3-γ-lactonyl complex (164) and an optically active benzylamine was found to proceed in similar fashion. Addition of (*R*)-(+)-α-methylbenzylamine to a dichloromethane solution of (164) resulted in the formation of a particularly insoluble bright yellow solid, obtained in 87% yield. This was fully characterised by mass and NMR spectroscopy as the zwitterionic η^2-olefin complex (170) (Figure 152). In particular, the ^1H and ^{13}C-{^1H} NMR spectra showed that (170) was formed as a 1:1 mixture of the (*R*, *R*/*S*)- and (*R*, *S*/*R*)-diastereoisomers (the configuration at molybdenum being ambiguous).

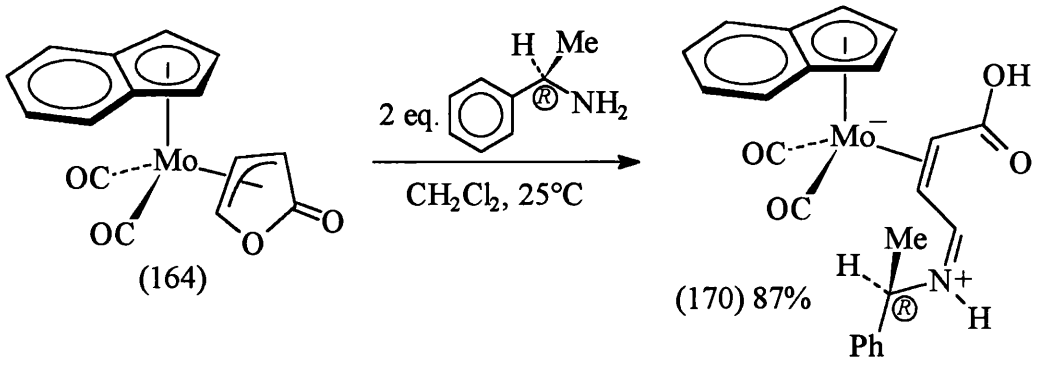

Figure 152

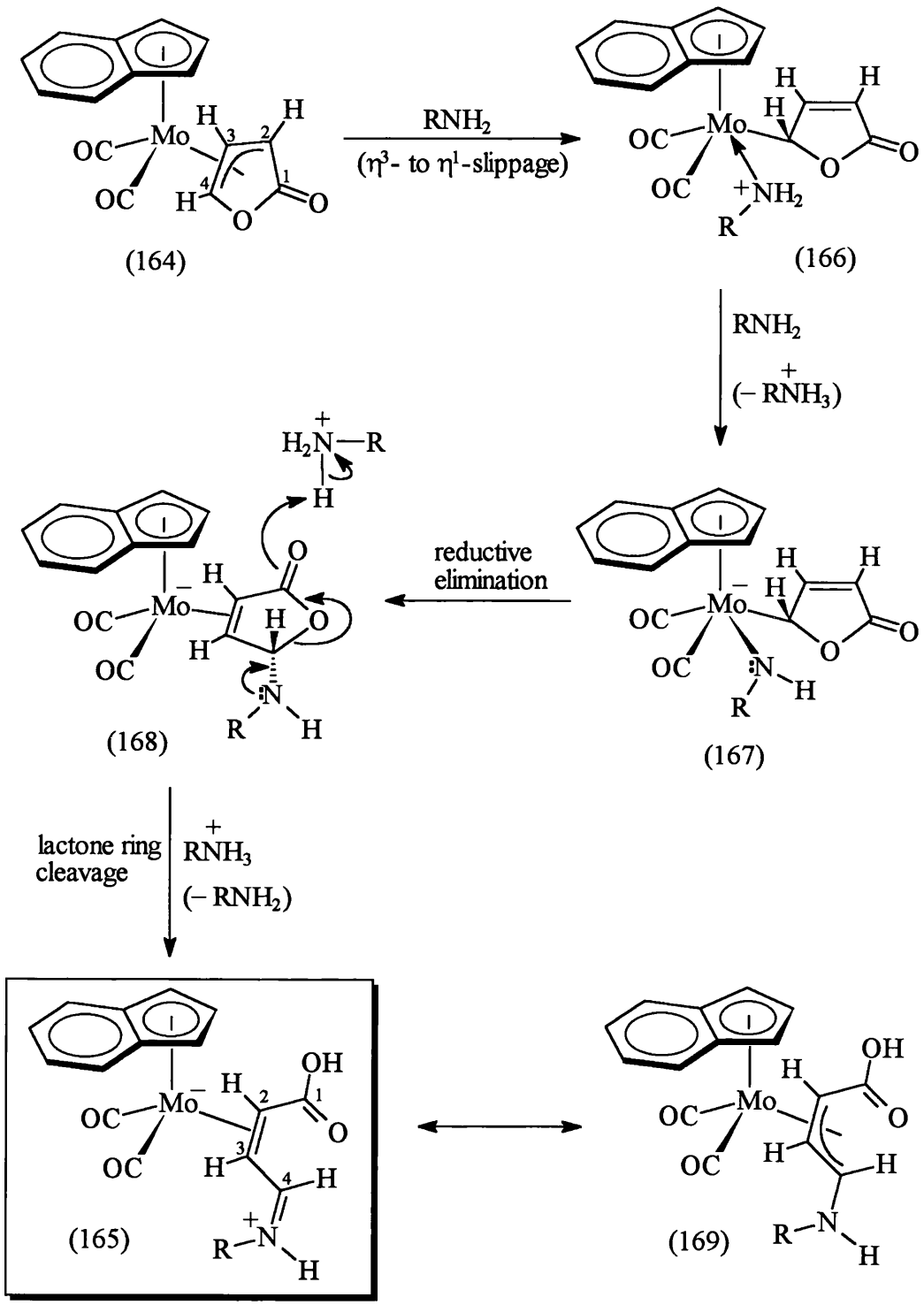

Figure 153. R = $PhCH_2$.

Mechanism for the formation of $[Mo(\eta^2\text{-}C_{11}H_{12}NO_2)(CO)_2(\eta^5\text{-}C_9H_7)]$ (165).

Following on from the benzylamine reactions, the reactivity of an η^3-γ-lactonyl complex towards the addition of an oxygen nucleophile was examined. Treatment of the cyclopentadienyl-lactonyl complex (163) with sodium methoxide (thf, 20°C) gave rise to a rapid reaction (0.5 h), and following work-up, a yellow powder was obtained in 83% yield. This was identified by mass and NMR spectroscopy as the methoxy- and carboxylate-substituted acyclic *anti*-η^3-allyl complex (171) (Fig. 154).

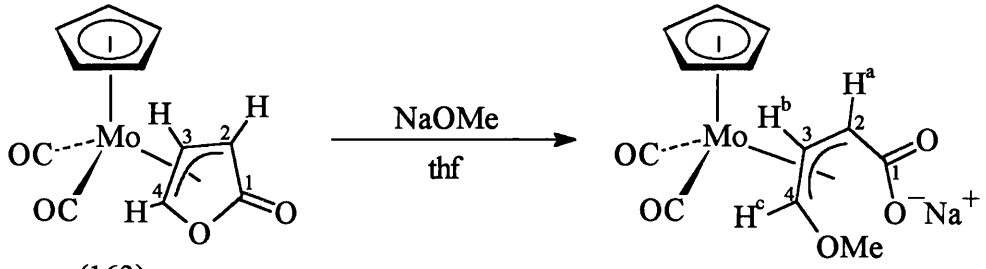

(163) *anti*-(171) 83%

Figure 154

Complex (171) was found to be soluble in only the more polar common organic solvents, as expected for such a charged species. The solution IR spectrum for (171) showed a broadened band at 1572 cm^{-1} attributed to the presence of the carboxylate anion. Two sets of metal-carbonyl bands were also observed (1946, 1871 and 1936, 1852 cm^{-1}) indicating the presence of *exo* and *endo* conformers of (171). This was confirmed from an examination of the ^1H NMR spectrum, which displayed two sets of well-resolved allylic resonances in the ratio 11:9. The relative chemical shift values for the allylic protons suggested that the *exo* conformer was the major isomer. In addition, the vicinal ^3J(H-H) couplings of the allylic protons [$J(H^aH^b) = J(H^bH^c) = 8.4$ Hz] implied that both the methoxy- and carboxylate-substituents were orientated in an *anti* configuration relative to the C_3 backbone of the allyl ligand.

Evidently, complex (171) is formed by means of an overall addition of methoxide at C^4 in (163) (NMR numbering), resulting in cleavage of the lactone ring. Presumably this process occurs in a similar manner to the benzylamine reactions, in which initial attack by the nucleophile takes place at the metal. The suggested mechanism is illustrated in Figure 155, overleaf. The first stage in this sequence

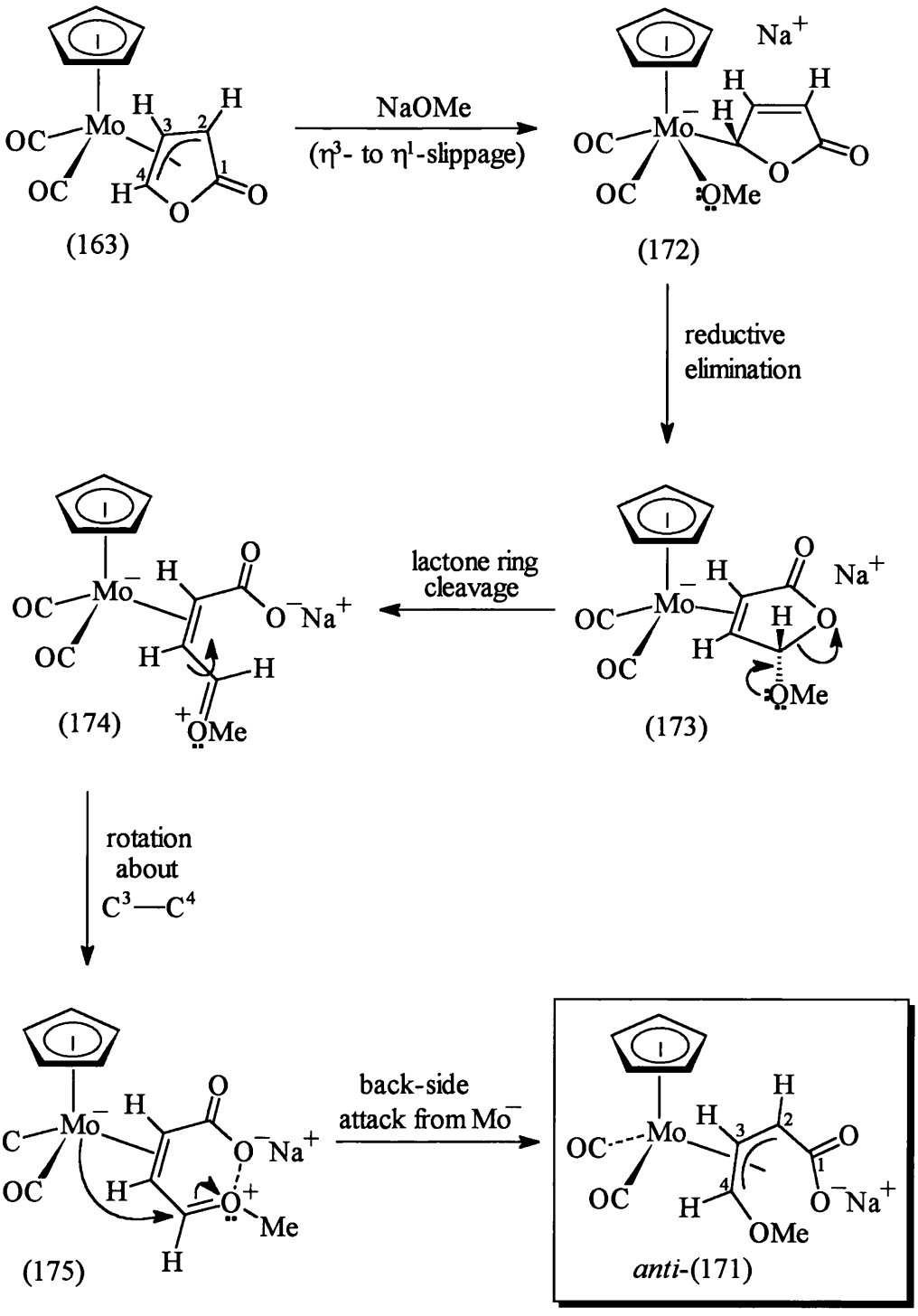

Figure 155

Mechanism for the formation of $[Mo(\eta^3\text{-}C_5H_6O_3Na)(CO)_2(\eta^5\text{-}C_5H_5)]$ (171).

involves direct attack of methoxide anion at the molybdenum centre in (163) with concomitant η^3- to η^1-slippage of the lactone ligand to form (172). A reductive elimination followed by a ring-opening reaction [*via* the lone-pair at the methoxy-oxygen atom in (173)] would give rise to a zwitterionic intermediate (174) containing a carboxylate anion [analogous to complexes (165) and (170)]. Interestingly, this species was not isolated, the actual product (171) being an *anti*-η^3-allyl complex. Conversion from (174) to (171) is thought to occur *via* rotation about the C^3-C^4 single bond in (174) to give the cisoid intermediate (175), in which the positive charge at the methoxy-oxygen atom is stabilised by its close proximity to the carboxylate moiety. Subsequent back-side nucleophilic attack from the molybdenum atom leads to the formation of complex (171).

From the results of these preliminary experiments, it is clear that the molybdenum η^3-γ-lactonyl complexes readily react with both benzylamine and the more nucleophilic methoxide anion at C^4 (the γ-carbon) of the lactone ring, most likely *via* initial coordination to the metal. The observed similarities between these reactions suggests that such reactivity is independent of the nature of the nucleophile. It is envisaged that the continuation of these studies will establish the generality of this process, by examining the reactivity of the η^3-γ-lactonyl complexes with a more diverse range of nucleophiles.

2.4.4 Reactivity of a Molybdenum η^3-γ-Lactonyl Complex Towards Protonation

It has been previously mentioned that the 4-oxo-η^3-cyclohexenyl and 4-oxo-η^3-butenyl complexes readily undergo selective *O*-protonation upon treatment with $HBF_4.OEt_2$ to give hydroxy-substituted η^4-1,3-diene cations (see Sections 2.1.3 and 2.3.2). Similarly, Liebeskind has shown that the molybdenum η^3-δ-lactonyl complex (159) reacts with Et_3OPF_6 to form an ethoxy-substituted η^4-1,3-diene cation (160)[35] (see Section 2.4.1, Figure 140). It was therefore anticipated that protonation of our η^3-γ-lactonyl complexes would occur at the lactone carbonyl oxygen atom, allowing the

formation of cationic η^4-furan species such as (176) (Figure 156). Indeed, this type of reaction can be predicted from the results of the EHMO study carried out on the η^3-lactonyl complex (162) (see Figure 149, Section 2.4.3). The lactone carbonyl oxygen atom in this complex is the most electronegative atom (having a calculated localised negative charge of -1.131), and thus would be the most likely site of electrophilic attack.

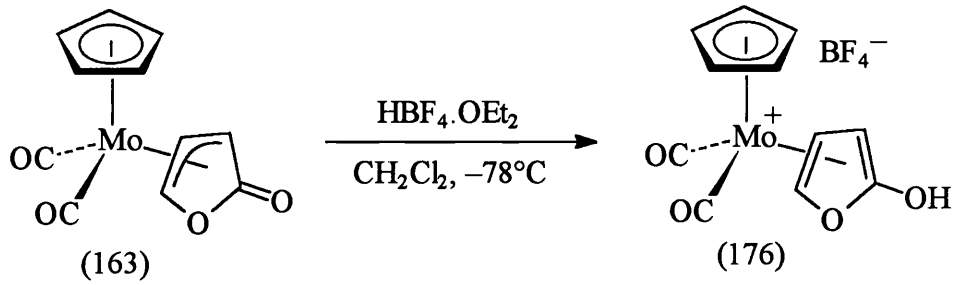

Figure 156

Cationic η^4-diene complexes such as (176) would be expected to undergo stereoselective nucleophilic addition reactions at C^1 of the furan ring (i.e. the hydroxy-substituted carbon), thereby providing a possible route to various stereodefined furan-based compounds. Hence, the formation of (176), *via* the protonation of the cyclopentadienyl η^3-γ-lactonyl complex (163), was attempted.

Low temperature addition of $HBF_4.OEt_2$ (-78°C) to a dichloromethane solution of (163) resulted in a rapid reaction and, following standard work-up procedures, a particularly air-sensitive orange powder was isolated. The insolubility of the product in Et_2O suggested it to be cationic. However, the readiness with which this compound decomposed on exposure to air made it extremely difficult to obtain any accurate information regarding its elemental composition. As such, the product could not be unambiguously identified on the sole basis of its IR and NMR spectral data.

The IR spectrum displayed two metal-carbonyl bands at 1927 and 1914 cm^{-1}, along with a distinct band at 1744 cm^{-1}, characteristic of an organic carbonyl group. Such relatively low frequency metal-carbonyl bands suggested that there was no localised positive charge at the molybdenum atom. In addition to a single resonance

due to an η^5-C_5H_5 ligand, the ^1H NMR spectrum showed three slightly broadened resonances at 5.49, 3.43 and 3.03 ppm, characteristic of three η^3-allylic protons. In particular the vicinal ^3J(H-H) couplings between these signals (3.7 and 3.3 Hz) implied that the allylic protons were orientated *cis* to each other, remaining directly attached to a ring system (as in the η^3-γ-lactonyl complex starting material). The ^{13}C-{^1H} NMR spectrum displayed resonances due to two metal-carbonyls and an η^5-C_5H_5 ligand, along with resonances at 173.5, 79.1, 44.6 and 37.9 ppm.

In view of the above information, it was evident that the anticipated η^4-furan cation (176) had not been isolated (such a structure is not compatible with the observed spectral data). Instead, it seemed most likely that the product was composed of a heterocyclic organic ligand, containing a localised positive charge, bonded in an η^3-allylic fashion to a $CpMo(CO)_2$ fragment. It was initially thought that the product was some sort of η^3-allylic cation (177) as represented by the series of resonance structures shown in Figure 157. Such structures are consistent with protonation occurring at the lactone carbonyl oxygen atom, however they do not readily account for the presence of the organic carbonyl band at 1744 cm^{-1} in the IR spectrum.

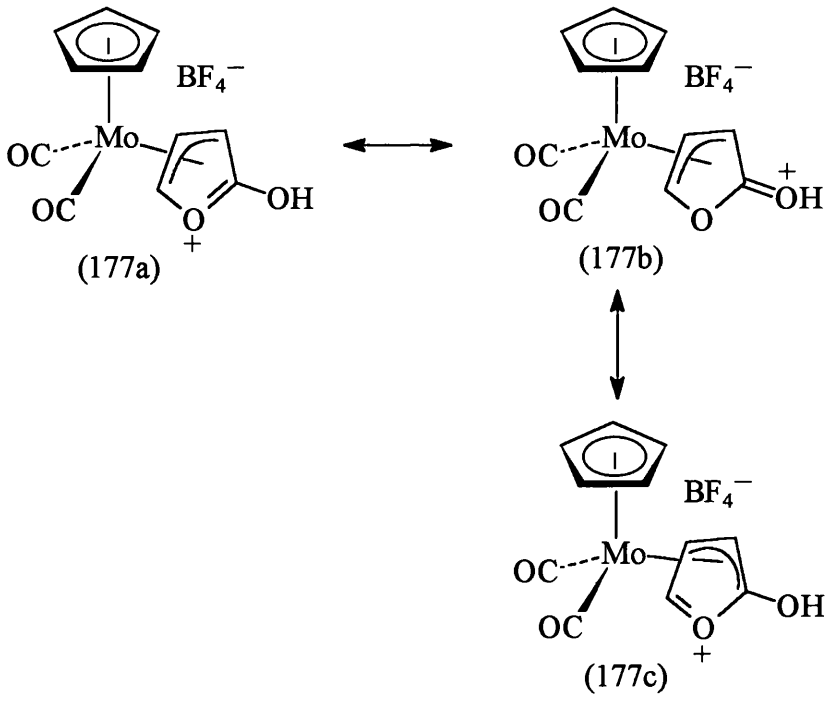

Figure 157

It would appear that the structure of the product from the reaction between the η^3-γ-lactonyl complex (163) and $HBF_4.OEt_2$ is of a rather more subtle nature. Ideally, an X-ray diffraction experiment is needed in order to clearly determine the exact identity of this species. It is hoped that the continuation of these studies will allow such an investigation in the near future.

2.4.5 Summary and Conclusions

The work discussed in this section has been concerned with the chemistry of certain furan-derived molybdenum complexes and a few useful conclusions may be drawn from these studies. It would appear that the direct coordination of furan to a $[CpMo(CO)_2]^+$ fragment, *via* the method of ligand substitution, is an unfavourable process. However, the use of a substituted furan, i.e. 2-(trimethylsilyloxy)furan, leads to the formation of a novel η^3-γ-lactonyl complex. The pentamethylcyclopentadienyl η^3-γ-lactonyl complex $[Mo(\eta^3\text{-}C_4H_3O_2)(CO)_2(\eta^5\text{-}C_5Me_5)]$ (162) and its η^5-indenyl and η^5-cyclopentadienyl analogues are all readily available by this route. Such species have been shown to undergo an interesting allyl-oxygen cleavage in their reaction with benzylamine or methoxide anion. Overall substituent addition takes place at the γ-carbon atom (C^4) of the lactone ring and is thought to occur by initial nucleophilic attack at the metal. Finally, the reactivity of an η^3-γ-lactonyl complex towards protonation has been examined. However, the exact nature of the protonation product has not been unambiguously determined. Further work is needed in this area in order to establish the structural identity of the product.

3. EXPERIMENTAL

General Experimental Procedures

All reactions were carried out under an atmosphere of dry, oxygen-free dinitrogen, using standard Schlenk line techniques, unless otherwise stated. Solvents were freshly distilled over an appropriate drying agent and further degassed before use where necessary. Reagents were obtained from commercial sources and were used as received, unless otherwise indicated. Chromatography columns used BDH alumina (Brockman activity II) or Florisil (100-200 mesh) as solid support.

^{1}H and ^{13}C-{^{1}H} NMR spectra were recorded on JEOL JNM GX270 (270 MHz) or EX400 (400 MHz) Fourier Transform spectrometers. Chemical shifts were referenced internally to the protio impurity in the deuteriated solvent. Coupling constants are in Hz.

Infrared spectra were recorded on a Nicolet 510P FT-IR spectrometer as solutions using sodium chloride cells.

FAB mass spectra and microanalyses were obtained courtesy of the University of Bath Analytical Services.

Preparation of Starting Materials

The following compounds were prepared according to the published literature procedures:

1-trimethylsilyloxycyclohexa-1,3-diene[164]

$[Mo(NCMe)_2(CO)_2(\eta^5\text{-}C_9H_7)][BF_4]$ (15)[38]

$[Mo(NCMe)_2(CO)_2(\eta^5\text{-}C_5Me_5)][BF_4]$ (16)[44]

$[Mo(\eta^3\text{-}C_3H_5)(CO)_2(\eta^5\text{-}C_5H_5)]$ (25)[28]

$[W(\eta^3\text{-}C_3H_5)(CO)_2(\eta^5\text{-}C_5H_5)]$ (138)[64]

$[Mo(\eta^3\text{-}C_3H_5)(CO)_2(\eta^5\text{-}C_9H_7)]$ (140)[64]

exo-syn-$[Ru(\eta^3\text{-}CH_2CHCHCHO)(CO)(\eta^5\text{-}C_5H_5)]$ (128a)[57,58]

exo-syn-$[Fe(\eta^3\text{-}CH_2CHCHCHO)(CO)(\eta^5\text{-}C_5H_5)]$ (130a)[110]

Preparation of $[Mo(\eta^3\text{-}C_6H_7O)(CO)_2(\eta^5\text{-}C_5Me_5)]$ (92)

To a solution of the blood-red complex *cis*-$[Mo(NCMe)_2(CO)_2(\eta^5\text{-}C_5Me_5)][BF_4]$ (16) (800 mg, 1.75 mmol) in CH_2Cl_2 (25 cm^3) was added 1-trimethylsilyloxy-cyclohexa-1,3-diene (886 mg, 5.25 mmol). The mixture was heated gently to reflux for 4 h giving a dark yellow solution. After cooling, the mixture was filtered through a small pad of alumina. The yellow filtrate was collected and concentrated to a small volume under reduced pressure, before being chromatographed on alumina. Elution with Et_2O afforded a bright yellow fraction which gave, after removal of solvent and recrystallisation from CH_2Cl_2/pentane, $[Mo(\eta^3\text{-}C_6H_7O)(CO)_2(\eta^5\text{-}C_5Me_5)]$ (92) (550 mg, 82%) as bright yellow *crystals*.

Microanalysis

$C_{18}H_{22}MoO_3$	requires:	C = 56.6, H = 5.8%
	found:	C = 56.5, H = 5.8%

Infrared Spectrum

ν_{CO}/cm^{-1} (CH_2Cl_2) at 1952 (vs), 1875 (s) and 1630 (m).

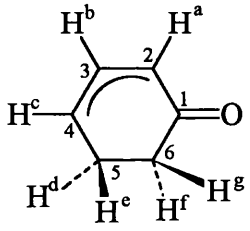

^{1}H NMR Spectrum

(CD_2Cl_2, 20°C): δ 3.45 (m, 2H, H^b and H^c), 3.20 [dd, 1H, H^a, $J(H^aH^b)$ = 5.7, $J(H^aH^c)$ = 2.0)], 2.37 [dddd, 1H, H^e, $J(H^eH^d)$ = 15.3, $J(H^eH^g)$ = 8.6, $J(H^eH^f)$ = 7.4, $J(H^eH^c)$ = 3.0], 2.00 [dddd, 1H, H^d, $J(H^dH^e)$ = 15.3, $J(H^dH^f)$ = 9.7, $J(H^dH^c)$ = 2.2, $J(H^dH^g)$ = 1.6], 1.88 (s, 15H, C_5Me_5), 1.69 [ddd, 1H, H^g, $J(H^gH^f)$ = 18.7, $J(H^gH^e)$ = 8.6, $J(H^gH^d)$ = 1.6] and 1.52 [ddd, 1H, H^f, $J(H^fH^g)$ = 18.7, $J(H^fH^d)$ = 9.7, $J(H^fH^e)$ = 7.4].

^{13}C-{^{1}H} NMR Spectrum

(CD_2Cl_2, 20°C): δ 236.4 (MoCO), 235.9 (MoCO), 197.7 (C^1), 104.7 (C_5Me_5), 74.8 (C^3), 59.7 (C^2 or C^4), 59.6 (C^2 or C^4), 30.6 (C^6), 22.1 (C^5) and 10.1 ($C_5\mathit{Me}_5$).

FAB Mass Spectrum

(+) FAB in NBA: 385, $[MH]^+$; 356, $[M\text{-}CO]^+$ and 328, $(M\text{-}2CO)^+$.

Preparation of $[Mo(\eta^4\text{-}C_6H_8O)(CO)_2(\eta^5\text{-}C_5Me_5)][BF_4]$ (94)

A solution of the yellow complex $[Mo(\eta^3\text{-}C_6H_7O)(CO)_2(\eta^5\text{-}C_5Me_5)]$ (92) (300 mg, 0.785 mmol) in CH_2Cl_2 (15 cm^{-3}) was cooled to -78°C and treated with $HBF_4.OEt_2$ (150 mg, 0.136 cm^3 of an 85% Et_2O solution, 0.785 mmol) causing a slight darkening in colour. The mixture was allowed to warm to ambient and stirred for 1 h. The resulting orange solution was filtered through Celite and then concentrated to a small volume under reduced pressure. Addition of Et_2O precipitated an orange solid which was washed with Et_2O and recrystallised from CH_2Cl_2/Et_2O to afford $[Mo(\eta^4\text{-}C_6H_8O)(CO)_2\text{-}(\eta^5\text{-}C_5Me_5)][BF_4]$ (94) (258 mg, 70%) as an orange powder.

Microanalysis

$C_{18}H_{23}BF_4MoO_3$	requires:	C = 46.0, H = 4.9%
	found:	C = 45.7, H = 4.8%

Infrared Spectrum

ν_{CO}/cm^{-1} (CH_2Cl_2) at 1993 (vs) and 1927 (vs).

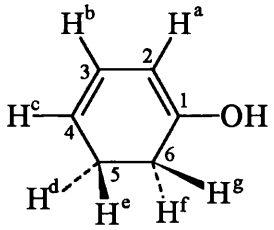

^{1}H NMR Spectrum

(CD_2Cl_2, 20°C): 4.44 [dd, 1H, H^a, $J(H^aH^b)$ = 5.0, $J(H^aH^c)$ = 1.3], 4.15 [dd, 1H, H^b, $J(H^bH^c)$ = 7.7, $J(H^bH^a)$ = 5.0], 3.87 [ddm, 1H, H^c, $J(H^cH^b)$ = 7.7, $J(H^cH^a)$ = 1.3], 2.40-1.95 (m, 4H, H^d, H^e, H^f, and H^g) and 1.98 (s, 15H, C_5Me_5).

^{13}C-{^{1}H} NMR Spectrum

(CD_2Cl_2, 20°C): δ 234.0 (CO), 232.0 (CO), 170.1 (C^1), 107.5 (C_5Me_5), 83.4 (C^2), 76.7 (C^3), 64.8 (C^4), 27.7 (C^5), 21.7 (C^6) and 10.3 (C_5Me_5).

FAB Mass Spectrum

(+) FAB in NBA: 385, $[M]^+$; 357, $[M\text{-}CO]^+$ and 329, $[M\text{-}2CO]^+$.

(-) FAB in NBA: 87, $[BF_4]^-$.

Deprotonation of $[Mo(\eta^4\text{-}C_6H_8O)(CO)_2(\eta^5\text{-}C_5Me_5)][BF_4]$ (94) with Et_3N

A solution of orange cation $[Mo(\eta^4\text{-}C_6H_8O)(CO)_2(\eta^5\text{-}C_5Me_5)][BF_4]$ (94) (115 mg, 0.244 mmol) in CH_2Cl_2 (10 cm^3) was treated with triethylamine (0.034 cm^{-3}, 0.244 mmol). The mixture was stirred for 1.5 h at ambient temperature causing a gradual change in colour to bright yellow. The solvent was removed under reduced pressure and the residue was chromatographed on alumina. Elution with Et_2O afforded a bright yellow solid, identified by infrared and NMR spectroscopy as the 4-oxo-η^3-allyl complex $[Mo(\eta^3\text{-}C_6H_7O)(CO)_2(\eta^5\text{-}C_5Me_5)]$ (92) (74 mg, 79%).

[Spectroscopic data for (92) as described above.]

Preparation of $[Mo(\eta^3\text{-}C_6H_9O)(CO)_2(\eta^5\text{-}C_5Me_5)]$ (95)

Sodium cyanoborohydride (0.249 cm^3 of a 1M solution in thf, 0.249 mmol) was added to a cooled (0°C) suspension of the orange cation $[Mo(\eta^4\text{-}C_6H_8O)(CO)_2(\eta^5\text{-}C_5Me_5)][BF_4]$ (94) (117 mg, 0.249 mmol) in thf (20 cm^3). The reaction mixture was stirred for 1 h at 0°C before being allowed to warm to ambient. After stirring the yellow solution for 1 h at room temperature, the solvent was removed *in vacuo* and the residue was chromatographed on alumina. Elution with Et_2O afforded a yellow fraction which gave, after removal of solvent and recrystallisation from CH_2Cl_2/pentane, $[Mo(\eta^3\text{-}C_6H_9O)(CO)_2(\eta^5\text{-}C_5Me_5)]$ (95) (79 mg, 83%) as bright yellow *crystals*.

Microanalysis

$C_{18}H_{24}MoO_3$	requires:	C = 56.3, H = 6.3%
	found:	C = 56.3, H = 6.3%

Infrared Spectrum

ν_{CO}/cm^{-1} (CH_2Cl_2) at 1921 (vs) and 1836 (s).

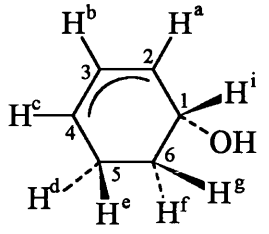

^{1}H NMR Spectrum

(CD_2Cl_2, 20°C): δ 3.97 (m, 1H, H^i), 3.26 (m, 1H, H^a), 3.07 (m, 1H, H^c), 2.79 [dd, 1H, H^b, $J(H^bH^a) = J(H^bH^c) = 7.2$], 1.95 [dddd, 1H, H^e, $J(H^eH^d) = 14.7$, $J(H^eH^f) = 11.9$, $J(H^eH^g) = 5.7$, $J(H^eH^c) = 2.6$], 1.88 (d, 1H, OH), 1.84 (s, 15H, C_5Me_5), 1.76 [dddd, 1H, H^d, $J(H^dH^e) = 14.7$, $J(H^dH^f) = 6.6$, $J(H^dH^c) = 3.0$, $J(H^dH^g) = 1.3$], 1.40 (dt, 1H, H^g, $J(H^gH^f) = 12.6$, $J(H^gH^e) = J(H^gH^i) = 5.7$] and 0.26-0.15 (m, 1H, H^f).

^{13}C-{^{1}H} NMR Spectrum

(CD_2Cl_2, 20°C): δ 243.8 (CO), 238.0 (CO), 103.9 (C_5Me_5), 68.5 (C^1), 67.9, 66.0 (C^2 and C^3), 60.3 (C^4), 32.0 (C^6), 23.2 (C^5) and 10.2 (C_5Me_5).

FAB Mass Spectrum

(+) FAB in NBA: 386, $[M]^+$; 369, $[M\text{-}OH]^+$; 306, $[M\text{-}OH\text{-}X]^+$; 278, $[M\text{-}OH\text{-}X\text{-}CO]^+$ and 250, $[M\text{-}OH\text{-}X\text{-}2CO]^+$.

Preparation of $[Mo(\eta^4\text{-}C_6H_6O)(CO)_2(\eta^5\text{-}C_5Me_5)][BF_4]$ (97)

Trityltetrafluoroborate (507 mg, 1.54 mmol, freshly recrystallised from CH_2Cl_2/Et_2O) was added to a cooled (0°C) solution of the yellow complex $[Mo(\eta^3\text{-}C_6H_7O)(CO)_2(\eta^5\text{-}C_5Me_5)]$ (92) (600 mg, 1.57 mmol) in CH_2Cl_2 (20 cm^3, further dried from P_2O_5) under a dry argon atmosphere. The resulting brown suspension was stirred for 2 h at 0°C and overnight at room temperature. The solution was transferred *via* cannula into 70 cm^3 of dry Et_2O being agitated with gaseous nitrogen, and a mustard-cream solid immediately precipitated. The supernatant liquid was removed *via* syringe

and the solid washed with several portions of Et_2O. A further purification was effected by recrystallisation form CH_2Cl_2/Et_2O to afford $[Mo(\eta^4\text{-}C_6H_6O)(CO)_2(\eta^5\text{-}C_5Me_5)]$ (97) (650 mg, 89%) as a mustard-cream powder.

Complex (97) is extremely air- and moisture-sensitive and turns olive green upon decomposition. H-H COSY experiments were used to assign the proton NMR signals.

Microanalysis

$C_{18}H_{21}BF_4MoO_3$	requires:	C = 46.2, H = 4.5%
	found:	C = 45.9, H = 4.6%

Infrared Spectrum

ν_{CO}/cm^{-1} (CH_2Cl_2) at 2056 (vs), 2012 (vs), 1703 (m) and 1686 (m).

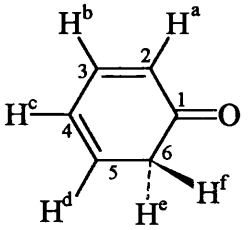

^1H NMR Spectrum

(CD_2Cl_2, 20°C): δ 5.75 [ddd, 1H, H^c, $J(H^cH^d)$ = 8.3, $J(H^cH^b)$ = 6.0, $J(H^cH^a)$ = 1.1], 5.49 [ddd, 1H, H^b, $J(H^bH^a)$ = 6.2, $J(H^bH^c)$ = 6.0, $J(H^bH^d)$ = 2.3], 4.23 [ddd, 1H, H^d, $J(H^dH^c)$ = 8.3, $J(H^dH^e)$ = 4.0, $J(H^dH^b)$ = 2.3], 3.51 [dd. 1H, H^a, $J(H^aH^b)$ = 6.2, $J(H^aH^c)$ = 1.1], 3,08 [d, 1H, H^f, $J(H^fH^e)$ = 19.6], 2.79 [dd, 1H, H^e, $J(H^eH^f)$ = 19.6, $J(H^eH^d)$ = 4.0], 2.09 (s, 15H, C_5Me_5).

$^{13}C\text{-}\{^1H\}$ NMR Spectrum

(CD_2Cl_2, 20°C): δ 217.6 (CO), 216.5 (CO), 194.3 (C^1), 109.0 (C_5Me_5), 95.8 (C^3), 75.8, 73.9, 67.8 (C^2, C^4 and C^5), 35.3 (C^6) and 10.7 (C_5Me_5).

FAB Mass Spectrum

(+) FAB in NBA: 383, $[M]^+$; 355, $[M\text{-}CO]^+$ and 327, $[M\text{-}2CO]^+$.

(-) FAB in NBA: 87, $[BF_4]^-$.

Reaction of $[Mo(\eta^4\text{-}C_6H_6O)(CO)_2(\eta^5\text{-}C_5Me_5)][BF_4]$ (97) with $Na[BH_3CN]$

Sodium cyanoborohydride (0.188 cm^3 of a 1M solution in thf, 0.188 mmol) was added to a cooled (0°C) suspension of the mustard-cream cation $[Mo(\eta^4\text{-}C_6H_6O)(CO)_2(\eta^5\text{-}C_5Me_5)][BF_4]$ (97) (88 mg, 0.188 mmol) in thf (25 cm^3). The reaction mixture was stirred for 2 h at 0°C and for 2 h at room temperature, causing a change in colour to a dirty yellow. The solvent was removed under reduced pressure and the residue was chromatographed on alumina. Elution with Et_2O afforded a bright yellow solid, identified by infrared and NMR spectroscopy as the 4-oxo-η^3-allyl complex $[Mo(\eta^3\text{-}C_6H_7O)(CO)_2(\eta^5\text{-}C_5Me_5)]$ (92) (57 mg, 80%).

[Spectroscopic data for (92) as described above.]

Reaction of $[Mo(\eta^4\text{-}C_6H_6O)(CO)_2(\eta^5\text{-}C_5Me_5)][BF_4]$ (97) with 1-pyrrolidino-1-cyclohexene

$[Mo(\eta^4\text{-}C_6H_6O)(CO)_2(\eta^5\text{-}C_5Me_5)][BF_4]$ (97) (105 mg, 0.224 mmol) in CH_2Cl_2 (20 cm^3, freshly distilled from P_2O_5) was treated at -78°C with 1-pyrrolidino-1-cyclohexene (0.047 cm^3, 0.292 mmol). Some darkening of colour was observed. The mixture was stirred for 5 h at -78°C and 30 h at room temperature to give a dark red solution. The reaction was hydrolysed with H_2O (0.17 cm^3, 42 equiv.) and stirred for 0.5 h at ambient. The solvents were removed *in vacuo* to give a red-black residue. This was dissolved in CH_2Cl_2, purified by column chromatography (Et_2O eluant, Florisil) and the red main fraction was collected. After vacuum removal of the solvent, $[Mo(\eta^5\text{-}C_5Me_5)(CO)_2]_2$[120] (99) (67 mg, 52%) was isolated as a red-purple solid.

Infrared Spectrum

ν_{CO}/cm^{-1} (CH_2Cl_2) at 1863 (s) and 1833 (s) cm^{-1}.

^1H NMR Spectrum

(CD_2Cl_2, 20°C): δ 1.93 (s, 30H, $2C_5Me_5$).

FAB Mass Spectrum

(+) FAB in NBA: 576, $[M]^+$; 548, $[M\text{-}CO]^+$; 520, $[M\text{-}2CO]^+$ and 464, $[M\text{-}4CO]^+$.

Reaction of $[Mo(\eta^4\text{-}C_6H_6O)(CO)_2(\eta^5\text{-}C_5Me_5)][BF_4]$ (97) with MeMgBr

$[Mo(\eta^4\text{-}C_6H_6O)(CO)_2(\eta^5\text{-}C_5Me_5)][BF_4]$ (97) (100 mg, 0.214 mmol) in thf (50 cm^3) was treated at -78°C with MeMgBr (0.277 cm^3 of a 1M solution in butylether, 0.277 mmol). Some darkening of colour was observed and the mixture was stirred at -78°C for 2 h. The solution was allowed to warm to ambient temperature and stirred for 1 h. The resulting dark red mixture was concentrated under reduced pressure to give a red-black residue. This was dissolved in CH_2Cl_2, purified by column chromatography (Et_2O eluant, Florisil) and the red-purple main fraction was collected. After vacuum removal of the solvent, $[Mo(\eta^5\text{-}C_5Me_5)(CO)_2]_2$[120] (99) (53 mg, 43% was isolated as a red-purple solid.

[Spectroscopic data for (99) as described above.]

Reaction of $[Mo(\eta^4\text{-}C_6H_6O)(CO)_2(\eta^5\text{-}C_5Me_5)][BF_4]$ (97) with 1,8-bis(dimethylamino)naphthalene

$[Mo(\eta^4\text{-}C_6H_6O)(CO)_2(\eta^5\text{-}C_5Me_5)][BF_4]$ (97) (80 mg, 0.17 mmol) in CH_2Cl_2 (20 cm^3, freshly distilled from P_2O_5) was treated at -78°C with 1,8-bis(dimethylamino)-naphthalene (40 mg, 0.188 mmol). Some darkening of colour was observed. The mixture was stirred for 1 h at -78°C and then allowed to warm to ambient temperature, causing an immediate colour change to dark red-purple. The solution was stirred for 1 h at room temperature and then concentrated under reduced pressure to leave a dark red residue. This was dissolved in CH_2Cl_2 and purified by column chromatography (Et_2O eluant, Florisil). The red-purple main fraction was collected and, after vacuum removal of the solvent, afforded $[Mo(\eta^5\text{-}C_5Me_5)(CO)_2]_2$[120] (99) (58 mg, 59%) as a red-purple solid.

[Spectroscopic data for (99) as described above.]

Preparation of $[Mo(\eta^3\text{-}C_7H_9O)(CO)_2(\eta^5\text{-}C_5Me_5)]$ (104)

$Li[N(SiMe_3)_2]$ (3.23 cm^3 of a 1M solution in thf, 3.23 mmol) was added to a cooled (-78°C) solution of the yellow complex $[Mo(\eta^3\text{-}C_6H_7O)(CO)_2(\eta^5\text{-}C_5Me_5)]$ (92) (950 mg, 2.46 mmol) in thf (50 cm^3), producing an immediate colour change to a deep orange. The mixture was stirred at -78°C for 0.5 h and then iodomethane (0.773 cm^3, 12.4 mmol) was added. The resulting orange-yellow mixture was stirred at -78°C for 1 h and at ambient temperature for 3 h. The solvent was removed *in vacuo* and the oily yellow residue was chromatographed on alumina. Elution with Et_2O afforded a bright yellow fraction which gave, after removal of solvent and recrystallisation from CH_2Cl_2/pentane, $[Mo(\eta^3\text{-}C_7H_9O)(CO)_2(\eta^5\text{-}C_5Me_5)]$ (104) (860 mg, 87%) as a bright yellow powder.

Microanalysis

$C_{19}H_{24}MoO_3$	requires:	C = 57.6, H = 6.1%
	found:	C = 57.0, H = 6.2%

Infrared Spectrum

ν_{CO}/cm^{-1} (CH_2Cl_2) at 1952 (vs), 1873 (s) and 1630 (m).

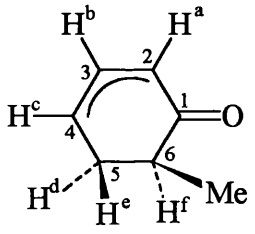

^{1}H NMR Spectrum

(CD_2Cl_2, 20°C): δ [dd, 1H, H^b, $J(H^bH^a) = J(H^bH^c) = 6.6$], 3.35 (m, 1H, H^c), 3.18 [dd, 1H, H^a, $J(H^aH^b) = 6.6$, $J(H^aH^c) = 1.6$], 2.25 [ddd, 1H, H^d, $J(H^dH^e) = 15.0$, $J(H^dH^f) = 7.7$, $J(H^dH^c) = 3.0$], 1,93 [ddd, 1H, H^e, $J(H^eH^d) = 15.0$, $J(H^eH^f) = 8.9$, $J(H^eH^c) = 2.9$], 1.84 (s, 15H, C_5Me_5), 1.63 (m, 1H, H^f) and 0.89 [d, 3H, Me, $J(H^fMe) = 7.2$].

^{13}C-{^{1}H} NMR Spectrum

(CD_2Cl_2, 20°C): δ 236.4 (CO), 235.9 (CO), 202.5 (C^1), 104.4 (C_5Me_5), 74.4 (C^2), 58.9 (C^3), 58.2 (C^4), 35.1 (C^6), 31.1 (C^5), 17.9 (Me) and 10.3 (C_5Me_5).

FAB Mass Spectrum

(+) FAB in NBA: 399, $[MH]^+$; 370, $[M\text{-}CO]^+$ and 342, $[M\text{-}2CO]^+$.

Reduction of $[Mo(\eta^3\text{-}C_6H_7O)(CO)_2(\eta^5\text{-}C_5Me_5)]$ (92) with $NaBH_4$

An excess of sodium borohydride (110 mg, 2.91 mmol) was added to a solution of the yellow complex $[Mo(\eta^3\text{-}C_6H_7O)(CO)_2(\eta^5\text{-}C_5Me_5)]$ (92) (752 mg, 1.97 mmol) in methanol (50 cm^3). The reaction mixture was stirred at ambient temperature for 3 h, after which the solvent was removed *in vacuo*. The yellow residue was redissolved in Et_2O and water (5 cm^3) was added whilst stirring rapidly. The etheral layer was separated and concentrated to a small volume under reduced pressure before being chromatographed on alumina. Elution with Et_2O afforded a yellow fraction which gave, after removal of solvent and recrystallisation from CH_2Cl_2/pentane, $[Mo(\eta^3\text{-}C_6H_9O)(CO)_2(\eta^5\text{-}C_5Me_5)]$ (95) (582 mg, 77%) as bright yellow *crystals*.

[Spectroscopic data for (95) as described above.]

Oppenauer Oxidation of $[Mo(\eta^3\text{-}C_6H_9O)(CO)_2(\eta^5\text{-}C_5Me_5)]$ (95)

An excess of dry acetone (20 cm^3, 273 mmol) was added to a solution of the yellow complex $[Mo(\eta^3\text{-}C_6H_9O)(CO)_2(\eta^5\text{-}C_5Me_5)]$ (95) (1.50 g, 3.90 mmol) in toluene (50 cm^3). To this was added aluminium isopropoxide (2.60 g, 12.73 mmol) and the mixture was heated to reflux for 7 h. Monitoring by infrared spectroscopy and TLC showed the formation of the oxidised product with complete consumption of the starting material. After cooling to ambient temperature, the solvent was removed *in vacuo* and the yellow residue was extracted with Et_2O. The etheral extracts were combined and concentrated to a small volume under reduced pressure, before being

chromatographed on alumina. Elution with Et_2O afforded a bright yellow solid, identified by infrared and NMR spectroscopy as the 4-oxo-η^3-allyl complex $[Mo(\eta^3\text{-}C_6H_7O)(CO)_2(\eta^5\text{-}C_5Me_5)]$ (92) (1.37 g, 92%).

[Spectroscopic data for (92) as described above.]

Preparation of $[Mo(\eta^3\text{-}C_{12}H_{13}O)(CO)_2(\eta^5\text{-}C_5Me_5)]$ (106)

Finely powdered anhydrous cerium(III) chloride (172 mg, 0.697 mmol) was heated under vacuum (0.1 mm Hg) at 140°C with stirring. After 2 h, the powder was cooled to 0°C in a flow of argon and thf (4 cm^3) was added with vigorous stirring. The resulting white suspension was allowed to warm to ambient temperature and left to stir overnight under argon. The mixture was then cooled to -78°C and treated with phenyllithium (0.387 cm^3 of an 1.8 M solution in thf, 0.697 mmol) causing the suspension to turn pale yellow in colour. After stirring for 0.5 at -78°C, a solution of the yellow complex $[Mo(\eta^3\text{-}C_6H_7O)(CO)_2(\eta^5\text{-}C_5Me_5)]$ (92) (205 mg, 0.536 mmol) in thf was added *via cannula* and stirring was continued at low temperature for 3 h. The orange mixture was allowed to warm to ambient and stirred for a further 15 h, causing a deepening in colour to an orange-red. This was treated with an excess of water (0.2 cm^3) and stirred for 1 h, after which the solvents were removed *in vacuo*. The orange residue was extracted with CH_2Cl_2 and the extracts were filtered through Celite giving an orange filtrate. This was concentrated to a small volume under reduced pressure and chromatographed on alumina. Elution with CH_2Cl_2/hexane (1:1) afforded a yellow fraction which gave, after removal of solvent and recrystallisation from CH_2Cl_2/hexane, $[Mo(\eta^3\text{-}C_{12}H_{13}O)(CO)_2(\eta^5\text{-}C_5Me_5)]$ (106) (170 mg, 69%) as a yellow-brown powder.

Microanalysis

$C_{24}H_{28}MoO_3$	requires:	C = 62.6, H = 6.1%
	found:	C = 62.4, H = 6.1%

Infrared Spectrum

ν_{CO}/cm^{-1} (CH_2Cl_2) at 1925 (vs) and 1838 (s).

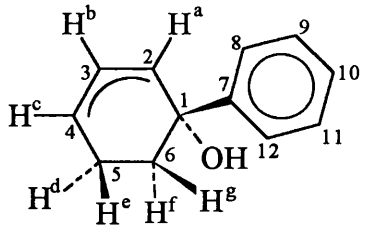

^{1}H NMR Spectrum

(CD_2Cl_2, 20°C): δ 7.69 (m, 2H, H^8 and H^{12}), 7.36 (m, 2H, H^9 and H^{11}), 7.22 (m, 1H, H^{10}), 3.24 (m, 3H, H^a, H^b and H^c), 2.50 (s, 1H, OH), 2.01-1.77 (m, 2H, H^d and H^e), 1.88 (s, 15H, C_5Me_5), 1.41 (m, 1H, H^g) and 0.75 (m, 1H, H^f).

^{13}C-{^{1}H} NMR Spectrum

(CD_2Cl_2, 20°C): δ 245.5 (CO), 238.2 (CO), 149.5 (C^7), 128.2 (C^8 and C^{12}), 126.8 (C^9 and C^{11}), 126.0 (C^{10}), 104.2 (C_5Me_5), 75.1 (C^1), 70.4, 69.0 (C^2 and C^3), 60.8 (C^4), 38.5 (C^6), 23.5 (C^5) and 10.3 (C_5Me_5).

FAB Mass Spectrum

(+) FAB in NBA: 462, $[M]^+$; 445, $[M-OH]^+$; 385, $[M-Ph]^+$; 306, $[M-Ph-X]^+$; 278, $[M-Ph-X-CO]^+$ and 250, $[M-Ph-X-2CO]^+$.

Preparation of $[Mo(\eta^3-C_{13}H_{15}O)(CO)_2(\eta^5-C_5Me_5)]$ (107)

Finely powdered anhydrous cerium(III) chloride (96 mg, 0.389 mmol) was heated under vacuum (0.1 mm Hg) at 140°C with stirring. After 2 h, the powder was cooled to 0°C in a flow of argon, and thf (2 cm^3) was added with vigorous stirring. The resulting white suspension was allowed to warm to ambient temperature and left to stir overnight under argon. The mixture was then cooled to -78°C and treated with phenyllithium (0.217 cm^3 of a 1.8 M solution in thf, 0.389 mmol), causing the suspension to turn pale yellow in colour. After stirring for 0.5 h at -78°C, a solution of the yellow complex $[Mo(\eta^3-C_7H_9O)(CO)_2(\eta^5-C_5Me_5)]$ (105) (119 mg, 0.300 mmol) in thf (5 cm^3) was added *via cannula*, and stirring was continued at low temperature for 3 h. The orange mixture was allowed to warm to ambient and stirred for a further 15 h,

causing a deepening in colour to an orange-red. This was treated with an excess of water (0.1 cm^3) and stirred for 1 h, after which the solvents were removed *in vacuo*. The orange residue was extracted with CH_2Cl_2 and the extracts were filtered through Celite giving a yellow filtrate. This was concentrated to a small volume under reduced pressure and chromatographed on alumina. Elution with hexane and then toluene afforded a yellow fraction which gave, after removal of solvent and recrystallisation from toluene/hexane, $[Mo(\eta^3\text{-}C_{13}H_{15}O)(CO)_2(\eta^5\text{-}C_5Me_5)]$ (107) (103 mg, 72%) as a yellow powder.

The molecular structure of (107) was determined by X-ray crystallography. X-ray quality *crystals* of (107) were obtained by toluene/hexane layer diffusion at room temperature. H-H and H-C COSY experiments were used to assign the proton and carbon NMR signals.

Microanalysis

$C_{24}H_{30}MoO_3$	requires:	C = 63.3, H = 6.4%
	found:	C = 63.0, H = 6.5%

Infrared Spectrum

ν_{CO}/cm^{-1} (CH_2Cl_2) at 1923 (vs) and 1836 (s).

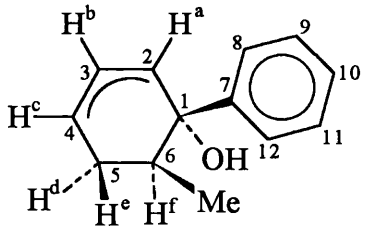

^{1}H NMR Spectrum

(CD_2Cl_2, 20°C): δ 7.67 (m, 2H, H^8 and H^{12}), 7.34 (m, 2H, H^9 and H^{11}), 7.21 (m, 1H, H^{10}), 3.24 (m, 3H, H^a, H^b and H^c), 2.41 (s, 1H, OH), 2.05-1.69 (complex m, 2H, H^d, H^e), 1.88 (s, 15H, C_5Me_5), 0.82 [mt, 1H, H^f, $J(H^f\,Me)$ = 6.8] and 0.28 [d, 3H, Me, $J(Me\,H^f)$ = 6.8].

^{13}C-{^{1}H} NMR Spectrum

(CD_2Cl_2, 20°C): δ 245.5 (CO), 238.2 (CO), 146.3 (C^7), 127.8 (C^8 and C^{12}), 126.8 (C^9 and C^{11}), 126.3 (C^{10}), 104.2 (C_5Me_5), 77.8 (C^1), 71.1, 70.4 (C^2 and C^3), 60.5 (C^4), 40.9 (C^6), 32.1 (C^5), 15.0 (Me) and 10.2 (C_5Me_5).

FAB Mass Spectrum

(+) FAB in NBA: 476, $[M]^+$; 459, $[M\text{-}OH]^+$; 399, $[M\text{-}Ph]^+$; 306, $[M\text{-}Ph\text{-}X]^+$; 278, $[M\text{-}Ph\text{-}X\text{-}CO]^+$; 250, $[M\text{-}Ph\text{-}X\text{-}2CO]^+$.

Preparation of $[Mo(\eta^5\text{-}C_5H_5)(CO)_3]$ (110)

Cyclopentadienylsodium (8.975 g, 0.102 mol) in thf (40 cm^3) was added dropwise under nitrogen, over 30 min, to a stirred solution of $Mo(CO)_6$ (24.5 g, 0.093 mol) in thf (50 cm^3). The mixture was brought carefully to a gentle reflux for 15 h (an initial rapid effervescence was observed). The resulting dark brown solution was cooled to ambient temperature followed by dropwise addition of methyl iodide (13.0 cm^3, 0.20 mol). The mixture was stirred overnight at ambient temperature and the solvents removed in vacuo to yield a brown slurry. This was redissolved in CH_2Cl_2 (50 cm^3) and filtered through a short column of alumina, eluting with CH_2Cl_2 . The material passing down the column was collected and reduced *in vacuo* to approximately 30 cm^3. This solution was re-purified by column chromatography as above, to yield $[Mo(\eta^5\text{-}C_5H_5)(CO)_3CH_3]$ (110) as a yellow crystalline solid [15.35 g, 64% from $Mo(CO)_6$].

Infrared Spectrum

ν_{CO}/cm^{-1} (CH_2Cl_2) at 2018 (s) and 1925 (bs).

Preparation of $[Mo(\eta^5\text{-}C_5H_5)(CO)_3(NCMe)][BF_4]$ (111)

Tetrafluoroboric acid diethyl etherate (10 cm^3, *ca.* 52.5 mmol) was added dropwise to a solution of $[Mo(\eta^5\text{-}C_5H_5)(CO)_3]$ (110) (13.64 g, 52.5 mmol) in dichloromethane (70 cm^3) at -78°C. The red solution was allowed to warm to warm to

ambient temperature and stirred for 30 minutes. The mixture was re-cooled to -78°C, acetonitrile (~15 cm^3) was added and the resultant solution stirred for 2 hours, allowing the temperature to rise slowly to ambient. The bulk of the solvents were removed *in vacuo*, to leave approximately 20 cm^3 and dry ether (100 cm^3) was added, with trituration, to precipitate the orange-red product. The solvents were decanted *via* syringe and the solid washed with further portions of Et_2O (4 x 30 cm^3). The solid was dissolved in dichloromethane (70 cm^3) and stirred with activated charcoal (2.5 g). The mixture was filtered through Celite, the bulk of the solvents removed *in vacuo*,leaving approximately, 30 cm^3 and the product re-precipitated by the addition of Et_2O (100 cm^3). The supernatant liquid was decanted *via* syringe and the resultant orange-red solid washed repeatedly with Et_2O until the washings were colourless (5 x 30 cm^3). The product was dried *in vacuo* to yield $[Mo(\eta^5\text{-}C_5H_5)(CO)_3(NCMe)][BF_4]$ (111) as an orange-red solid (17.51 g, 90%).

Infrared Spectrum

ν_{CO}/cm^{-1} (CH_2Cl_2) at 2075 (s) and 1994 (bs).

Preparation of *cis*-$[Mo(\eta^5\text{-}C_5H_5)(CO)_2(NCMe)_2][BF_4]$ (108)

cis-$[Mo(\eta^5\text{-}C_5H_5)(CO)_3(NCMe)][BF_4]$ (111) (17.51 g, 47 mmol) was dissolved in acetonitrile (50 cm^3) and heated to reflux for 8 h, giving a deep red solution. The solvent was removed *in vacuo* and the residue was taken up in dichloromethane (20 cm^3). Diethyl ether (60 cm^3) was added, with scratching, to precipitate the blood-red product. The solvents were decanted *via* syringe and the solid washed with diethyl ether (4 x 50 cm^3). Nitrogen was blown over the product which was then dried in vacuo to yield *cis*-$[Mo(\eta^5\text{-}C_5H_5)(CO)_2(NCMe)_2[BF_4]$ (108) as a blood-red solid (14.32 g, 79%).

Microanalysis

$C_{11}H_{11}BF_4MoN_2O_2$	requires:	C = 34.2, H = 2.9, N = 7.3%
	found:	C = 33.5, H = 2.9, N = 7.2%

Infrared Spectrum

ν_{CO}/cm^{-1} (CH_2Cl_2) at 1999 (s) and 1914 (s).

^1H NMR Spectrum

(CD_2Cl_2, 20°C): δ 5.75 (s, 5H, C_5H_5), 2.52 (s, 6H, MeCN).

^{13}C-{^1H} NMR Spectrum

(CD_2Cl_2, 20°C): δ 249.9 (CO), 143.1 (N*C*Me), 96.2 (C_5H_5) and 4.8 (NC*Me*).

FAB Mass Spectrum

(+) FAB in NBA: 301, $[M]^+$; 260, $[M\text{-}NCMe]^+$; 232, $[M\text{-}NCMe\text{-}CO]^+$ and 204, $[M\text{-}NCMe\text{-}2CO]^+$.

(-) FAB in NBA: 87, $[BF_4]^-$.

Preparation of $[Mo(\eta^4\text{-}C_5H_6)(CO)_2(\eta^5\text{-}C_5H_5)][BF_4]$ (112)

An excess of freshly distilled cyclopentadiene (1.10 cm^3, 12.95 mmol) was added to a *dilute* solution of the blood-red complex *cis*-$[Mo(NCMe)_2(CO)_2(\eta^5\text{-}C_5H_5)][BF_4]$ (108) (500 mg, 1.29 mmol) in CH_2Cl_2 (110 cm^3) at 20°C. After stirring for 1 h, the reaction mixture was warmed to ambient and stirred for a further 2 d, causing a gradual change in colour from red to a yellow/green solution. This was filtered through Celite and then concentrated to a small volume under reduced pressure, following which, addition of Et_2O precipitated a yellow solid. Further washing with Et_2O and then pentane, gave, after removal of the supernatant liquid and drying *in vacuo*, $[Mo(\eta^4\text{-}C_5H_6)(CO)_2(\eta^5\text{-}C_5H_5)][BF_4]$ (112) (430 mg, 90%) as a yellow powder.

Complex (112) is air-sensitive and readily goes off to $[Mo(CO)H(\eta^5\text{-}C_5H_5)_2][BF_4]$ (113) when left as a concentrated solution.

Microanalysis

$C_{12}H_{11}BF_4MoO_2$	requires:	C = 39.0, H = 3.0%
	found:	C = 38.7, H = 3.0%

Infrared Spectrum

ν_{CO}/cm^{-1} (CH_2Cl_2) at 2052 (ms), 2025 (m), 1998 (ms) and 1972 (m).

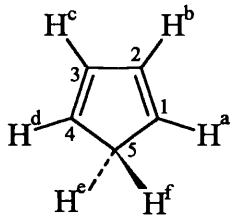

^{1}H NMR Spectrum

(CD_3NO_2, 20°C): δ 6.35 [dd, 2H, H^b and H^c, $J(H^bH^a) = J(H^cH^d) = 2.9$, $J(H^bH^d) = J(H^cH^a) = 2.8$], 5.85 (s, 5H, C_5H_5), 4.65 (m, 2H, H^a and H^d), 3.90 [dm, 1H, H^e or H^f, $J(H^eH^f) = 14.8$] and 3.50 [dm, 1H, H^e or H^f, $J(H^eH^f) = 14.8$].

^{13}C-{^{1}H} NMR Spectrum

(CD_3NO_2, 20°C): δ 217.8 (2CO), 89.3 (C_5H_5), 85.5 (C^2 and C^3), 72.1 (C^1 and C^4) and 44.0 (C^5).

FAB Mass Spectrum

(+) FAB in NBA: 285, $[M]^+$; 257, $[M\text{-}CO]^+$ and 229, $[M\text{-}2CO]^+$.

(-) FAB in NBA: 87, $[BF_4]^-$.

Binuclear reaction of $[Mo(\eta^4\text{-}C_5H_6)(CO)_2(\eta^5\text{-}C_5H_5)][BF_4]$ (112)

A sample of the yellow complex $[Mo(\eta^4\text{-}C_5H_6)(CO)_2(\eta^5\text{-}C_5H_5)][BF_4]$ (112) (195 mg. 0.53 mmol) was dissolved in dry $MeNO_2$ (7 cm^3) to give a *concentrated* solution and slow evolution of CO was observed. The reaction mixture was stirred for 3 h at ambient temperature causing a slight darkening in colour. Infrared spectroscopy showed complete consumption of the starting material and the formation of a new product. Slow addition of Et_2O precipitated a yellow solid which was washed with several portions of Et_2O and pentane. Recrystallisation from $MeNO_2/Et_2O$ gave $[Mo(CO)H(\eta^5\text{-}C_5H_5)_2][BF_4]$ (113) (160 mg, 89%), isolated as a yellow powder.

Complex (113) was found to exhibit corresponding experimental data to that previously reported for the hexafluorophosphate salt of this compound.[139]

Microanalysis

$C_{11}H_{11}BF_4MoO$ requires: C = 38.6, H = 3.2%

found: C = 38.7, H = 3.3%

Infrared Spectrum

ν_{CO}/cm^{-1} (CH_2Cl_2) at 2027 (vs).

^1H NMR Spectrum

[$(CD_3)_2CO$, 20°C]: δ 5.97 (s, 10H, $2C_5H_5$) and -8.15 (s, 1H, MoH).

^{13}C-{^1H} NMR Spectrum

[$(CD_3)_2CO$, 20°C]: δ 222.3 (CO) and 88.3 ($2C_5H_5$).

FAB Mass Spectrum

(+) FAB in NBA: 257, $[M]^+$ and 228, $[M-H-CO]^+$.

(-) FAB in NBA: 87, $[BF_4]^-$.

Reaction of $[Mo(\eta^4\text{-}C_5H_6)(CO)_2(\eta^5\text{-}C_5H_5)][BF_4]$ (112) with $Li[N(SiMe_3)_2]$

A cooled (-78°C) suspension of the yellow complex $[Mo(\eta^4\text{-}C_5H_6)(CO)_2(\eta^5\text{-}C_5H_5)][BF_4]$ (112) (150 mg, 0.405 cm^3) in thf, (15 cm^3) was treated with $Li[N(SiMe_3)_2]$ (0.405 cm^3 of a 1.0M solution in thf, 0.405 mmol) producing an immediate change in colour to a bottle green solution. The mixture was allowed to warm to ambient temperature and stirred for 0.5 h. Monitoring by infrared spectroscopy showed complete consumption of starting material and the formation of a new compound, tentatively identified as $[Mo(\eta^3\text{-}C_5H_5)(CO)_2(\eta^5\text{-}C_5H_5)]$ (118), [ν_{CO}/cm^{-1} at 1952 (ms) and 1861 (m)]. The solvent was removed under reduced pressure and the residue chromatographed on alumina. Elution with hexane afforded a green band which gave, after vacuum removal of solvent, a green solid identified as $[Mo(\eta^5\text{-}C_5H_5)_2(CO)]$ (121)[146] (42 mg, 41%).

Infrared Spectrum

ν_{CO}/cm^{-1} (CH_2Cl_2) at 1916 (s).

Reaction of [Mo(η^3-C_3H_5)(CO)$_2$(η^5-C_5H_5)] (25) with 2,4-cyclopentadien-1-yltrimethylsilane.

A *dilute* solution of the yellow complex [Mo(η^3-C_3H_5)(CO)$_2$(η^5-C_5H_5)] (25) (652 mg, 2.53 mmol) in CH_2Cl_2 (100 cm^3) was cooled to -78°C. To this, was added dropwise $HBF_4.OEt_2$ (481 mg, 0.437 cm^3 of an 85% Et_2O solution, 2.53 mmol) causing an immediate change in colour to a deep reddish violet. After stirring for 2 h at -78°C, an excess of 2,4-cyclopentadien-1-yltrimethylsilane (2.90 cm^3, 17.7 mmol) was added and the mixture stirred for a further 1.5 h at low temperature. The mixture was then allowed to warm to ambient and left to stir for 15 h, before filtering through Celite to give a reddish yellow solution. This was concentrated to a small volume under reduced pressure, following which dropwise addition of Et_2O precipitated a yellow solid. Further washing with Et_2O and then pentane, gave, after removal of the supernatant liquid and drying *in vacuo*, [Mo(η^4-C_5H_6)(CO)$_2$(η^5-C_5H_5)][BF_4] (112) (654 mg, 70%) as a yellow powder.

[Spectroscopic data for (112) as described above.]

Preparation of [Mo(η^3-C_5H_7)(CO)$_2$(η^5-C_5H_5)] (123)

Sodium cyanoborohydride (0.473 cm^3 of a 1.0M solution in thf, 0.47 mol) was added to a cooled (-78°C) suspension of the yellow complex [Mo(η^4-C_5H_6)(CO)$_2$(η^5-C_5H_5)][BF_4] (112) (175 mg, 0.47 mmol) in thf (25 cm^3). The mixture was allowed to warm to ambient and stirred for 1 h giving a yellow solution. Solvent was removed *in vacuo* and the resulting oily yellow residue loaded onto an alumina column. Elution with hexane afforded a yellow fraction which gave, after removal of solvent and recrystallisation from hexane, [Mo(η^3-C_5H_7)(CO)$_2$(η^5-C_5H_5)] (123) (94 mg, 70%) as a yellow powder.

Complex (123) was found to exhibit corresponding experimental data to that previously reported for this compound.[147]

Microanalysis

$C_{12}H_{12}MoO_2$ requires: C = 50.7, H = 4.3%

found: C = 50.4, H = 4.2%

Infrared Spectrum

ν_{CO}/cm^{-1} (CH_2Cl_2) at 1935 (vs) and 1854 (s).

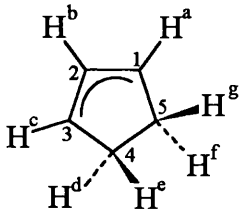

^{1}H NMR Spectrum

($CDCl_3$, 20°C): δ 5.28 (s, 5H, C_5H_5), 4.18 [dd, 1H, H^b, $J(H^bH^a) = J(H^bH^c) = 4.0$], 3.74 (m, 2H, H^a and H^c), 2.01 (d, 2H, H^d and H^f, $J = 11.0$) and 1.55 (dm, 2H, H^e and H^g, $J = 11.0$).

^{13}C-{^{1}H} NMR Spectrum

(C_6D_6, 20°C): δ 235.8 (2CO), 91.4 (C_5H_5), 60.5 (C^2), 57.9 (C^1 and C^3) and 30.1 (C^4 and C^5).

Reaction of $[Mo(\eta^4\text{-}C_5H_6)(CO)_2(\eta^5\text{-}C_5H_5)][BF_4]$ (112) with MeMgI

To a cooled (-78°C) suspension of the yellow complex $[Mo(\eta^4\text{-}C_5H_6)(CO)_2(\eta^5\text{-}C_5H_5)][BF_4]$ (112) (222 mg, 0.60 mmol) in thf (20 cm^3) was added MeMgI (0.200 cm^3 of a 3.0 M solution in thf, 0.60 mmol). After warming to ambient temperature, the resulting red-mauve solution was stirred for 1 h. Monitoring by infrared spectroscopy showed complete consumption of starting material and the formation of a new compound, tentatively identified as $[Mo(\eta^3\text{-}C_6H_9)(CO)_2(\eta^5\text{-}C_5H_5)]$ (124) [ν_{CO}/cm^{-1} at 1937 (vs) and 1862 (s)]. All attempts to isolate this species were thwarted by its tendency to decompose following column chromatography on alumina.

Preparation of *endo-anti*-[Ru(η^3-$CH_2CHCHCHO$)(CO)(η^5-C_5H_5)] (128d)

A solution of the yellow complex *exo-syn*-[Ru(η^3-$CH_2CHCHCHO$)(CO)(η^5-C_5H_5)] (128a)[57,58] (310 mg, 1.18 mmol) in CH_2Cl_2 (15 cm^3) was cooled to -78°C. To this was added $HBF_4.OEt_2$ (0.225 cm^3, 245 mg of an 85% Et_2O solution, 1.30 mmol) and the mixture was allowed to warm to ambient temperature, causing a slight darkening in colour. Stirring was continued for 2 h and monitoring by infrared spectroscopy showed the complete formation of a cationic species (ν_{CO}/cm^{-1} at 2010), tentatively identified as *endo-s-cis*-[Ru(η^4-$CH_2CHCHCHOH$)(CO)(η^5-C_5H_5)][BF_4] (129d). Triethylamine (0.202 cm^3, 147 mg, 1.45 mmol) was added and the yellow solution was stirred at ambient temperature for 2 h. Solvent was removed *in vacuo* and the residue was chromatographed on alumina. Elution with CH_2Cl_2 afforded a lemon-yellow fraction which gave, after removal of solvent and recrystallisation from CH_2Cl_2/hexane, *endo-anti*-[Ru(η^3-$CH_2CHCHCHO$)(CO)(η^5-C_5H_5)] (128d) (270 mg, 87%) as a pale yellow powder.

Microanalysis

$C_{10}H_{10}RuO_2$	requires:	C = 45.6, H = 3.8%
	found:	C = 45.7, H = 3.8%

Infrared Spectrum

ν_{CO}/cm^{-1} (CH_2Cl_2) at 1962 (s) and 1657 (ms).

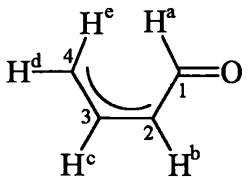

^{1}H NMR Spectrum

(CD_2Cl_2, 20°C): δ 7.78 [d, 1H, H^a, $J(H^aH^b)$ = 7.7], 5.14 (s, 5H, C_5H_5), 4.66 [ddd, 1H, H^c, $J(H^cH^e)$ = 11.4, $J(H^cH^d)$ = 7.9, $J(H^cH^b)$ = 6.8], 4.40 [ddd, 1H, H^b, $J(H^bH^a)$ = 7.7, $J(H^bH^c)$ = 6.8, $J(H^bH^d)$ = 0.7], 3.19 [ddd, 1H, H^d, $J(H^dH^c)$ = 7.9, $J(H^dH^e)$ = 2.2, $J(H^dH^b)$ = 0.7] and 2.16 [dd, 1H, H^e, $J(H^eH^c)$ = 11.4, $J(H^eH^d)$ = 2.2].

^{13}C-{^{1}H} NMR Spectrum

(CD_2Cl_2, 20°C): δ 206.9 (CO), 190.1 (C^1), 82.2 (C_5H_5), 71.9 (C^3), 55.5 (C^2) and 33.0 (C^4).

Preparation of *endo-anti*-[Fe(η^3-$CH_2CHCHCHO$)(CO)(η^5-C_5H_5)] (130d)

A solution of the orange complex *exo-syn*-[Fe(η^3-$CH_2CHCHCHO$)(η^5-C_5H_5)] (130a)[110] (360 mg, 1.65 mmol) in CH_2Cl_2 (30 cm^3) was cooled to -78°C. To this was added $HBF_4.OEt_2$ (0.343 cm^3, 377 mg of an 85% Et_2O solution, 1.98 mmol) causing the solution to turn red in colour. The mixture was allowed to warm to ambient temperature and stirred for 2 h before treatment with triethylamine (0.331 cm^3, 241 mg, 2.38 mmol). Stirring was continued for a further 1 h during which the colour of the solution turned gradually yellow. Solvent was removed under reduced pressure and the residue was chromatographed on alumina. Elution with hexane afforded a bright yellow band which gave, after removal of solvent, *endo-anti*-[Fe(η^3-$CH_2CHCHCHO$)(CO)(η^5-C_5H_5)] (130d) (331 mg, 92%) as a yellow powder.

Microanalysis

$C_{10}H_{10}FeO_2$	requires:	C = 55.1, H = 4.6%
	found:	C = 55.6, H = 4.9%

Infrared Spectrum

ν_{CO}/cm^{-1} (CH_2Cl_2) at 1960 (s) and 1650 (ms).

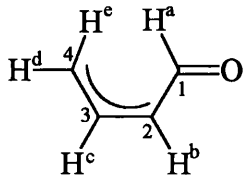

^{1}H NMR Spectrum

($CDCl_3$, 20°C): δ 7.35 (br s, 1H, H^a), 5.25 [ddd, 1H, H^c, $J(H^cH^e)$ = 11.9, $J(H^cH^d)$ = 7.9, $J(H^cH^b)$ = 7.3], 4.67 (s, 5H, C_5H_5), 4.30 [dd, 1H, H^b, $J(H^bH^a) = J(H^bH^c)$ = 7.3],

3.05 [dd, 1H, H^d, $J(H^dH^c)$ = 7.9, $J(H^dH^e)$ = 2.4] and 1.31 [dd, 1H, H^e, $J(H^eH^c)$ = 11.9, $J(H^eH^d)$ = 2.4].

$^{13}C-\{^1H\}$ NMR Spectrum

(CD_2Cl_2, 20°C): δ 221.4 (CO), 191.0 (C^1), 79.9 (C_5H_5), 77.6 (C^3), 56.0 (C^2) and 36.3 (C^4).

Preparation of *s-cis*-[Mo(η^4-$CH_2CHCHCHOAc$)$(CO)_2$(η^5-C_5Me_5)][BF_4] (133)

An excess of 1-acetoxy-1,3-butadiene (0.460 cm^3, 435 mg, 3.88 mmol) was added to a solution of the blood-red complex *cis*-[Mo$(NCMe)_2(CO)_2$(η^5-C_5Me_5)][BF_4] (16) (177 mg, 0.388 mmol) in CH_2Cl_2 (25 cm^3) and the mixture was stirred at room temperature for 4 d. Monitoring by infrared spectroscopy showed the gradual consumption of the starting material and the formation of a new product. The solvent was removed *in vacuo*, and the resulting green-brown residue was extracted with CH_2Cl_2 and filtered through Celite. The bottle-green filtrate was concentrated to a small volume under reduced pressure, following which addition of Et_2O precipitated a green solid. The supernatant liquid was removed *via* syringe and the solid washed with several portions of Et_2O and then pentane. A further purification was effected by recrystallisation from CH_2Cl_2/Et_2O to afford *s-cis*-[Mo(η^4-$CH_2CHCHCHOAc$)$(CO)_2$-(η^5-C_5Me_5)][BF_4] (133) (133 mg, 71.1%) as a green powder.

Microanalysis

$C_{18}H_{23}BF_4MoO_4$	requires:	C = 44.5, H = 4.8%
	found:	C = 45.0, H = 5.0%

Infrared Spectrum

ν_{CO}/cm^{-1} (CH_2Cl_2) at 2053 (vs), 2006 (s) and 1759 (mw).

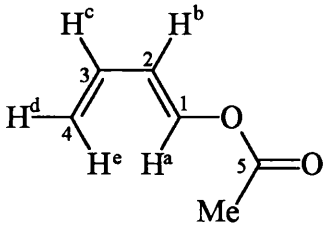

^{1}H NMR Spectrum

(CD_2Cl_2, 20°C): δ 6.08 (m, 1H, H^c), 5.97 (m, 1H, H^b), 4.58 [d, 1H, H^a, $J(H^aH^b)$ = 6.8], 2.57 [d, 1H, H^d, $J(H^dH^c)$ = 7.8], 2.03 (s, 3H, Me), 1.98 (s, 15H, C_5Me_5) and 1.05 [d, 1H, H^e, $J(H^eH^c)$ = 10.7]

^{13}C-{^{1}H} NMR Spectrum

(CD_2Cl_2, 20°C): δ 221.6 (CO), 220.3 (CO), 169.3 (C^5), 106.1 (C_5Me_5), 100.1 (C^1), 95.3 (C^2 or C^3), 89.0 (C^2 or C^3), 59.5 (C^4), 20.5 (Me) and 10.8 (C_5Me_5).

FAB Mass Spectrum

(+) FAB in NBA: 401, $[M]^+$; 373, $[M\text{-}CO]^+$ and 345, $[M\text{-}2CO]^+$.

(-) FAB in NBA: 87, $[BF_4]^-$.

Preparation of *exo-anti*-[Mo(η^3-$CH_2CHCHCHO$)(CO)$_2$(η^5-C_5Me_5)] (126c)

Sodium hydrogen carbonate (50 cm^3, 50 g of a 0.1 M aqueous solution, pH 8.5, *ca.* 5.0 mmol) was added to a solution of the green complex *s-cis*-[Mo(η^4-CH_2CHCH-$CHOAc$)(CO)$_2$(η^5-C_5Me_5)][BF_4] (133) (1.94 g, 3.99 mmol) in CH_2Cl_2 (50 cm^3). The two-phase system was vigorously stirred at room temperature, causing the mixture to turn yellowish in colour. After 2 h, the aqueous layer was removed and extracted several times with CH_2Cl_2. The extracts and organic layer were combined and washed with several portions of water before drying over magnesium sulphate. The mixture was filtered and the yellow filtrate was concentrated to a small volume under reduced pressure before being chromatographed on alumina. Elution with Et_2O afforded a single yellow fraction which gave, after removal of solvent and recrystallisation from Et_2O, *exo-anti*-[Mo(η^3-$CH_2CHCHCHO$)(CO)$_2$(η^5-C_5Me_5)] (126c)[44] (1.15g, 81%) as bright yellow *crystals*.

The molecular structure of (126c) was determined by X-ray crystallography. X-ray quality crystals were obtained by CH_2Cl_2/Et_2O/hexane layer diffusion at room temperature.

Microanalysis

$C_{16}H_{20}MoO_3$ requires: C = 53.9, H = 5.7%

found: C = 54.0, H = 5.7%

Infrared Spectrum

ν_{CO}/cm^{-1} (CH_2Cl_2) at 1960 (vs), 1883 (s) and 1644 (m).

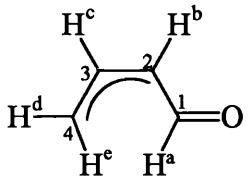

^{1}H NMR Spectrum

(CD_2Cl_2, 20°C): δ 7.00 [d, 1H, H^a, $J(H^aH^b)$ = 7.8], 3.51 [ddd, 1H, H^c, $J(H^cH^e)$ = 11.6, $J(H^cH^d)$ = 8.4, $J(H^cH^b)$ = 7.1], 3.42 (m, 1H, H^b), 2.28 [ddd, 1H, H^d, $J(H^dH^c)$ = 8.4, $J(H^dH^e)$ = 2.8, $J(H^dH^b)$ = 1.4], 1.88 (s, 15H, C_5Me_5) and 1.75 [dd, 1H, H^e, $J(H^eH^c)$ = 11.6, $J(H^eH^d)$ = 2.8].

^{13}C-{^{1}H} NMR Spectrum

(CD_2Cl_2, 20°C): δ 237.5 (CO), 237.2 (CO), 184.8 (C^1), 104.9 (C_5Me_5), 80.1 (C^3), 65.0 (C^2), 42.4 (C^4) and 10.4 (C_5Me_5).

FAB Mass Spectrum

(+) FAB in NBA: 359, $[MH]^+$; 330, $[M\text{-}CO]^+$ and 302, $[M\text{-}2CO]^+$.

Preparation of *s-cis*-[Mo(η^4-$CH_2CHCHCHOAc$)$(CO)_2(\eta^5$-C_5H_5)][BF_4] (134)

An excess of 1-acetoxy-1,3-butadiene (9.40 cm^3, 79.0 mmol) was added to a solution of the blood-red complex *cis*-[Mo$(NCMe)_2(CO)_2(\eta^5$-$C_5H_5)$][BF_4] (108) (3.05 g, 7.90 mmol) in CH_2Cl_2 (55 cm^3). After stirring at ambient temperature for 2 d a bright yellow precipitate was observed. Stirring was continued for a further 2 d, resulting in the formation of more precipitate. The mixture was filtered *via* cannula and the yellow solid was washed with several portions of CH_2Cl_2 and then pentane. Removal of the solvent followed by drying, first under nitrogen and then *in vacuo*, afforded *s-cis*-

$[Mo(\eta^4\text{-}CH_2CHCHCHOAc)(CO)_2(\eta^5\text{-}C_5H_5)][BF_4]$ (134) (2.80 g, 85%) obtained as a pale yellow powder.

Microanalysis

$C_{13}H_{13}BF_4MoO_4$	requires:	C = 37.5, H = 3.1 %
	found:	C = 37.0, H = 3.2%

Infrared Spectrum

ν_{CO}/cm^{-1} ($MeNO_2$) at 2068 (vs), 2020 (s) and 1759 (mw).

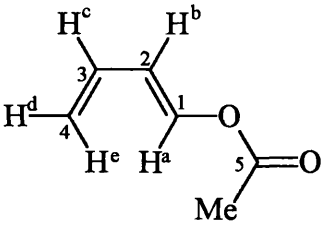

^{1}H NMR Spectrum

[$(CD_3)_2CO$, 20°C]: δ 6.48 (br m, 1H, H^b), 6.29 (br m, 1H, H^c), 6.12 (s, 5H, C_5H_5), 6.07 [br d, 1H, H^a, $J(H^aH^b)$ = 6.8], 3.01 [ddd, 1H, H^d, $J(H^dH^c)$ = 7.8, $J(H^dH^e)$ = 2.0, $J(H^dH^b)$ = 1.4], 2.38 [br d, 1H, H^e, $J(H^eH^c)$ = 10.7] and 2.06 (s, 3H, Me).

^{13}C-{^{1}H} NMR Spectrum

[$(CD_3)_2CO$, 20°C]: δ 220.2 (CO), 219.2 (CO), 167.9 (C^5). 102.8 (C^1), 93.9 (C^2 or C^3), 91.6 (C_5H_5), 88.3 (C^2 or C^3), 50.0 (C^4) and (Me).

FAB Mass Spectrum

(+) FAB in NBA:	331, $[M]^+$; 303, $[M\text{-}CO]^+$; 275, $[M\text{-}2CO]^+$ and
	232, $[M\text{-}2CO\text{-}Ac]^+$.
(-) FAB in NBA:	87, $[BF_4]^-$.

Preparation of *anti*-$[Mo(\eta^3\text{-}CH_2CHCHCHO)(CO)_2(\eta^5\text{-}C_5H_5)]$ (135)

Method A: Sodium hydrogen carbonate (75 cm^3, 70 g of a 0.1 M aqueous solution, pH 8.5, *ca.* 7.50 mmol) was added to a solution of the yellow complex *s-cis*-$[Mo(\eta^4\text{-}CH_2CHCHCHOAc)(CO)_2(\eta^5\text{-}C_5H_5)][BF_4]$ (134) (3.00 g, 7.21 mmol) in CH_2Cl_2 (60 cm^3). The two-phase system was vigorously stirred at room temperature for 0.5 h. The

aqueous layer was removed and extracted several times with CH_2Cl_2. The extracts and organic layer were combined and washed with several portions of water, before drying over magnesium sulphate. The mixture was filtered and the yellow filtrate was concentrated to a small volume under reduced pressure, before being chromatographed on alumina. Elution with CH_2Cl_2 afforded a bright yellow band which gave, after removal of solvent and recrystallisation from CH_2Cl_2/hexane, *anti*-[Mo(η^3-CH_2CHCH-CHO)$(CO)_2(\eta^5$-$C_5H_5)$] (135) (1.80 g, 87%) as a bright yellow powder.

Method B: A solution of the yellow complex [Mo(η^3-C_3H_5)$(CO)_2(\eta^5$-$C_5H_5)$] (25) (607 mg, 2.35 mmol) in CH_2Cl_2 (30 cm^3) was cooled to -78°C. To this was added dropwise HBF_4.OEt (0.411 cm^3, 452 mg of an 85% Et_2O solution, 2.38 mmol) causing an immediate change in colour to a deep reddish violet. After stirring for 0.5 h at -78°C, the mixture was treated with 1-acetoxy-1,3-butadiene (0.698, 659 mg, 5.89 mmol) and allowed to warm to ambient temperature. The dark green-brown mixture was stirred for a further 2 h and then filtered through Celite to give a dark green solution. This was concentrated to about 30 cm^3 *in vacuo* and treated with sodium hydrogen carbonate (35 cm^3 of a 0.1 M aqueous solution, pH 8.5, *ca* 3.50 mmol). The two-phase system was vigorously stirred at room temperature for 0.5 h causing the mixture to turn yellowish in colour. The aqueous layer was removed and extracted several times with CH_2Cl_2. The extracts and organic layer were combined and washed with several portions of water before drying over magnesium sulphate. The mixture was filtered through a small pad of alumina, and the orange-yellow filtrate was concentrated to a small volume under reduced pressure, before being chromatographed on alumina. Elution with CH_2Cl_2 afforded a bright yellow band which gave, after removal of solvent and recrystallisation from CH_2Cl_2/hexane, *anti*-[Mo(η^3-CH_2CHCH-CHO)$(CO)_2(\eta^5$-$C_5H_5)$ (135) (3,63 mg, 54%) as a bright yellow powder.

NMR spectroscopy showed (135) to exist in solution at room temperature as a 10:1 mixture of the *exo* and *endo* isomers (135c) and (135d). Low temperature NMR experiments were necessary for the determination of the coupling constants.

Microanalysis

$C_{11}H_{10}MoO_3$ requires: C = 46.2, H = 3.5%

found: C = 46.3, H = 3.5%

Infrared Spectrum

ν_{CO}/cm^{-1} (CH_2Cl_2) at 1973 (vs), 1896 (s) and 1649 (m).

Exo-anti isomer (135c) (major)

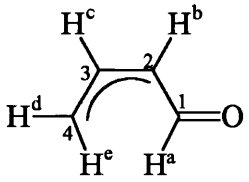

^{1}H NMR Spectrum

(CD_2Cl_2, 20°C): δ 7.14 (br s, 1H, H^a), 5.40 (br s, 5H, C_5H_5), 4.76 (br s, 1H, H^c), 4.05 (br s, 1H, H^b), 3.03 (br s, 1H, H^d) and 1.77 (br s, 1H, H^e).

(CD_2Cl_2, -40°C): δ 6.98 [d, 1H, H^a, $J(H^aH^b)$ = 7.9], 5.40 (s, 5H, C_5H_5), 4.78 [ddd, 1H, H^c, $J(H^cH^e)$ = 11.9, $J(H^cH^d)$ = 8.2, $J(H^cH^b)$ = 7.0], 4.00 [ddd, 1H, H^b, $J(H^bH^a)$ = 7.9, $J(H^bH^c)$ = 7.0, $J(H^bH^d)$ = 1.4], 3.02 [ddd, 1H, H^d, $J(H^dH^c)$ = 8.2, $J(H^dH^e)$ = 2.7, $J(H^dH^b)$ = 1.4 and 1.68 [dd, 1H, H^e, $J(H^eH^c)$ = 11.9, $J(H^cH^d)$ = 2.7].

^{13}C-{^{1}H} NMR Spectrum

(CD_2Cl_2, 20°C): δ 234.7 (br s, CO), 234.3 (br s, CO), 186.7 (br s, C^1), 92.2 (br s, C_5H_5), 72.2 (br s, C^3), 59.5 (br s, C^2) and 40.2 (br s, C^4).

(CD_2Cl_2, -50°C): δ 234.7 (CO), 234.5 (CO), 186.1 (C^1), 92.0 (C_5H_5), 71.8 (C^3) 58.7 (C^2) and 40.0 (C^4).

Endo-anti isomer (135d) (minor)

^{1}H NMR Spectrum

(CD_2Cl_2, 20°C): δ 7.84 (br s, 1H, H^a), 5.30 (br s, 5H, C_5H_5), 4.50 (br s, 1H, H^c), 4.19 (br s, 1H, H^b), 2.78 (br s 1H, H^d) and 2.65 (br s, 1H, H^e).

(CD_2Cl_2, -40°C): δ 7.71 [d, 1H, H^a, $J(H^aH^b)$ = 7.9], 5.30 (s, 5H, C_5H_5), 4.46 [ddd, 1H, H^c, $J(H^cH^e)$ = 11.2, $J(H^cH^d)$ = 7.3, $J(H^cH^b)$ = 6.2], 4.28 [dd, 1H, H^b, $J(H^bH^a)$ = 7.9, $J(H^bH^c)$ = 6.2], 2.77 [d, 1H, H^d, $J(H^dH^c)$ = 7.3] and 2.65 [d, 1H, H^e, $J(H^eH^c)$ = 11.2].

^{13}C-{^{1}H} NMR Spectrum

(CD_2Cl_2, 20°C): δ 234.7 (br s, CO), 234.3 (br s, CO), 186.7 (br, s, C^1), 92.2 (br s, C_5H_5), 72.2 (br s, C^3), 59.5 (br s, C^2) and 40.2 (br s, C^4).

(CD_2Cl_2, -50°C): δ 235.4 (CO), 235.1 (CO), 186.6 (C^1), 90.9 (C_5H_5), 86.4 (C^3), 61.0 (C^2) and 34.2 (C^4).

FAB Mass Spectrum

(+) FAB in NBA: 288, $[M]^+$; 260, $[M-CO]^+$ and 232, $[M-2CO]^+$.

Preparation of *anti*-[W(η³-$CH_2CHCHCHO$)(CO)₂)(η⁵-C_5H_5)] (139)

A solution of the yellow complex [W(η³-C_3H_5)(CO)₂(η⁵-C_5H_5)] (138) (150 mg, 0.433 mmol) in CH_2Cl_2 (15 cm^3) was cooled to -78°C. To this was added $HBF_4.OEt_2$ (0.075 cm^3, 83 mg of an 85% Et_2O solution, 0.443 mmol) resulting in an immediate colour change to a dark red. After stirring for 0.5 h at -78°C, the mixture was treated with 1-acetoxy-1,3-butadiene (0.128 cm^3, 121 mg, 1.08 mmol) and allowed to warm to ambient temperature. The green-black viscous mixture produced was stirred for a further 2 h and then filtered through Celite to give a dark green solution. Solvent was removed *in vacuo* and the residue redissolved in CH_2Cl_2 (30 cm^3) and treated with sodium hydrogen carbonate (11.0 cm^3 of a 0.1M aqueous solution, pH8.5, *ca* 1.1 mmol). The two-phase system was vigorously stirred at room temperature for 0.5 h causing the mixture to turn orange-yellow in colour. The aqueous layer was removed and extracted several times with CH_2Cl_2. The extracts and organic layer were combined and washed with several portions of water before drying over magnesium sulphate. The mixture was filtered through a small pad of alumina, and the orange-yellow filtrate was concentrated to a small volume under reduced pressure before being chromatographed on alumina. Elution with CH_2Cl_2 afforded a bright yellow band which gave, after removal of solvent and recrystallisation from toluene/hexane, *anti*-[W(η³-CH_2CHCH-CHO)(CO)₂(η⁵-C_5H_5)] (139) (70 mg, 4.3 %) as yellow *crystals*.

NMR spectroscopy showed (139) to exist in solution at room temperature as a 14:1 mixture of the *exo* and *endo* isomers (139c) and (139d). Low temperature NMR experiments were necessary to clearly distinguish between the isomers and determine the coupling constants.

Microanalysis

$C_{11}H_{10}O_3W$	requires:	C = 35.3, H = 2.7%
	found:	C = 35.6, H = 2.7%

Infrared Spectrum

ν_{CO}/cm^{-1} (CH_2Cl_2) at 1966 (vs), 1885 (s) and 1651 (m).

Exo-anti isomer (139c) (major)

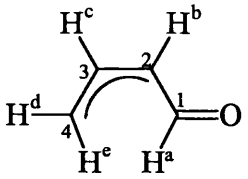

^{1}H NMR Spectrum

(CD_2Cl_2, 20°C): δ 7.02 (br s, 1H, H^a), 5.52 (br s, 5H, C_5H_5), 4.41 (br m, 1H, H^c), 4.05 (br m, 1H, H^b), 2.92 (br s, 1H, H^d) and 1.84 (br s, 1H, H^e).

(CD_2Cl_2, -30°C): δ 6.89 [d, 1H, H^a, $J(H^aH^b)$ = 8.2], 5.52 (s, 5H, C_5H_5), 4.39 [ddd, 1H, H^c, $J(H^cH^e)$ = 11.2, $J(H^cH^d)$ = 8.2, $J(H^cH^b)$ = 6.9], 4.02 [ddd, 1H, H^b, $J(H^bH^a)$ = 8.2, $J(H^bH^c)$ = 6.9, $J(H^bH^d)$ = 1.2], 2.90 [ddd, 1H, H^d, $J(H^dH^c)$ = 8.2, $J(H^dH^e)$ = 2.9, $J(H^dH^b)$ = 1.2] and 1.78 [dd, 1H, H^e, $J(H^eH^c)$ = 11.2, $J(H^eH^d)$ = 2.9].

^{13}C-{^{1}H} NMR Spectrum

(CD_2Cl_2, 20°C): δ 222.0 (br s, CO), 221.3 (br s, CO), 186.4 (br s, C^1), 90.8 (br s, C_5H_5), 63.9 (br s, C^3), 53.9 (br s, C^2) and 31.4 (br s, C^4).

(CD_2Cl_2, -30°C): δ 222.5 (CO), 221.4 (CO), 186.0 (C^1), 90.8 (C_5H_5), 63.6 (C^3), 54.1 (C^2) and 31.4 (C^4).

Endo-anti isomer (139d) (minor)

^{1}H NMR Spectrum

(CD_2Cl_2, 20°C): δ 7.75 (br s 1H, H^a), 5.52 (br s, 5H, C_5H_5), 4.41 (br m, 1H, H^c), 4.05 (br m, 1H, H^b), 2.73 (br s, 1H, H^d) and 2.70 (br s, 1H, H^e).

(CD_2Cl_2, -30°C): δ 7.63 [d, 1H, H^a, $J(H^aH^b) = 8.3$], 5.39 (s, 5H, C_5H_5), 4.47 (m, 1H, H^c), 4.24 [dd, 1H, H^b, $J(H^bH^a) = 8.3$, $J(H^bH^c) = 6.6$], 2.64 [d, 1H, H^d, $J(H^dH^c) = 6.8$] and 2.55 [d, 1H, H^e, $J(H^eH^c) = 9.9$].

^{13}C-{^{1}H} NMR Spectrum

(CD_2Cl_2, 20°C): δ 234.7 (br s, CO), 234.3 (br s, CO), 186.7 (br s, C^1), 92.2 (br s, C_5H_5), 72.2 (br s, C^3), 59.5 (br s, C^2) and 40.2 (br s, C^4).

(CD_2Cl_2, -30°C): δ 89.0 (C_5H_5). (The remaining resonances were too weak to be observed.)

FAB Mass Spectrum

(+) FAB in NBA: 375, $[MH]^+$; 346, $[M-CO]^+$ and 318, $[M-2CO]^+$.

Preparation of *exo-anti*-[Mo(η^3-$CH_2CHCHCHO$)$(CO)_2$(η^5-C_9H_7)] (125c)

A solution of the yellow complex [Mo(η^3-C_3H_5)$(CO)_2$(η^5-C_9H_7)] (140) (2.83 g, 9.19 mmol) in CH_2Cl_2 (50 cm^3) was cooled to -50°C. To this was added $HBF_4.OEt_2$ (1.74 cm^3, 2.01 g of an 85% Et_2O solution, 10.57 mmol) resulting in an immediate colour change to dark red. After stirring for 0.5 h at -50°C, the mixture was treated with 1-acetoxy-1,3-butadiene (2.73 cm^3, 22.98 mmol) and allowed to warm to ambient temperature, producing a green-black viscous mixture. This was stirred for a further 1 h and then filtered through Celite to give a dark green solution. The filtrate was concentrated to a dark residue *in vacuo*, redissolved in CH_2Cl_2 (80 cm^3) and treated with sodium hydrogen carbonate (135 cm^3 of an aqueous solution, pH 8.5, *ca.* 13.79 mmol). The two-phase system was vigorously stirred at room temperature for 0.5 h, causing the mixture to turn dark yellow in colour. The aqueous layer was removed and extracted several times with CH_2Cl_2. The extracts and organic layer were combined and

washed with several portions of water before drying over magnesium sulphate. The mixture was filtered through a pad of alumina and the orange-yellow filtrate was concentrated to a small volume under reduced pressure before being chromatographed on alumina. Elution with CH_2Cl_2 afforded a bright yellow fraction which gave, after removal of solvent and recrystallisation from CH_2Cl_2/hexane, *exo-anti*-[Mo(η^3-$CH_2CHCHCHO$)$(CO)_2$($\eta^5C_9H_7$)] (125c)[44] (1.51 g, 49%) as bright yellow *crystals*.

Microanalysis

$C_{15}H_{12}MoO_3$	requires:	C = 53.6, H = 3.6%
	found:	C = 53.5, H = 3.6%

Infrared Spectrum

ν_{CO}/cm^{-1} (CH_2Cl_2) at 1973 (vs), 1896 (s) and 1649 (m).

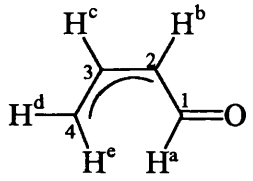

^{1}H NMR Spectrum

(CD_2Cl_2, -20°C): δ 7.25-7.08 (m, 4H, indenyl), 6.86 [d, 1H, H^a, $J(H^aH^b)$ = 8.2], 6.18 (m, 1H, indenyl), 6.06 (m, 1H, indenyl), 5.60 (m, 1H, indenyl), 3.35 [ddd, 1H, H^b, $J(H^bH^a)$ = 8.2, $J(H^bH^c)$ = 7.4, $J(H^bH^d)$ = 1.3], 2.52 [ddd, 1H, H^d, $J(H^dH^c)$ = 8.7, $J(H^dH^e)$ = 2.2, $J(H^dH^b)$ = 1.3], 1.83 [dd, 1H, H^e, $J(H^eH^c)$ = 12.2, $J(H^eH^d)$ = 2.2] and 0.40 [ddd, 1H, H^c, $J(H^cH^e)$ = 12.2, $J(H^cH^d)$ = 8.7, $J(H^cH^b)$ = 7.4].

^{13}C-{^{1}H} NMR Spectrum

(CD_2Cl_2, 20°C): δ 235.2 (CO), 234.1 (CO), 185.6 (C^1), 126.5, 126.4 (indenyl), 124.4, 124.0 (indenyl), 112.6, 112.3 (indenyl), 89.5 (indenyl), 87.9 (C^3), 81.0, 80.2 (indenyl), 69.2 (C^2) and 48.2 (C^4).

FAB Mass Spectrum

(+) FAB in NBA: 339, $[MH]^+$; 310, $[M\text{-}CO]^+$ and 282, $[M\text{-}2CO]^+$.

Preparation of *exo-anti*-[Mo(η^3-$CH_2CHCHCH_2OH$)$(CO)_2$(η^3-C_5H_5)] (141c)

Sodium borohydride (20 mg, 0.529 mmol) was added to a solution of the yellow complex *anti*-[Mo(η^3-$CH_2CHCHCHO$)$(CO)_2$(η^5-C_5H_5)] (135) (100 mg, 0.349 mmol) in methanol (10 cm^3) and the mixture was stirred at ambient temperature for 0.5 h. Monitoring by infrared spectroscopy indicated the complete consumption of starting material and the formation of a new product. Water (0.5 cm^3) was added and the mixture was stirred for 0.5 h before the solvents were removed *in vacuo*. The yellow residue was extracted with several portions of Et_2O which were concentrated to a small volume under reduced pressure and chromatographed on alumina. Elution with Et_2O/hexane (1:1) afforded a yellow fraction which gave, after removal of solvents and recrystallisation from CH_2Cl_2/pentane, *exo-anti*-[Mo(η^3-$CH_2CHCHCH_2OH$)$(CO)_2$(η^3-C_5H_5)] (141c) (65 mg, 65%) as yellow *crystals.*

Microanalysis

$C_{11}H_{12}MoO_3$	requires:	C = 45.9, H = 4.2%
	found:	C = 46.0, H = 4.2%

Infrared Spectrum

ν_{CO}/cm^{-1} (CH_2Cl_2) at 1948 (vs) and 1865 (s).

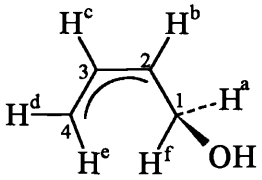

^{1}H NMR Spectrum

($CDCl_3$, 20°C): δ 5.28 (s, 5H, C_5H_5), 4.12 [ddd, 1H, H^c, $J(H^cH^e)$ = 11.4, $J(H^cH^b)$ = 7.7, $J(H^cH^d)$ = 7.5], 3.93(m, 1H, H^b), 3.78 (m, 1H, H^a), 2.94 [ddd, 1H, H^d, $J(H^dH^c)$ = 7.5, $J(H^dH^e)$ = 2.4, $J(H^dH^b)$ = 1.6], 2.14 [dd, 1H, H^f, $J(H^fH^b)$ = 11.0], 1.50 (br s, 1H, OH) and 1.41 [dd, 1H, H^e, $J(H^eH^c)$ = 11.4, $J(H^eH^d)$ = 2.4].

^{13}C-{^{1}H} NMR Spectrum

($CDCl_3$, 20°C): δ 236.8 (CO), 236.3 (CO), 91.6 (C_5H_5), 69.1 (C^1), 66.6 (C^3), 53.9 (C^2) and 38.1 (C^4).

FAB Mass Spectrum

(+) FAB in NBA: 273, $[M\text{-}OH]^+$; 245, $[M\text{-}OH\text{-}CO]^+$ and 217, $[M\text{-}OH\text{-}2CO]^+$.

Reaction of *anti*-[Mo(η^3-$CH_2CHCHCHO$)$(CO)_2$(η^5-C_5H_5)] (135) with $NaBD_4$

Sodium borodeuteride (20 mg, 0.478 mmol) was added to a solution of the yellow complex *anti*-[Mo(η^3-$CH_2CHCHCHO$)$(CO)_2$(η^5-C_5H_5)] (135) (85 mg, 0.297 mmol) in methanol (10 cm^3) and the mixture was stirred at ambient temperature for 0.5 h. Monitoring by infrared spectroscopy indicated the complete consumption of starting material and the formation of a new product. Water (0.5 cm^3) was added and the mixture was stirred for 0.5 h before the solvents were removed *in vacuo*. The yellow residue was extracted with several portions of Et_2O which were concentrated to a small volume under reduced pressure and chromatographed on alumina. Elution with Et_2O/hexane (1:1) afforded a yellow fraction which gave, after removal of solvents and recrystallisation from CH_2Cl_2/pentane, *exo-anti*-[Mo(η^3-$CH_2CHCHCHO$)$(CO)_2$(η^5-C_5H_5)] (142c) (57 mg, 67%) as yellow *crystals*.

Microanalysis

$C_{11}H_{11}DMoO_3$	requires:	C = 45.7, H = 3.8%
		C = 45.8, H = 4.0%

Infrared Spectrum

ν_{CO}/cm^{-1} (CH_2Cl_2) at 1948 (vs) and 1863 (s).

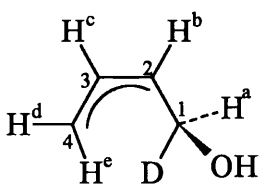

^{1}H NMR Spectrum

(CD_2Cl_2, 20°C): δ 5.30 (s, 5H, C_5H_5), 4.14 [ddd, 1H, H^c, $J(H^cH^e)$ = 11.4, $J(H^cH^b)$ = 7.7, $J(H^cH^d)$ = 7.5], 3.93 (m, 1H, H^b), 3.71 (m, 1H, H^a), 2.95[ddd, 1H, H^d, $J(H^dH^c)$ = 7.5, $J(H^dH^e)$ = 2.4, $J(H^dH^b)$ = 1.6] and 1.38 [dd, 1H, H^e, $J(H^eH^c)$ = 11.4, $J(H^eH^d)$ = 2.4].

^{13}C-{^{1}H} NMR Spectrum

($CDCl_3$, 20°C): δ 237.0 (CO), 236.6 (CO), 91.6 (C_5H_5), 69.0 (C^1), 66.6 (C^3), 53.8 (C^2) and 38.1 (C^4).

Preparation of *exo-anti*-[Mo(η^3-$CH_2CHCHCH_2OMe$)(CO)$_2$(η^5-C_5H_5)] (143c)

An excess of sodium borohydride (20 mg, 0.529 mmol) was added to a solution of the yellow complex *anti*-[Mo(η^3-$CH_2CHCHCHO$)(CO)$_2$(η^5-C_5H_5)] (135) (100 mg, 0.349 mmol) in methanol (10 cm^3) and the mixture was stirred at ambient temperature for 30 h. Monitoring by TLC showed the formation of a new product (R_f = 0.9, alumina/CH_2Cl_2). Water (0.5 cm^3) was added and the mixture was stirred for 0.5 h, after which the solvents were removed *in vacuo*. The yellow residue was extracted with several portions of Et_2O, which were concentrated to an oil under reduced pressure and redissolved in a small volume of hexane, before being chromatographed on alumina. Elution with hexane afforded a yellow band which gave, after removal of solvent and recrystallisation from hexane (-30°C), *exo-anti*-[Mo(η^3-$CH_2CHCHCH_2OMe$)(CO)$_2$(η^5-C_5H_5)] (143c) (73 mg, 69%) as yellow *crystals*.

The molecular structure of (143c) was identified by X-ray crystallography. X-ray quality *crystals* were obtained by slow recrystallisation from a concentrated solution of (143c) in hexane at 10°C. H-H COSY and off-resonance techniques were used to assign the proton and carbon NMR signals.

Microanalysis

$C_{12}H_{14}MoO_3$	requires:	C = 47.7, H = 4.7%
	found:	C = 47.6, H = 4.7%

Infrared Spectrum

ν_{CO}/cm^{-1} (CH_2Cl_2) at 1948 (vs) and 1863 (s).

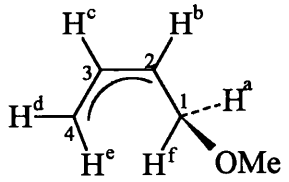

^{1}H NMR Spectrum

(CD_2Cl_2, 20°C): δ 5.30 (s, 5H, C_5H_5), 4.21 [ddd, 1H, H^c, $J(H^cH^e)$ = 11.4, $J(H^cH^b)$ = 7.7, $J(H^cH^d)$ = 7.6], 3.77 [dddd, 1H, H^b, $J(H^bH^f)$ = 11.2, $J(H^bH^c)$ = 7.7, $J(H^bH^a)$ = 3.7, $J(H^bH^d)$ = 1.6], 3.62[dd, 1H, H^a, $J(H^aH^f)$ = 11.0, $J(H^aH^b)$ = 3.7], 3.21 (s, 3H, OMe), 2.96 [ddd, 1H, H^f, $J(H^fH^b)$ = 11.2, $J(H^fH^a)$ = 11.0] and 1.35 [dd, 1H, H^e, $J(H^eH^c)$ = 11.4, $J(H^eH^d)$ = 2.4].

^{13}C-{^{1}H} NMR Spectrum

(CD_2Cl_2, 20°C): δ 237.5, (CO), 237.0 (CO), 92.0 (C_5H_5), 71.7 (C^1), 67.1 (C^3), 57.2 (OMe), 53.9 (C^2) and 38.0 (C^4).

FAB Mass Spectrum

(+) FAB in NBA: 304, $[M]^+$; 273, $[M\text{-}OMe]^+$; 245, $[M\text{-}OMe\text{-}CO]^+$ and 217, $[M\text{-}OMe\text{-}2CO]^+$.

Preparation of *s-cis*-[Mo(η^4-$CH_2CHCHCH_2$)(CO)$_2$(η^5-C_5H_5)] (9)

To a cooled (-78°C) solution of the yellow complex *exo-anti*-[Mo(η^3-CH_2CH-$CHCH_2OH$)(CO)$_2$(η^5-C_5H_5)] (141c) (105 mg, 0.364 mmol) in CH_2Cl_2 (15 cm^3) was added $HBF_4.OEt_2$ (0.069 cm^3, 76 mg of an 85% Et_2O solution, 0.401 mmol), resulting in the formation of a yellow precipitate. The mixture was stirred at -78°C for 1 h and at ambient temperature for a further 0.5 h. Solvent volume was reduced *in vacuo*, following which slow addition of pentane precipitated more of the yellow solid. This was washed with pentane and dried *in vacuo* to afford *s-cis*-[Mo(η^4-$CH_2CHCHCH_2$)-(CO)$_2$(η^5-C_5H_5)] (9) (111 mg, 85%) as a yellow powder.

Complex (9) was found to exhibit corresponding experimental data to that previously reported for this compound.[31] The broadness of the NMR signals was attributed to the presence of an *exo-endo* equilibrium.

Microanalysis

$C_{11}H_{11}BF_4MoO_2$	requires:	C = 36.9, H = 3.1%
	found:	C = 36.9, H = 3.1%

Infrared Spectrum

ν_{CO}/cm^{-1} ($MeNO_2$) at 2064 (vs) and 2016 (s).

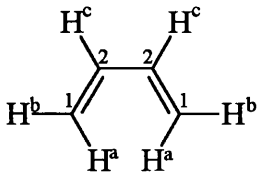

^{1}H NMR Spectrum

[$(CD_3)_2CO$, 20°C]: δ 6.39 (br m, 2H, H^c), 6.08 (s, 5H, C_5H_5), 3.18 (br s, 2H, H^a) and 2.22 (br m, 2H, H^b).

^{13}C-{^{1}H} NMR Spectrum

[$(CD_3)_2CO$, 20°C]: δ 220.3 (br s, 2CO), 100.4 (br s, C^2), 91.8 (br s, C_5H_5) and 51.8 (br s, C^1).

FAB Mass Spectrum

(+) FAB in NBA: 273, $[M]^+$; 245, $[M\text{-}CO]^+$ and 217, $[M\text{-}2CO]^+$.

(-) FAB in NBA: 87, $[BF_4]^-$.

Reaction of *anti*-[Mo(η^3-$CH_2CHCHCHO$)$(CO)_2$(η^5-C_5H_5)] (135) with $NaBD_4$

An excess of sodium borodeuteride (12 mg, 0.287 mmol) was added to a solution of the yellow complex *anti*-[Mo(η^3-$CH_2CHCHCHO$)$(CO)_2$(η^5-C_5H_5)] (135) (60 mg, 0.210 mmol) in methanol (7 cm^3) and the mixture was stirred for 30 h. Water (0.5 cm^3) was added and the mixture was stirred for 0.5 h, after which the solvents were removed *in vacuo*. The yellow residue was extracted with several portions of Et_2O,

which were concentrated to an oil under reduced pressure and redissolved in a small volume of hexane, before being chromatographed on alumina. Elution with hexane afforded a single yellow fraction which gave, after removal of solvent and recrystallisation from hexane (-30°C), a 1:1 isomeric mixture of *exo-anti*-[Mo(η^3-CH_2-CHCHCH(OMe)D)$(CO)_2$(η^5-C_5H_5)] (144c) and *exo-anti*-[Mo(η^3-CHDCHCHCH_2-OMe)$(CO)_2$(η^5-C_5H_5)] (145c) obtained as a yellow solid (38 mg, 60%).

Microanalysis

$C_{12}H_{13}DMoO_3$	requires:	C = 47.5, H = 4.3%
	found:	C = 46.9, H = 4.6%

Infrared Spectrum

ν_{CO}/cm^{-1} (CH_2Cl_2) at 1948 (vs) and 1865 (s).

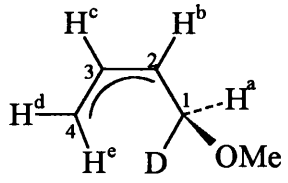

^{1}H NMR Spectrum (144c)

($CDCl_3$, 20°C): δ 5.28 (s, 5H, C_5H_5), 4.18 [ddd, 1H, H^c, $J(H^cH^e)$ = 11.4, $J(H^cH^b)$ = 7.7, $J(H^cH^d)$ = 7.6], 3.78 (m, 1H, H^b), 3.62 (m, 1H, H^a), 3.25 (s, 3H, OMe), 2.95 [dd, 1H, H^d, $J(H^dH^c)$ = 7.6, $J(H^dH^e)$ = 2.4] and 1.38 [dd, 1H, H^e, $J(H^eH^d)$ = 2.4].

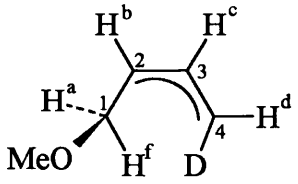

^{1}H NMR Spectrum (145c)

($CDCl_3$, 20°C): δ 5.28 (s, 5H, C_5H_5), 4.18 (m, 1H, H^c), 3.78 (m, 1H, H^b), 3.64 [dd, 1H, H^a, $J(H^aH^f)$ = 10.9, $J(H^aH^b)$ = 3.7], 3.25 (s, 3H, OMe), 2.95 [dt, 1H, H^d, $J(H^dH^c)$ = 7.6, $J(H^dD)$ = 2.4] and 1.85 [dd, 1H, H^f, $J(H^fH^b)$ = 11.1, $J(H^fH^a)$ = 10.9].

^{13}C-{^{1}H} NMR Spectrum (144c) and (145c)

($CDCl_3$, 20°C): δ 237.6 (CO), 237.1 (CO), 91.7 (C_5H_5), 71.8 (br s, C^1), 66.6 (C^3), 57.6 (OMe), 53.4 (C^2) and 38.1 (br s, C^4).

Preparation of *exo-anti*-[Mo(η^3-$CH_2CHCHCH_2OH$)(CO)$_2$(η^5-C_5Me_5)] (147c)

Sodium borohydride (13 mg, 0.321 mmol) was added to a solution of the yellow complex *exo-anti*-[Mo(η^3-$CH_2CHCHCHO$)(CO)$_2$(η^5-C_5Me_5)] (126c) (104 mg, 0.292 mmol) in methanol (10 cm^3) and the mixture was stirred at ambient temperature for 1h. Monitoring by infrared spectroscopy indicated the complete consumption of starting material and the formation of a new product. Water (0.5 cm^3) was added and the mixture was stirred for 0.5 h before the solvents were removed *in vacuo*. The yellow residue was extracted with several portions of Et_2O which were concentrated to a small volume under reduced pressure and chromatographed on alumina. Elution with Et_2O afforded a yellow band which gave, after removal of solvent and recrystallisation from CH_2Cl_2/hexane, *exo-anti*-[Mo(η^3-$CH_2CHCHCH_2OH$)(CO)$_2$(η^5-C_5Me_5)] (147c) (65 mg, 62%) as a yellow powder.

Off resonance spectra were used to assign the ^{13}C-{^{1}H} NMR signals.

Microanalysis

$C_{16}H_{22}MoO_3$	requires:	C = 53.6, H = 6.2%
	found:	C = 53.3, H = 6.0%

Infrared Spectrum

ν_{CO}/cm^{-1} (CH_2Cl_2) at 1935 (vs) and 1852 (s).

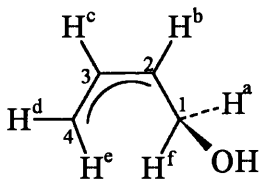

^{1}H NMR Spectrum

(CD_2Cl_2, 20°C): δ 3.64 [dd, 1H, H^a, $J(H^aH^f)$ = 11.4, $J(H^aH^b)$ = 3.6], 3.22[ddddd, 1H, H^b, $J(H^bH^f)$ = 11.2, $J(H^bH^c)$ = 7.6, $J(H^bH^a)$ = 3.6, $J(H^bH^d)$ = 1.5, $J(H^bH^e)$ = 0.6], 2.85 [ddd, 1H, H^c, $J(H^cH^e)$ = 11.9, $J(H^cH^d)$ = $J(H^cH^b)$ = 7.6], 2.25 [ddd, 1H, H^d, $J(H^dH^c)$ = 7.6, $J(H^dH^e)$ = 2.4, $J(H^dH^b)$ = 1.5], 2.07 [dd, 1H, H^f, $J(H^fH^a)$ = 11.4, $J(H^fH^b)$ = 11.2], 1.86 (s, 15H, C_5Me_5), 1.51 (br s, 1H, OH) and 1.46 [ddd, 1H, H^e, $J(H^eH^c)$ = 11.9, $J(H^eH^d)$ = 2.4, $J(H^eH^b)$ = 0.6].

^{13}C-{^{1}H} NMR Spectrum

δ 240.3 (CO), 239.8 (CO), 103.9 (C_5Me_5), 74.0 (C^3), 62.4 (C^1), 61.8 (C^2), 41.9 (C^4) and 10.3 (C_5Me_5).

FAB Mass Spectrum

(+) FAB in NBA: 359, $[MH]^+$; 330, $[M-2H-CO]^+$ and 302, $[M-2H-2CO]^+$.

Preparation of *exo-anti*-[Mo(η^3-$CH_2CHCHCH_2OMe$)(CO)$_2$(η^5-C_5Me_5)

An excess of sodium borohydride (21 mg, 0.544 mmol) was added to a solution of the yellow complex *exo-anti*-[Mo(η^3-$CH_2CHCHCHO$)(CO)$_2$(η^5-C_5Me_5)] (126c) (97 mg, 0.272 mmol) in methanol (10 cm^3) and the mixture was stirred at ambient temperature for 2 d. Monitoring by TLC showed the formation of a new product (R_f = 0.92, alumina/CH_2Cl_2). Water (0.5 cm^3) was added and the mixture was stirred for 0.5 h, after which the solvents were removed *in vacuo*. The yellow residue was extracted with several portions of Et_2O, which were concentrated to an oil under reduced pressure and redissolved in a small volume of hexane, before being chromatographed on alumina. Elution with hexane afforded a yellow band which gave, after removal of solvent and recrystallisation from hexane (-30°C), *exo-anti*-[Mo(η^3-$CH_2CHCHCH_2OMe$)(CO)$_2$(η^5-C_5Me_5) (148c) (66 mg, 65%) as a yellow solid.

Off-resonance experiments were used to assign the ^{13}C-{^{1}H} NMR signals.

Microanalysis

$C_{17}H_{24}MoO_3$ requires: C = 54.8, H = 6.5%

found: C = 54.4, H = 6.7%

Infrared Spectrum

ν_{CO}/cm^{-1} (CH_2Cl_2) at 1935 (vs) and 1850 (s).

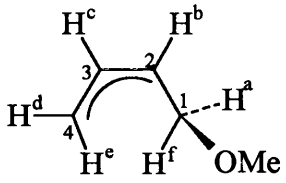

^{1}H NMR Spectrum

(CD_2Cl_2, 20°C): δ 3.56 [dd, 1H, H^a, $J(H^aH^f)$ = 10.9, $J(H^aH^b)$ = 3.6], 3.20 (s, 3H, OMe), 3.05 [dddd, 1H, H^b, $J(H^bH^f)$ = 11.1, $J(H^bH^c)$ = 7.8, $J(H^bH^a)$ = 3.6, $J(H^bH^d)$ = 1.6], 2.92 [ddd, 1H, H^c, $J(H^cH^e)$ = 11.2, $J(H^cH^b)$ = 7.8, $J(H^cH^d)$ = 7.5], 2.25 [ddd, 1H, H^d, $J(H^dH^c)$ = 7.5, $J(H^dH^e)$ = 2.4, $J(H^dH^b)$ = 1.6], 1.86 (s, 15H, C_5Me_5), 1.80 [dd, 1H, H^f, $J(H^fH^b)$ = 11.1, $J(H^fH^a)$ = 10.9] and 1.43 [dd, 1H, H^e, $J(H^eH^c)$ = 11.2, $J(H^eH^d)$ = 2.4].

^{13}C-{^{1}H} NMR Spectrum

(CD_2Cl_2, 20°C): δ 240.6 (CO), 240.0 (CO), 103.9 (C_5Me_5), 75.2 (C^3), 72.0 (C^1), 57.9 (C^2), 57.0 (OMe), 41.8 (C^4) and 10.3 (C_5Me_5).

FAB Mass Spectrum

(+) FAB in NBA: 343, $[M\text{-}OMe]^+$; 315, $[M\text{-}OMe\text{-}CO]^+$ and 287, $[M\text{-}OMe\text{-}2CO]^+$.

Preparation of *exo-anti*-[Mo(η^3-$CH_2CHCHCH(OH)Me$)$(CO)_2$(η^5-C_5H_5)] (149c)

Methylmagnesium iodide (2.10 cm^3 of a 3.0 M solution in thf, 6.29 mmol) was added to a cooled (-20°C) solution of the yellow complex *anti*-[Mo(η^3-$CH_2CHCHCHO$)$(CO)_2$(η^5-C_5H_5)] (135) (1.44 g, 5.03 mmol) in thf (50 cm^3). The mixture was allowed to warm to ambient temperature and stirred for 2 h. Monitoring by infrared spectroscopy indicated that the reaction had gone to completion. The mixture was

quenched with water (1 cm^3) and stirred for a further 0.5 h, causing the mixture to turn red-brown in colour. The solvents were removed *in vacuo* and the residue extracted with CH_2Cl_2 and filtered through a small pad of alumina. The red filtrate was concentrated to a small volume under reduced pressure before being chromatographed on alumina. Elution with CH_2Cl_2 afforded a major yellow fraction which gave, after removal of solvent and recrystallisation from CH_2Cl_2/hexane, *exo-anti*-[Mo(η^3-$CH_2CHCHCH(OH)Me)(CO)_2(\eta^5$-$C_5H_5)$] (149c) (1.07 g, 70%) as a yellow powder.

Microanalysis

$C_{12}H_{14}MoO_3$	requires:	C = 47.7, H = 4.7%
	found:	C = 47.2, H = 4.6%

Infrared Spectrum

ν_{CO}/cm^{-1} (CH_2Cl_2) at 1943 (vs) and 1850 (s).

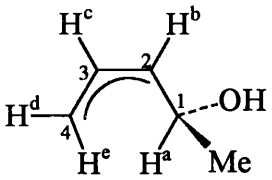

^{1}H NMR Spectrum

(CD_2Cl_2, 20°C): δ 5.30 (s, 5H, C_5H_5), 4.01 [ddd, 1H, H^c, $J(H^cH^e)$ = 11.7, $J(H^cH^b)$ = $J(H^cH^d)$ = 7.9], 3.82 [ddd, 1H, H^b, $J(H^bH^a)$ = 8.3, $J(H^bH^c)$ = 7.9, $J(H^bH^d)$ = 1.8], 3.04 [ddd, 1H, H^d, $J(H^dH^c)$ = 7.9, $J(H^dH^e)$ = 2.0, $J(H^dH^b)$ = 1.8], 2.89 [dqd, 1H, H^a, $J(H^aH^b)$ = 8.3, $J(H^aMe)$ = 6.2, $J(H^aOH)$ = 3.3], 2.35 [d, 1H, OH, $J(H^aOH)$ = 3.3], 1.44 [dd, 1H, H^e, $J(H^eH^c)$ = 11.7, $J(H^eH^d)$ = 2.0] and 1.18 [d, 1H, Me, $J(MeH^a)$ = 6.2].

^{13}C-{^{1}H} NMR Spectrum

(CD_2Cl_2, 20°C): δ 242.5 (CO), 237.6 (CO), 92.2 (C_5H_5), 70.5 (C^1), 68.5 (C^3), 65.2 (C^2), 40.8 (C^4) and 29.3 (Me).

FAB Mass Spectrum

(+) FAB in NBA: 304, $[M]^+$; 287, $[M\text{-}OH]^+$; 259, $[M\text{-}OH\text{-}CO]^+$ and 231, $[M\text{-}OH\text{-}2CO]^+$.

Preparation of *exo-anti*-[Mo(η^3-$CH_2CHCHCH(OH)Et$)$(CO)_2(\eta^5$-C_5H_5)] (150c)

Ethylmagnesium bromide (0.46 cm^3 of a 3.0 M solution in Et_2O, 1.38 mmol) was added to a cooled (0°C) solution of the yellow complex *anti*-[Mo(η^3-CH_2CHCH-CHO)$(CO)_2(\eta^5$-C_5H_5)] (135) (200 mg, 0.66 mmol) in thf (20 cm^3). The mixture was allowed to warm to ambient temperature and stirred for 2 h. Monitoring by infrared spectroscopy indicated that the reaction had gone to completion. The mixture was quenched with water (1 cm^3) and stirred for a further 0.5 h at room temperature. Solvents were removed *in vacuo* and the residue extracted with Et_2O and filtered through Celite. The filtrate was concentrated to an oily residue under reduced pressure before being chromatographed on alumina. Elution with hexane afforded a major yellow fraction which gave, after removal of solvent and recrystallisation from hexane, *exo-anti*-[Mo(η^3-$CH_2CHCHCH(OH)Et$)$(CO)_2(\eta^5$-C_5H_5)] (150c) (110 mg, 53%) as yellow *crystals*.

Microanalysis

$C_{13}H_{16}MoO_3$	requires:	C = 49.4, H = 5.1%
	found:	C = 49.4, H = 5.1%

Infrared Spectrum

ν_{CO}/cm^{-1} (CH_2Cl_2) at 1941 (vs) and 1850 (s).

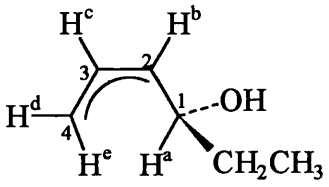

^{1}H NMR Spectrum

($CDCl_3$, 20°C): δ 5.28 (s, 5H, C_5H_5), 4.00 [ddd, 1H, H^c, $J(H^cH^e)$ = 11.6, $J(H^cH^b)$ = 8.1, $J(H^cH^d)$ = 7.9], 3.79 [ddd, 1H, H^b, $J(H^bH^a)$ = 8.5, $J(H^bH^c)$ = 8.1, $J(H^bH^d)$ = 1.9], 3.05 [ddd, 1H, H^d, $J(H^dH^c)$ = 7.9, $J(H^dH^e)$ = 2.1, $J(H^dH^b)$ = 1.9], 2.63 (m, 1H, H^a), 2.47 [d, 1H, OH, J(OH, H^a) = 3.1], 1.66-1.46 (m, 2H, CH_2), 1.41 [dd, 1H, H^e, $J(H^eH^c)$ = 11.6, $J(H^eH^d)$ = 2.1] and 0.90 [t, 3H, CH_3, $J(CH_3CH_2)$ = 7.4].

^{13}C-{^{1}H} NMR Spectrum

($CDCl_3$, 20°C): δ 241.4 (CO), 236.4 (CO), 91.9 (C_5H_5), 75.2 (C^1), 66.9 (C^3), 65.2 (C^2), 40.9 (C^4), 36.2 (CH_2) and 10.2 (CH_3).

FAB Mass Spectrum

(+) FAB in NBA: 318, $[M]^+$; 301, $[M\text{-}OH]^+$; 273, $[M\text{-}OH\text{-}CO]^+$ and 245, $[M\text{-}OH\text{-}2CO]^+$.

Preparation of *exo-anti*-[Mo(η^3-$CH_2CHCHCH(OH)Ph$)$(CO)_2$(η^5-C_5H_5)] (151c)

Phenylmagnesium chloride (0.70 cm^3 of a 2.0 M solution in thf, 1.40 mmol) was added to a cooled (0°C) solution of the yellow complex *anti*-[Mo(η^3-$CH_2CHCHCHO$)-$(CO)_2$(η^5-C_5H_5)] (135) (200 mg, 0.66 mmol) in thf (20 cm^3). The mixture was allowed to warm to ambient temperature and stirred for 2h. Monitoring by infrared spectroscopy indicated that the reaction had gone to completion. The mixture was quenched with water (0.5 cm^3) and stirred for a further 0.5 h at room temperature. Solvents were removed *in vacuo* and the residue extracted with Et_2O and filtered through Celite. The filtrate was concentrated to an oily residue under reduced pressure and chromatographed on alumina. Elution with hexane gave, after removal of solvent and recrystallisation from hexane, *exo-anti*-[Mo(η^3-$CH_2CHCHCH(OH)Ph$)$(CO)_2$(η^5-C_5H_5)] (151c) (138, 57%) as a yellow solid.

Microanalysis

$C_{17}H_{16}MoO_3$	requires:	C = 56.1, H = 4.4%
	found:	C = 56.7, H = 4.1%

Infrared Spectrum

ν_{CO}/cm^{-1} (CH_2Cl_2) at 1946 (vs) and 1858 (s).

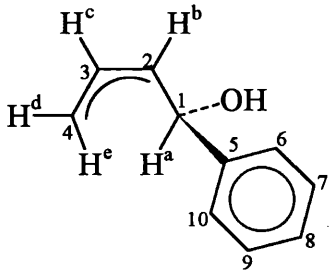

^{1}H NMR Spectrum

($CDCl_3$, 20°C): δ 7.31-7.18 (m, 5H, C_6H_5), 5.24 (s, 5H, C_5H_5), 4.01 [ddd, 1H, H^b, $J(H^bH^a)$ = 8.9, $J(H^bH^c)$ = 8.4, $J(H^bH^d)$ = 1.8], 3.85 [ddd, 1H, H^c, $J(H^cH^e)$ = 11.7, $J(H^cH^b)$ = 8.4, $J(H^cH^d)$ = 7.9], 3.67 [dd, 1H, H^a, $J(H^aH^b)$ = 8.9, $J(H^aOH)$ = 2.9], 3.04 [ddd, 1H, H^d, $J(H^dH^c)$ = 7.9, $J(H^dH^e)$ = 2.2, $J(H^dH^b)$ = 1.8], 2.61 [d, 1H, OH, $J(OH.H^a)$ = 2.9] and 1.58 [dd, 1H, H^e, $J(H^eH^c)$ = 11.7, $J(H^eH^d)$ = 2.2].

^{13}C-{^{1}H} NMR Spectrum

($CDCl_3$, 20°C): δ 147.5 (C^5), 128.4 (C^6 and C^{10}), 127.3 (C^7 and C^9), 125.5 (C^8), 91.9 (C_5H_5), 75.7 (C^1), 66.8 (C^3), 65.1 (C^2) and 42.3 (C^4).

FAB Mass Spectrum

(+) FAB in NBA: 366, $[M]^+$; 349, $[M\text{-}OH]^+$; 321, $[M\text{-}OH\text{-}CO]^+$ and 293, $[M\text{-}OH\text{-}2CO]^+$.

Preparation of *exo-anti*-[Mo(η^3-$CH_2CHCHCH(OH)Me$)$(CO)_2$(η^5-C_5Me_5)] (152c)

Methyllithium (0.305 cm^3 of a 1.4 M solution in Et_2O, 0.427 mmol) was added to a cooled (-78°C) solution of the yellow complex *exo-anti*-[Mo(η^3-$CH_2CHCHCHO$)-$(CO)_2$(η^5-C_5Me_5)] (126c) (0.117, 0.328 mmol) in thf (10 cm^3). The mixture was stirred at -78°C for 1 h and at ambient temperature for 15 h, during which time the colour of the solution turned red. An excess of water (0.060 cm^3, 3.28 mmol) was added and the mixture stirred for a further 2 h at room temperature. The solvents were removed *in vacuo* and the orange-red residue was extracted with CH_2Cl_2 and filtered through Celite. The orange filtrate was reduced to a small volume under reduced pressure before being chromatographed on alumina. Elution with hexane and then

CH_2Cl_2/hexane (1:3) afforded a yellow fraction which gave, after removal of solvent and recrystallisation from pentane (-35°C), *exo-anti*-[Mo(η^3-$CH_2CHCHCH(OH)Me$)$(CO)_2$-(η^5-C_5Me_5)] (92 mg, 75%) as a yellow solid.

H-H COSY and DEPT experiments were used to assign the proton and carbon NMR signals.

Microanalysis

$C_{17}H_{24}MoO_3$ requires: C = 54.8, H = 6.5%

requires: C = 54.6, H = 6.4%

Infrared Spectrum

ν_{CO}/cm^{-1} (CH_2Cl_2) at 1929 (vs) and 1836 (s).

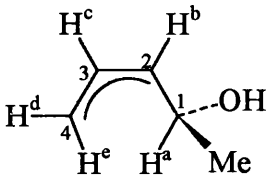

^{1}H NMR Spectrum

(CD_2Cl_2, 20°C): δ 3.12 [dddd, 1H, H^b, $J(H^bH^a)$ = 8.2, $J(H^bH^c)$ = 7.8, $J(H^bH^d)$ = 1.7, $J(H^bH^e)$ = 0.7], 2.87 [dqd, 1H, H^a, $J(H^aH^b)$ = 8.2, $J(H^aMe)$ = 6.1, $J(H^aOH)$ = 3.2], 2.71 [ddd, 1H, H^c, $J(H^cH^e)$ = 11.7, $J(H^cH^d)$ = 8.4, $J(H^cH^b)$ = 7.8], 2.32 [ddd, 1H, H^d, $J(H^dH^c)$ = 8.4, $J(H^dH^e)$ = 2.2, $J(H^dH^b)$ = 1.7], 1.86 (s, 15H, C_5Me_5), 1.53 [ddd, 1H, H^e, $J(H^eH^c)$ = 11.7, $J(H^eH^d)$ = 2.2, $J(H^eH^b)$ = 0.7] and 1.41 [d, 3H, Me, $J(MeH^a)$ = 6.1].

^{13}C-{^{1}H} NMR Spectrum

(CD_2Cl_2, 20°C): δ 245.6 (CO), 239.8 (CO), 104.0 (C_5Me_5), 73.5, 73.4 (C^1 and C^3), 71.0 (C^2), 43.7 (C^4), 28.9 (Me) and 10.3 (C_5Me_5).

Attempted Oppenauer oxidation of *exo-anti*-[Mo(η^3-$CH_2CHCHCH(OH)Me$)$(CO)_2$(η^5-C_5H_5)] (149c)

An excess of dry acetone (15 cm^3, 204 mmol) was added to a solution of the yellow complex *exo-anti*-[Mo(η^3-$CH_2CHCHCH(OH)Me$)$(CO)_2$(η^5-C_5H_5)] (149c) (700

mg, 2.32 mmol) in toluene (37 cm^3). To this was added aluminium isopropoxide (1.42 g, 6.95 mmol) and the mixture was heated to reflux for 5.5 h. Monitoring by infrared spectroscopy and TLC indicated the formation of a new compound. After cooling to ambient temperature, the solvent was removed *in vacuo* and the yellow residue was extracted with CH_2Cl_2. The organic extracts were combined and concentrated to an oil before being chromatographed on alumina. Elution with hexane-CH_2Cl_2 (5:1) afforded a major yellow fraction which gave, after removal of solvent and recrystallisation from hexane (-30°C), *exo-anti*-[Mo(η^3-$CH_2CHCHCHCH_2$)$(CO)_2$(η^5-C_5H_5)] (154c) (310 mg, 47%) as a yellow solid.

The molecular structure of (154c) was identified by X-ray crystallography. X-ray quality *crystals* of (154c) were obtained by slow recrystallisation from a concentrated hexane solution at 10°C. H-H COSY techniques were used to assign the proton NMR signals.

Microanalysis

$C_{12}H_{12}MoO_2$	requires:	C = 50.7, H = 4.3%
	found:	C = 50.4, H = 4.2%

Infrared Spectrum

ν_{CO}/cm^{-1} (CH_2Cl_2) at 1950 cm^{-1} and 1867 (s).

$\nu_{C=C}/cm^{-1}$ (CH_2Cl_2) at 1617 (m).

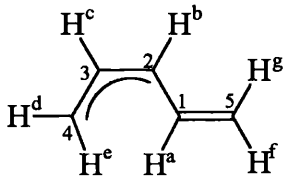

^{1}H NMR Spectrum

(CD_2Cl_2, 20°C): δ 5.29 (s, 5H, C_5H_5), 4.99 [dd, 1H, H^g, $J(H^gH^a)$ = 16.2, $J(H^gH^f)$ = 1.6], 4.72 [dd, 1H, H^f, $J(H^fH^a)$ = 10.3, $J(H^fH^g)$ = 1.6], 4.50 [ddd, 1H, H^b, $J(H^bH^a)$ = 10.1, $J(H^bH^c)$ = 7.7, $J(H^bH^d)$ = 1.4], 4.33 [ddd, 1H, H^a, $J(H^aH^g)$ = 16.2, $J(H^aH^f)$ = 10.3, $J(H^aH^b)$ = 10.1], 4.19 [ddd, 1H, H^c, $J(H^cH^e)$ = 11.5, $J(H^cH^b)$ = 7.7, $J(H^cH^d)$ = 7.5], 2.84

[ddd, 1H, H^d, $J(H^dH^c)$ = 7.5, $J(H^dH^e)$ = 2.5, $J(H^dH^b)$ = 1.4] and 1.47 [dd, 1H, H^e, $J(H^eH^c)$ = 11.5, $J(H^eH^d)$ = 2.5].

$^{13}C-\{^1H\}$ NMR Spectrum

(CD_2Cl_2, 20°C): δ 237.6 (CO), 236.6 (CO), 134.8 (C^1), 110.8 (C^5), 91.7 (C_5H_5), 66.5 (C^3), 64.6 (C^2) and 34.7 (C^4).

FAB Mass Spectrum

(+) FAB in NBA: 287, $[MH]^+$; 258, $[M-CO]^+$ and 230, $[M-2CO]^+$.

Preparation of $[Mo(\eta^3-C_4H_3O_2)(CO)_2(\eta^5-C_5Me_5)]$ (162)

An excess of 2-(trimethylsilyloxy)furan (1.84 cm^3, 10.96 mmol) was added to a suspension of the blood-red complex *cis*-$[Mo(NCMe)_2(CO)_2(\eta^5-C_5Me_5)][BF_4]$ (16) (1.00g, 2.19 mmol) in CH_2Cl_2 (30 cm^3). After stirring for 4 d at room temperature, the resulting dark yellow solution was filtered through a small pad of alumina. The yellow filtrate was collected and concentrated to a small volume before being chromatographed on alumina. Elution with CH_2Cl_2 afforded a single yellow fraction which gave, after removal of solvent and recrystallisation from CH_2Cl_2/pentane, $[Mo(\eta^3-C_4H_3O_2)(CO)_2-(\eta^5-C_5Me_5)]$ (162) (503 mg, 62%) as a bright yellow powder.

NMR and infrared spectroscopy showed (162) to exist in solution at room temperature as a 3:1 mixture of *exo* and *endo* isomers. X-ray quality *crystals* of the *exo* isomer were obtained by CH_2Cl_2/toluene/pentane layer diffusion at room temperature. Low temperature NMR experiments were necessary to distinguish between the isomers and for the determination of the coupling constants. H-H and H-C COSY techniques were used to assign the proton and carbon NMR signals.

Microanalysis

$C_{16}H_{18}MoO_4$	requires:	C = 51.9, H = 4.9%
	found:	C = 51.9, H = 4.9%

Exo isomer (major)

Infrared Spectrum

ν_{CO}/cm^{-1} (CH_2Cl_2) at 1968 (vs), 1892 (s) and 1748 (ms).

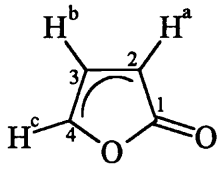

^{1}H NMR Spectrum

(CD_2Cl_2, 20°C): δ 6.38 (br s, 1H, H^c), 4.99 (br s, 1H, H^b), 3.02 (br s, 1H, H^a) and 1.92 (br s, 15H, C_5Me_5).

(CD_2Cl_2, -80°C): δ 6.46 [dd, 1H, H^c, $J(H^cH^b) = 2.7$, $J(H^cH^a) = 2.5$]., 5.00 [dd, 1H, H^b, $J(H^bH^a) = J(H^bH^c) = 2.7$], 2.97 [dd, 1H, H^a, $J(H^aH^b) = 2.7$, $J(H^aH^c) = 2.5$] and 1.85 (s, 15H, C_5Me_5).

^{13}C-{^{1}H} NMR Spectrum

(CD_2Cl_2, 20°C): δ 235.8 (br s, 2CO), 175.3 (br s, C^1), 105.5 (br s, C_5Me_5), 95.9 (br s, C^4), 75.8 (br s, C^3), 38.0 (br s, C^2) and 10.2 (br s, C_5Me_5).

(CD_2Cl_2, -50°C): δ 240.2 (CO), 236.1 (CO), 175.9 (C^1), 105.4 (C_5Me_5), 95.4 (C^4), 75.4 (C^3), 37.9 (C^2) and 10.2 (C_5Me_5).

Endo Isomer (minor)

Infrared Spectrum

ν_{CO}/cm^{-1} (CH_2Cl_2) at 1985 (m), 1917 (m) and 1721 (w).

^{1}H NMR Spectrum

(CD_2Cl_2, 20°C): δ 6.38 (br s, 1H, H^c), 4.99 (br s, 1H, H^b), 3.02 (br s, 1H, H^a) and 1.92 (br s, 15H, C_5Me_5).

(CD_2Cl_2, -80°C): δ 5.84 [dd, 1H, H^c, $J(H^cH^b) = 2.7$, $J(H^cH^a) = 2.5$], 5.78 [dd, 1H, H^b, $J(H^bH^a) = J(H^bH^c) = 2.7$], 3.06 [dd, 1H, H^a, $J(H^aH^b) = 2.7$, $J(H^aH^c) = 2.5$] and 1.81 (s, 15H, C_5Me_5).

^{13}C-{^{1}H} NMR Spectrum

(CD_2Cl_2, 20°C): δ 235.8 (br s, 2CO), 175.3 (br s, C^1), 105.5 (br s, C_5Me_5), 95.9 (br s, C^4), 75.8 (br s, C^3), 38.0 (br s, C^2) and 10.2 (br s, C_5Me_5).

(CD_2Cl_2, -50°C): δ 235.7 (CO), 233.9 (CO), 174.6 (C^1), 104.6 (C_5Me_5), 90.4 (C^4), 80.2 (C^3), 37.0 (C^2) and 9.8 (C_5Me_5).

FAB Mass Spectrum

(+) FAB in NBA: 372, $[M]^+$; 344, $[M-CO]^+$; 316, $[M-2CO]^+$ and 288, $[M-3CO]^+$.

Preparation of $[Mo(\eta^3-C_4H_3O_2)(CO)_2(\eta^5-C_5H_5)]$ (163)

Method A: An excess of 2-(trimethylsilyloxy)furan (3.27 cm^3, 19.43 mmol) was added to a suspension of the blood-red complex *cis*-$[Mo(NCMe)_2(CO)_2(\eta^5-C_5H_5)][BF_4]$ (108) (1.50 g, 3.89 mmol) in CH_2Cl_2 (40 cm^3). After stirring for 3 d at room temperature, the resulting dark yellow solution was filtered through a small pad of alumina. The yellow filtrate was concentrated to a small volume and chromatographed on alumina. Elution with CH_2Cl_2 afforded a single yellow fraction which gave, after removal of solvent and recrystallisation from CH_2Cl_2/pentane, $[Mo(\eta^3-C_4H_3O_2)(CO)_2(\eta^5-C_5H_5)]$ (163) (645 mg, 55%) obtained as a bright yellow powder.

Method B: A solution of the yellow complex $[Mo(\eta^3-C_3H_5)(CO)_2(\eta^5-C_5H_5)]$ (25) (324 mg, 1.26 mmol) in CH_2Cl_2 (30 cm^3) was cooled to -78°C. To this was added dropwise $HBF_4.OEt_2$ (0.22 cm^3, 242 mg of an 85% Et_2O solution, 1.27 mmol) causing an immediate change in colour to a deep reddish-violet. After stirring for 0.5 h at -78°C, the mixture was treated with an excess of 2-(trimethylsilyloxy)furan (1.06 cm^3, 6.28 mmol) and then allowed to warm to ambient. The reaction mixture was stirred for a further 2 h and then filtered through Celite to give a reddish yellow solution. This was concentrated to a small volume under reduced pressure and chromatographed on alumina. Elution with CH_2Cl_2 afforded a single yellow fraction which gave, after removal of solvent and recrystallisation from CH_2Cl_2/pentane, $[Mo(\eta^3-C_4H_3O_2)(CO)_2$-$(\eta^5-C_5H_5)]$ (163) (139 mg, 37%) as a bright yellow powder.

NMR and infrared spectroscopy showed (163) to exist in solution at room temperature as a 2:1 mixture of *exo* and *endo* isomers. Low temperature NMR experiments were necessary to distinguish between the two isomers and for the determination of the coupling constants.

Microanalysis

$C_{11}H_8MoO_4$ requires: C = 44.0, H = 2.7%

found: C = 43.8, H = 2.7%

Exo isomer (major)

Infrared Spectrum

ν_{CO}/cm^{-1} (CH_2Cl_2) at 2000 (vs), 1935 (s) and 1750 (ms).

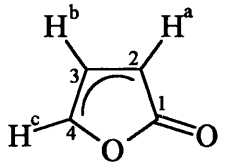

^{1}H NMR Spectrum

(CD_2Cl_2, 20°C): δ 6.47 (br s, 1H, H^c), 5.82 (br s, 1H, H^b), 5.39 (br s, 5H, C_5H_5) and 3.55 (br s, 1H, H^a).

(CD_2Cl_2, -60°C): δ 6.43 [dd, 1H, H^c, $J(H^cH^b)$ = 2.5, $J(H^cH^a)$ = 2.4], 5.86 [dd, 1H, H^b, $J(H^bH^a)$ = $J(H^bH^c)$ = 2.5], 5.37 (s, 5H, C_5H_5) and 3.54 [dd, 1H, H^a, $J(H^aH^b)$ = 2.5, $J(H^aH^c)$ = 2.4].

^{13}C-{^{1}H} NMR Spectrum

(CD_2Cl_2, 20°C): δ 233.1 (br s, 2CO), 177 (br s, C^1), 94.4 (br s, C_5H_5), 92.1 (br s, C^4), 81.3 (br s, C^3) and 38.3 (br s, C^2).

(CD_2Cl_2, -50°C): δ 233.1 (CO), 232.3 (CO), 177.2 (C^1). 94.1 (C_5H_5), 91.2 (C^4), 81.0 (C^3) and 37.9 (C^2).

Endo isomer (minor)

Infrared Spectrum

ν_{CO}/cm^{-1} (CH_2Cl_2) at 1986 (ms), 1912 (m) and 1721 (m).

^{1}H NMR Spectrum

(CD_2Cl_2, 20°C): δ 6.58 (br s, 1H, H^c), 5.96 (br s, 1H, H^b), 5.42 (br s, 5H, C_5H_5) and 3.49 (br s, 1H, H^a).

(CD_2Cl_2, -60°C): δ 6.62 [dd, 1H, H^c, $J(H^cH^b) = 2.7$, $J(H^cH^a) = 2.5$], 6.08 [dd, 1H, H^b, $J(H^bH^a) = J(H^bH^c) = 2.7$], 5.45 (s, 5H, C_5H_5) and 3.43 [dd, 1H, H^a, $J(H^aH^b) = 2.7$, $J(H^aH^c) = 2.5$].

^{13}C-{^{1}H} NMR Spectrum

(CD_2Cl_2, 20°C): δ 233.1 (br s, 2CO), 177.0 (br s, C^1), 94.4 (br s, C_5H_5), 92.1 (br s, C^4), 81.3 (br s, C^3) and 38.3 (br s, C^2).

(CD_2Cl_2, -50°C): δ 236.6 (CO), 232.8 (CO), 175.9 (C^1), 94.8 (C^4), 92.8 (C_5H_5), 67.4 (C^3) and 33.9 (C^2).

FAB Mass Spectrum

(+) FAB in NBA: 302, $[M]^+$; 274, $[M-CO]^+$; 246, $[M-2CO]^+$ and 218, $[M-3CO]^+$.

Preparation of $[Mo(\eta^3\text{-}C_4H_3O_2)(CO)_2(\eta^5\text{-}C_9H_7)]$ (164)

An excess of 2-(trimethylsilyloxy)furan (2.47 cm^3, 14.71 mmol) was added to a suspension of the blood-red complex *cis*-$[Mo(NCMe)_2(CO)_2(\eta^5\text{-}C_9H_7)][BF_4]$ (15) (1.20 g, 2.94 mmol) in CH_2Cl_2 (35 cm^3). After stirring for 3 d at room temperature, the resulting dark yellow solution was filtered through a small pad of alumina. The yellow filtrate was collected and concentrated to a small volume before being chromatographed on alumina. Elution with CH_2Cl_2 afforded a single yellow fraction which gave, after removal of solvent and recrystallisation from CH_2Cl_2/pentane, $[Mo(\eta^3\text{-}C_4H_3O_2)(CO)_2\text{-}(\eta^5\text{-}C_9H_7)]$ (164) (590 mg, 57%) as a bright yellow powder.

NMR and infrared spectroscopy indicated the predominance of an *exo* conformation for (164) in solution. Low temperature NMR experiments were necessary for the determination of the coupling constants. H-H and H-C COSY techniques were used to assign the proton and carbon NMR signals.

Microanalysis

$C_{15}H_{10}O_4Mo$	requires:	C = 51.5, H = 2.9%
	found:	C = 51.4, H = 2.8%

Infrared Spectrum

ν_{CO}/cm^{-1} (CH_2Cl_2) at 1979 (vs), 1904 (s) and 1752 (ms).

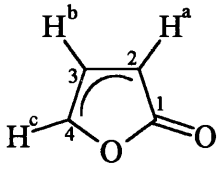

^{1}H NMR Spectrum

(CD_2Cl_2, 20°C): δ 7.32-7.16 (m, 4H, indenyl), 6.57 (br s 1H, H^c), 6.18 (br m, 1H, indenyl), 5.96 (br m, 1H, indenyl), 5.62 (dd, 1H, indenyl), 3.15 (br s, 1H, H^a) and 1.73 (br s, 1H, H^b).

(CD_2Cl_2, -45°C): δ 7.32-7.11 (m, 4H, indenyl), 6.62 [dd, 1H, H^c, $J(H^cH^b)$ = 2.7, $J(H^cH^a)$ = 2.4], 6.22 (m, 1H, indenyl), 5.98 (m, 1H, indenyl), 5.60 (dd, 1H, indenyl), 3.14 [dd, 1H, H^a, $J(H^aH^b)$ = 2.7, $J(H^aH^c)$ = 2.4] and 1.26 [dd, 1H, H^b, $J(H^bH^a)$ = 2.7, $J(H^bH^c)$ = 2.7].

^{13}C-{^{1}H} NMR Spectrum

(CD_2Cl_2, 20°C): δ 237.2 (CO), 232.4 (CO), 173.2 (C^1) 127.1, 126.1 (indenyl), 124.6, 123.8 (indenyl), 113.0, 111.6 (indenyl), 100.0 (C^4), 89.0 (indenyl), 84.9 (C^3), 81.4, 81.2 (indenyl) and 44.8 (C^2).

(CD_2Cl_2, -45°C): δ 237.7 (CO), 232.6 (CO), 173.1 (C^1), 126.9, 125.7 (indenyl), 124.5, 123.1 (indenyl), 112.5, 110.8 (indenyl), 99.9 (C^4), 88.2 (indenyl), 85.7 (C^3), 81.0, 80.8 (indenyl) and 45.1 (C^2).

FAB Mass Spectrum

(+) FAB in NBA: 352, $[M]^+$; 324, $[M-CO]^+$; 296, $[M-2CO]^+$ and 268, $[M-3CO]^+$.

Preparation of $[Mo(\eta^2\text{-}C_{11}H_{12}NO_2)(CO)_2(\eta^5\text{-}C_9H_7)]$ (165)

Benzylamine (0.686 cm^3, 67 mg, 0.628 mmol) was added to a solution of the yellow complex $[Mo(\eta^3\text{-}C_4H_3O)(CO)_2(\eta^5\text{-}C_9H_7)]$ (164) (110 mg, 0.314 mmol) in CH_2Cl_2 (15 cm^3). The mixture was left to stir overnight at room temperature resulting in a bright orange solution. Analysis by TLC and infrared spectroscopy showed the complete consumption of starting material and the formation of a new product. The mixture was concentrated to a small volume *in vacuo*, following which slow addition of pentane precipitated a bright yellow solid. This was washed with pentane and recrystallised from CH_2Cl_2/pentane to afford $[Mo(\eta^2\text{-}C_{11}H_{12}NO_2)(CO)_2(\eta^5\text{-}C_9H_7)]$ (165) (122 mg, 85%) as a bright yellow powder.

The molecular structure of (165) was determined from the results of an X-ray diffraction experiment, which also showed that (165) crystallised with one molecule of CH_2Cl_2 in the unit cell. X-ray quality *crystals* of (165) were obtained by CH_2Cl_2/Et_2O/pentane layer diffusion at room temperature. DEPT, H-H and H-C COSY techniques were used to assign the proton and carbon NMR signals.

Microanalysis

$C_{22}H_{19}MoNO_4.CH_2Cl_2$	requires:	C = 50.9, H = 3.9, N = 2.6%
	found:	C = 51.4, H = 3.9, N = 2.7%

Infrared Spectrum

ν_{CO}/cm^{-1} (CH_2Cl_2) at 1933 (vs), 1842 (s) and 1653 (mw).

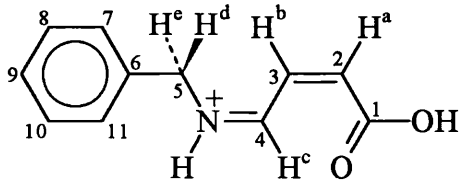

^{1}H NMR Spectrum

[$(CD_3)_2CO$, 20°C]: δ 9.72 (br s, 1H, OH), 7.52-7.49 (m, 4H, indenyl), 7.48-7.38 (m, 3H, phenyl), 7.21-7.12 (m, 2H, phenyl), 6.79 [dm, 1H, H^c, $J(H^cH^b)$ = 11.2], 6.61 (br m, 1H, NH), 6.20 (m, 1H, indenyl), 6.11 (m, 1H, indenyl), 5.65 (dd, 1H, indenyl), 4.17

[dm, 2H, H^d and H^e, $J(H^dH^e)$ = 5.1], 1.70 [d, 1H, H^a, $J(H^aH^b)$ = 7.4] and 1.13 [dd, 1H, H^b, $J(H^bH^c)$ = 11.2, $J(H^bH^a)$ = 7.4].

^{13}C-{^1H} NMR Spectrum

[$(CD_3)_2CO$, 20°C]: δ 247.2 (CO), 240.9 (CO), 177.7 (C^1), 137.7 (C^6), 133.9 (C^4), 128.8, 128.0, 127.7 (C^7-C^{11}), 125.0, 124.4, 124.2 (indenyl), 112.9, 112.5 (indenyl), 89.7 (indenyl), 80.2 (indenyl), 55.2 (C^3), 48.6 (C^5) and 41.9 (C^2).

FAB Mass Spectrum

(+) FAB in NBA: 459, $[M]^+$; 431, $[M\text{-}CO]^+$ and 403, $[M\text{-}2CO]^+$.

Preparation of $[Mo(\eta^2\text{-}C_{12}H_{14}NO_2)(CO)_2(\eta^5\text{-}C_9H_7)]$ (170)

(*R*)-(+)-α-methylbenzylamine (0.132 cm^3, 121 mg, 1.00 mmol) was added to a solution of the yellow complex $[Mo(\eta^3\text{-}C_4H_3O)(CO)_2(\eta^5\text{-}C_9H_7)]$ (164) (175 mg, 0.500 mmol) in CH_2Cl_2 (30 cm^3). The mixture was left to stir overnight at room temperature resulting in the precipitation of a bright yellow solid. Analysis by TLC and infrared spectroscopy showed the complete consumption of the starting material and the formation of a new product. The solvent volume was reduced *in vacuo*, following which slow addition of pentane precipitated more of the bright yellow solid. This was washed with pentane and dried *in vacuo* to afford $[Mo(\eta^2\text{-}C_{12}H_{14}NO_2)(CO)_2(\eta^5\text{-}C_9H_7)]$ (170) (205 mg, 87%) as a bright yellow powder.

NMR spectroscopy showed (170) to exist as a 1:1 mixture of the (*R*, *R*/*S*)- and (*R*, *S*/*R*)-diastereoisomers. H-H and H-C COSY techniques were used to assign the proton and carbon NMR signals.

Microanalysis

$C_{23}H_{21}MoNO_4$	requires:	C = 58.6, H = 4.5, N = 3.0%
	found:	C = 58.8, H = 4.5, N = 3.0%

Infrared Spectrum

ν_{CO}/cm^{-1} (CH_2Cl_2) at 1933 (vs), 1844 (s) and 1653 (mw).

(*R, R/S*)-Diastereoisomer

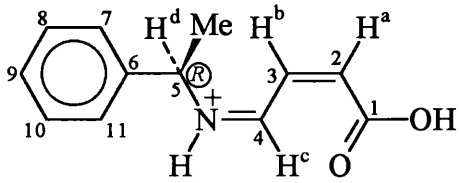

^{1}H NMR Spectrum

[$(CD_3)_2CO$, 20°C]: δ 9.73 (br s, 1H, OH), 7.60-7.52 (m, 4H, indenyl), 7.47-7.36 (m, 3H, phenyl), 7.25-7.08 (m, 2H, phenyl), 6.72 [dm, 1H, H^c, $J(H^cH^b)$ = 11.2], 6.48 (br m, 1H, NH), 6.16 (m, 1H, indenyl), 6.08 (m, 1H, indenyl), 5.64 (dd, 1H, indenyl), 4.58 [q, 1H, H^d, $J(H^dMe)$ = 6.8], 1.64 [d, 1H, H^a, $J(H^aH^b)$ = 7.3], 1.63 [d, 3H, Me, $J(MeH^d)$ = 6.8] and 1.11 [dd, 1H, H^b, $J(H^bH^c)$ = 11.2, $J(H^bH^a)$ = 7.3].

^{13}C-{^{1}H} NMR Spectrum

[$(CD_3)_2CO$, 20°C]: δ 247.6 (CO), 241.4 (CO), 178.0 (C^1), 143.6 (C^6), 133.3 (C^4), 128.9, 127.6, 126.5 (C^7-C^{11}), 125.1, 124.4, 124.2 (indenyl), 112.9, 112.5 (indenyl), 90.5, 81.2, 79.8 (indenyl), 55.8 (C^3), 54.6 (C^5), 42.6 (C^2) and 23.2 (Me).

(*R, S/R*)-Diastereoisomer

^{1}H NMR Spectrum

[$(CD_3)_2CO$, 20°C]: δ 9.73 (br s, 1H, OH), 7.60-7.52 (m, 4H, indenyl), 7.47-7.36 (m, 3H, phenyl), 7.25-7.08 (m, 2H, phenyl), 6.67 [dm, 1H, H^c, $J(H^cH^b)$ = 11.2], 6.48 (br m, 1H, NH), 6.16 (m, 1H, indenyl), 6.08 (m, 1H, indenyl), 5.60 (dd, 1H, indenyl), 4.14 [q, 1H, H^d, $J(H^dMe)$ = 6.8], 1.66 [d, 1H, H^a, $J(H^aH^b)$ = 7.3], 1.60 [d, 3H, Me, $J(MeH^d)$ = 6.8] and 1.38 [dd, 1H, H^b, $J(H^bH^c)$ = 11.2, $J(H^bH^a)$ = 7.3].

^{13}C-{^{1}H} NMR Spectrum

[$(CD_3)_2CO$, 20°C]: δ 247.3 (CO), 240.9 (CO), 177.6 (C^1), 143.2 (C^6), 131.8 (C^4), 128.9, 127.4, 126.2 (C^7-C^{11}), 124.7, 124.3, 124.0 (indenyl), 112.8, 111.8 (indenyl), 89.9, 80.2, 79.8 (indenyl), 54.6 (C^3), 54.0 (C^5), 41.6 (C^2) and 22.9 (Me).

FAB Mass Spectrum

(+) FAB in NBA: 473, $[M]^+$; 445, $[M\text{-}CO]^+$ and 417, [M-2CO].

Preparation of *anti*-[Mo(η^3-$C_5H_6O_3Na$)$(CO)_2$(η^5-C_5H_5)] (171)

NaOMe (0.740 cm^3 of a 0.23 M solution in thf, 0.17 mmol) was added to a solution of the yellow complex [Mo(η^3-$C_4H_3O_2$)$(CO)_2$(η^5-C_5H_5)] (163) (51 mg, 0.17 mmol) in thf (10 cm^3). The mixture was allowed to stir at ambient temperature for 0.5 h, after which the volatiles were removed under reduced pressure and the resultant yellow residue was extracted with several portions of thf. The extracts were combined and filtered through Celite and the filtrate was reduced to a small volume (*ca.* 2 cm^3) *in vacuo*. Slow addition of Et_2O afforded *anti*-[Mo(η^3-$C_5H_6O_3Na$)$(CO)_2$(η^5-C_5H_5)] (171) (50 mg, 83%) as a yellow powder.

NMR and infrared spectroscopy showed that (171) existed in solution at room temperature as an 11:9 mixture of *exo* and *endo* isomers.

Exo isomer (major)

Infrared Spectrum

ν_{CO}/cm^{-1} (thf) at 1946 (vs) and (1871) (s).

$\nu_{O=CO}$-/cm^{-1} (thf) at 1572 (br m).

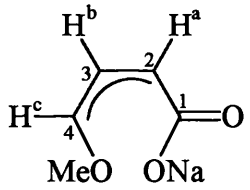

^{1}H NMR Spectrum

[$(CD_3)_2CO$, 20°C]: δ 5.98 [d, 1H, H^c, $J(H^cH^b)$ = 8.4], 5.42 (s, 5H, C_5H_5), 4.41 [dd, 1H, H^b, $J(H^bH^a)$ = $J(H^bH^c)$ = 8.4], 3.60 (s, 3H, OMe) and 3.57 [d, 1H, H^a, $J(H^aH^b)$ = 8.4].

^{13}C-{^{1}H} NMR Spectrum

[$(CD_3)_2CO$, 20°C]: δ 243.4 (CO), 241.8 (CO), 181.6 (C^1), 109.3 (C^4), 92.7 (C_5H_5), 75.4 (C^3), 58.8 (C^2) and 44.1 (OMe).

Endo isomer (minor)

Infrared Spectrum

ν_{CO}/cm^{-1} (thf) at 1936 (vs) and 1852 (s).

$\nu_{O=CO}-/cm^{-1}$ (thf) at 1572 (br m).

^1H NMR Spectrum

[$(CD_3)_2CO$, 20°C]: δ 7.01 [d, 1H, H^c, $J(H^cH^b)$ = 8.4], 5.31 (s, 5H, C_5H_5), 3.90 [dd, 1H, H^b, $J(H^bH^a)$ = $J(H^bH^c)$ = 8.4], 3.63 [d, 1H, H^a, $J(H^aH^b)$ = 8.4] and 3.54 (s, 3H, OMe).

$^{13}C-\{^1H\}$ NMR Spectrum

[$(CD_3)_2CO$, 20°C]: δ 242.8 (CO), 239.5 (CO), 181.8 (C^1), 115.8 (C^4), 93.1 (C_5H_5), 59.6 (C^3), 58.4 (C^2) and 41.3 (OMe).

FAB Mass Spectrum

(+) FAB in NBA: 355, $[M]^+$ and 327, $[M-CO]^+$.

Protonation of [Mo(η^3-$C_4H_3O_2$)(CO)$_2$(η^5-C_5H_5)] (163)

A solution of the yellow complex [Mo(η^3-$C_4H_3O_2$)(CO)$_2$(η^5-C_5H_5)] (163) (100 mg, 0.27 mmol) in CH_2Cl_2 (10 cm^3) was cooled to -78°C and treated with $HBF_4.OEt_2$ (0.047 cm^3, 515 mg of an 85% Et_2O solution, 0.27 mmol) producing an immediate change in colour to orange-red. The mixture was allowed to warm to ambient temperature and stirred for 1 h. The resulting orange solution was filtered through Celite and then concentrated to a small volume under reduced pressure. Addition of Et_2O precipitated an orange solid, which was washed with Et_2O and recrystallised from CH_2Cl_2/Et_2O to afford an unidentified protonation product (64 mg), as a particularly air-sensitive orange powder.

Infrared Spectrum

ν_{CO}/cm^{-1} (thf) at 1927 (vs), 1914 (s) and 1744 (s).

^{1}H NMR Spectrum

(CD_3CN, 20°C): δ 5.49 [dd, 1H, J(H-H) = 3.7, J(H-H) = 3.3], 5.12 (s. 5H, C_5H_5), 3.43 [d, 1H, J(H-H) = 3.3] and 3.03 [d, 1H, J(H-H) = 3.7].

^{13}C-{^{1}H} NMR Spectrum

(CD_3CN, 20°C): δ 246.8 (2CO), 173.5 (br s), 96.7 (C_5H_5), 79.1, 44.6 and 37.9.

4. REFERENCES

1. S. G. Davies, *Organotransition Metal Chemistry: Applications to Organic Synthesis*, Pergamon Press, Oxford, 1982.
2. A. J. Pearson, *Metallo-organic Chemistry*, Wiley, Chichester, 1985.
3. J. P. Collman, L. S. Hegedus, J. R. Norton and R. G. Finke, *Principles and Applications of Organotransition Metal Chemistry*, University Science Books, Mill Valley, CA, 1987.
4. Ch. Elschenbroich and A. Salzer, *Organometallics*, VCH, Weinham, 1989.
5. S. G. Davies, *Aldrichimica Acta*, 1990, **23**, 31.
6. S. G. Davies, I. M. Dordon-Hedgecock, R. J. C. Easton, S. C. Preston, K. H. Sutton and J. C. Walker, *Bull. Soc. Chim. France*, 1987, 609.
7. A. J. Pearson, *Synlett*, 1990, 10.
8. A. J. Pearson, *Cyclohexadienes*, in *Second Supplements to the 2nd edition of Rodd's Chemistry of Carbon Compounds*, ed. M. Sainsbury, Elsevier Science Publishers, Amsterdam, 1992, vol. IIA and B, p. 447.
9. A. J. Pearson, *Recent Developments in the Synthetic Applications of Organoiron and Organomolybdenum Chemistry*, in *Advances in Metal-Organic Chemistry*, ed. L. S. Liebeskind, JAI Press, London, 1989, vol. 1, p. 1.
10. R. Gree, *Synthesis*, 1989, 341.
11. M. Uemura, *Tricarbonyl(η^6-Arene)chromium Complexes in Organic Synthesis*, in *Advances in Metal-Organic Chemistry*, ed. L. S. Liebeskind, JAI Press, London, 1991, vol. 2, p. 195.
12. W. D. Wulff, *Transition Metal Carbene Complexes in Organic Synthesis*, in *Advances in Metal-Organic Chemistry*, ed. L. S. Liebeskind, JAI Press, London, 1989, vol. 1, p. 209.
13. H. Reichlen, A. Gruhl, G. Von Hessling and O. Pfrengle, *Justus Liebigs. Am. Chem*, 1930, **482**, 161.
14. R. Pettit and G. F. Emerson, *Adv. Organomet. Chem.*, 1964, **1**, 1.
15. R. B. King, *The Organic Chemistry of Iron*, Academic Press, New York, 1978, **1**, 525.

16. Y. Shvo and E. Hazum, *J. Chem. Soc., Chem. Commun.*, 1975, 829

17. A. J. Birch, K. B. Chamberlain, M. A. Haas and D. J. Thompson, *J. Chem. Soc., Perkin Trans. I*, 1973, 1882 .

18. A. J. Pearson and C. W. Ong, *J. Am. Chem. Soc.*, 1981, **103**, 6686.

19. P. McArdle and T. Higgins, *Inorg. Chim. Acta*, 1978, **30**, L303.

20. G. F. Emerson, J. E. Mahler and R. Pettit, *J. Org. Chem.*, 1964, **29**, 3620.

21. J. A. S. Howell, B. F. G. Johnson, P. L. Josty and J. Lewis, *J. Organomet. Chem.*, 1972, **39**, 329.

22. G. Cardaci and G. Bellachioma, *Inorg. Chem.*, 1977, **16**, 3099.

23. M. Brookhart and G. O. Nelson, *J. Organomet. Chem.*, 1979, **164**, 193.

24. S. Sarel, R. Ben-Sharhan and B. Kirson, *Israel J. Chem.*, 1972, **10**, 787.

25. T. M. Whitesides and R. W. Slaven, *J. Organomet. Chem.*, 1974, **67**, 99.

26. E. H. Braye and W. Hübel, *J. Organomet. Chem.*, 1965, **3**, 38.

27. M. Supozynski, I. Wolszczak and P. Karztoowicz, *Inorg. Chim. Acta*, 1979, **33**, L97.

28. R. G. Hayter, *J. Organomet. Chem.*, 1968, **13**, P1.

29. J. W. Faller, H. H. Murray, D. L. White and K. H. Chao, *Organometallics*, 1983, **2**, 400.

30. A. J. Pearson and M. N. I. Khan, *J. Org. Chem.*, 1985, **50**, 5276.

31. J. W. Faller and A. M. Rosan, *J. Am. Chem. Soc.*, 1977, **99**, 4858.

32. J. W. Faller and A. M. Rosan, *Ann. N. Y. Acad. Sci.*, 1977, **295**, 186.

33. L. S. Liebeskind and A. Bombrun, *J. Am. Chem. Soc.*, 1991, **113**, 8736.

34. J. W. Faller and C. Lambert, *Tetrahedron*, 1985, **41**, 5755.

35. A. Rubio and L. S. Liebeskind, *J. Am. Chem. Soc.*, 1993, **115**, 891.

36. J. W. Faller and D. Linebarrier, *Organometallics*, 1988, **7**, 1670.

37. J. S. McCallum, J. T. Sterbenz and L. S. Liebeskind, *Organometallics*, 1993, **12**, 927.

38. M. Bottrill and M. Green, *J. Chem. Soc., Dalton Trans.*, 1977, 2365.

39. M. Green, S. Greenfield and M. Kersting, *J. Chem. Soc., Chem. Commun.*, 1985, 18.

40. M. Green, S. Greenfield, M. J. Grimshire, M. Kersting, A. G. Orpen and R. A. Rodrigues, *J. Chem. Soc., Chem. Commun.*, 1987, 97.

41. J. S. Baxter, M. Green and T. V. Lee, *J. Chem. Soc. Chem. Commun.*, 1989, 1595.

42. S. A. Benyunes and M. Green, *J. Organomet. Chem.*, 1990, **390**, C32.

43. S. A. Benyunes, M. Green and M. J. Grimshire, *Organometallics*, 1989, **8**, 2268.

44. S. A. Benyunes, A. Binelli, M. Green and M. J. Grimshire, *J. Chem. Soc., Dalton Trans.*, 1991, 895.

45. S. A. Benyunes, R. J. Deeth, A. Fries. M. Green, M. McPartlin and C. B. M. Nation, *J. Chem. Soc., Dalton Trans.*, 1992, 3453.

46. A. J. Pearson, in *Chemistry of the Carbon-Metal Bond*, eds. F. R. Hartley and S. Patai, Wiley, Chichester, 1987, vol. 4.

47. V. V. Krivykh, O. V. Gusev, M. G. Peterleitner, L. I. Denisovich and M. I. Rybinskaya, *Izv. Akad. Nauk SSSR, Ser. Khim.*, 1986, 1440.

48. V. V. Krivykh, O. V. Gusev and M. I. Rybinskaya, *J. Organomet. Chem.*, 1989, **362**, 351.

49. O. V. Gusev, V. V. Krivykh, P. V. Petrovskii and M. I. Rybinskaya, *Izv. Akad. Nauk SSSR, Ser. Khim.*, 1987, 1655.

50. J. Markham, K. Menard and A. Cutler, *Inorg. Chem.*, 1985, **24**, 1581.

51. J. Chatt and L. A. Duncanson, *J. Chem. Soc.*, 1953, 2939.

52. M. J. S. Dewar, *Bull. Soc. Chim. France*, 1951, C71.

53. H. Yasuda, K. Tatsumi and A. Nakamura, *Accts. Chem. Res.*, 1985, **18**, 120.

54. R. D. Ernsy, *Accts. Chem. Res.*, 1985, **18**, 56.

55. L. Kruczynski and J. Takats, *J. Am. Chem. Soc.*, 1974, **96**, 932

56. L. Kruczynski and J. Takats, *Inorg. Chem.*, 1976, **15**, 3140.

57. T. L. Waring, Ph.D. Thesis, University of Bristol, 1987.

58. S. A. Benyunes, J. P. Day, M. Green, A. W. Al-Saadoon and T. L. Waring, *Angew. Chem. Int. Ed. Engl.*, 1990, **29**, 1416.

59. G. Erker, J. Wicher, K. Engel, F. Rosenfeldt, W. Dietrich and C. Krüger, *J. Am. Chem. Soc.*, 1980, **102**, 6344.

60. N. J. Christensen, A. D. Hunter and P. Legzdins, *Organometallics*, 1989, **8**, 930.

61. A. Davison and W. C. Rode, *Inorg. Chem.*, 1967, **6**, 2125.

62. J. W. Faller and M. J. Incorvia, *Inorg. Chem.*, 1968, **7**, 840.

63. J. W. Faller and A. Jakubowski, *J. Organomet. Chem.*, 1971, **31**, C75.

64. J. W. Faller, C. C. Chen, M. J. Mattina and A. Jakubowski, *J. Organomet. Chem.*, 1973, **52**, 361.

65. M. R. Churchill and R. Mason, *Proc. Roy. Soc. Ser. A.*, 1964, **279**, 191.

66. A. N. Nesmeyanov and N. A. Vol'Kenau, *Izvest. Akad. Nauk. SSSR. Ser. Khim*, 1975, 1151.

67. J. E. Bäckvall, *Acc. Chem. Res.*, 1983, **16**, 335.

68. S. G. Davies, M. L. H. Green and D. M. P. Mingos, *Tetrahedron*, 1978, **34**, 3047.

69. E. O. Greaves, G. R. Knox and P. L. Pauson, *J. Chem. Soc., Chem. Commun.*, 1969, 1124.

70. R. E. Graf and C. P. Lillya, *J. Organomet. Chem.*, 1979, **166**, 53.

71. M. F. Semmelhack and J. W. Herndon, *Organometallics*, 1983, **2**, 363.

72. E. O. Fischer and R. D. Fischer, *Angew. Chem.*, 1960, **72**, 919.

73. A. J. Birch and D. H, Williamson, *J. Chem. Soc., Perkin Trans.*, 1973, **1**, 1892.

74. A. J. Birch, I. D. Jenkins and A. J. Liepa, *Tetrahedron Lett.*, 1975, 1723.

75. F. Franke and I. D. Jenkins, *Aust. J. Chem.*, 1978, **31**, 595.

76. B. F. G. Johnson, J. Lewis, D. G. Parker, P. R. Raithby and G. M. Sheldrick, *J. Organomet. Chem.*, 1978, **150**, 115.

77. B. F. G. Johnson, K. D. Karlin, J. Lewis and D. G. Parker, *J. Organomet. Chem.*, 1978, **157**, C67.

78. B. M. R. Bandara, A. J. Birch and T. C. Khor, *Tetrahedron Lett.*, 1980, **21**, 3625.

79. A. J. Pearson and C. W. Ong, *J. Org. Chem.*, 1982, **47**, 3780.

80. A. J. Pearson, S. L. Kole and J. Yoon, *Organometallics*, 1986, **5**, 2075.

81. I. Paterson and M. M. Mansuri, *Tetrahedron*, 1985, **41**, 3569.

82. A. J. Pearson, S. L. Kole and B. Chen, *J. Am. Chem. Soc.*, 1983, **105**, 4483.

83. A. J. Pearson, S. L. Kole and T. Ray, *J. Am. Chem. Soc.*, 1984, **106**, 6060.

84. A. J. Pearson, *J. Chem. Soc., Perkin Trans. I*, 1979, 1255.

85. A. J. Pearson, N. I. Khan, J. C. Clardy and H. Cun-heng, J. Am. Chem. Soc., 1985, **107**, 2748.

86. A. J. Pearson and N. I. Khan, *Tetrahedron Lett.*, 1985, **26**, 1407.

87. B. E. R. Schilling, R. Hoffmann and J. W. Faller, *J. Am. Chem. Soc.*, 1979, **101**, 592.

88. R. D. Adams, D. F. Chodosh, J. W. Faller and A. M. Rosan, *J. Am. Chem. Soc.*, 1979, **101**, 2570.

89. D. J. Thompson, *J. Organomet. Chem.*, 1976, 108, 381.

90. D. H. R. Barton, A. A. L. Guantilaka, T. Nakanishi, H. Patin, D. A. Widdowson and B. R. Worth, *J. Chem. Soc., Perkin Trans. I*, 1976, 821.

91. C. H. Mauldin, E. R. Biehl and B. C. Reeves, *Tetrahedron Lett.*, 1972, 2955.

92. E. J. Corey and G. Moinet, *J. Am. Chem. Soc.*, 1973, **95**, 7185.

93. Y. Shvo and E. Hazum, *J. Chem. Soc., Chem. Commun.*, 1974, 336.

94. H. Alper, *J. Organomet. Chem.*, 1975, **96**, 95.

95. M. Frank-Neumann and D. Martina, *Tetrahedron Lett.*, 1972, 2955.

96. P. Caddy, M. Green, E. O'Brien, L. E. Smart and P. Woodward, *J. Chem. Soc., Dalton Trans.*, 1980, 962.

97. J. W. Faller, J. A. John and M. R. Mazzieri, *Tetrahedron Lett.*, 1989, **30**, 1769.

98. V. I. Sokolov, *Chirality and Optical Activity in Organometallic Compounds*, Gordon and Breach, London, 1990.

99. H. Brunner, *Adv. Organomet. Chem.*, 1980, **18**, 151.

100. J. W. Faller and Y. Shvo, *J. Am. Chem. Soc.*, 1980, **102**, 5396.

101. J. W. Faller, Y. Shvo, K. Chao and H. H. Murray, *J. Organomet. Chem.*, 1982, **226**, 251.

102. A. J. Birch and B. M. R. Bandara, *Tetrahedron Lett.*, 1980, **21**, 2981.

103. M. Green and M. E. Vamon Rao, unpublished work.

104. A. J. Pearson, S. L. Blystone, H. Nar, A. A. Pinkerton, B. A. Roden and J. Yoon, *J. Am. Chem. Soc.*, 1989, **111**, 134.

105. A. J. Pearson, V. D. Khetani and B. A. Roden, *J. Org. Chem.*, 1989, **54**, 5141.

106. A. J. Pearson, S. L. Blystone and B. A. Roden, *Tetrahedron Lett.*, 1987, **28**, 2459.

107. A. J. Pearson and J. Yoon, J. Chem. Soc., *Chem. Commun.*, 1986, 1467.

108. P. W. Howard, G. R. Stephenson and S. C. Taylor, *J. Chem. Soc., Chem. Commun.*, 1988, 1603.

109. S. Hansson, J. F. Miller and L. S. Liebeskind, *J. Am. Chem. Soc.*, 1990, **112**, 9660.

110. M. Bamber, Ph.D. Thesis, University of London, 1991.

111. A. J. Pearson and M. W. D. Perry, *J. Chem. Soc., Chem. Commun.*, 1989, 389.

112. A. J. Pearson, S. Mallik, R. Mortezaei, M. W. D. Perry, R. J. Shively and W. J. Youngs, *J. Am. Chem. Soc.*, 1990, 112, 8034.

113. A. J. Pearson, S. Mallik, A. A. Pinkerton, J. P. Adams and S. Zheng, *J. Org. Chem.*, 1992, 57, 2910.

114. R. H. Yu. J. S. McCallum and L. S. Liebeskind, *Organometallics*, 1994, **13**, 1476.

115. R. A. Rodrigues, Ph.D. Thesis, University of Bristol, 1987.

116. F. H. Allen, O. Kennard, D. G. Watson, L. Brammer, A. G. Orpen and R. Taylor, *J. Chem. Soc., Perkin Trans. II*, 1987, S1.

117. D. H. Williams and I. Fleming, *Spectroscopic Methods in Organic Chemistry*, McGraw-Hill, London, 1987.

118. A. J. Birch and K. B. Chamberlain, *Organic Synthesis*, 1977, **57**, 107.

119. N. A. Grabowski, R. P. Hughes, B. S. Jaynes and A. L. Rheingold, *J. Chem. Soc., Chem. Commun.*, 1986, 1694.

120. R. B. King, M. Z. Iqbal and A. D. King, *J. Organomet. Chem.*, 1979, **171**, 53.

121. F. Naf, R. Decorzant and W. Thommen, *Helv. Chim. Acta*, 1975, **58**, 1808.

122. J. M. Fortunato and B. Gavern, *J. Org. Chem.*, 1976, **41**, 2194.

123. G. Stork, P. Rosen and N. L. Goldman, *J. Am. Chem. Soc.*, 1961, **83**, 2965.

124. C. Djerassi, *Organic Reactions*, 1951, **6**, 207.

125. T. Imamato, Y. Sugiura and N. Takiyama, *Tetrahedron Lett.*, 1984, **25**, 4233.

126. T. Imamato, N. Takiyama, K. Nakamura, T. Hatajima and Y. Kamiya, *J. Am. Chem. Soc.*, 1989, **111**, 4392.

127. T. Imamoto, *Pure and Appl. Chem.*, 1990, **62**, 747.

128. K. Utimoto, A. Nakamura and S. Matsubara, *J. Am. Chem. Soc.*, 1990, **112**, 8189.

129. A. G. Orpen, L. Brammer, F. H. Allen, O. Kennard, D. G. Watson and R. Taylor, *J. Chem. Soc., Dalton Trans.*, 1989, S1.

130. G. Bringmann, R. Walter and R. Weirich, *Angew. Chem., Int. Ed. Engl.*, 1990, **29**, 977.

131. R. Noyori, *Chem. Soc. Rev.*, 1989, **18**, 187.

132. E. J. Thomas, *Aliphatic Compounds*, in *The Chemistry of Natural Products*, ed. R. H. Thomson, Blackie, London, 1985, p. 80.

133. T. W. Hart, *Nat. Prod. Reports*, 1988, **5**, 14.

134. G. Sembdner and C. Klose, *Biol. Rundsch.*, 1985, **23**, 29.

135. B. M. Trost and D. L. Vanvranken, *J. Am. Chem. Soc.*, 1993, **115**, 444.

136. B. M. Trost, L. P. Li and S. D. Guile, *J. Am. Chem. Soc.*, 1992, **114**, 8745.

137. M. L. Falckpedersen, T. Benneche and K. Undheim, *Acta Chim. Scand.*, 1993, **47**, 72.

138. K. W. Barnet, P. M. Treichel and R. L. Shubkin, *J. Organomet. Chem.*, 1967., **7**, 449.

139. F. W. S. Benfield and M. L. H. Green, *J. Chem. Soc., Dalton Trans.*, 1974, 1324.

140. H. J. Müller, U. Nagel, M. Steimann, K. Polburn and W. Beck, *Chem. Ber.*, 1989, **122**, 1387.

141. L. G. Bell, H. H. Brintzinger, *J. Organomet. Chem.*, 1977, **135**, 173.

142. G. Huttner, H. H. Brintzinger and L. G. Bell, J. Organomet. Chem., 1978, **145**, 329.

143. K. L. T. Wong and H. H. Brintzinger, *J. Am. Chem. Soc.*, 1975, **97**, 5143.

144. S. Mönkeberg, E. van Raaij, H. Kiesele and H. H. Brintzinger, *J. Organomet. Chem.*, 1989, **365**, 285.

145. J. March, *Advanced Organic Chemistry: Reactions, Mechanisms and Structure*, Wiley, Chichester, 1985.

146. G. L. Geoffroy and M. G. Bradley, *Inorg. Chem.*, 1978, **17**, 2410.

147. B. R. Francis, M. L. H. Green, T. Luong-thi and G. A. Moser, *J. Chem. Soc., Dalton Trans.*, 1976, 1339.

148. M. Suzuki, Y. Oda, R. Noyori, *J. Am. Chem. Soc.*, 1979, **101**, 1623.

149. W. J. Vong, S. H. Lin, R. S. Liu, G. H. Lee and S. M. Peng, *J. Chem. Soc., Chem Commun.*, 1990, 1285.

150. W.J. Vong, S. M. Peng, S. H. Lin, W. J. Lu and R. S. Liu, *J. Am. Chem. Soc.*, 1991, **113**, 573.

151. S. H. Lin, G. H. Lee, S. H. Peng and R. S. Liu, *Organometallics*, 1993, **12**, 2591.

152. D. H. G. Crout and M. Christen, *Biotransformations in Organic Synthesis*, in *Modern Synthetic Methods*, ed. R. Scheffold, Springer-Verlag, 1989, vol. 5, p. 1.

153. N. W. Alcock, D. H. G. Crout, C. M. Henderson and S. E. Thomas, *J. Chem. Soc., Chem. Commun.*, 1988, 746.

154. J. W. Faller, D. F. Chodosh and D. Katahira, *J. Organomet. Chem.*, 1980, **187**, 227.

155. J. L. Davidson, M. Green, J. Z. Nyathi, C. Scott, F. G. A. Stone, A. J. Welch and P. Woodward, *J. Chem. Soc., Chem. Commun.*, 1976, 714.

156. M. Green, J. Z. Nyathi, C. Scott, F. G. A. Stone, A. J. Welch and P. Woodward, *J. Chem. Soc., Dalton Trans.*, 1978, 1067.

157. W. H. Myers, M. Sabat and W. D. Harman, *J. Am. Chem. Soc.*, 1991, **113**, 6682.

158. S. G. Davies and M. R. Shipton, *J. Chem. Soc., Perkin Trans. I*, 1991, 757.

159. R. Cordone, W. D. Harman and H. Taube, *J. Am. Chem. Soc.*, 1989, **111**, 2896.

160. J. Zakrzewski, *J. Organomet. Chem.*, 1987, **326**, C17.

161. H. Felkin and J. Zakrzewski, *J. Am. Chem. Soc.*, 1985, **107**, 3374.

162. J. M. O'Conner and C. P. Casey, *Chem. Ber.*, 1987, **87**, 302.

163. EHMO calculation employed the program system developed by Mealli and Proserpio: C. Mealli and M. Proserpio, *J. Chem. Educ.*, 1990, **67**, 399.

164. G. M. Rubottom and J. M. Gruber, *J. Org. Chem.*, 1977, **42**, 1051.

165. G. M. Sheldrick, SHELX86 program for crystal structure determination, University of Göttingen, 1986.

166. G. M. Sheldrick, SHELX76 program for crystal structure determination, University of Cambridge, 1976.

167. N. Walker and D. Stewart, *Acta Crystallogr.*, Sect. A, 1983, **39**, 158.

5. APPENDIX

Note on [Mo(η^3-$C_{13}H_{15}O$)(CO_2)(η^5-C_5Me_5)] (107).

A crystal of approximate dimensions 0.2 x 0.2 x 0.2 mm was used for data collection.

Crystal data: $C_{25}H_{30}O_3Mo$, M = 474.5 triclinic, a = 8.557(2), b = 10.582(3), c = 13.056(3)Å, α = 80.35(2), β = 87.16(2), γ = 73.53(2)°, U = 1117.7 Å^3, space group $P\bar{1}$, Z = 2, D_c = 1.41 gcm^{-3}, μ(Mo-K_α) = 5.9 cm^{-1}, F(000) = 492. Data were measured at room temperature on a CAD4 automatic four-circle diffractometer in the range $2 \leq \theta \leq 24^\circ$. 3762 reflections were collected of which 2985 were unique with $I \geq 2\sigma(I)$. Data were corrected for Lorentz and polarization but not for absorption. The structure was solved by Patterson methods and refined using the SHELX[165,166] suite of programs. In the final least squares cycles all atoms were allowed to vibrate anisotropically. Hydrogen atoms were included at calculated positions except in the instance of the H3, H131, H141 and H151 (attached to O3, C13, C14 and C15 respectively). These protons were located in an advanced Difference Fourier and refined at a distance of 0.96 Å from the relevant parent atoms.

Final residuals after 12 cycles of least squares were R = 0.0258, R_w = 0.0286, for a weighting scheme of $w = 0.9678/[\sigma^2(F) + 0.001390(F)^2]$. Max. final shift/esd was 0.018. The max. and min. residual densities were 0.15 and -0.13 eÅ^{-3} respectively. Final fractional atomic coordinates and isotropic thermal parameters, bond distances and angles are given in Tables A1-A6. Tables of anisotropic temperature factors are available as supplementary data. The asymmetric unit is shown in Fig. 83, along with the labelling scheme used.

TABLE A1

Fractional atomic co-ordinates ($x10^4$) for complex (107)

	x	y	z
Mo(1)	3928.0(3)	2981.0(2)	2921.9(2)
O(1)	2055(3)	5116(2)	3292(2)
O(2)	86(3)	2635(3)	5319(2)
O(3)	-1191(3)	6988(2)	2419(2)
C(1)	1357(4)	4370(3)	3142(2)
C(2)	186(4)	2778(3)	4428(3)
C(3)	2457(4)	2259(3)	1737(2)
C(4)	2906(3)	1494(3)	2744(3)
C(5)	1817(4)	709(3)	3020(3)
C(6)	681(4)	994(3)	2209(3)
C(7)	1070(4)	1948(3)	1405(3)
C(8)	3394(5)	3099(4)	1087(3)
C(9)	4447(4)	1381(4)	3309(3)
C(10)	1961(5)	-354(4)	3967(4)
C(11)	-646(5)	310(4)	2174(4)
C(12)	290(5)	2437(4)	366(3)
C(13)	-1479(3)	4896(3)	2054(2)
C(14)	-2091(3)	3771(3)	2315(2)
C(15)	-2403(3)	3414(3)	3374(3)
C(16)	-3167(4)	4502(3)	4008(2)
C(17)	-2544(3)	5747(3)	3739(2)
C(18)	-2239(3)	6129(3)	2559(2)
C(19)	-3660(4)	6902(4)	4217(3)
C(20)	-3826(4)	6936(3)	1982(2)
C(21)	-4115(4)	8282(3)	1621(3)
C(22)	-5574(5)	9016(3)	1132(3)
C(23)	-6754(5)	8436(4)	991(3)
C(24)	-6491(4)	7087(4)	1350(3)
C(25)	-5053(4)	6353(3)	1827(3)

TABLE A2

Anisotropic temperature factors (Å $x10^3$) for complex (107)

	U_{11}	U_{22}	U_{33}	U_{23}	U_{13}	U_{23}
Mo(1)	35.7(2)	35.6(2)	43.1(2)	-9.1(1)	0.7(1)	-12.1(1)
O(1)	64(1)	63(1)	88(2)	-17(1)	-7(1)	-35(1)
O(2)	81(2)	79(2)	49(1)	-7(1)	0(1)	-33(1)
O(3)	58(1)	47(1)	70(1)	-4(1)	-3(1)	-24(1)
C(1)	44(2)	47(2)	49(2)	-9(1)	3(1)	-12(1)
C(2)	46(2)	45(2)	53(2)	-8(1)	-1(1)	-15(1)
C(3)	57(2)	51(2)	56(2)	-25(1)	15(1)	-20(1)
C(4)	40(2)	53(2)	62(2)	-23(1)	6(1)	-10(1)
C(5)	47(2)	40(2)	67(2)	-11(1)	10(1)	-4(1)
C(6)	46(2)	42(2)	83(2)	-26(2)	6(2)	-15(1)
C(7)	55(2)	51(2)	56(2)	-23(1)	1(1)	-14(1)
C(8)	93(3)	81(3)	80(3)	-33(2)	37(2)	-46(2)
C(9)	44(2)	93(3)	90(3)	-36(2)	-3(2)	-5(2)
C(10)	84(3)	51(2)	107(3)	7(2)	19(2)	0(2)
C(11)	59(2)	66(2)	157(4)	-50(3)	13(2)	-32(2)
C(12)	91(3)	94(3)	64(2)	-31(2)	-8(2)	-22(2)
C(13)	45(1)	46(2)	40(1)	-8(1)	-3(1)	-11(1)
C(14)	40(1)	47(2)	57(2)	-15(1)	-7(1)	-10(1)
C(15)	39(1)	47(2)	65(2)	-4(1)	-3(1)	-20(1)
C(16)	40(1)	57(2)	53(2)	-3(1)	6(1)	-12(1)
C(17)	41(1)	47(2)	47(2)	-12(1)	-2(1)	-6(1)
C(18)	44(1)	39(1)	51(2)	-9(1)	0(1)	-14(1)
C(19)	62(2)	64(2)	59(2)	-20(2)	4(2)	-1(2)
C(20)	50(2)	43(2)	43(2)	-9(1)	1(1)	-7(1)
C(21)	65(2)	44(2)	61(2)	-16(1)	2(2)	-8(1)
C(22)	82(2)	44(2)	59(2)	-7(1)	-1(2)	8(2)
C(23)	62(2)	63(2)	65(2)	-11(2)	-11(2)	5(2)
C(24)	58(2)	73(2)	79(2)	-5(2)	-16(2)	-13(2)
C(25)	55(2)	52(2)	69(2)	0(2)	-14(2)	-11(1)

TABLE A3

Hydrogen fractional atomic co-ordinates ($x10^4$) and isotropic temperature factors ($Å^2$ $x10^3$) for complex (107)

	x	y	z	U
H(3)	-368(39)	6678(40)	2947(24)	92(2)
H(81)	4277(5)	3159(4)	1485(3)	92(2)
H(82)	2680(5)	3976(4)	875(3)	92(2)
H(83)	3821(5)	2706(4)	484(3)	92(2)
H(92)	4475(4)	814(4)	3968(3)	92(2)
H(92)	4471(4)	2250(4)	3418(3)	92(2)
H(93)	5375(4)	1004(4)	2903(3)	92(2)
H(101)	1070(5)	-741(4)	3983(4)	92(2)
H(102)	1936(5)	37(4)	4582(4)	92(2)
H(103)	2972(5)	-1035(4)	3938(4)	92(2)
H(111)	-1258(5)	670(4)	1543(4)	92(2)
H(112)	-1358(5)	459(4)	2759(4)	92(2)
H(113)	-164(5)	-632(4)	2197(4)	92(2)
H(121)	-622(5)	2085(4)	337(3)	92(2)
H(122)	1065(5)	2144(4)	-162(3)	92(2)
H(123)	-79(5)	3395(4)	254(3)	92(2)
H(131)	-1044(46)	5119(41)	1378(13)	92(2)
H(141)	-2232(53)	3226(34)	1828(24)	92(2)
H(151)	-2638(51)	2568(21)	3547(32)	92(2)
H(161)	-4323(4)	4770(3)	3898(2)	92(2)
H(162)	-2939(4)	4143(3)	4728(2)	92(2)
H(171)	-1485(3)	5529(3)	4046(2)	92(2)
H(191)	-3261(4)	7673(4)	4042(3)	92(2)
H(192)	-3678(4)	6657(4)	4958(3)	92(2)
H(193)	-4743(4)	7105(4)	3948(3)	92(2)
H(211)	-3299(4)	8719(3)	1708(3)	92(2)
H(221)	-5748(5)	9952(3)	887(3)	92(2)
H(231)	-7754(5)	8950(4)	647(3)	92(2)
H(241)	-7323(4)	6665(4)	1269(3)	92(2)
H(251)	-4884(4)	5414(3)	2058(3)	92(2)

TABLE A4

Bond lengths (Å) for complex (107)

C(1)-Mo(1)	1.943(5)	C(2)-Mo(1)	1.946(5)	H(112)-C(11)	0.960	H(113)-C(11)	0.960
C(3)-Mo(1)	2.336(5)	C(4)-Mo(1)	2.304(5)	H(121)-C(12)	0.960	H(122)-C(12)	0.960
C(5)-Mo(1)	2.352(5)	C(6)-Mo(1)	2.386(5)	H(123)-C(12)	0.960	H(131)-C(13)	0.960(2)
C(7)-Mo(1)	2.389(5)	C(13)-Mo(1)	2.350(5)	H(141)-C(14)	0.960(2)	H(151)-C(15)	0.960(2)
C(14)-Mo(1)	2.187(5)	C(15)-Mo(1)	2.368(5)	H(161)-C(16)	0.960	H(162)-C(16)	0.960
C(1)-O(1)	1.161(5)	C(2)-O(2)	1.149(5)	H(171)-C(17)	0.960	H(191)-C(19)	0.960
C(18)-O(3)	1.433(4)	C(4)-C(3)	1.431(5)	H(192)-C(19)	0.960	H(193)-C(19)	0.960
C(7)-C(3)	1.423(5)	C(8)-C(3)	1.496(5)	H(211)-C(21)	0.960	H(221)-C(22)	0.960
C(5)-C(4)	1.412(5)	C(9)-C(4)	1.508(6)	H(231)-C(23)	0.960	H(241)-C(24)	0.960
C(6)-C(5)	1.409(6)	C(10)-C(5)	1.510(7)	H(251)-C(25)	0.960		
C(7)-C(6)	1.426(6)	C(11)-C(6)	1.516(6)				
C(12)-C(7)	1.487(6)	C(14)-C(13)	1.417(5)				
C(18)-C(13)	1.524(6)	C(15)-C(14)	1.404(5)				
C(16)-C(15)	1.510(6)	C(17)-C(16)	1.538(6)				
C(18)-C(17)	1.555(6)	C(19)-C(17)	1.526(6)				
C(20)-C(18)	1.539(6)	C(21)-C(20)	1.378(5)				
C(25)-C(20)	1.398(5)	C(22)-C(21)	1.390(6)				
C(23)-C(22)	1.356(6)	C(24)-C(23)	1.383(6)				
C(25)-C(24)	1.370(6)	H(3)-O(3)	0.960(2)				
H(81)-C(8)	0.960	H(82)-C(8)	0.960				
H(83)-C(8)	0.960	H(92)-C(9)	0.960				
H(92)-C(9)	0.960	H(93)-C(9)	0.960				
H(101)-C(10)	0.960	H(102)-C(10)	0.960				
H(103)-C(10)	0.960	H(111)-C(11)	0.960				

TABLE A5

Bond angles (deg.) for complex (107)

C(2)-Mo(1)-C(1)	82.0(2)	C(3)-Mo(1)-C(1)	90.1(2)	C(5)-C(4)-C(3)	108.0(4)	C(9)-C(4)-C(3)	124.8(4)
C(3)-Mo(1)-C(2)	136.0(1)	C(4)-Mo(1)-C(1)	92.4(2)	C(9)-C(4)-C(5)	126.4(4)	C(6)-C(5)-C(4)	108.2(4)
C(4)-Mo(1)-C(2)	100.9(2)	C(4)-Mo(1)-C(3)	35.9(1)	C(10)-C(5)-C(4)	125.5(4)	C(10)-C(5)-C(6)	126.0(4)
C(5)-Mo(1)-C(1)	124.8(2)	C(5)-Mo(1)-C(2)	91.0(2)	C(7)-C(6)-C(5)	108.6(4)	C(11)-C(6)-C(5)	125.0(4)
C(5)-Mo(1)-C(3)	58.8(2)	C(5)-Mo(1)-C(4)	35.3(1)	C(11)-C(6)-C(7)	126.2(4)	C(6)-C(7)-C(3)	107.3(4)
C(6)-Mo(1)-C(1)	147.5(1)	C(6)-Mo(1)-C(2)	115.0(2)	C(12)-C(7)-C(3)	125.5(4)	C(12)-C(7)-C(6)	126.9(4)
C(6)-Mo(1)-C(3)	58.1(2)	C(6)-Mo(1)-C(4)	58.3(2)	C(18)-C(13)-C(14)	119.0(4)	C(15)-C(14)-C(13)	115.9(4)
C(6)-Mo(1)-C(5)	34.6(1)	C(7)-Mo(1)-C(1)	120.0(2)	C(16)-C(15)-C(14)	118.9(4)	C(17)-C(16)-C(15)	114.3(3)
C(7)-Mo(1)-C(2)	148.3(1)	C(7)-Mo(1)-C(3)	35.0(1)	C(18)-C(17)-C(16)	113.7(3)	C(19)-C(17)-C(16)	110.2(4)
C(7)-Mo(1)-C(4)	58.8(2)	C(7)-Mo(1)-C(5)	58.1(2)	C(19)-C(17)-C(18)	113.0(3)	C(13)-C(18)-O(3)	109.8(3)
C(7)-Mo(1)-C(6)	34.8(1)	C(13)-Mo(1)-C(1)	78.8(2)	C(17)-C(18)-O(3)	109.3(3)	C(17)-C(18)-C(13)	111.5(3)
C(13)-Mo(1)-C(2)	113.5(2)	C(13)-Mo(1)-C(3)	107.2(2)	C(20)-C(18)-O(3)	105.8(3)	C(20)-C(18)-C(13)	108.7(3)
C(13)-Mo(1)-C(4)	142.6(1)	C(13)-Mo(1)-C(5)	149.3(1)	C(20)-C(18)-C(17)	111.6(3)	C(21)-C(20)-C(18)	121.0(4)
C(13)-Mo(1)-C(6)	114.9(2)	C(13)-Mo(1)-C(7)	94.2(2)	C(25)-C(20)-C(18)	121.9(4)	C(25)-C(20)-C(21)	117.1(4)
C(14)-Mo(1)-C(1)	113.0(2)	C(14)-Mo(1)-C(2)	106.0(2)	C(22)-C(21)-C(20)	120.8(4)	C(23)-C(22)-C(21)	121.4(4)
C(14)-Mo(1)-C(3)	116.9(2)	C(14)-Mo(1)-C(4)	145.0(1)	C(24)-C(23)-C(22)	118.7(4)	C(25)-C(24)-C(23)	120.3(5)
C(14)-Mo(1)-C(5)	121.5(2)	C(14)-Mo(1)-C(6)	89.8(2)	C(24)-C(25)-C(20)	121.7(4)	C(18)-O(3)-H(3)	108.9(26)
C(14)-Mo(1)-C(7)	87.0(2)	C(14)-Mo(1)-C(13)	36.2(1)	H(81)-C(8)-C(3)	109.7(3)	H(82)-C(8)-C(3)	109.0(3)
C(15)-Mo(1)-C(1)	113.9(2)	C(15)-Mo(1)-C(2)	71.0(2)	H(82)-C(8)-H(81)	109.5	H(83)-C(8)-C(3)	109.7(3)
C(15)-Mo(1)-C(3)	148.1(1)	C(15)-Mo(1)-C(4)	150.3(1)	H(83)-C(8)-H(81)	109.5	H(83)-C(8)-H(82)	109.5
C(15)-Mo(1)-C(5)	115.1(2)	C(15)-Mo(1)-C(6)	98.2(2)	H(92)-C(9)-C(4)	109.3(3)	H(92)-C(9)-C(4)	109.6(3)
C(15)-Mo(1)-C(7)	113.4(2)	C(15)-Mo(1)-C(13)	60.9(2)	H(92)-C(9)-H(92)	109.5	H(93)-C(9)-C(4)	109.5(3)
C(15)-Mo(1)-C(14)	35.6(1)	C(7)-C(3)-C(4)	107.8(4)	H(93)-C(9)-H(92)	109.5	H(93)-C(9)-H(92)	109.5
C(8)-C(3)-C(4)	126.3(4)	C(8)-C(3)-C(7)	125.5(4)	H(101)-C(10)-C(5)	109.6(3)	H(102)-C(10)-C(5)	109.5(3)
				H(102)-C(10)-H(101)	109.5	H(103)-C(10)-C(5)	109.3(3)
				H(103)-C(10)-H(101)	109.5	H(103)-C(10)-H(102)	109.5
				H(111)-C(11)-C(6)	109.5(3)	H(112)-C(11)-C(6)	109.3(3)
				H(112)-C(11)-H(111)	109.5	H(113)-C(11)-C(6)	109.6(3)
				H(113)-C(11)-H(111)	109.5	H(113)-C(11)-H(112)	109.5

Table A5 continued...

H(121)-C(12)-C(7)	109.3(3)	H(122)-C(12)-C(7)	109.5(3)
H(122)-C(12)-H(121)	109.5	H(123)-C(12)-C(7)	109.6(3)
H(123)-C(12)-H(121)	109.5	H(123)-C(12)-H(122)	109.5
C(14)-C(13)-H(131)	121.9(26)	C(18)-C(13)-H(131)	112.0(26)
H(141)-C(14)-C(13)	124.4(27)	C(15)-C(14)-H(141)	119.5(27)
H(151)-C(15)-C(14)	114.3(27)	C(16)-C(15)-H(151)	119.2(27)
H(161)-C(16)-C(15)	108.3(3)	H(162)-C(16)-C(15)	108.2(3)
H(162)-C(16)-H(161)	109.5	C(17)-C(16)-H(161)	108.3(2)
C(17)-C(16)-H(162)	108.1(3)	H(171)-C(17)-C(16)	107.3(2)
C(18)-C(17)-H(171)	104.1(2)	C(19)-C(17)-H(171)	108.0(3)
H(191)-C(19)-C(17)	109.4(3)	H(192)-C(19)-C(17)	109.6(3)
H(192)-C(19)-H(191)	109.5	H(193)-C(19)-C(17)	109.5(3)
H(193)-C(19)-H(191)	109.5	H(193)-C(19)-H(192)	109.5
H(211)-C(21)-C(20)	119.6(3)	C(22)-C(21)-H(211)	119.6(3)
H(221)-C(22)-C(21)	119.3(3)	C(23)-C(22)-H(221)	119.3(3)
H(231)-C(23)-C(22)	120.7(3)	C(24)-C(23)-H(231)	120.5(3)
H(241)-C(24)-C(23)	119.8(3)	C(25)-C(24)-H(241)	119.9(3)
H(251)-C(25)-C(20)	119.3(3)	H(251)-C(25)-C(24)	119.1(3)

TABLE A6

Selected non-bonded distances (Å) for complex (107)

Intramolecular:

O(1)-Mo(1)	3.101	O(2)-Mo(1)	3.096
C(8)-Mo(1)	3.438	C(9)-Mo(1)	3.423
C(10)-Mo(1)	3.464	C(11)-Mo(1)	3.489
C(12)-Mo(1)	3.489	H(131)-Mo(1)	2.799
H(141)-Mo(1)	2.649	H(151)-Mo(1)	2.810
C(16)-Mo(1)	3.382	C(17)-Mo(1)	3.554
H(171)-Mo(1)	3.262	C(18)-Mo(1)	3.423
H(3)-O(1)	2.265	H(162)-O(2)	2.699
C(1)-O(3)	3.036	C(13)-O(3)	2.421
H(131)-O(3)	2.553	C(17)-O(3)	2.437
H(171)-O(3)	2.454	C(19)-O(3)	3.086
C(20)-O(3)	2.371	C(21)-O(3)	2.657
H(211)-O(3)	2.279	C(1)-H(3)	2.447
C(13)-H(3)	2.772	C(17)-H(3)	2.452
H(171)-H(3)	2.094	C(18)-H(3)	1.966
C(2)-C(1)	2.551	C(3)-C(1)	3.042
C(4)-C(1)	3.076	C(13)-C(1)	2.743
H(171)-C(1)	2.706	C(18)-C(1)	3.166
C(5)-C(2)	3.079	C(15)-C(2)	2.530
C(16)-C(2)	2.952	H(162)-C(2)	2.699
C(5)-C(3)	2.300	C(6)-C(3)	2.295
H(81)-C(3)	2.031	H(82)-C(3)	2.024

Table A6 continued...

H(83)-C(3)	2.031	C(9)-C(3)	2.605	C(17)-C(13)	2.546	C(20)-C(13)	2.489
C(12)-C(3)	2.587	C(6)-C(4)	2.285	C(25)-C(13)	3.014	C(14)-H(131)	2.089
C(7)-C(4)	2.306	C(8)-C(4)	2.611	C(18)-H(131)	2.084	C(20)-H(131)	2.778
H(81)-C(4)	2.682	H(92)-C(4)	2.038	H(151)-C(14)	2.001	C(16)-C(14)	2.511
H(92)-C(4)	2.042	H(93)-C(4)	2.040	C(17)-C(14)	2.958	C(18)-C(14)	2.535
C(10)-C(4)	2.598	C(7)-C(5)	2.303	C(25)-C(14)	3.154	H(251)-C(14)	2.525
C(9)-C(5)	2.607	H(92)-C(5)	2.681	C(15)-H(141)	2.055	H(151)-H(141)	2.275
H(101)-C(5)	2.043	H(102)-C(5)	2.042	H(161)-C(15)	2.028	H(162)-C(15)	2.027
H(103)-C(5)	2.040	C(11)-C(5)	2.595	C(17)-C(15)	2.561	C(18)-C(15)	2.932
C(10)-C(6)	2.602	H(101)-C(6)	2.674	C(16)-H(151)	2.149	H(171)-C(16)	2.041
H(111)-C(6)	2.047	H(112)-C(6)	2.045	C(18)-C(16)	2.590	C(19)-C(16)	2.513
H(113)-C(6)	2.049	C(12)-C(6)	2.605	H(192)-C(16)	2.694	H(193)-C(16)	2.691
H(121)-C(6)	2.672	C(8)-C(7)	2.595	H(162)-H(161)	1.568	C(17)-H(161)	2.054
C(11)-C(7)	2.624	H(111)-C(7)	2.691	C(19)-H(161)	2.578	C(17)-H(162)	2.051
H(121)-C(7)	2.019	H(122)-C(7)	2.022	H(171)-H(162)	2.231	C(19)-H(162)	2.778
H(123)-C(7)	2.022	C(14)-C(7)	3.153	H(191)-C(17)	2.055	H(192)-C(17)	2.057
C(9)-C(8)	3.177	C(12)-C(8)	3.156	H(193)-C(17)	2.056	C(20)-C(17)	2.559
H(82)-H(81)	1.568	H(83)-H(81)	1.568	C(18)-H(171)	2.017	C(19)-H(171)	2.039
C(9)-H(81)	2.758	H(83)-H(82)	1.568	H(191)-H(171)	2.345	H(192)-H(171)	2.313
C(10)-C(9)	3.184	H(92)-H(92)	1.568	C(19)-C(18)	2.569	H(191)-C(18)	2.696
H(93)-H(92)	1.568	C(10)-H(92)	2.769	C(21)-C(18)	2.540	H(211)-C(18)	2.690
H(93)-H(92)	1.568	C(11)-C(10)	3.167	C(25)-C(18)	2.568	H(251)-C(18)	2.721
H(102)-H(101)	1.568	H(103)-H(101)	1.568	C(20)-C(19)	2.922	H(192)-H(191)	1.568
C(11)-H(101)	2.741	H(103)-H(102)	1.568	H(193)-H(191)	1.568	H(193)-H(192)	1.568
H(112)-H(111)	1.568	H(113)-H(111)	1.568	C(20)-H(193)	2.667	H(211)-C(20)	2.032
H(121)-H(111)	2.146	H(113)-H(112)	1.568	C(22)-C(20)	2.406	C(23)-C(20)	2.802
H(122)-H(121)	1.568	H(123)-H(121)	1.568	C(24)-C(20)	2.417	H(251)-C(20)	2.046
H(123)-H(122)	1.568	H(141)-C(13)	2.114	H(221)-C(21)	2.039	C(23)-C(21)	2.395
C(15)-C(13)	2.391	C(16)-C(13)	2.896	C(24)-C(21)	2.745	C(25)-C(21)	2.368

Table A6 continued...

C(22)-H(211)	2.042	H(221)-H(211)	2.333
H(231)-C(22)	2.023	C(24)-C(22)	2.356
C(25)-C(22)	2.726	C(23)-H(221)	2.009
H(231)-H(221)	2.317	H(241)-C(23)	2.038
C(25)-C(23)	2.387	C(24)-H(231)	2.045
H(241)-H(231)	2.348	H(251)-C(24)	2.019
C(25)-H(241)	2.027	H(251)-H(241)	2.315

Intermolecular:

H(3)-O(2a)	2.533	H(101)-O(2b)	2.500
H(193)-H(103c)	2.347		

Key to symmetry operations relating
designated atoms to reference atoms
at (x,y,z):

(a) -x,1.0-y,1.0-z
(b) -x,-y,1.0-z
(c) -1.0+x,1.0+y,z

Note on *exo-anti*-[Mo(η^3-$CH_2CHCHCHO$)$(CO)_2$(η^5-C_5Me_5)] (126c)

A crystal of approximate dimensions 0.2 x 0.2 x 0.2 mm was used for data collection.

Crystal data: $C_{16}H_{20}O_3Mo$, M = 356.3 monoclinic, a = 10.919(2), b = 10.578(2), c = 13.724(2)Å, β = 90.18(2)°, U = 1585.1 Å^3, space group $P2_1/n$, Z = 4, D_c = 1.49 gcm^{-3}, μ(Mo-K_α) = 1.60 cm^{-1}, F(000) = 728. Data were measured at room temperature on a CAD4 automatic four-circle diffractometer in the range $2 \leq \theta \leq 22^\circ$. 2194 reflections were collected of which 1584 were unique with $I \geq 2\sigma(I)$. Data were corrected for Lorentz and polarization but not for absorption. The structure was solved by Patterson methods and refined using the SHELX[165,166] suite of programs. However a 'Rolls-Royce' refinement was hampered by disorder of both the allyl methoxy group and the carbonyls in the ratio 70:30. The minor structure containing the 30% occupancy atoms (O1', O2', O3', C11', C12', and C16') is effectively the mirror image of the major structure and it is the latter which is illustrated in the ORTEP plot. In the final least squares cycles all atoms except for those with primed labels were allowed to vibrate anisotropically. Hydrogen atoms were included at calculated positions on the pentamethyl cp moiety. Disorder precluded the location of the remaining hydrogens.

Final residuals after 12 cycles of least squares were R = 0.0499, R_w = 0.0578, for a weighting scheme of $w = 4.7460/[\sigma^2(F) + 0.000316(F)^2]$. Max. final shift/esd was 0.000. The max. and min. residual densities were 0.25 and -0.17 eÅ^{-3} respectively. Final fractional atomic coordinates and isotropic thermal parameters, bond distances and angles are given in Tables B1-B7. Tables of anisotropic temperature factors are available as supplementary data. The asymmetric unit is shown in Fig. 113 , along with the labelling scheme used.

TABLE B1

Fractional atomic co-ordinates ($x10^4$) and equivalent isotropic temperature factors ($Å^2$ $x10^3$) for complex (126c).

	x	y	z
Mo(1)	-56(1)	1486(1)	2564
O(1)	-2452(11)	2000(12)	1466(9)
O(2)	-1912(11)	1227(13)	4251(8)
O(3)	-1799(15)	-668(16)	631(9)
C(1)	898(7)	3136(8)	3411(6)
C(2)	284(8)	3651(8)	2563(6)
C(3)	852(8)	3145(8)	1727(6)
C(4)	1841(7)	2335(8)	2050(6)
C(5)	1853(8)	2340(9)	3070(6)
C(6)	652(10)	3467(11)	4468(7)
C(7)	-697(9)	4605(10)	2574(8)
C(8)	600(10)	3469(10)	699(7)
C(9)	2804(11)	1774(11)	1430(10)
C(10)	2765(10)	1652(11)	3729(8)
C(11)	-1566(14)	1746(14)	1880(11)
C(12)	-1215(12)	1265(15)	3649(11)
C(13)	211(12)	-413(12)	3357(10)
C(14)	785(11)	-372(11)	2446(13)
C(15)	132(12)	-220(13)	1541(11)
C(16)	-1183(16)	-754(16)	1394(13)

TABLE B2

Anisotropic temperature factors ($Å$ $x10^3$) for complex (126c).

	U_{11}	U_{22}	U_{33}	U_{23}	U_{13}	U_{12}
Mo(1)	46(1)	47(1)	52(1)	-3	0	0
O(1)	78(8)	127(10)	115(9)	35(7)	-56(7)	-33(7)
O(2)	84(7)	171(12)	85(7)	-30(7)	28(6)	-33(8)
O(3)	192(14)	235(18)	100(8)	-104(10)	37(9)	-132(13)
C(1)	47(5)	59(6)	77(6)	-16(5)	-6(4)	1(4)
C(2)	45(5)	42(6)	90(7)	0(5)	-6(5)	-1(4)
C(3)	62(6)	52(5)	67(5)	6(4)	-8(4)	-13(5)
C(4)	46(5)	48(6)	84(6)	-4(5)	9(5)	-2(4)
C(5)	50(5)	62(6)	78(6)	-9(5)	-24(4)	-6(5)
C(6)	85(7)	114(9)	75(6)	-43(6)	-7(5)	-7(6)
C(7)	59(6)	65(7)	136(9)	-4(6)	-5(5)	20(6)
C(8)	92(8)	93(9)	84(7)	29(6)	-17(6)	-25(6)
C(9)	82(8)	80(8)	145(10)	-35(7)	42(7)	1(6)
C(10)	74(7)	114(10)	110(8)	4(7)	-61(6)	20(7)
C(11)	67(10)	52(9)	92(10)	16(8)	-20(9)	-22(7)
C(12)	55(8)	89(11)	60(8)	-15(8)	3(8)	-13(8)
C(13)	98(9)	76(8)	126(9)	19(7)	-24(8)	-4(7)
C(14)	81(8)	45(7)	211(15)	-10(9)	-7(9)	21(6)
C(15)	91(9)	99(10)	166(12)	-68(9)	54(9)	-40(8)
C(16)	98(13)	107(14)	98(11)	-49(10)	14(9)	-42(11)

The temperature factor exponent takes the form:

$-2\ (U_{11}.h.a^* + \ldots + 2U_{12}.h.k.a^*.b^*)$

TABLE B4

Hydrogen fractional atomic co-ordinates ($x10^4$) and isotropic temperature factors ($Å^2$ $x10^3$) for complex (126c).

	x	y	z	U
H(61)	-43(10)	4020(11)	4504(7)	179(16)
H(62)	1356(10)	3883(11)	4741(7)	179(16)
H(63)	488(10)	2709(11)	4829(7)	179(16)
H(71)	-922(9)	4784(10)	3236(8)	179(16)
H(72)	-1398(9)	4289(10)	2227(8)	179(16)
H(73)	-413(9)	5366(10)	2268(8)	179(16)
H(81)	-99(10)	4018(10)	664(7)	179(16)
H(82)	436(10)	2710(10)	338(7)	179(16)
H(83)	1299(10)	3890(10)	427(7)	179(16)
H(91)	2592(11)	1890(11)	756(10)	179(16)
H(92)	2873(11)	888(11)	1568(10)	179(16)
H(93)	3573(11)	2182(11)	1562(10)	179(16)
H(101)	3323(10)	1172(11)	3336(8)	179(16)
H(102)	2331(10)	1093(11)	4157(8)	179(16)
H(103)	3215(10)	2259(11)	4107(8)	179(16)

TABLE B3

Fractional atomic co-ordinates ($x10^4$) for complex (126c).

	x	y	z	U
O(1′)	-1808(26)	1022(26)	784(19)	103(9)
O(2′)	-2536(27)	2081(28)	3522(21)	105(9)
O(3′)	-1801(33)	-662(32)	4361(24)	153(13)
C(11′)	-1120(36)	1141(41)	1378(30)	87(11)
C(12′)	-1576(42)	1684(42)	3172(32)	87(13)
C(16′)	-1116(46)	-770(70)	3638(54)	210(30)

TABLE B5

Bond lengths (Å) for complex (126c).

C(1)-Mo(1)	2.339(10)	C(2)-Mo(1)	2.319(11)	C(9)-C(4)	1.479(13)	Mo(1)-C(5)	2.373(10)
C(3)-Mo(1)	2.322(10)	C(4)-Mo(1)	2.366(10)	C(1)-C(5)	1.420(13)	C(4)-C(5)	1.401(12)
C(5)-Mo(1)	2.373(10)	C(11)-Mo(1)	1.915(17)	C(10)-C(5)	1.527(14)	C(1)-C(6)	1.518(14)
C(11')-Mo(1)	2.030(44)	C(12)-Mo(1)	1.971(16)	C(2)-C(7)	1.472(13)	C(3)-C(8)	1.476(12)
C(12')-Mo(1)	1.872(45)	C(13)-Mo(1)	2.303(14)	C(4)-C(9)	1.479(13)	C(5)-C(10)	1.527(14)
C(14)-Mo(1)	2.176(13)	C(15)-Mo(1)	2.297(13)	Mo(1)-C(11)	1.915(17)	O(1)-C(11)	1.153(17)
O(1')-O(1)	1.563(31)	C(11)-O(1)	1.153(17)	O(1')-C(11)	1.708(32)	C(11')-C(11)	1.060(40)
C(11')-O(1)	1.720(45)	O(1)-O(1')	1.563(31)	C(12')-C(11)	1.775(47)	Mo(1)-C(11')	2.030(44)
O(3)-O(1')	1.800(32)	C(11)-O(1')	1.707(32)	O(1)-C(11')	1.720(45)	O(1')-C(11')	1.114(41)
C(11')-O(1')	1.114(41)	C(16)-O(1')	2.166(36)	C(11)-C(11')	1.060(40)	C(15)-C(11')	1.997(45)
O(2')-O(2)	1.509(32)	O(3')-O(2)	2.007(37)	C(16)-C(11')	2.006(46)	Mo(1)-C(12)	1.971(16)
C(12)-O(2)	1.126(15)	C(12')-O(2)	1.601(45)	O(2)-C(12)	1.126(15)	O(2')-C(12)	1.690(34)
O(2)-O(2')	1.509(32)	C(12)-O(2')	1.690(34)	C(12')-C(12)	0.882(41)	C(16')-C(12)	2.155(76)
C(12')-O(2')	1.228(46)	O(1')-O(3)	1.800(32)	Mo(1)-C(12')	1.872(45)	O(2)-C(12')	1.601(45)
C(16)-O(3)	1.246(23)	O(2)-O(3')	2.007(37)	O(2')-C(12')	1.228(46)	C(11)-C(12')	1.775(47)
C(16')-O(3')	1.250(61)	Mo(1)-C(1)	2.339(10)	C(12)-C(12')	0.882(41)	Mo(1)-C(13)	2.303(14)
C(2)-C(1)	1.448(12)	C(4)-C(1)	2.298(13)	C(14)-C(13)	1.401(18)	C(16')-C(13)	1.547(45)
C(5)-C(1)	1.420(13)	C(6)-C(1)	1.518(14)	Mo(1)-C(14)	2.176(13)	C(13)-C(14)	1.401(18)
Mo(1)-C(2)	2.319(11)	C(1)-C(2)	1.448(12)	C(15)-C(14)	1.439(20)	Mo(1)-C(15)	2.297(13)
C(3)-C(2)	1.412(12)	C(7)-C(2)	1.472(13)	C(11')-C(15)	1.997(45)	C(14)-C(15)	1.439(20)
Mo(1)-C(3)	2.322(10)	C(2)-C(3)	1.412(12)	C(16)-C(15)	1.555(21)	O(1')-C(16)	2.166(36)
C(4)-C(3)	1.447(13)	C(8)-C(3)	1.476(12)	O(3)-C(16)	1.246(23)	C(11')-C(16)	2.006(46)
Mo(1)-C(4)	2.366(10)	C(1)-C(4)	2.298(13)	C(15)-C(16)	1.555(21)	O(3')-C(16')	1.250(61)
C(3)-C(4)	1.447(13)	C(5)-C(4)	1.401(12)	C(12)-C(16')	2.155(76)	C(13)-C(16')	1.547(45)

TABLE B6

Bond angles (deg.) for complex (126c).

C(2)-Mo(1)-C(1)	36.2(3)	C(3)-Mo(1)-C(1)	59.5(4)
C(3)-Mo(1)-C(2)	35.4(3)	C(4)-Mo(1)-C(1)	58.5(4)
C(4)-Mo(1)-C(2)	59.0(4)	C(4)-Mo(1)-C(3)	36.0(3)
C(5)-Mo(1)-C(1)	35.1(3)	C(5)-Mo(1)-C(2)	59.0(4)
C(5)-Mo(1)-C(3)	58.8(4)	C(5)-Mo(1)-C(4)	34.4(3)
C(11)-Mo(1)-C(1)	121.2(6)	C(11)-Mo(1)-C(2)	89.7(6)
C(11)-Mo(1)-C(3)	91.0(5)	C(11)-Mo(1)-C(4)	123.5(6)
C(11)-Mo(1)-C(5)	147.5(5)	C(11')-Mo(1)-C(1)	141.8(12)
C(11')-Mo(1)-C(2)	105.6(13)	C(11')-Mo(1)-C(3)	89.0(12)
C(11')-Mo(1)-C(4)	109.2(12)	C(11')-Mo(1)-C(5)	143.4(11)
C(11')-Mo(1)-C(11)	31.0(11)	C(12)-Mo(1)-C(1)	90.0(5)
C(12)-Mo(1)-C(2)	102.7(6)	C(12)-Mo(1)-C(3)	137.7(5)
C(12)-Mo(1)-C(4)	146.6(4)	C(12)-Mo(1)-C(5)	112.9(5)
C(12)-Mo(1)-C(11)	80.4(7)	C(12)-Mo(1)-C(11')	102.5(13)
C(12')-Mo(1)-C(1)	95.1(14)	C(12')-Mo(1)-C(2)	91.8(15)
C(12')-Mo(1)-C(3)	121.1(15)	C(12')-Mo(1)-C(4)	150.3(14)
C(12')-Mo(1)-C(5)	127.3(15)	C(12')-Mo(1)-C(11)	55.9(16)
C(12')-Mo(1)-C(11')	82.6(19)	C(12')-Mo(1)-C(12)	26.4(12)
C(13)-Mo(1)-C(1)	111.1(5)	C(13)-Mo(1)-C(2)	147.3(4)
C(13)-Mo(1)-C(3)	147.2(4)	C(13)-Mo(1)-C(4)	111.3(5)
C(13)-Mo(1)-C(5)	94.8(5)	C(13)-Mo(1)-C(11)	117.6(6)
C(13)-Mo(1)-C(11')	107.0(13)	C(13)-Mo(1)-C(12)	67.6(7)
C(13)-Mo(1)-C(12')	89.9(15)	C(14)-Mo(1)-C(1)	121.6(5)
C(14)-Mo(1)-C(2)	145.6(4)	C(14)-Mo(1)-C(3)	117.7(6)
C(14)-Mo(1)-C(4)	87.2(5)	C(14)-Mo(1)-C(5)	89.8(5)
C(14)-Mo(1)-C(11)	117.1(7)	C(14)-Mo(1)-C(11')	91.0(14)
C(14)-Mo(1)-C(12)	102.7(7)	C(14)-Mo(1)-C(12')	120.6(15)
C(14)-Mo(1)-C(13)	36.3(5)	C(15)-Mo(1)-C(1)	148.2(4)
C(15)-Mo(1)-C(2)	139.6(4)	C(15)-Mo(1)-C(3)	104.6(5)
C(15)-Mo(1)-C(4)	92.1(4)	C(15)-Mo(1)-C(5)	113.5(5)
C(15)-Mo(1)-C(11)	83.7(7)	C(15)-Mo(1)-C(11')	54.6(13)
C(15)-Mo(1)-C(12)	115.3(6)	C(15)-Mo(1)-C(12')	116.2(15)
C(15)-Mo(1)-C(13)	65.9(7)	C(15)-Mo(1)-C(14)	37.4(5)
C(11)-O(1)-O(1')	76.2(16)	C(11')-O(1)-O(1')	39.3(15)
C(11')-O(1)-C(11)	37.1(15)	O(3)-O(1')-O(1)	136.8(18)
C(11)-O(1')-O(1)	41.0(9)	C(11)-O(1')-O(3)	123.2(18)
C(11')-O(1')-O(1)	77.9(29)	C(11')-O(1')-O(3)	101.2(32)
C(11')-O(1')-C(11)	37.1(23)	C(16)-O(1')-O(1)	119.0(16)
C(16)-O(1')-O(3)	35.1(8)	C(16)-O(1')-C(11)	90.1(15)
C(16)-O(1')-C(11')	66.7(28)	O(3')-O(2)-O(2')	132.3(16)
C(12)-O(2)-O(2')	78.3(16)	C(12)-O(2)-O(3')	92.8(16)
C(12')-O(2)-O(2')	46.4(17)	C(12')-O(2)-O(3')	110.8(21)
C(12')-O(2)-C(12)	32.1(17)	C(12)-O(2')-O(2)	40.7(9)
C(12')-O(2')-O(2)	70.8(26)	C(12')-O(2')-C(12)	30.3(21)
C(16)-O(3)-O(1')	88.7(14)	C(16')-O(3')-O(2)	93.9(43)
C(2)-C(1)-Mo(1)	71.1(6)	C(4)-C(1)-Mo(1)	61.4(4)
C(4)-C(1)-C(2)	72.1(6)	C(5)-C(1)-Mo(1)	73.8(6)
C(5)-C(1)-C(2)	107.3(8)	C(5)-C(1)-C(4)	35.2(4)
C(6)-C(1)-Mo(1)	124.6(7)	C(6)-C(1)-C(2)	126.8(9)
C(6)-C(1)-C(4)	160.7(7)	C(6)-C(1)-C(5)	125.7(9)
C(1)-C(2)-Mo(1)	72.6(6)	C(3)-C(2)-Mo(1)	72.4(6)
C(3)-C(2)-C(1)	107.9(8)	C(7)-C(2)-Mo(1)	124.1(8)
C(7)-C(2)-C(1)	125.8(9)	C(7)-C(2)-C(3)	126.1(9)

Table B6 continued...

C(2)-C(3)-Mo(1)	72.2(6)	C(4)-C(3)-Mo(1)	73.7(6)	O(2')-C(12')-Mo(1)	166.3(37)	O(2')-C(12')-O(2)	62.9(24)
C(4)-C(3)-C(2)	107.7(8)	C(8)-C(3)-Mo(1)	124.8(7)	C(11)-C(12')-Mo(1)	63.3(16)	C(11)-C(12')-O(2)	159.6(30)
C(8)-C(3)-C(2)	127.5(10)	C(8)-C(3)-C(4)	124.5(10)	C(11)-C(12')-O(2')	112.7(38)	C(12)-C(12')-Mo(1)	83.1(36)
C(1)-C(4)-Mo(1)	60.2(4)	C(3)-C(4)-Mo(1)	70.3(5)	C(12)-C(12')-O(2)	42.8(22)	C(12)-C(12')-O(2')	105.2(43)
C(3)-C(4)-C(1)	72.2(6)	C(5)-C(4)-Mo(1)	73.1(6)	C(12)-C(12')-C(11)	139.1(44)	C(14)-C(13)-Mo(1)	66.9(8)
C(5)-C(4)-C(1)	35.7(5)	C(5)-C(4)-C(3)	108.0(8)	C(16')-C(13)-Mo(1)	102.3(29)	C(16')-C(13)-C(14)	130.7(30)
C(9)-C(4)-Mo(1)	130.1(7)	C(9)-C(4)-C(1)	159.5(8)	C(13)-C(14)-Mo(1)	76.8(8)	C(15)-C(14)-Mo(1)	75.8(8)
C(9)-C(4)-C(3)	126.3(10)	C(9)-C(4)-C(5)	124.9(10)	C(15)-C(14)-C(13)	123.5(12)	C(11')-C(15)-Mo(1)	55.9(14)
C(1)-C(5)-Mo(1)	71.1(6)	C(4)-C(5)-Mo(1)	72.5(6)	C(14)-C(15)-Mo(1)	66.7(7)	C(14)-C(15)-C(11')	120.9(16)
C(4)-C(5)-C(1)	109.1(9)	C(10)-C(5)-Mo(1)	124.2(8)	C(16)-C(15)-Mo(1)	106.3(9)	C(16)-C(15)-C(11')	67.4(15)
C(10)-C(5)-C(1)	124.5(10)	C(10)-C(5)-C(4)	126.4(10)	C(16)-C(15)-C(14)	121.7(14)	O(3)-C(16)-O(1')	56.2(14)
O(1)-C(11)-Mo(1)	174.7(13)	O(1')-C(11)-Mo(1)	119.9(16)	C(11')-C(16)-O(1')	30.7(12)	C(11')-C(16)-O(3)	86.4(19)
O(1')-C(11)-O(1)	62.8(14)	C(11')-C(11)-Mo(1)	80.5(26)	C(15)-C(16)-O(1')	91.4(13)	C(15)-C(16)-O(3)	125.4(16)
C(11')-C(11)-O(1)	101.9(28)	C(11')-C(11)-O(1')	39.4(23)	C(15)-C(16)-C(11')	66.9(15)	C(12)-C(16')-O(3')	82.7(44)
C(12')-C(11)-Mo(1)	60.8(17)	C(12')-C(11)-O(1)	119.6(22)	C(13)-C(16')-O(3')	137.6(60)	C(13)-C(16')-C(12)	78.7(29)
C(12')-C(11)-O(1')	149.6(19)	C(12')-C(11)-C(11')	129.2(31)				
O(1)-C(11')-Mo(1)	109.3(24)	O(1')-C(11')-Mo(1)	171.9(39)				
O(1')-C(11')-O(1)	62.8(26)	C(11)-C(11')-Mo(1)	68.5(25)				
C(11)-C(11')-O(1)	41.0(18)	C(11)-C(11')-O(1')	103.5(40)				
C(15)-C(11')-Mo(1)	69.5(14)	C(15)-C(11')-O(1)	162.1(24)				
C(15)-C(11')-O(1')	117.4(38)	C(15)-C(11')-C(11)	132.7(33)				
C(16)-C(11')-Mo(1)	101.0(20)	C(16)-C(11')-O(1)	119.9(23)				
C(16)-C(11')-O(1')	82.7(32)	C(16)-C(11')-C(11)	125.5(31)				
C(16)-C(11')-C(15)	45.7(11)	O(2)-C(12)-Mo(1)	174.7(16)				
O(2')-C(12)-Mo(1)	114.3(16)	O(2')-C(12)-O(2)	61.0(14)				
C(12')-C(12)-Mo(1)	70.5(32)	C(12')-C(12)-O(2)	105.1(35)				
C(12')-C(12)-O(2')	44.5(30)	C(16')-C(12)-Mo(1)	94.7(18)				
C(16')-C(12)-O(2)	90.2(21)	C(16')-C(12)-O(2')	123.5(19)				
C(16')-C(12)-C(12')	121.2(39)	O(2)-C(12')-Mo(1)	125.8(31)				

TABLE B7

Selected non-bonded distances (Å) for complex (126c).

Intramolecular:

O(1)-Mo(1)	3.065	O(1')-Mo(1)	3.137
O(2)-Mo(1)	3.094	O(2')-Mo(1)	3.079
O(3)-Mo(1)	3.979	O(3')-Mo(1)	3.861
C(6)-Mo(1)	3.436		

Intermolecular:

O(3')-O(1a)	2.840

Key to symmetry operations relating
designated atoms to reference atoms
at (x,y,z):

(a) -1.0+

Note on *exo-anti*-[Mo(η^3-$CH_2CHCHCH_2OMe$)$(CO)_2$(η^5-C_5H_5)] (143c)

A crystal of approximate dimensions 0.4 x 0.4 x 0.3 mm was used for data collection.

Crystal data: $C_{12}H_{14}O_3Mo$, M = 302.2 monoclinic, a = 8.338(2), b = 7.511(2), c = 19.661(6)Å, β = 98.34(2)°, U = 1218.3 Å^3, space group $P2_1/c$, Z = 4, D_c = 1.65 gcm^{-3}, μ(Mo-K_α) = 10.4 cm^{-1}, F(000) = 608. Data were measured at 150° K on a CAD4 automatic four-circle diffractometer in the range $2\leq\theta\leq24^\circ$. 2240 reflections were collected of which 1715 were unique with $I\geq2\sigma(I)$. Data were corrected for Lorentz and polarization and also for absorption.[167] (Max. and Min. absorption corrections; 1.187, 0.714 respectively). The structure was solved by Patterson methods and refined using the SHELX[165,166] suite of programs. In the final least squares cycles all atoms were allowed to vibrate anisotropically. Hydrogen atoms were included at calculated positions except for those protons attached to C8, C9 and C10. These hydrogens (H81, H82, H91, H101) were located in an advanced Difference Fourier and refined at a distance of 0.98 Å from the parent atoms.

Final residuals after 10 cycles of least squares were R = 0.0336, R_w = 0.0408, for a weighting scheme of $w = 3.1608/[\sigma^2(F) + 0.000449(F)^2]$. Max. final shift/esd was 0.000. The max. and min. residual densities were 0.39 and -0.32 eÅ^{-3} respectively. Final fractional atomic coordinates and isotropic thermal parameters, bond distances and angles are given in Tables C1-C7. Tables of anisotropic temperature factors are available as supplementary data. The asymmetric unit is shown in Fig. 124, along with the labelling scheme used.

TABLE C1

Fractional atomic co-ordinates ($x10^4$) and equivalent isotropic temperature factors ($Å^2$ $x10^3$) for complex (143c)

	x	y	z	U
Mo(1)	2140	176(1)	1296	27
O(1)	3114(4)	-1064(5)	-97(2)	56(1)
O(2)	614(5)	3293(5)	373(2)	74(1)
O(3)	5698(5)	4716(5)	1410(2)	62(1)
C(1)	-322(8)	-122(8)	1730(4)	63(3)
C(2)	844(8)	-429(9)	2264(3)	61(2)
C(3)	1739(6)	-1927(10)	2133(4)	84(3)
C(4)	964(7)	-2543(7)	1459(3)	60(2)
C(5)	-260(6)	-1348(8)	1259(3)	52(2)
C(6)	2775(5)	-560(7)	426(3)	41(2)
C(7)	1204(6)	2160(7)	717(3)	45(2)
C(8)	4941(6)	-157(6)	1513(3)	42(2)
C(9)	4369(6)	1138(7)	1943(2)	43(2)
C(10)	3660(5)	2718(6)	1654(2)	39(1)
C(11)	4360(6)	3676(6)	1105(2)	41(2)
C(12)	6485(8)	5540(9)	907(3)	66(2)

TABLE C2

Fractional atomic co-ordinates ($x10^4$) for complex (143c)

	x	y	z
Mo(1)	2140	176(1)	1296
O(1)	3114(4)	-1064(5)	-97(2)
O(2)	614(5)	3293(5)	373(2)
O(3)	5698(5)	4716(5)	1410(2)
C(1)	-322(8)	-122(8)	1730(4)
C(2)	844(8)	-429(9)	2264(3)
C(3)	1739(6)	-1927(10)	2133(4)
C(4)	964(7)	-2543(7)	1459(3)
C(5)	-260(6)	-1348(8)	1259(3)
C(6)	2775(5)	-560(7)	426(3)
C(7)	1204(6)	2160(7)	717(3)
C(8)	4941(6)	-157(6)	1513(3)
C(9)	4369(6)	1138(7)	1943(2)
C(10)	3660(5)	2718(6)	1654(2)
C(11)	4360(6)	3676(6)	1105(2)
C(12)	6485(8)	5540(9)	907(3)

TABLE C3

Anisotropic temperature factors (Å $x10^3$) for complex (143c)

	U_{11}	U_{22}	U_{33}	U_{23}	U_{13}	U_{12}
Mo(1)	27	28	27	1	4	-8
O(1)	55(2)	79(3)	37(2)	-16(2)	17(2)	-11(2)
O(2)	81(3)	46(2)	82(3)	15(2)	-32(2)	-2(2)
O(3)	80(3)	70(3)	36(2)	-4(2)	5(2)	-49(2)
C(1)	49(4)	74(5)	72(4)	-12(3)	26(3)	-10(3)
C(2)	65(4)	80(4)	43(3)	-8(3)	25(3)	-22(3)
C(3)	29(3)	116(6)	101(5)	92(5)	-6(3)	-17(3)
C(4)	75(4)	28(3)	89(4)	-3(3)	53(3)	-15(3)
C(5)	38(3)	57(3)	62(3)	7(3)	6(2)	-26(2)
C(6)	32(2)	44(3)	44(3)	4(2)	2(2)	-11(2)
C(7)	43(3)	38(3)	50(3)	-4(2)	-7(2)	-10(2)
C(8)	36(3)	49(3)	40(3)	6(2)	4(2)	-1(2)
C(9)	38(2)	50(3)	37(2)	8(2)	-6(2)	-20(2)
C(10)	43(3)	41(3)	32(2)	-9(2)	7(2)	-18(2)
C(11)	52(3)	39(3)	32(2)	-3(2)	5(2)	-19(2)
C(12)	68(4)	79(4)	50(3)	3(3)	7(3)	-53(3)

The temperature factor exponent takes the form:

$-2\ (U\ .h\ .a^*\ +\ \ldots\ \ +2U\ .h.k.a^*.b^*)$

TABLE C4

Hydrogen fractional atomic co-ordinates ($x10^4$) and isotropic temperature factors (Å^2 $x10^3$) for complex (143c)

	x	y	z	U
H(11)	-1081(8)	845(8)	1697(4)	82(6)
H(21)	1032(8)	278(9)	2674(3)	82(6)
H(31)	2654(6)	-2437(10)	2420(4)	82(6)
H(41)	1250(7)	-3565(7)	1209(3)	82(6)
H(51)	-977(6)	-1403(8)	831(3)	82(6)
H(81)	5513(63)	205(59)	1132(22)	49(16)
H(82)	5531(59)	-1168(56)	1762(26)	69(17)
H(91)	4287(72)	887(85)	2424(16)	82(6)
H(101)	3087(66)	3247(77)	2035(23)	82(6)
H(111)	3553(6)	4439(6)	858(2)	82(6)
H(112)	4719(6)	2831(6)	793(2)	82(6)
H(121)	7382(8)	6232(9)	1127(3)	82(6)
H(122)	5736(8)	6305(9)	628(3)	82(6)
H(123)	6875(8)	4646(9)	623(3)	82(6)

TABLE C5

Bond lengths (Å) for complex (143c)

C(1)-Mo(1)	2.345(8)	C(2)-Mo(1)	2.365(7)	Mo(1)-C(10)	2.342(6)	C(9)-C(10)	1.409(8)
C(3)-Mo(1)	2.340(7)	C(4)-Mo(1)	2.308(7)	C(11)-C(10)	1.486(7)	O(3)-C(11)	1.421(6)
C(5)-Mo(1)	2.298(6)	C(6)-Mo(1)	1.942(7)	C(10)-C(11)	1.486(7)	O(3)-C(12)	1.408(8)
C(7)-Mo(1)	1.967(7)	C(8)-Mo(1)	2.325(7)	H(11)-C(1)	0.960	C(1)-H(11)	0.960
C(9)-Mo(1)	2.216(6)	C(10)-Mo(1)	2.342(6)	H(21)-C(2)	0.960	C(2)-H(21)	0.960
C(6)-O(1)	1.168(7)	C(7)-O(2)	1.152(7)	H(31)-C(3)	0.960	C(3)-H(31)	0.960
C(11)-O(3)	1.421(6)	C(12)-O(3)	1.408(8)	H(41)-C(4)	0.960	C(4)-H(41)	0.960
Mo(1)-C(1)	2.345(8)	C(2)-C(1)	1.343(11)	H(51)-C(5)	0.960	C(5)-H(51)	0.960
C(3)-C(1)	2.241(11)	C(4)-C(1)	2.214(10)	H(81)-C(8)	0.984(28)	H(82)-C(8)	0.994(28)
C(5)-C(1)	1.311(9)	Mo(1)-C(2)	2.365(7)	C(8)-H(81)	0.984(28)	C(8)-H(82)	0.994(28)
C(1)-C(2)	1.343(11)	C(3)-C(2)	1.395(10)	H(91)-C(9)	0.976(28)	C(9)-H(91)	0.976(28)
C(4)-C(2)	2.254(10)	C(5)-C(2)	2.167(10)	H(101)-C(10)	1.025(28)	C(10)-H(101)	1.025(28)
Mo(1)-C(3)	2.340(7)	C(1)-C(3)	2.241(11)	H(111)-C(11)	0.960	H(112)-C(11)	0.960
C(2)-C(3)	1.395(10)	C(4)-C(3)	1.463(10)	C(11)-H(111)	0.960	C(11)-H(112)	0.960
C(5)-C(3)	2.256(9)	Mo(1)-C(4)	2.308(7)	H(121)-C(12)	0.960	H(122)-C(12)	0.960
C(1)-C(4)	2.214(10)	C(2)-C(4)	2.254(10)	H(123)-C(12)	0.960	C(12)-H(121)	0.960
C(3)-C(4)	1.463(10)	C(5)-C(4)	1.372(9)	C(12)-H(122)	0.960	C(12)-H(123)	0.960
Mo(1)-C(5)	2.298(6)	C(1)-C(5)	1.311(9)				
C(2)-C(5)	2.167(10)	C(3)-C(5)	2.256(9)				
C(4)-C(5)	1.372(9)	Mo(1)-C(6)	1.942(7)				
O(1)-C(6)	1.168(7)	Mo(1)-C(7)	1.967(7)				
O(2)-C(7)	1.152(7)	Mo(1)-C(8)	2.325(7)				
C(9)-C(8)	1.416(9)	Mo(1)-C(9)	2.216(6)				
C(8)-C(9)	1.416(9)	C(10)-C(9)	1.409(8)				

TABLE C6

Bond angles (deg.) for complex (143c)

C(2)-Mo(1)-C(1)	33.1(2)	C(3)-Mo(1)-C(1)	57.2(3)	C(3)-C(1)-C(2)	35.8(4)	C(4)-C(1)-Mo(1)	60.7(3)
C(3)-Mo(1)-C(2)	34.5(2)	C(4)-Mo(1)-C(1)	56.8(3)	C(4)-C(1)-C(2)	74.1(5)	C(4)-C(1)-C(3)	38.3(3)
C(4)-Mo(1)-C(2)	57.7(3)	C(4)-Mo(1)-C(3)	36.7(2)	C(5)-C(1)-Mo(1)	71.6(4)	C(5)-C(1)-C(2)	109.5(7)
C(5)-Mo(1)-C(1)	32.8(2)	C(5)-Mo(1)-C(2)	55.4(3)	C(5)-C(1)-C(3)	73.6(5)	C(5)-C(1)-C(4)	35.3(3)
C(5)-Mo(1)-C(3)	58.2(3)	C(5)-Mo(1)-C(4)	34.7(2)	C(1)-C(2)-Mo(1)	72.6(4)	C(3)-C(2)-Mo(1)	71.8(4)
C(6)-Mo(1)-C(1)	131.1(2)	C(6)-Mo(1)-C(2)	150.3(2)	C(3)-C(2)-C(1)	109.9(6)	C(4)-C(2)-Mo(1)	59.9(3)
C(6)-Mo(1)-C(3)	120.8(4)	C(6)-Mo(1)-C(4)	92.6(3)	C(4)-C(2)-C(1)	70.9(5)	C(4)-C(2)-C(3)	39.0(3)
C(6)-Mo(1)-C(5)	100.2(3)	C(7)-Mo(1)-C(1)	89.3(3)	C(5)-C(2)-Mo(1)	60.7(3)	C(5)-C(2)-C(1)	34.8(3)
C(7)-Mo(1)-C(2)	115.0(3)	C(7)-Mo(1)-C(3)	146.4(2)	C(5)-C(2)-C(3)	75.1(5)	C(5)-C(2)-C(4)	36.1(2)
C(7)-Mo(1)-C(4)	127.6(3)	C(7)-Mo(1)-C(5)	95.1(3)	C(1)-C(3)-Mo(1)	61.5(3)	C(2)-C(3)-Mo(1)	73.7(4)
C(7)-Mo(1)-C(6)	80.9(3)	C(8)-Mo(1)-C(1)	146.3(2)	C(2)-C(3)-C(1)	34.3(3)	C(4)-C(3)-Mo(1)	70.5(4)
C(8)-Mo(1)-C(2)	113.3(3)	C(8)-Mo(1)-C(3)	92.3(3)	C(4)-C(3)-C(1)	69.8(4)	C(4)-C(3)-C(2)	104.1(6)
C(8)-Mo(1)-C(4)	108.4(3)	C(8)-Mo(1)-C(5)	143.0(2)	C(5)-C(3)-Mo(1)	60.0(3)	C(5)-C(3)-C(1)	33.9(2)
C(8)-Mo(1)-C(6)	74.7(3)	C(8)-Mo(1)-C(7)	119.4(3)	C(5)-C(3)-C(2)	68.2(5)	C(5)-C(3)-C(4)	35.9(3)
C(9)-Mo(1)-C(1)	121.9(3)	C(9)-Mo(1)-C(2)	92.5(3)	C(1)-C(4)-Mo(1)	62.4(3)	C(2)-C(4)-Mo(1)	62.4(3)
C(9)-Mo(1)-C(3)	90.6(3)	C(9)-Mo(1)-C(4)	123.1(3)	C(2)-C(4)-C(1)	35.0(3)	C(3)-C(4)-Mo(1)	72.8(4)
C(9)-Mo(1)-C(5)	146.6(2)	C(9)-Mo(1)-C(6)	106.6(3)	C(3)-C(4)-C(1)	71.8(5)	C(3)-C(4)-C(2)	36.9(3)
C(9)-Mo(1)-C(7)	108.4(3)	C(9)-Mo(1)-C(8)	36.2(2)	C(5)-C(4)-Mo(1)	72.3(4)	C(5)-C(4)-C(1)	33.5(3)
C(10)-Mo(1)-C(1)	115.6(3)	C(10)-Mo(1)-C(2)	101.9(3)	C(5)-C(4)-C(2)	68.5(5)	C(5)-C(4)-C(3)	105.4(6)
C(10)-Mo(1)-C(3)	117.7(3)	C(10)-Mo(1)-C(4)	154.4(2)	C(1)-C(5)-Mo(1)	75.6(4)	C(2)-C(5)-Mo(1)	63.9(3)
C(10)-Mo(1)-C(5)	147.8(2)	C(10)-Mo(1)-C(6)	107.0(3)	C(2)-C(5)-C(1)	35.8(4)	C(3)-C(5)-Mo(1)	61.8(3)
C(10)-Mo(1)-C(7)	73.1(3)	C(10)-Mo(1)-C(8)	63.1(3)	C(3)-C(5)-C(1)	72.5(6)	C(3)-C(5)-C(2)	36.7(3)
C(10)-Mo(1)-C(9)	35.9(2)	C(12)-O(3)-C(11)	111.2(5)	C(4)-C(5)-Mo(1)	73.1(4)	C(4)-C(5)-C(1)	111.2(7)
C(2)-C(1)-Mo(1)	74.2(4)	C(3)-C(1)-Mo(1)	61.3(3)	C(4)-C(5)-C(2)	75.4(5)	C(4)-C(5)-C(3)	38.7(3)
				O(1)-C(6)-Mo(1)	177.2(4)	O(2)-C(7)-Mo(1)	178.0(4)
				C(9)-C(8)-Mo(1)	67.7(4)	C(8)-C(9)-Mo(1)	76.1(4)
				C(10)-C(9)-Mo(1)	77.0(3)	C(10)-C(9)-C(8)	119.7(5)
				C(9)-C(10)-Mo(1)	67.2(3)	C(11)-C(10)-Mo(1)	115.4(4)
				C(11)-C(10)-C(9)	121.0(5)	C(10)-C(11)-O(3)	109.0(4)

Table C6 continued...

H(11)-C(1)-Mo(1)	120.5(3)	C(2)-C(1)-H(11)	125.3(5)
C(3)-C(1)-H(11)	161.1(3)	C(4)-C(1)-H(11)	160.6(3)
C(5)-C(1)-H(11)	125.3(5)	H(21)-C(2)-Mo(1)	122.2(2)
H(21)-C(2)-C(1)	125.0(5)	C(3)-C(2)-H(21)	125.1(5)
C(4)-C(2)-H(21)	164.1(3)	C(5)-C(2)-H(21)	159.8(2)
H(31)-C(3)-Mo(1)	120.0(2)	H(31)-C(3)-C(1)	162.2(3)
H(31)-C(3)-C(2)	127.9(5)	C(4)-C(3)-H(31)	128.0(5)
C(5)-C(3)-H(31)	163.9(3)	H(41)-C(4)-Mo(1)	119.6(2)
H(41)-C(4)-C(1)	160.8(3)	H(41)-C(4)-C(2)	164.2(3)
H(41)-C(4)-C(3)	127.3(5)	C(5)-C(4)-H(41)	127.3(5)
H(51)-C(5)-Mo(1)	118.6(2)	H(51)-C(5)-C(1)	124.4(5)
H(51)-C(5)-C(2)	160.2(2)	H(51)-C(5)-C(3)	163.1(3)
H(51)-C(5)-C(4)	124.4(5)	H(81)-C(8)-Mo(1)	114.5(34)
H(82)-C(8)-Mo(1)	125.8(33)	H(82)-C(8)-H(81)	109.0(45)
C(9)-C(8)-H(81)	120.5(29)	C(9)-C(8)-H(82)	114.6(34)
H(91)-C(9)-Mo(1)	108.8(37)	H(91)-C(9)-C(8)	121.5(40)
C(10)-C(9)-H(91)	118.0(40)	H(101)-C(10)-Mo(1)	104.3(36)
H(101)-C(10)-C(9)	104.1(35)	C(11)-C(10)-H(101)	128.1(36)
H(111)-C(11)-O(3)	109.6(4)	H(111)-C(11)-C(10)	109.6(4)
H(112)-C(11)-O(3)	109.6(4)	H(112)-C(11)-C(10)	109.6(4)
H(112)-C(11)-H(111)	109.5	H(121)-C(12)-O(3)	109.5(4)
H(122)-C(12)-O(3)	109.5(5)	H(122)-C(12)-H(121)	109.5
H(123)-C(12)-O(3)	109.5(5)	H(123)-C(12)-H(121)	109.5
H(123)-C(12)-H(122)	109.5		

TABLE C7

Selected non-bonded distances (Å) for complex (143c)

Intramolecular:

O(1)-Mo(1)	3.109	O(2)-Mo(1)	3.118
H(11)-Mo(1)	2.950	H(21)-Mo(1)	2.988
H(31)-Mo(1)	2.940	H(41)-Mo(1)	2.905
H(51)-Mo(1)	2.883	H(81)-Mo(1)	2.877
H(82)-Mo(1)	3.017	H(91)-Mo(1)	2.694
H(101)-Mo(1)	2.778	C(11)-Mo(1)	3.268
H(111)-Mo(1)	3.560	H(112)-Mo(1)	3.193
Mo(1)-O(1)	3.109	C(8)-O(1)	3.377
Mo(1)-O(2)	3.118	C(6)-O(2)	3.403
C(10)-O(2)	3.335	C(11)-O(2)	3.256
H(111)-O(2)	2.641	C(9)-O(3)	3.144
C(10)-O(3)	2.367	H(101)-O(3)	2.871
H(111)-O(3)	1.964	H(112)-O(3)	1.964
H(121)-O(3)	1.951	H(122)-O(3)	1.951
H(123)-O(3)	1.951	H(21)-C(1)	2.051
H(51)-C(1)	2.016	C(7)-C(1)	3.042
Mo(1)-H(11)	2.950	C(2)-H(11)	2.053
H(21)-H(11)	2.449	C(5)-H(11)	2.023
H(51)-H(11)	2.408	C(7)-H(11)	3.064
H(11)-C(2)	2.053	H(31)-C(2)	2.124
C(9)-C(2)	3.311	H(91)-C(2)	3.009
Mo(1)-H(21)	2.988	C(1)-H(21)	2.051

Table C7 continued...

H(11)-H(21)	2.449	C(3)-H(21)	2.099	H(82)-H(81)	1.611	C(9)-H(81)	2.095
H(31)-H(21)	2.536	H(21)-C(3)	2.099	C(10)-H(81)	2.732	C(11)-H(81)	2.777
H(41)-C(3)	2.183	C(8)-C(3)	3.365	H(112)-H(81)	2.155	Mo(1)-H(82)	3.017
C(9)-C(3)	3.238	H(91)-C(3)	2.993	H(81)-H(82)	1.611	C(9)-H(82)	2.041
Mo(1)-H(31)	2.940	C(2)-H(31)	2.124	H(91)-H(82)	2.354	O(3)-C(9)	3.144
H(21)-H(31)	2.536	C(4)-H(31)	2.189	C(2)-C(9)	3.311	C(3)-C(9)	3.238
H(41)-H(31)	2.635	H(31)-C(4)	2.189	C(6)-C(9)	3.338	C(7)-C(9)	3.395
H(51)-C(4)	2.072	C(6)-C(4)	3.083	H(81)-C(9)	2.095	H(82)-C(9)	2.041
Mo(1)-H(41)	2.905	C(3)-H(41)	2.183	H(101)-C(9)	1.934	C(11)-C(9)	2.520
H(31)-H(41)	2.635	C(5)-H(41)	2.098	H(112)-C(9)	2.648	Mo(1)-H(91)	2.694
H(51)-H(41)	2.497	H(11)-C(5)	2.023	C(2)-H(91)	3.009	C(3)-H(91)	2.993
H(41)-C(5)	2.098	C(6)-C(5)	3.261	C(8)-H(91)	2.098	H(82)-H(91)	2.354
C(7)-C(5)	3.154	Mo(1)-H(51)	2.883	C(10)-H(91)	2.056	H(101)-H(91)	2.123
C(1)-H(51)	2.016	H(11)-H(51)	2.408	O(2)-C(10)	3.335	O(3)-C(10)	2.367
C(4)-H(51)	2.072	H(41)-H(51)	2.497	C(6)-C(10)	3.452	C(7)-C(10)	2.583
O(2)-C(6)	3.403	C(4)-C(6)	3.083	C(8)-C(10)	2.442	H(81)-C(10)	2.732
C(5)-C(6)	3.261	C(7)-C(6)	2.537	H(91)-C(10)	2.056	H(111)-C(10)	2.022
C(8)-C(6)	2.608	H(81)-C(6)	2.559	H(112)-C(10)	2.022	Mo(1)-H(101)	2.778
C(9)-C(6)	3.338	C(10)-C(6)	3.452	O(3)-H(101)	2.871	C(7)-H(101)	2.944
H(112)-C(6)	3.049	C(1)-C(7)	3.042	C(9)-H(101)	1.934	H(91)-H(101)	2.123
H(11)-C(7)	3.064	C(5)-C(7)	3.154	C(11)-H(101)	2.267	H(111)-H(101)	2.563
C(6)-C(7)	2.537	C(9)-C(7)	3.395	Mo(1)-C(11)	3.268	O(2)-C(11)	3.256
C(10)-C(7)	2.583	H(101)-C(7)	2.944	C(7)-C(11)	2.867	C(8)-C(11)	3.009
C(11)-C(7)	2.867	H(111)-C(7)	2.586	H(81)-C(11)	2.777	C(9)-C(11)	2.520
H(112)-C(7)	2.956	O(1)-C(8)	3.377	H(101)-C(11)	2.267	C(12)-C(11)	2.335
C(3)-C(8)	3.365	C(6)-C(8)	2.608	H(122)-C(11)	2.531	H(123)-C(11)	2.530
H(91)-C(8)	2.098	C(10)-C(8)	2.442	Mo(1)-H(111)	3.560	O(2)-H(111)	2.641
C(11)-C(8)	3.009	H(112)-C(8)	2.646	O(3)-H(111)	1.964	C(7)-H(111)	2.586
Mo(1)-H(81)	2.877	C(6)-H(81)	2.559	C(10)-H(111)	2.022	H(101)-H(111)	2.563

Table C7 continued...

H(112)-H(111)	1.568	C(12)-H(111)	2.570	H(121)-H(51j)	2.366	O(1)-H(51a)	2.819
H(122)-H(111)	2.392	Mo(1)-H(112)	3.193	O(2)-H(51a)	2.814	C(6)-H(51a)	3.075
O(3)-H(112)	1.964	C(6)-H(112)	3.049	C(7)-H(51a)	3.075	H(51)-C(6a)	3.075
C(7)-H(112)	2.956	C(8)-H(112)	2.646	H(51)-C(7a)	3.075	O(1)-H(81b)	2.558
H(81)-H(112)	2.155	C(9)-H(112)	2.648	H(101)-H(82g)	2.515	O(3)-C(9g)	3.417
C(10)-H(112)	2.022	H(111)-H(112)	1.568	H(31)-C(9e)	2.823	O(3)-H(91g)	2.453
C(12)-H(112)	2.503	H(123)-H(112)	2.319	H(82)-H(101e)	2.515	H(41)-H(111c)	2.606
C(11)-C(12)	2.335	H(111)-C(12)	2.570	O(1)-H(112b)	2.760	C(5)-H(121k)	2.663
H(112)-C(12)	2.503	O(3)-H(121)	1.951	H(51)-H(121k)	2.366	H(21)-H(121e)	2.629
H(122)-H(121)	1.568	H(123)-H(121)	1.568	O(1)-H(123b)	2.883		
O(3)-H(122)	1.951	C(11)-H(122)	2.531				
H(111)-H(122)	2.392	H(121)-H(122)	1.568				
H(123)-H(122)	1.568	O(3)-H(123)	1.951	Key to symmetry operations relating			
C(11)-H(123)	2.530	H(112)-H(123)	2.319	designated atoms to reference atoms			
H(121)-H(123)	1.568	H(122)-H(123)	1.568	at (x,y,z):			

Intermolecular:

H(51)-O(1a)	2.819	H(81)-O(1b)	2.558
H(112)-O(1b)	2.760	H(123)-O(1b)	2.883
H(41)-O(2c)	2.881	O(2)-O(2d)	3.055
H(51)-O(2a)	2.814	H(31)-O(3e)	2.979
C(9)-O(3e)	3.417	H(91)-O(3e)	2.453
C(3)-H(11f)	2.960	H(31)-H(11f)	2.658
C(4)-H(21f)	3.029	H(121)-H(21g)	2.629
H(11)-C(3h)	2.960	O(3)-H(31g)	2.979
H(11)-H(31h)	2.658	C(9)-H(31g)	2.823
H(21)-C(4h)	3.029	O(2)-H(41i)	2.881
H(111)-H(41i)	2.606	H(121)-C(5j)	2.663

(a) -x,-y,-z
(b) 1.0-x,-y,-z
(c) x,-1.0+y,z
(d) -x,1.0-y,-z
(e) 1.0-x,-0.5+y,0.5-z
(f) -x,-0.5+y,0.5-z
(g) 1.0-x,0.5+y,0.5-z
(h) -x,0.5+y,0.5-z
(i) x,1.0+y,z
(j) 1.0+x,1.0+y,z
(k) -1.0+x,-1.0+y,z

Note on *exo-anti*-[Mo(η^3-$CH_2CHCHCHCH_2$)$(CO)_2$(η^5-C_5H_5)] (154c)

A crystal of approximate dimensions 0.2 x 0.2 x 0.2 mm was used for data collection.

Crystal data: $C_{12}H_{12}O_2Mo$, M = 300.2, monoclinic, a = 9.001(1), b = 8.699(1), c = 14.522(2)Å, β = 101.249(9)°, U = 1115.2 Å^3, space group $P2_1/c$, Z = 4, D_c = 1.79 gcm^{-3}, μ(Mo-K_α) = 11.3 cm^{-1}, F(000) = 600. Data were measured at 170° K on a CAD4 automatic four-circle diffractometer in the range $2\leq\theta\leq24^\circ$. 2010 reflections were collected of which 1492 were unique with $I\geq2\sigma(I)$. Data were corrected for Lorentz and polarization but not for absorption. The structure was solved by Patterson methods and refined using the SHELX[165,166] suite of programs. In the final least squares cycles all atoms were allowed to vibrate anisotropically. Hydrogen atoms were located in the penultimate Difference Fourier and positionally refined.

Final residuals after 12 cycles of least squares were R = 0.0317, R_w = 0.0356, for a weighting scheme of $w = 1.0595/[\sigma^2(F) + 0.002924(F)^2]$. Max. final shift/esd was 0.000. The max. and min. residual densities were 0.41 and -0.51 eÅ^{-3} respectively. Final fractional atomic coordinates and isotropic thermal parameters, bond distances and angles are given in Tables D1-D7. Tables of anisotropic temperature factors are available as supplementary data. The asymmetric unit is shown in Fig. 137, along with the labelling scheme used.

TABLE D1

Fractional atomic co-ordinates ($x10^4$) and equivalent isotropic temperature factors ($Å^2$ $x10^3$) for complex (154c)

	x	y	z	U
Mo(1)	2230.8(4)	2081.4(3)	2319.6(2)	16.0(3)
O(1)	-120(4)	2285(4)	3615(2)	30(1)
O(2)	3347(4)	4969(3)	3513(2)	30(1)
C(1)	775(5)	2193(4)	3141(3)	20(1)
C(2)	2966(5)	3883(5)	3081(3)	22(1)
C(3)	2509(6)	3230(5)	912(3)	30(2)
C(4)	991(6)	3456(6)	1037(3)	30(2)
C(5)	292(6)	2006(5)	984(3)	26(2)
C(6)	1347(5)	890(5)	839(3)	24(1)
C(7)	2722(5)	1642(6)	783(3)	25(2)
C(8)	2420(5)	-222(5)	3164(3)	25(1)
C(9)	3737(5)	80(5)	2802(3)	23(1)
C(10)	4697(5)	1338(5)	3151(3)	23(1)
C(11)	5037(5)	1781(5)	4129(3)	25(1)
C(12)	6319(6)	2461(6)	4550(4)	29(1)

TABLE D2

Fractional atomic co-ordinates ($x10^4$) for complex (154c)

	x	y	z
Mo(1)	2230.8(4)	2081.4(3)	2319.6(2)
O(1)	-120(4)	2285(4)	3615(2)
O(2)	3347(4)	4969(3)	3513(2)
C(1)	775(5)	2193(4)	3141(3)
C(2)	2966(5)	3883(5)	3081(3)
C(3)	2509(6)	3230(5)	912(3)
C(4)	991(6)	3456(6)	1037(3)
C(5)	292(6)	2006(5)	984(3)
C(6)	1347(5)	890(5)	639(3)
C(7)	2722(5)	1642(6)	783(3)
C(8)	2420(5)	-222(5)	3164(3)
C(9)	3737(5)	80(5)	2802(3)
C(10)	4697(5)	1338(5)	3151(3)
C(11)	5037(5)	1781(5)	4129(3)
C(12)	6319(6)	2461(6)	4550(4)

TABLE D3

Anisotropic temperature factors (Å $x10^3$) for complex (154c)

	U_{11}	U_{22}	U_{33}	U_{23}	U_{13}	U_{12}
Mo(1)	14.7(3)	14.3(3)	19.1(3)	-1.5(1)	4.0(2)	0.3(1)
O(1)	27(2)	29(2)	35(2)	3(1)	15(2)	4(1)
O(2)	34(2)	22(2)	36(2)	-8(2)	12(1)	-3(1)
C(1)	21(2)	14(2)	26(2)	3(2)	4(2)	0(2)
C(2)	23(2)	20(2)	24(2)	-1(2)	7(2)	-1(2)
C(3)	48(3)	21(2)	22(2)	-3(2)	13(2)	-11(2)
C(4)	42(3)	24(2)	22(2)	2(2)	3(2)	13(2)
C(5)	19(2)	39(3)	19(2)	-5(2)	0(2)	2(2)
C(6)	28(2)	21(2)	22(2)	-3(2)	2(2)	-5(2)
C(7)	28(2)	29(2)	20(2)	-7(2)	10(2)	0(2)
C(8)	30(2)	19(2)	23(2)	3(2)	2(2)	-2(2)
C(9)	18(2)	18(2)	31(3)	4(2)	1(2)	3(2)
C(10)	22(2)	19(2)	28(2)	1(2)	3(2)	4(2)
C(11)	22(2)	24(2)	29(2)	1(2)	7(2)	4(2)
C(12)	28(3)	27(2)	30(3)	-3(2)	-1(2)	1(2)

The temperature factor exponent takes the form:

$-2\ (U_{11}.h.a^* + \ldots + 2U_{23}.h.k.a^*.b^*)$

TABLE D4

Hydrogen fractional atomic co-ordinates ($x10^4$) and isotropic temperature factors (Å^2 $x10^3$) for complex (154c)

	x	y	z	U
H(31)	3254(56)	3988(58)	897(32)	28(4)
H(41)	548(54)	4433(59)	1129(33)	28(4)
H(51)	-688(65)	1757(57)	937(35)	28(4)
H(61)	1151(54)	-125(57)	846(33)	28(4)
H(71)	3661(56)	1161(53)	669(32)	28(4)
H(81)	1788(58)	-985(60)	2920(34)	28(4)
H(82)	2388(55)	-108(56)	3738(37)	28(4)
H(91)	3980(51)	-518(59)	2212(32)	28(4)
H(101)	5528(55)	1553(58)	2699(33)	28(4)
H(111)	4235(59)	1679(58)	4523(34)	28(4)
H(121)	6478(60)	2710(52)	5248(38)	28(4)
H(122)	6987(70)	2619(58)	4193(39)	28(4)

TABLE D5

Bond lengths (Å) for complex (154c)

C(1)-Mo(1)	1.939(6)	C(2)-Mo(1)	1.957(6)
C(3)-Mo(1)	2.332(7)	C(4)-Mo(1)	2.310(7)
C(5)-Mo(1)	2.344(7)	C(6)-Mo(1)	2.380(6)
C(7)-Mo(1)	2.389(6)	C(8)-Mo(1)	2.338(6)
C(9)-Mo(1)	2.234(6)	C(10)-Mo(1)	2.400(6)
C(1)-O(1)	1.160(7)	C(2)-O(2)	1.149(6)
C(4)-C(3)	1.426(8)	C(7)-C(3)	1.412(8)
C(5)-C(4)	1.405(8)	C(6)-C(5)	1.402(7)
C(7)-C(6)	1.416(7)	C(9)-C(8)	1.412(7)
C(10)-C(9)	1.426(7)	C(11)-C(10)	1.446(8)
C(12)-C(11)	1.334(8)	H(31)-C(3)	0.944(52)
H(41)-C(4)	0.959(52)	H(51)-C(5)	0.898(56)
H(61)-C(6)	0.901(50)	H(71)-C(7)	0.985(49)
H(81)-C(8)	0.901(55)	H(82)-C(8)	0.845(52)
H(91)-C(9)	1.060(48)	H(101)-C(10)	1.103(47)
H(111)-C(11)	1.009(51)	H(121)-C(12)	1.020(54)
H(122)-C(12)	0.877(60)		

TABLE D6

Bond angles (deg.) for complex (154c)

C(2)-Mo(1)-C(1)	78.9(3)	C(3)-Mo(1)-C(1)	135.9(2)
C(3)-Mo(1)-C(2)	94.0(3)	C(4)-Mo(1)-C(1)	101.1(3)
C(4)-Mo(1)-C(2)	95.6(3)	C(4)-Mo(1)-C(3)	35.8(2)
C(5)-Mo(1)-C(1)	91.6(3)	C(5)-Mo(1)-C(2)	127.2(3)
C(5)-Mo(1)-C(3)	58.4(3)	C(5)-Mo(1)-C(4)	35.1(2)
C(6)-Mo(1)-C(1)	115.5(3)	C(6)-Mo(1)-C(2)	151.1(2)
C(6)-Mo(1)-C(3)	57.9(3)	C(6)-Mo(1)-C(4)	58.2(3)
C(6)-Mo(1)-C(5)	34.5(2)	C(7)-Mo(1)-C(1)	148.6(2)
C(7)-Mo(1)-C(2)	123.5(3)	C(7)-Mo(1)-C(3)	34.8(2)
C(7)-Mo(1)-C(4)	58.5(3)	C(7)-Mo(1)-C(5)	57.7(3)
C(7)-Mo(1)-C(6)	34.5(2)	C(8)-Mo(1)-C(1)	73.1(3)
C(8)-Mo(1)-C(2)	114.1(3)	C(8)-Mo(1)-C(3)	144.9(2)
C(8)-Mo(1)-C(4)	147.3(2)	C(8)-Mo(1)-C(5)	112.1(3)
C(8)-Mo(1)-C(6)	94.5(3)	C(8)-Mo(1)-C(7)	110.2(3)
C(9)-Mo(1)-C(1)	106.7(3)	C(9)-Mo(1)-C(2)	109.2(3)
C(9)-Mo(1)-C(3)	116.5(3)	C(9)-Mo(1)-C(4)	145.5(2)
C(9)-Mo(1)-C(5)	123.1(3)	C(9)-Mo(1)-C(6)	91.1(3)
C(9)-Mo(1)-C(7)	87.5(3)	C(9)-Mo(1)-C(8)	35.9(2)
C(10)-Mo(1)-C(1)	112.0(3)	C(10)-Mo(1)-C(2)	75.8(3)
C(10)-Mo(1)-C(3)	108.0(3)	C(10)-Mo(1)-C(4)	143.1(2)
C(10)-Mo(1)-C(5)	151.1(1)	C(10)-Mo(1)-C(6)	116.8(3)
C(10)-Mo(1)-C(7)	96.0(3)	C(10)-Mo(1)-C(8)	62.6(2)
C(10)-Mo(1)-C(9)	35.6(2)	C(7)-C(3)-C(4)	108.0(5)
C(5)-C(4)-C(3)	107.4(5)	C(6)-C(5)-C(4)	108.7(5)

Table D6 continued...

C(7)-C(6)-C(5)	108.3(5)	C(6)-C(7)-C(3)	107.6(5)
C(10)-C(9)-C(8)	120.3(5)	C(11)-C(10)-C(9)	123.5(5)
C(12)-C(11)-C(10)	124.5(6)	H(31)-C(3)-C(4)	127.5(30)
H(31)-C(3)-C(7)	124.4(30)	H(41)-C(4)-C(3)	125.0(29)
H(41)-C(4)-C(5)	127.5(30)	H(51)-C(5)-C(4)	130.0(33)
H(51)-C(5)-C(6)	120.4(34)	H(61)-C(6)-C(5)	122.4(32)
H(61)-C(6)-C(7)	129.0(32)	H(71)-C(7)-C(3)	125.5(28)
H(71)-C(7)-C(6)	126.9(28)	H(81)-C(8)-C(9)	120.1(31)
H(82)-C(8)-C(9)	122.6(35)	H(82)-C(8)-H(81)	109.6(47)
H(91)-C(9)-C(8)	122.1(27)	H(91)-C(9)-C(10)	117.2(27)
H(101)-C(10)-C(9)	110.7(27)	H(101)-C(10)-C(11)	120.1(26)
H(111)-C(11)-C(10)	119.7(30)	H(111)-C(11)-C(12)	115.5(30)
H(121)-C(12)-C(11)	119.4(30)	H(122)-C(12)-C(11)	115.5(38)
H(122)-C(12)-H(121)	125.0(49)		

TABLE D7

Selected non-bonded distances (Å) for complex (154c)

Intramolecular:

O(1)-Mo(1)	3.099	O(2)-Mo(1)	3.105
C(11)-Mo(1)	3.281	H(31)-Mo(1)	2.934
H(41)-Mo(1)	2.906	H(51)-Mo(1)	2.992
H(61)-Mo(1)	2.898	H(71)-Mo(1)	3.040
H(81)-Mo(1)	2.858	H(82)-Mo(1)	2.788
H(91)-Mo(1)	2.777	H(101)-Mo(1)	2.947
H(111)-Mo(1)	3.370	C(11)-O(2)	3.205
C(2)-C(1)	2.475	C(4)-C(1)	3.288
C(5)-C(1)	3.082	C(8)-C(1)	2.567
H(82)-C(1)	2.525	C(3)-C(2)	3.148
C(4)-C(2)	3.170	C(10)-C(2)	2.698
C(11)-C(2)	2.834	C(5)-C(3)	2.282
C(6)-C(3)	2.282	H(41)-C(3)	2.127
H(71)-C(3)	2.141	C(6)-C(4)	2.281
C(7)-C(4)	2.297	H(31)-C(4)	2.137
H(51)-C(4)	2.098	C(7)-C(5)	2.284
H(41)-C(5)	2.130	H(61)-C(5)	2.033
C(9)-C(6)	3.295	H(51)-C(6)	2.012
H(71)-C(6)	2.157	C(9)-C(7)	3.199
H(31)-C(7)	2.096	H(61)-C(7)	2.103
H(91)-C(7)	2.864	C(10)-C(8)	2.461
C(11)-C(8)	3.043	H(91)-C(8)	2.170

Table D7 continued...

H(111)-C(8)	2.835	C(11)-C(9)	2.529
H(81)-C(9)	2.020	H(82)-C(9)	1.998
H(101)-C(9)	2.088	H(111)-C(9)	2.819
C(12)-C(10)	2.461	H(82)-C(10)	2.705
H(91)-C(10)	2.130	H(111)-C(10)	2.134
H(122)-C(10)	2.562	H(82)-C(11)	2.860
H(101)-C(11)	2.215	H(121)-C(11)	2.038
H(122)-C(11)	1.885	H(101)-C(12)	2.758
H(111)-C(12)	1.988	H(61)-H(51)	2.350
H(82)-H(81)	1.427	H(91)-H(81)	2.430
H(111)-H(82)	2.395	H(101)-H(91)	2.302
H(121)-H(111)	2.272	H(122)-H(121)	1.684

Intermolecular:

H(41)-O(1a)	2.549	H(61)-O(1b)	2.614
H(121)-O(2c)	2.689	H(101)-O(2d)	2.592
H(111)-C(3e)	2.777	H(31)-C(11f)	2.879
H(111)-H(31e)	2.406		

Key to symmetry operations relating designated atoms to reference atoms at (x,y,z):

(a) -x,0.5+y,0.5-z

(b) -x,-0.5+y,0.5-z

(c) 1.0-x,1.0-y,1.0-z

(d) 1.0-x,-0.5+y,0.5-z

(e) x,0.5-y,0.5+z

(f) 1.0-x,0.5+y,0.5-z

Note on [Mo(η^3-$C_4H_3O_2$)(CO)$_2$(η^5-C_5Me_5)] (162)

A crystal of approximate dimensions 0.2 x 0.2 x 0.2 mm was used for data collection.

Crystal data: $C_{16}H_{18}O_4Mo$, M = 370.2 monoclinic, a = 28.077(4), b = 8.895(2), c = 12.767(2)Å, β = 104.49(1)°, U = 3087.1 Å^3, space group $C2/c$, Z = 8, D_c = 1.59 gcm^{-3}, μ(Mo-K_α) = 8.40 cm^{-1}, F(000) = 1504. Data were measured at room temperature on a CAD4 automatic four-circle diffractometer in the range $2 \leq \theta \leq 24^\circ$. 2649 reflections were collected of which 2018 were unique with $I \geq 2\sigma(I)$. Data were corrected for Lorentz and polarization but not for absorption. The structure was solved by Patterson methods and refined using the SHELX[165,166] suite of programs. In the final least squares cycles all atoms were allowed to vibrate anisotropically. Hydrogen atoms were included at calculated positions except in the instance of H141, H151, and H161 (attached to C14, C15, and C16 respectively). These protons were located in an advanced Difference Fourier and refined at a distance of 0.96 Å from the relevant parent atoms.

Final residuals after 10 cycles of least squares were R = 0.0262, R_w = 0.0273, for a weighting scheme of $w = 2.9285/[\sigma^2(F) + 0.000292(F)^2]$. Max. final shift/esd was 0.001. The max. and min. residual densities were 0.31 and -0.13 eÅ^{-3} respectively. Final fractional atomic coordinates and isotropic thermal parameters, bond distances and angles are given in Tables E1-E7. Tables of anisotropic temperature factors are available as supplementary data. The asymmetric unit is shown in Fig. 143, along with the labelling scheme used.

TABLE E1

Fractional atomic co-ordinates ($x10^4$) and equivalent isotropic temperature factors ($Å^2 x10^3$) for complex (162)

	x	y	z	U
Mo(1)	3687	2732	3180	33
O(1)	4169(1)	5880(3)	3450(3)	86(1)
O(2)	4010(1)	2609(3)	1025(3)	72(1)
O(3)	2901(1)	4246(4)	284(2)	77(1)
O(4)	2996(1)	5208(3)	1939(2)	59(1)
C(1)	3975(2)	4730(4)	3315(3)	53(1)
C(2)	3887(1)	2692(4)	1808(3)	44(1)
C(3)	3696(1)	293(3)	3972(3)	38(1)
C(4)	4145(1)	516(4)	3671(3)	40(1)
C(5)	4393(1)	1755(4)	4283(3)	43(1)
C(6)	4096(1)	2290(4)	4968(3)	44(1)
C(7)	3665(1)	1382(4)	4771(2)	41(1)
C(8)	3329(1)	-956(4)	3579(3)	56(1)
C(9)	4354(2)	-466(4)	2941(3)	59(2)
C(10)	4906(1)	2275(5)	4294(4)	65(2)
C(11)	4237(2)	3480(5)	5828(3)	69(2)
C(12)	3270(2)	1449(5)	5372(3)	63(2)
C(13)	2942(1)	4000(4)	1231(3)	49(1)
C(14)	2934(1)	2639(4)	1835(3)	48(1)
C(15)	2892(1)	3056(5)	2878(3)	53(1)
C(16)	3056(2)	4536(5)	2982(3)	56(1)

TABLE E2

Fractional atomic co-ordinates ($x10^4$) for complex (162)

	x	y	z
Mo(1)	3687	2732	3180
O(1)	4169(1)	5880(3)	3450(3)
O(2)	4010(1)	2609(3)	1025(3)
O(3)	2901(1)	4246(4)	284(2)
O(4)	2996(1)	5208(3)	1939(2)
C(1)	3975(2)	4730(4)	3315(3)
C(2)	3887(1)	2692(4)	1808(3)
C(3)	3696(1)	293(3)	3972(3)
C(4)	4145(1)	516(4)	3671(3)
C(5)	4393(1)	1755(4)	4283(3)
C(6)	4096(1)	2290(4)	4968(3)
C(7)	3665(1)	1382(4)	4771(2)
C(8)	3329(1)	-956(4)	3579(3)
C(9)	4354(2)	-466(4)	2941(3)
C(10)	4906(1)	2275(5)	4294(4)
C(11)	4237(2)	3480(5)	5828(3)
C(12)	3270(2)	1449(5)	5372(3)
C(13)	2942(1)	4000(4)	1231(3)
C(14)	2934(1)	2639(4)	1835(3)
C(15)	2892(1)	3056(5)	2878(3)
C(16)	3056(2)	4536(5)	2982(3)

TABLE E3

Anisotropic temperature factors (Å $\times 10^3$) for complex (162)

	U_{11}	U_{22}	U_{33}	U_{23}	U_{13}	U_{12}
Mo(1)	34	30	33	2	8	0
O(1)	125(3)	43(2)	83(2)	3(2)	11(2)	-32(2)
O(2)	70(2)	98(3)	56(2)	8(1)	32(2)	14(2)
O(3)	75(2)	108(3)	45(2)	19(2)	9(1)	13(2)
O(4)	67(2)	54(2)	56(2)	13(1)	15(1)	18(1)
C(1)	69(3)	43(2)	44(2)	6(2)	7(2)	-3(2)
C(2)	41(2)	49(2)	44(2)	4(2)	14(2)	5(2)
C(3)	42(2)	32(2)	37(2)	6(1)	3(1)	-2(1)
C(4)	39(2)	35(2)	44(2)	6(1)	6(1)	1(1)
C(5)	37(2)	42(2)	42(2)	9(2)	-3(1)	-2(2)
C(6)	57(2)	36(2)	32(2)	3(1)	1(2)	-6(2)
C(7)	48(2)	41(2)	35(2)	9(1)	10(1)	-2(2)
C(8)	55(2)	48(2)	64(2)	0(2)	11(2)	-18(2)
C(9)	59(2)	50(2)	69(3)	-1(2)	22(2)	11(2)
C(10)	43(2)	71(3)	74(3)	15(2)	3(2)	-13(2)
C(11)	100(4)	58(3)	44(2)	-7(2)	7(2)	-23(2)
C(12)	73(3)	75(3)	49(2)	8(2)	28(2)	-2(2)
C(13)	38(2)	67(3)	41(2)	6(2)	8(2)	11(2)
C(14)	39(2)	52(2)	51(2)	3(2)	4(2)	2(2)
C(15)	36(2)	72(3)	52(2)	20(2)	15(2)	11(2)
C(16)	59(2)	64(3)	47(2)	0(2)	14(2)	24(2)

The temperature factor exponent takes the form:

$-2\ (U_{11}.h.a^* + \ldots + 2U_{23}.h.k.a^*.b^*)$

TABLE E4

Hydrogen fractional atomic co-ordinates ($\times 10^4$) and isotropic temperature factors (Å^2 $\times 10^3$) for complex (162)

	x	y	z	U
H(81)	3431(1)	-1539(4)	3041(3)	136(6)
H(82)	3011(1)	-531(4)	3270(3)	136(6)
H(83)	3313(1)	-1592(4)	4177(3)	136(6)
H(91)	4116(2)	-1218(4)	2622(3)	136(6)
H(92)	4647(2)	-945(4)	3353(3)	136(6)
H(93)	4430(2)	136(4)	2381(3)	136(6)
H(101)	4991(1)	3126(5)	4766(4)	136(6)
H(102)	4918(1)	2555(5)	3575(4)	136(6)
H(103)	5135(1)	1474(5)	4547(4)	136(6)
H(111)	4544(2)	3929(5)	5792(3)	136(6)
H(112)	4272(2)	3033(5)	6527(3)	136(6)
H(113)	3986(2)	4239(5)	5712(3)	136(6)
H(121)	3331(2)	2283(5)	5865(3)	136(6)
H(122)	3271(2)	532(5)	5770(3)	136(6)
H(123)	2956(2)	1574(5)	4867(3)	136(6)
H(141)	2823(13)	1707(22)	1477(27)	63(7)
H(151)	2751(14)	2440(35)	3340(26)	63(7)
H(161)	3043(14)	5231(32)	3550(21)	63(7)

TABLE E5

Bond lengths (Å) for complex (162)

C(1)-Mo(1)	1.942(6)	C(2)-Mo(1)	1.969(6)
C(3)-Mo(1)	2.391(5)	C(4)-Mo(1)	2.352(5)
C(5)-Mo(1)	2.296(5)	C(6)-Mo(1)	2.318(5)
C(7)-Mo(1)	2.374(5)	C(14)-Mo(1)	2.369(6)
C(15)-Mo(1)	2.189(5)	C(16)-Mo(1)	2.358(6)
C(1)-O(1)	1.151(5)	C(2)-O(2)	1.139(6)
C(13)-O(3)	1.205(5)	C(13)-O(4)	1.388(5)
C(16)-O(4)	1.431(5)	C(4)-C(3)	1.422(6)
C(7)-C(3)	1.425(5)	C(8)-C(3)	1.513(6)
C(5)-C(4)	1.428(6)	C(9)-C(4)	1.498(6)
C(6)-C(5)	1.431(6)	C(10)-C(5)	1.510(7)
C(7)-C(6)	1.425(6)	C(11)-C(6)	1.505(7)
C(12)-C(7)	1.499(6)	C(14)-C(13)	1.439(6)
C(15)-C(14)	1.415(7)	C(16)-C(15)	1.390(7)
H(81)-C(8)	0.960	H(82)-C(8)	0.960
H(83)-C(8)	0.960	H(91)-C(9)	0.960
H(92)-C(9)	0.960	H(93)-C(9)	0.960
H(101)-C(10)	0.960	H(102)-C(10)	0.960
H(103)-C(10)	0.960	H(111)-C(11)	0.960
H(112)-C(11)	0.960	H(113)-C(11)	0.960
H(121)-C(12)	0.960	H(122)-C(12)	0.960
H(123)-C(12)	0.960	H(141)-C(14)	0.960(2)
H(151)-C(15)	0.960(2)	H(161)-C(16)	0.960(2)

TABLE E6

Bond angles (deg.) for complex (162)

C(2)-Mo(1)-C(1)	83.7(3)	C(3)-Mo(1)-C(1)	146.4(1)
C(3)-Mo(1)-C(2)	112.6(2)	C(4)-Mo(1)-C(1)	123.8(2)
C(4)-Mo(1)-C(2)	87.9(2)	C(4)-Mo(1)-C(3)	34.9(1)
C(5)-Mo(1)-C(1)	90.9(2)	C(5)-Mo(1)-C(2)	98.3(2)
C(5)-Mo(1)-C(3)	58.7(2)	C(5)-Mo(1)-C(4)	35.8(1)
C(6)-Mo(1)-C(1)	88.6(2)	C(6)-Mo(1)-C(2)	133.8(1)
C(6)-Mo(1)-C(3)	58.6(2)	C(6)-Mo(1)-C(4)	59.5(2)
C(6)-Mo(1)-C(5)	36.1(1)	C(7)-Mo(1)-C(1)	119.1(2)
C(7)-Mo(1)-C(2)	145.7(1)	C(7)-Mo(1)-C(3)	34.8(1)
C(7)-Mo(1)-C(4)	58.5(2)	C(7)-Mo(1)-C(5)	59.1(2)
C(7)-Mo(1)-C(6)	35.3(1)	C(14)-Mo(1)-C(1)	111.9(2)
C(14)-Mo(1)-C(2)	75.9(2)	C(14)-Mo(1)-C(3)	100.8(2)
C(14)-Mo(1)-C(4)	119.6(2)	C(14)-Mo(1)-C(5)	155.3(1)
C(14)-Mo(1)-C(6)	147.2(1)	C(14)-Mo(1)-C(7)	113.1(2)
C(15)-Mo(1)-C(1)	106.2(3)	C(15)-Mo(1)-C(2)	110.6(2)
C(15)-Mo(1)-C(3)	95.5(2)	C(15)-Mo(1)-C(4)	128.6(2)
C(15)-Mo(1)-C(5)	147.6(1)	C(15)-Mo(1)-C(6)	115.4(2)
C(15)-Mo(1)-C(7)	88.5(2)	C(15)-Mo(1)-C(14)	35.9(1)
C(16)-Mo(1)-C(1)	70.8(3)	C(16)-Mo(1)-C(2)	107.0(2)
C(16)-Mo(1)-C(3)	126.2(2)	C(16)-Mo(1)-C(4)	161.0(1)
C(16)-Mo(1)-C(5)	146.5(1)	C(16)-Mo(1)-C(6)	113.3(2)
C(16)-Mo(1)-C(7)	104.8(2)	C(16)-Mo(1)-C(14)	55.6(2)
C(16)-Mo(1)-C(15)	35.4(2)	C(16)-O(4)-C(13)	104.6(4)
C(7)-C(3)-C(4)	108.5(4)	C(8)-C(3)-C(4)	126.1(4)

Table E6 continued...

C(8)-C(3)-C(7)	125.3(4)	C(5)-C(4)-C(3)	107.6(4)
C(9)-C(4)-C(3)	126.7(4)	C(9)-C(4)-C(5)	125.3(4)
C(6)-C(5)-C(4)	108.2(4)	C(10)-C(5)-C(4)	125.0(4)
C(10)-C(5)-C(6)	126.4(4)	C(7)-C(6)-C(5)	107.7(4)
C(11)-C(6)-C(5)	126.3(4)	C(11)-C(6)-C(7)	125.8(5)
C(6)-C(7)-C(3)	108.0(4)	C(12)-C(7)-C(3)	125.4(4)
C(12)-C(7)-C(6)	126.3(4)	O(4)-C(13)-O(3)	118.7(5)
C(14)-C(13)-O(3)	132.9(4)	C(14)-C(13)-O(4)	108.4(4)
C(15)-C(14)-C(13)	107.5(4)	C(16)-C(15)-C(14)	103.6(4)
C(15)-C(16)-O(4)	110.3(4)	H(81)-C(8)-C(3)	109.5(3)
H(82)-C(8)-C(3)	109.5(3)	H(82)-C(8)-H(81)	109.5
H(83)-C(8)-C(3)	109.5(3)	H(83)-C(8)-H(81)	109.5
H(83)-C(8)-H(82)	109.5	H(91)-C(9)-C(4)	109.5(3)
H(92)-C(9)-C(4)	109.5(3)	H(92)-C(9)-H(91)	109.5
H(93)-C(9)-C(4)	109.5(3)	H(93)-C(9)-H(91)	109.5
H(93)-C(9)-H(92)	109.5	H(101)-C(10)-C(5)	109.5(3)
H(102)-C(10)-C(5)	109.5(3)	H(102)-C(10)-H(101)	109.5
H(103)-C(10)-C(5)	109.5(3)	H(103)-C(10)-H(101)	109.5
H(103)-C(10)-H(102)	109.5	H(111)-C(11)-C(6)	109.5(3)
H(112)-C(11)-C(6)	109.5(3)	H(112)-C(11)-H(111)	109.5
H(113)-C(11)-C(6)	109.5(3)	H(113)-C(11)-H(111)	109.5
H(113)-C(11)-H(112)	109.5	H(121)-C(12)-C(7)	109.5(3)
H(122)-C(12)-C(7)	109.5(3)	H(122)-C(12)-H(121)	109.5
H(123)-C(12)-C(7)	109.5(3)	H(123)-C(12)-H(121)	109.5
H(123)-C(12)-H(122)	109.5	H(141)-C(14)-C(13)	121.2(24)
C(15)-C(14)-H(141)	125.5(24)	H(151)-C(15)-C(14)	125.0(25)
C(16)-C(15)-H(151)	131.2(24)	H(161)-C(16)-O(4)	114.6(24)
H(161)-C(16)-C(15)	127.5(24)		

TABLE E7

Selected non-bonded distances (Å) for complex (162)

Intramolecular:

O(1)-Mo(1)	3.091	O(2)-Mo(1)	3.106
O(4)-Mo(1)	3.097	C(8)-Mo(1)	3.506
C(9)-Mo(1)	3.460	C(10)-Mo(1)	3.386
C(11)-Mo(1)	3.412	C(12)-Mo(1)	3.486
C(13)-Mo(1)	3.039	H(141)-Mo(1)	2.967
H(151)-Mo(1)	2.701	O(4)-O(3)	2.232
C(14)-O(3)	2.425	C(1)-O(4)	2.900
C(14)-O(4)	2.292	C(15)-O(4)	2.315
H(161)-O(4)	2.028	C(2)-C(1)	2.609
C(5)-C(1)	3.030	C(6)-C(1)	2.986
C(16)-C(1)	2.515	H(161)-C(1)	2.744
C(4)-C(2)	3.011	H(93)-C(2)	2.733
C(13)-C(2)	2.822	C(14)-C(2)	2.686
C(5)-C(3)	2.300	C(6)-C(3)	2.306
H(81)-C(3)	2.044	H(82)-C(3)	2.044
H(83)-C(3)	2.044	C(9)-C(3)	2.610
H(91)-C(3)	2.682	C(12)-C(3)	2.599
C(6)-C(4)	2.316	C(7)-C(4)	2.310
C(8)-C(4)	2.616	H(81)-C(4)	2.683
H(91)-C(4)	2.031	H(92)-C(4)	2.031
H(93)-C(4)	2.031	C(10)-C(4)	2.606
C(7)-C(5)	2.305	C(9)-C(5)	2.600

Table E7 continued...

H(101)-C(5)	2.042	H(102)-C(5)	2.042
H(103)-C(5)	2.042	C(11)-C(5)	2.620
H(111)-C(5)	2.687	C(10)-C(6)	2.625
H(101)-C(6)	2.694	H(111)-C(6)	2.037
H(112)-C(6)	2.037	H(113)-C(6)	2.037
C(12)-C(6)	2.609	H(121)-C(6)	2.677
C(8)-C(7)	2.610	C(11)-C(7)	2.608
H(121)-C(7)	2.032	H(122)-C(7)	2.032
H(123)-C(7)	2.032	C(15)-C(7)	3.185
C(12)-C(8)	3.168	H(82)-H(81)	1.568
H(83)-H(81)	1.568	H(91)-H(81)	2.141
H(83)-H(82)	1.568	C(10)-C(9)	3.161
H(92)-H(91)	1.568	H(93)-H(91)	1.568
H(93)-H(92)	1.568	H(102)-H(101)	1.568
H(103)-H(101)	1.568	H(111)-H(101)	2.151
H(103)-H(102)	1.568	C(12)-C(11)	3.193
H(121)-C(11)	2.771	H(112)-H(111)	1.568
H(113)-H(111)	1.568	H(113)-H(112)	1.568
H(122)-H(121)	1.568	H(123)-H(121)	1.568
H(123)-H(122)	1.568	H(151)-H(123)	2.041
H(141)-C(13)	2.103	C(15)-C(13)	2.302
C(16)-C(13)	2.230	H(151)-C(14)	2.117
C(16)-C(14)	2.204	C(15)-H(141)	2.122
H(161)-C(15)	2.116	C(16)-H(151)	2.148

Intermolecular:

H(161)-O(3a)	2.392	H(112)-H(91b)	2.248

Key to symmetry operations relating designated atoms to reference atoms at (x,y,z):

(a) x,1.0-y,0.5+z (b) x,-y,0.5+z

Note on $[Mo(\eta^2\text{-}C_{11}H_{12}NO_2)(CO)_2(\eta^5\text{-}C_9H_7)]$ (165)

A crystal of approximate dimensions 0.2 x 0.2x 0.15 mm was used for data collection.

Crystal data: $C_{22}H_{19}N_3O_4Mo.CH_2Cl_2$, M = 542.3, monoclinic, a = 13.809(5), b = 8.598(2), c = 18.908(5)Å, β = 95.57(4)°, U = 2234.3 Å^3, space group $P2_1/n$, Z = 4, D_c = 1.61 gcm^{-3}, μ(Mo-K_α) = 8.4 cm^{-1}, F(000) = 1096. Data were measured at 170° K on a CAD4 automatic four-circle diffractometer in the range $2\leq\theta\leq24^\circ$. 3943 reflections were collected of which 2354 were unique with $I\geq2\sigma(I)$. Data were corrected for Lorentz and polarization but not for absorption. The structure was solved by Patterson methods and refined using the SHELX[165,166] suite of programs. In the final least squares cycles all atoms were allowed to vibrate anisotropically. Hydrogen atoms were included at calculated positions except for H1, H4, H131, H141 and H151 (attached to N1, O4, C13, C14 and C15 respectively). These hydrogens were located in an advanced Difference Fourier and refined at a distance of 0.96 Å from the relevent parent atoms in all cases barring H4, which was refined at a fixed distance of 1.08 Å from O4.

Final residuals after 12 cycles of least squares were R = 0.0458, R_w = 0.0417, for a weighting scheme of $w = 2.4318/[\sigma^2(F) + 0.000402(F)^2]$. Max. final shift/esd was 0.017. The max. and min. residual densities were 0.34 and -0.44 eÅ^{-3} respectively. Final fractional atomic coordinates and isotropic thermal parameters, bond distances and angles are given in Tables F1-F7. Tables of anisotropic temperature factors are available as supplementary data. The asymmetric unit is shown in Fig. 148, along with the labelling scheme used.

TABLE F1

Fractional atomic co-ordinates ($x10^4$) and equivalent isotropic

temperature factors ($Å^2$ $x10^3$) for complex (165)

	x	y	z	U
Mo(1)	4753.9(4)	1346.1(7)	1804.0(3)	20.8(3)
Cl(1)	2595(1)	1376(3)	3548(1)	43(1)
Cl(2)	3893(2)	-393(3)	4532(1)	58(1)
N(1)	4131(4)	4804(7)	2914(3)	25(2)
O(1)	4076(4)	1565(7)	193(3)	50(2)
O(2)	2566(4)	2097(6)	1828(3)	35(2)
O(3)	4745(3)	5093(5)	824(2)	27(2)
O(4)	5980(3)	3849(6)	393(2)	29(2)
C(1)	4345(5)	1484(9)	801(4)	31(3)
C(2)	3393(6)	1866(8)	1836(4)	31(3)
C(3)	5597(5)	-90(8)	2796(4)	32(2)
C(4)	4646(5)	-692(8)	2597(4)	34(3)
C(5)	4617(5)	-1310(9)	1910(4)	38(3)
C(6)	5532(5)	-1010(8)	1640(4)	34(3)
C(7)	6144(5)	-278(8)	2196(4)	25(2)
C(8)	7123(5)	230(8)	2235(4)	35(3)
C(9)	7514(6)	936(8)	2851(5)	42(3)
C(10)	6976(6)	1123(9)	3433(4)	44(3)
C(11)	6039(6)	634(9)	3424(4)	36(3)
C(12)	5447(5)	4157(8)	919(3)	22(2)
C(13)	5732(5)	3315(7)	1570(3)	20(2)
C(14)	5363(5)	3640(8)	2246(3)	25(2)
C(15)	4499(5)	4414(8)	2313(4)	23(2)
C(16)	4474(5)	4164(8)	3613(3)	25(2)
C(17)	5419(5)	4869(8)	3960(3)	23(2)
C(18)	5795(5)	6281(9)	3762(4)	30(2)
C(19)	6650(5)	6862(8)	4108(4)	34(3)
C(20)	7147(5)	6024(8)	4656(4)	33(3)
C(21)	6762(5)	4617(9)	4867(4)	35(3)
C(22)	5906(5)	4071(8)	4523(4)	31(2)
C(23)	2682(5)	228(9)	4325(4)	34(3)

TABLE F2

Fractional atomic co-ordinates ($x10^4$) for complex (165)

	x	y	z
Mo(1)	4753.9(4)	1346.1(7)	1804.0(3)
Cl(1)	2595(1)	1376(3)	3548(1)
Cl(2)	3893(2)	-393(3)	4532(1)
N(1)	4131(4)	4804(7)	2914(3)
O(1)	4076(4)	1565(7)	193(3)
O(2)	2566(4)	2097(6)	1828(3)
O(3)	4745(3)	5093(5)	824(2)
O(4)	5980(3)	3849(6)	393(2)
C(1)	4345(5)	1484(9)	801(4)
C(2)	3393(6)	1866(8)	1836(4)
C(3)	5597(5)	-90(8)	2796(4)
C(4)	4646(5)	-692(8)	2597(4)
C(5)	4617(5)	-1310(9)	1910(4)
C(6)	5532(5)	-1010(8)	1640(4)
C(7)	6144(5)	-278(8)	2196(4)
C(8)	7123(5)	230(8)	2235(4)
C(9)	7514(6)	936(8)	2851(5)
C(10)	6976(6)	1123(9)	3433(4)
C(11)	6039(6)	634(9)	3424(4)
C(12)	5447(5)	4157(8)	919(3)
C(13)	5732(5)	3315(7)	1570(3)
C(14)	5363(5)	3640(8)	2246(3)
C(15)	4499(5)	4414(8)	2313(4)
C(16)	4474(5)	4164(8)	3613(3)
C(17)	5419(5)	4869(8)	3960(3)
C(18)	5795(5)	6281(9)	3762(4)
C(19)	6650(5)	6862(8)	4108(4)
C(20)	7147(5)	6024(8)	4656(4)
C(21)	6762(5)	4617(9)	4867(4)
C(22)	5906(5)	4071(8)	4523(4)
C(23)	2682(5)	228(9)	4325(4)

TABLE F3

Anisotropic temperature factors (Å x10^3) for complex (165)

	U_{11}	U_{22}	U_{33}	U_{23}	U_{13}	U_{12}
Mo(1)	22.2(3)	21.7(3)	18.6(3)	1.9(3)	-3.7(2)	-2.1(2)
Cl(1)	31(1)	40(1)	55(1)	14(1)	-12(1)	-5(1)
Cl(2)	43(1)	87(2)	43(1)	32(1)	2(1)	21(1)
N(1)	22(3)	28(3)	24(3)	-4(3)	1(3)	3(3)
O(1)	57(4)	68(4)	24(3)	1(3)	-12(3)	-19(3)
O(2)	21(3)	40(3)	42(3)	15(3)	-2(2)	-3(2)
O(3)	28(3)	33(3)	20(2)	8(2)	5(2)	11(2)
O(4)	25(2)	36(3)	25(2)	11(3)	5(2)	4(2)
C(1)	25(4)	35(4)	30(4)	-1(4)	-3(3)	-14(4)
C(2)	34(5)	30(4)	26(4)	12(3)	-5(3)	-3(3)
C(3)	42(5)	20(4)	32(4)	14(3)	-1(4)	7(3)
C(4)	30(4)	27(4)	45(5)	15(4)	4(4)	-1(3)
C(5)	37(5)	22(4)	53(5)	0(4)	-10(4)	-8(4)
C(6)	42(5)	22(4)	37(4)	-4(3)	-7(4)	7(4)
C(7)	25(4)	25(4)	26(4)	2(3)	-3(3)	2(3)
C(8)	39(5)	24(4)	42(5)	17(4)	9(4)	10(4)
C(9)	33(5)	26(5)	62(6)	6(4)	-17(4)	-1(3)
C(10)	58(5)	32(5)	36(4)	6(4)	-22(4)	-4(4)
C(11)	52(5)	34(4)	20(4)	6(3)	-6(4)	7(4)
C(12)	22(4)	20(4)	22(4)	6(3)	0(3)	-4(3)
C(13)	25(4)	14(4)	20(3)	6(3)	-1(3)	4(3)
C(14)	29(4)	21(3)	22(3)	4(4)	-6(3)	-4(4)
C(15)	19(4)	28(4)	23(4)	4(3)	0(3)	-6(3)
C(16)	31(4)	26(4)	19(3)	-1(3)	0(3)	-2(3)
C(17)	27(4)	26(4)	16(3)	-3(3)	2(3)	0(3)
C(18)	28(4)	30(4)	33(4)	1(4)	-2(3)	8(4)
C(19)	41(5)	22(4)	39(5)	-4(3)	1(4)	-8(3)
C(20)	30(4)	35(5)	33(4)	-9(3)	-7(3)	3(3)
C(21)	45(5)	36(5)	23(4)	-4(3)	-12(4)	7(4)
C(22)	39(4)	26(4)	28(4)	5(3)	1(3)	-1(3)
C(23)	38(4)	35(5)	30(4)	1(4)	3(3)	-2(4)

TABLE F4

Hydrogen fractional atomic co-ordinates ($x10^4$) and isotropic temperature factors ($Å^2$ $x10^3$) for complex (165)

	x	y	z	U
H(1)	3526(24)	5278(70)	3006(35)	31(4)
H(4)	6516(36)	4726(56)	307(34)	31(4)
H(41)	4112(5)	-675(8)	2886(4)	31(4)
H(51)	4076(5)	-1845(9)	1663(4)	31(4)
H(61)	5703(5)	-1253(8)	1172(4)	31(4)
H(81)	7505(5)	85(8)	1842(4)	31(4)
H(91)	8171(6)	1313(8)	2880(5)	31(4)
H(101)	7279(6)	1611(9)	3855(4)	31(4)
H(111)	5684(6)	773(9)	3831(4)	31(4)
H(131)	6366(21)	2853(71)	1578(34)	31(4)
H(141)	5761(38)	3425(75)	2680(18)	31(4)
H(151)	4117(40)	4833(70)	1906(21)	31(4)
H(161)	3976(5)	4335(8)	3925(3)	31(4)
H(162)	4573(5)	3067(8)	3559(3)	31(4)
H(181)	5460(5)	6865(9)	3381(4)	31(4)
H(191)	6898(5)	7847(8)	3969(4)	31(4)
H(201)	7749(5)	6408(8)	4887(4)	31(4)
H(211)	7093(5)	4033(9)	5250(4)	31(4)
H(221)	5638(5)	3114(8)	4678(4)	31(4)
H(231)	2267(5)	-665(9)	4250(4)	31(4)
H(232)	2482(5)	831(9)	4713(4)	31(4)

Table F5

Bond lengths (Å) for complex (165)

C(1)-Mo(1)	1.929(9)	C(2)-Mo(1)	1.938(10)
C(3)-Mo(1)	2.445(9)	C(4)-Mo(1)	2.320(9)
C(5)-Mo(1)	2.302(10)	C(6)-Mo(1)	2.328(9)
C(7)-Mo(1)	2.431(8)	C(13)-Mo(1)	2.237(8)
C(14)-Mo(1)	2.272(9)	Cl(2)-Cl(1)	2.887(6)
C(23)-Cl(1)	1.765(9)	C(23)-Cl(2)	1.762(9)
C(15)-N(1)	1.333(9)	C(16)-N(1)	1.467(9)
C(1)-O(1)	1.177(9)	C(2)-O(2)	1.158(9)
C(12)-O(3)	1.259(9)	C(12)-O(4)	1.319(8)
C(4)-C(3)	1.427(11)	C(7)-C(3)	1.433(11)
C(11)-C(3)	1.424(11)	C(5)-C(4)	1.400(11)
C(6)-C(4)	2.297(13)	C(7)-C(4)	2.299(12)
C(6)-C(5)	1.432(11)	C(7)-C(6)	1.430(10)
C(8)-C(7)	1.416(11)	C(9)-C(8)	1.375(11)
C(10)-C(9)	1.396(12)	C(11)-C(10)	1.359(12)
C(13)-C(12)	1.449(10)	C(14)-C(13)	1.450(10)
C(15)-C(14)	1.382(10)	C(17)-C(16)	1.528(11)
C(18)-C(17)	1.386(10)	C(22)-C(17)	1.384(10)
C(19)-C(18)	1.386(10)	C(20)-C(19)	1.387(11)
C(21)-C(20)	1.395(11)	C(22)-C(21)	1.376(11)
H(1)-N(1)	0.960(2)	H(4)-O(4)	1.079(20)
H(41)-C(4)	0.960	H(51)-C(5)	0.960
H(61)-C(6)	0.960	H(81)-C(8)	0.960
H(91)-C(9)	0.960	H(101)-C(10)	0.960
H(111)-C(11)	0.960	H(131)-C(13)	0.960(2)
H(141)-C(14)	0.960(2)	H(151)-C(15)	0.960(2)
H(161)-C(16)	0.960	H(162)-C(16)	0.960

Table F5 continued...

H(181)-C(18)	0.960	H(191)-C(19)	0.960
H(201)-C(20)	0.960	H(211)-C(21)	0.960
H(221)-C(22)	0.960	H(231)-C(23)	0.960
H(232)-C(23)	0.960		

TABLE F6

Bond angles (deg.) for complex (165)

C(2)-Mo(1)-C(1)	79.9(4)	C(3)-Mo(1)-C(1)	149.1(3)
C(3)-Mo(1)-C(2)	118.9(4)	C(4)-Mo(1)-C(1)	130.6(3)
C(4)-Mo(1)-C(2)	91.8(4)	C(4)-Mo(1)-C(3)	34.7(2)
C(5)-Mo(1)-C(1)	97.4(4)	C(5)-Mo(1)-C(2)	97.9(4)
C(5)-Mo(1)-C(3)	57.9(4)	C(5)-Mo(1)-C(4)	35.3(2)
C(6)-Mo(1)-C(1)	91.0(4)	C(6)-Mo(1)-C(2)	131.8(3)
C(6)-Mo(1)-C(3)	58.1(4)	C(6)-Mo(1)-C(4)	59.2(4)
C(6)-Mo(1)-C(5)	36.0(3)	C(7)-Mo(1)-C(1)	118.8(4)
C(7)-Mo(1)-C(2)	149.6(3)	C(7)-Mo(1)-C(3)	34.2(2)
C(7)-Mo(1)-C(4)	57.8(3)	C(7)-Mo(1)-C(5)	58.2(3)
C(7)-Mo(1)-C(6)	34.9(2)	C(13)-Mo(1)-C(1)	83.3(4)
C(13)-Mo(1)-C(2)	115.9(4)	C(13)-Mo(1)-C(3)	106.4(3)
C(13)-Mo(1)-C(4)	141.0(2)	C(13)-Mo(1)-C(5)	145.5(2)
C(13)-Mo(1)-C(6)	109.7(4)	C(13)-Mo(1)-C(7)	91.2(3)
C(14)-Mo(1)-C(1)	111.8(4)	C(14)-Mo(1)-C(2)	96.5(4)
C(14)-Mo(1)-C(3)	91.4(3)	C(14)-Mo(1)-C(4)	117.6(3)
C(14)-Mo(1)-C(5)	149.3(2)	C(14)-Mo(1)-C(6)	130.2(3)
C(14)-Mo(1)-C(7)	97.7(3)	C(14)-Mo(1)-C(13)	37.5(2)
C(23)-Cl(1)-Cl(2)	35.0(2)	C(23)-Cl(2)-Cl(1)	35.1(2)
C(16)-N(1)-C(15)	123.9(7)	O(1)-C(1)-Mo(1)	178.6(6)
O(2)-C(2)-Mo(1)	175.7(7)	C(4)-C(3)-Mo(1)	67.9(5)
C(7)-C(3)-Mo(1)	72.4(5)	C(7)-C(3)-C(4)	107.0(7)
C(11)-C(3)-Mo(1)	123.5(6)	C(11)-C(3)-C(4)	133.5(7)
C(11)-C(3)-C(7)	119.5(8)	C(3)-C(4)-Mo(1)	77.4(5)
C(5)-C(4)-Mo(1)	71.7(5)	C(5)-C(4)-C(3)	109.0(8)
C(6)-C(4)-Mo(1)	60.5(3)	C(6)-C(4)-C(3)	72.8(6)
C(6)-C(4)-C(5)	36.3(4)	C(7)-C(4)-Mo(1)	63.5(3)

Table F6 continued...

C(7)-C(4)-C(3)	36.6(4)	C(7)-C(4)-C(5)	72.5(6)	C(6)-C(5)-H(51)	125.8(5)	H(61)-C(6)-Mo(1)	118.1(3)
C(7)-C(4)-C(6)	36.2(3)	C(4)-C(5)-Mo(1)	73.1(5)	H(61)-C(6)-C(4)	161.6(3)	H(61)-C(6)-C(5)	126.4(5)
C(6)-C(5)-Mo(1)	73.0(5)	C(6)-C(5)-C(4)	108.4(7)	C(7)-C(6)-H(61)	126.4(5)	H(81)-C(8)-C(7)	120.9(5)
C(4)-C(6)-Mo(1)	60.2(4)	C(5)-C(6)-Mo(1)	71.0(5)	C(9)-C(8)-H(81)	120.8(6)	H(91)-C(9)-C(8)	119.3(6)
C(5)-C(6)-C(4)	35.3(4)	C(7)-C(6)-Mo(1)	76.5(5)	C(10)-C(9)-H(91)	119.2(6)	H(101)-C(10)-C(9)	118.9(6)
C(7)-C(6)-C(4)	72.0(6)	C(7)-C(6)-C(5)	107.2(8)	C(11)-C(10)-H(101)	118.9(6)	H(111)-C(11)-C(3)	120.7(6)
C(3)-C(7)-Mo(1)	73.4(5)	C(4)-C(7)-Mo(1)	58.7(3)	H(111)-C(11)-C(10)	120.8(6)	H(131)-C(13)-Mo(1)	104.5(41)
C(4)-C(7)-C(3)	36.4(4)	C(6)-C(7)-Mo(1)	68.6(5)	H(131)-C(13)-C(12)	113.1(40)	C(14)-C(13)-H(131)	117.7(41)
C(6)-C(7)-C(3)	108.2(7)	C(6)-C(7)-C(4)	71.8(6)	H(141)-C(14)-Mo(1)	107.9(42)	H(141)-C(14)-C(13)	119.7(40)
C(8)-C(7)-Mo(1)	124.1(6)	C(8)-C(7)-C(3)	119.9(8)	C(15)-C(14)-H(141)	116.3(40)	H(151)-C(15)-N(1)	111.3(41)
C(8)-C(7)-C(4)	156.3(6)	C(8)-C(7)-C(6)	131.9(7)	H(151)-C(15)-C(14)	121.4(41)	H(161)-C(16)-N(1)	108.0(4)
C(9)-C(8)-C(7)	118.3(8)	C(10)-C(9)-C(8)	121.6(8)	H(162)-C(16)-N(1)	108.1(4)	H(162)-C(16)-H(161)	109.5
C(11)-C(10)-C(9)	122.2(8)	C(10)-C(11)-C(3)	118.5(8)	C(17)-C(16)-H(161)	107.9(4)	C(17)-C(16)-H(162)	108.1(5)
O(4)-C(12)-O(3)	119.9(7)	C(13)-C(12)-O(3)	125.6(7)	H(181)-C(18)-C(17)	119.6(5)	C(19)-C(18)-H(181)	119.6(5)
C(13)-C(12)-O(4)	114.5(7)	C(12)-C(13)-Mo(1)	115.3(5)	H(191)-C(19)-C(18)	119.9(5)	C(20)-C(19)-H(191)	119.9(5)
C(14)-C(13)-Mo(1)	72.5(5)	C(14)-C(13)-C(12)	124.3(7)	H(201)-C(20)-C(19)	120.3(5)	C(21)-C(20)-H(201)	120.4(5)
C(13)-C(14)-Mo(1)	69.9(5)	C(15)-C(14)-Mo(1)	99.2(5)	H(211)-C(21)-C(20)	120.2(5)	C(22)-C(21)-H(211)	120.2(5)
C(15)-C(14)-C(13)	123.6(7)	C(14)-C(15)-N(1)	127.1(7)	H(221)-C(22)-C(17)	119.2(5)	H(221)-C(22)-C(21)	119.1(5)
C(17)-C(16)-N(1)	115.2(6)	C(18)-C(17)-C(16)	123.9(7)	H(231)-C(23)-Cl(1)	109.4(4)	H(231)-C(23)-Cl(2)	109.4(4)
C(22)-C(17)-C(16)	117.7(7)	C(22)-C(17)-C(18)	118.3(7)	H(232)-C(23)-Cl(1)	109.4(4)	H(232)-C(23)-Cl(2)	109.4(4)
C(19)-C(18)-C(17)	120.8(8)	C(20)-C(19)-C(18)	120.2(8)	H(232)-C(23)-H(231)	109.5		
C(21)-C(20)-C(19)	119.3(8)	C(22)-C(21)-C(20)	119.7(8)				
C(21)-C(22)-C(17)	121.7(8)	Cl(2)-C(23)-Cl(1)	109.9(5)				
C(15)-N(1)-H(1)	132.3(41)	C(16)-N(1)-H(1)	101.9(42)				
C(12)-O(4)-H(4)	114.5(36)	H(41)-C(4)-Mo(1)	117.3(3)				
H(41)-C(4)-C(3)	125.6(5)	C(5)-C(4)-H(41)	125.5(5)				
C(6)-C(4)-H(41)	161.5(3)	C(7)-C(4)-H(41)	162.0(3)				
H(51)-C(5)-Mo(1)	120.0(3)	H(51)-C(5)-C(4)	125.8(5)				

TABLE F7

Selected non-bonded distances (Å) for **complex (165)**

Intramolecular:

O(1)-Mo(1)	3.105	O(2)-Mo(1)	3.094	H(151)-C(2)	2.738	H(41)-C(3)	2.134
H(41)-Mo(1)	2.889	H(51)-Mo(1)	2.903	C(5)-C(3)	2.301	C(6)-C(3)	2.319
H(61)-Mo(1)	2.905	C(8)-Mo(1)	3.431	C(8)-C(3)	2.466	C(9)-C(3)	2.783
C(11)-Mo(1)	3.443	C(12)-Mo(1)	3.141	C(10)-C(3)	2.392	H(111)-C(3)	2.085
H(131)-Mo(1)	2.646	H(141)-Mo(1)	2.725	H(51)-C(4)	2.110	C(11)-C(4)	2.620
C(15)-Mo(1)	2.841	H(151)-Mo(1)	3.136	C(5)-H(41)	2.107	H(61)-C(5)	2.145
O(2)-Cl(1)	3.306	C(2)-Cl(1)	3.545	C(7)-C(5)	2.303	C(6)-H(51)	2.139
H(41)-Cl(1)	3.094	C(16)-Cl(1)	3.526	C(8)-C(6)	2.599	C(7)-H(61)	2.143
H(162)-Cl(1)	3.092	H(231)-Cl(1)	2.272	H(81)-C(7)	2.079	C(9)-C(7)	2.397
H(232)-Cl(1)	2.272	H(111)-Cl(2)	3.084	C(10)-C(7)	2.779	C(11)-C(7)	2.468
H(231)-Cl(2)	2.269	H(232)-Cl(2)	2.269	H(91)-C(8)	2.026	C(10)-C(8)	2.419
C(14)-N(1)	2.430	H(141)-N(1)	2.619	C(11)-C(8)	2.841	H(131)-C(8)	2.734
H(151)-N(1)	1.904	H(161)-N(1)	1.986	C(9)-H(81)	2.041	H(91)-H(81)	2.337
H(162)-N(1)	1.987	C(17)-N(1)	2.529	H(101)-C(9)	2.041	C(11)-C(9)	2.412
C(18)-N(1)	2.958	H(181)-N(1)	2.640	C(10)-H(91)	2.044	H(101)-H(91)	2.328
C(15)-H(1)	2.102	H(151)-H(1)	2.339	H(111)-C(10)	2.026	C(11)-H(101)	2.007
C(16)-H(1)	1.911	H(161)-H(1)	1.962	H(111)-H(101)	2.314	H(131)-C(12)	2.028
O(4)-O(3)	2.232	C(13)-O(3)	2.410	C(14)-C(12)	2.563	C(15)-C(12)	3.063
C(14)-O(3)	3.013	C(15)-O(3)	2.927	H(141)-C(13)	2.098	C(15)-C(13)	2.496
H(151)-O(3)	2.310	C(13)-O(4)	2.329	H(151)-C(13)	2.713	C(14)-H(131)	2.078
H(131)-O(4)	2.409	C(12)-H(4)	2.021	H(151)-C(14)	2.052	C(16)-C(14)	3.000
C(2)-C(1)	2.482	C(5)-C(1)	3.187	C(15)-H(141)	2.002	C(16)-H(141)	2.698
C(6)-C(1)	3.048	C(12)-C(1)	2.753	C(16)-C(15)	2.471	H(162)-C(15)	2.619
C(13)-C(1)	2.778	C(4)-C(2)	3.069	C(18)-C(16)	2.574	H(181)-C(16)	2.749
C(14)-C(2)	3.149	C(15)-C(2)	2.771	C(22)-C(16)	2.493	H(221)-C(16)	2.613
				H(162)-H(161)	1.568	C(17)-H(161)	2.039
				C(17)-H(162)	2.041	C(22)-H(162)	2.608
				H(181)-C(17)	2.039	C(19)-C(17)	2.411
				C(20)-C(17)	2.793	C(21)-C(17)	2.410
				H(221)-C(17)	2.033	H(191)-C(18)	2.042
				C(20)-C(18)	2.403	C(21)-C(18)	2.766
				C(22)-C(18)	2.379	C(19)-H(181)	2.039

Table F7 continued...

H(191)-H(181)	2.338	H(201)-C(19)	2.047
C(21)-C(19)	2.400	C(22)-C(19)	2.754
C(20)-H(191)	2.043	H(201)-H(191)	2.351
H(211)-C(20)	2.053	C(22)-C(20)	2.396
C(21)-H(201)	2.055	H(221)-C(21)	2.025
C(22)-H(211)	2.035	H(221)-H(211)	2.326
H(232)-H(231)	1.568		

Intermolecular:

H(51)-Cl(1a)	2.765	H(151)-Cl(1b)	2.773
Cl(2)-Cl(2c)	3.449	H(111)-Cl(2c)	3.111
H(221)-Cl(2c)	2.818	O(2)-H(1a)	2.216
H(61)-O(1d)	2.641	O(4)-O(3e)	2.584
H(4)-O(3e)	2.628	H(232)-O(4f)	2.559
C(23)-H(4f)	2.574	H(232)-H(4f)	1.888
H(181)-C(4g)	2.747	C(19)-H(81h)	2.708
C(21)-H(161i)	2.743		

Key to symmetry operations relating designated atoms to reference atoms at (x,y,z):

(a) 0.5-x,-0.5+y,0.5-z
(b) 0.5-x,0.5+y,0.5-z
(c) 1.0-x,-y,1.0-z
(d) 1.0-x,-y,-z
(e) 1.0-x,1.0-y,-z
(f) -0.5+x,0.5-y,0.5+z
(g) x,1.0+y,z
(h) 1.5-x,0.5+y,0.5-z
(i) 1.0-x,1.0-y,1.0-z